ASPECTS OF THE GEOCHEMISTRY OF THE KARROO DOLERITES AND BASALTS OF THE NORTH-EASTERN CAPE.

by

J. v A. ROBEY, B.Sc. (Hons.)

Thesis presented for the degree of Master of Science at Rhodes University, Grahamstown.

January, 1976.

DECLARATION.

All work in this thesis is the original work of the author except where specific acknowledgement is made to the work of others.

signed: ..J.v.A.Robey.....

J. v A. Robey,
Department of Geology,
Rhodes University,
Grahamstown.

January, 1976.

ABSTRACT

The Birds River Gabbro Complex is intruded into sediments of the Karroo Stormberg Group in the area SW of Dordrecht in the north-eastern Cape.

A geochemical investigation, restricted to the igneous rock suite, gabbro-ferrogabbro-ferrotholeiite, presents new major-element data as well as data for twelve trace elements - Ba, Sr, Rb, Zr, Y, Nb, Zn, Cu, Ni, Co, V and Cr. The strong degree of differentiation of Kokstad-type tholeiitic magma in the Birds River intrusion, as noted by previous investigators, is revealed in variation diagrams in which data are plotted against a simple index of fractionation. Later differentiates are strongly enriched in Si, Ti, Fe, Na, K, P, Ba, Rb, Zr, Y, Nb, Zn and Cu but depleted in Mg, Ca, Al, Ni, Co and Cr. Extreme differentiation resulted in a strong depletion of Ti, Fe, P, Cu and V in the most highly evolved ferrotholeiites.

Field evidence suggests the initial emplacement of strongly fractionated magmatic residua derived from fractional crystallization processes in a magma chamber at depth during cauldron subsidence of a mass of sediments within an annular fracture. These porphyritic, in part glassy, ferrotholeiites are enriched in Si, Na, K, Ba, Zr, Rb, Y, Nb and Zn and were engulfed by a later episode of renewed hypabyssal intrusive activity from the original source area. The younger gabbro was emplaced in a series of closely-spaced heaves or pulses of relatively undifferentiated Kokstad-type magma. The gabbro differentiated in place to form ferrogabbros which chemically closely approximate ferro-tholeiite compositions. Residual liquids crystallized as a pegma-toidal facies.

A simple fractional crystallization path, modelled on the assumption that the gabbro and ferrotholeiite form a continuous series, indicates that the least evolved ferrotholeiite can be derived from the initial gabbro composition by the fractionation of major amounts of plagioclase and pyroxene but lesser amounts of olivine. Crystalli-zation and removal of magnetite and other Fe-oxides were relatively more important during the later stages of differentiation.

The variation of major- and trace-elements in tholeiitic Karroo magma under conditions of strong differentiation at Birds River serves as a framework for the regional study of the geochemistry of other Karroo dolerites and volcanics of the north-eastern Cape.

New geochemical data are presented for a sample of thirty chilled and coarse-grained Karroo dolerites collected throughout the north-

eastern Cape. For the most part, the chilled dolerites are relatively undifferentiated and the average composition differs only slightly from that determined by Walker and Poldervaart (1949). Variation diagrams reveal the steady increase in Si, Al, Ca, Na, K and P and the residual trace elements Ba, Zr, Rb, Y, Nb and Zn with increasing differentiation of the dolerites from more basic types. The concentrations of K, Ba and Rb are highly variable in some Karroo dolerites while new data suggest that Nb levels in the dolerites are low, being generally less than 10 ppm.

The strong variation of the K-related elements (K, Ba and Rb) as well as the large ranges determined for certain inter-element ratios, such as K/Rb, Zr/Nb and K/Zr in the chilled Karroo dolerites, suggest that factors other than fractional crystallization processes need to be considered to account for individual variations. Little correlation exists between petrographic type as defined by Walker and Poldervaart (1949) and geochemical character.

New geochemical data are also presented for ten Karroo basaltic lavas from the lowermost horizons of the lava sequence exposed in the Barkly East area. Major- and trace-element data indicate that these earliest Karroo extrusives are on average enriched in Si and Rb but depleted in Co and Ni when compared with the averaged chilled Karroo dolerite. Compared with basalts from Lesotho, the Barkly East basalts are enriched in Si but depleted in Ni and possibly Nb, Cu and V. The andesite is markedly enriched in Si, Na, K, Ba, Sr, Rb, Zr and Nb but depleted in Mg, Ca, V, Ni, Cu, Co and Cr. The subdued rate of Ni depletion and the absence of olivine as a major phenocryst phase in the series basalt to andesite, in the Barkly East area, suggests that differentiation trends may be controlled by the fractional crystallization of orthopyroxene and plagioclase, the two common phenocrysts present in these volcanics. The strong depletion of V and Cu in the andesite may indicate some magnetite removal during fractional crystallization.

CONTENTS

PAGE

ACKNOWLEDGEMENTS

Grateful acknowledgement is made to the Council for Scientific and Industrial Research, Pretoria for financial support during the period that I held the position of Research Officer at Rhodes University, within the framework of the SACUGS contribution to the INTERNATIONAL GEODYNAMICS PROGRAM. Financial support was made available for this work within Working Group 4 "GEODYNAMICS OF CONTINENTAL AND OCEANIC RIFTS (b) Comparative Geochemical Studies of Oceanic and Continental Volcanics Rocks".

I am extremely grateful to Professor H.V. Eales for the guidance and many helpful suggestions he so often gave during the course of this work and in particular for his advice and interest in problems relating to the Birds River intrusion. Professor Eales is also to be thanked for critically reading the manuscript.

I also warmly thank Dr. J.S. Marsh for the many hours of fruitful discussion held with him and especially for his assistance and advice in the treatment of trace element data particularly that involving computer analysis. I am also indebted to Dr. Marsh for critically reviewing sections of the manuscript and for the interest he took in the progress of this work.

The help and guidance given by Dr. B.E. Lock during a field trip to the Barkly East area is also appreciated.

Furthermore, I am greatly indebted to members of the Geochemistry Research Department, University of Cape Town, in particular Professors L.H. Ahrens and A.J. Erlank, Dr. A.R. Duncan and Mr. J.P. Willis for guidance and assistance in the use of analytical facilities and X.R.F. data reduction programs. I have not named all the other members of the Geochemistry Department who helped and encouraged me but their friendliness will never be forgotten.

I thank Mr. and Mrs. D. Tennant of the farm Denwood in the Birds River area for the hospitality they so readily gave.

I also wish to thank Mrs. U. Tarr for undertaking the arduous task of typing the manuscript.

Finally, I thank Liz for her unstinted encouragement throughout the duration of this study.

1. SCOPE OF STUDY:

This thesis is divided into two main sections. The first section discusses some aspects of the geochemistry of the Birds River differentiated intrusion. The second section presents new major- and trace-element data from some lower Karroo basalts in the Barkly East area and for a sample of Karroo dolerites, collected throughout the north-eastern Cape and Border regions.

Birds River Complex.

Previous chemical investigations into the gabbro-ferrotholeiite differentiated igneous suite at Birds River have tended to be confined to a study of the type-section exposed on the farm Denwood, along the south-western edge of the complex. These investigations are reported in Eales and Booth (1974) and Eales and Robey (in press).

This gabbro-ferrotholeiite sequence is also known to be exposed in some deep stream sections cut into the western edge of the complex. The aim of the present study was to investigate the sequence exposed in the Stapelbergkloof stream section on the farm Stapelberg's Vlei, further to the west of Denwood. Samples collected in Stapelbergkloof were analysed for major elements as well as 12 trace elements. The trace element data thus extend the partial trace element studies carried out by Eales and Robey (op.cit.).

This study compares geochemical data from Stapelbergkloof with that from Denwood. The variation of trace elements in the highly fractionated Birds River sequence indicates the relative degrees of enrichment or depletion that can be expected in trace element levels in other, highly differentiated Karroo intrusive bodies.

Karroo Dolerites and Barkly East basalts.

The aim of the second section of this thesis was to collect and provide new major- and trace-element data for a number of chilled Karroo dolerites in the north-eastern Cape and Border regions. Comparable studies were aimed at Karroo basalts and andesites erupted during the earliest stages of lava effusion in the Barkly East area.

These studies were aimed at providing new chemical data for the different dolerite types of Walker and Poldervaart (1949). It was also hoped to determine to what extent these different types represent different magma batches.

The study of the Barkly East basalts forms a preliminary investigation to a more thorough geochemical study at present being

undertaken by research workers in the Department of Geology, Rhodes University.

Finally, it was hoped to perform mineralogical investigations on all three rock suites, with the aid of microprobe techniques. Due to circumstances beyond the author's control, this has not been possible.

2. THE BIRDS RIVER DIFFERENTIATED COMPLEX.

2.1 Introduction.

Booth (1971) and Eales and Booth(1974) present an adequate historical review of investigations, prior to 1971, into the nature and form of the Birds River Complex, situated some 20 km west-south-west of Dordrecht in the North Eastern Cape.

Prior to 1971, investigations are limited to the work of du Toit, who first mentions and describes the complex as "an old volcanic centre, of Stormberg age, which was invaded at some later period by vast masses of Karroo dolerite, the sedimentary rocks being much tilted, dislocated, and portions highly metamorphozed" (du Toit, 1905, quoted by Eales and Booth, op.cit.). In later reports, du Toit (1911, 1920) more fully discusses this dolerite intrusion and describes the shape of the complex as being in the form of a bell-jar intrusion.

In 1969, a re-investigation into the nature of the Birds River intrusion was instigated and directed by Professor H.V. Eales. This subsequently lead to the more complete geological and structural interpretation presented by Booth (op.cit.) and summarized by Eales and Booth (op.cit.). While the former work concentrated more on the geology and structure of the area, the highly differentiated character of the Birds River Complex is first discussed in some detail by Eales and Booth (op.cit.). In this latter work, the petrology and petrography of the representative igneous rock suites are discussed in terms of new whole-rock major element analyses, as well as presenting new microprobe chemical data for the olivine and Ca-rich pyroxene mineral series. Particular attention is paid to the highly differentiated tholeiites (later termed ferrotholeiites by Eales and Robey (in press) and textures exhibited by these rocks are discussed in detail.

A later investigation by Eales and Robey (op.cit.) confirms the highly differentiated character of the Birds River Complex in terms of new partial trace element data for the representative rock types. In the latter discussion it is noted that "regular trends in the content of Rb, Sr, Y, Zr and Nb correlate well with fractionation indices based on major element chemistry". Also discussed in some detail are trace element variations across the intrusive contacts in the Denwood type-section (Eales and Robey, op.cit.). Here, the sharp discontinuity noted in the levels of trace element contents

across the gabbro-ferrotholeiite contact support the contention that the ferrotholeiites are not in-situ differentiates of the younger gabbro, but rather that they belong to an earlier, highly fractionated pulse. Regular cyclic trends of increasing Rb, Zr and Y levels within the younger gabbro-ferrogabbro series, however, suggest that differentiation in place led to the formation of the ferrogabbro and pegmatoidal series, found adjacent to the inner contact with the ferrotholeiites.

The present study is an investigation into major and trace element variations within the gabbro-ferrotholeiite series, exposed in Stapelbergkloof, some 5 km north-west of the Denwood type-section. New major element data are presented as well as new data for 12 trace elements - Sr, Ba, Rb, Zr, Y, Nb, Zn, Cu, Co, Ni, V and Cr. Though these data are from a different part of the complex, the strong degree of differentiation discussed by Eales and Booth (1974) and Eales and Robey (in press) is upheld. Previously published analyses for the gabbro-ferrotholeiite series are combined with the new data and in the major and trace element variation diagrams, it is seen that analyses fall on nearly smooth trends. While the gabbros and ferrogabbros from Stapelbergkloof are very similar to those from Denwood, the ferrotholeiites from Stapelbergkloof are, for the most part, slightly less differentiated than similar petrographic types from the type-section.

A concluding section attempts to formulate a simple fractional crystallization model for part of the gabbro-ferrotholeiite sequence at Stapelbergkloof. This suggests that, though the ferrotholeiite suite is an earlier-intruded pulse of highly fractionated magma derived from a magma source at some depth below the Birds River intrusion (Eales and Booth, op.cit.), the ferrotholeiites can be derived by the fractional crystallization of a magma source similar to that that gave rise to the gabbros that were emplaced in voluminous quantitites at some later time.

2.2. Location, Geological Setting and Sample Collection.

The geological map and structural interpretation of the Birds River Complex, after Eales and Booth (1974), is presented in Figs. 1(a and b). The more salient, geological features of the Birds River Complex presented in this section, are summarized from the above-mentioned work.

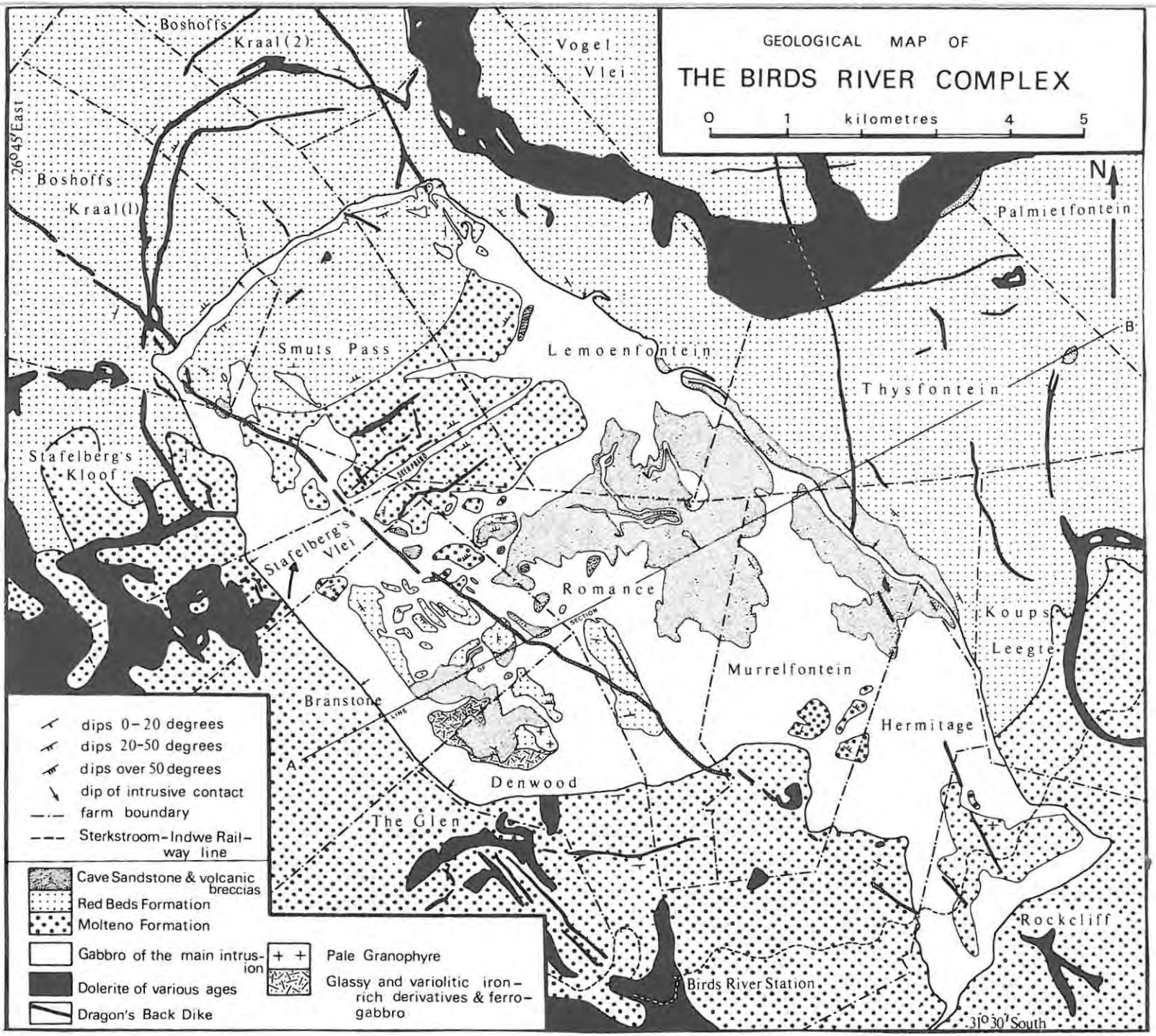

Fig.1(a): Geological map of the Birds River Complex (from Eales and Booth, 1974, Plate 1).

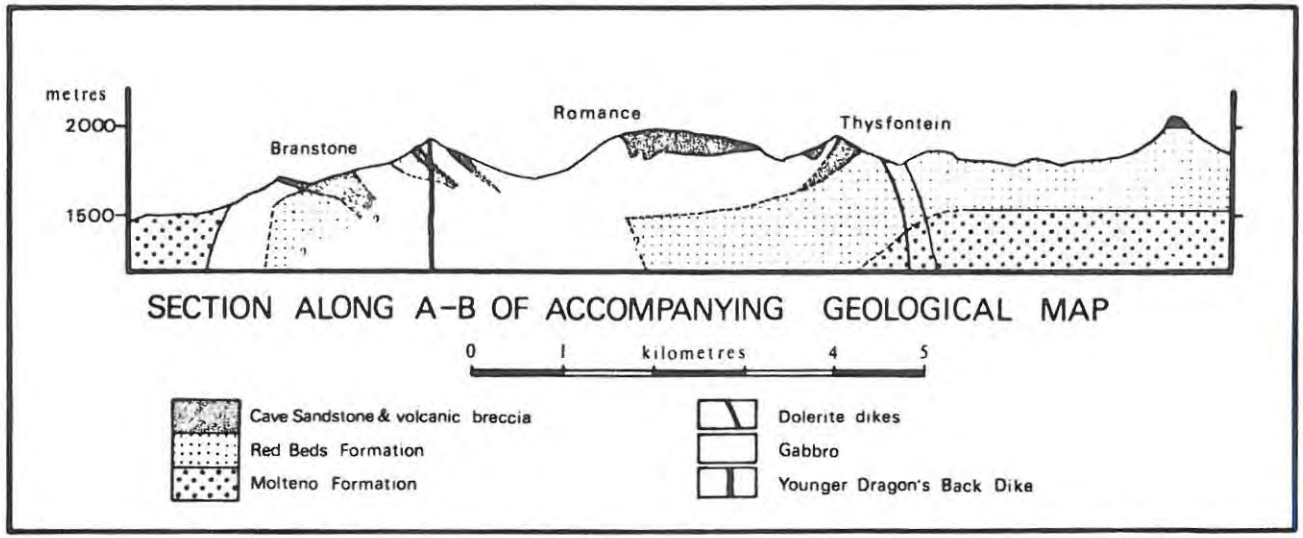

Fig.1(b): Interpretation of the structure of the Birds River Complex. Section along A-B in map shown in Fig.1(b) (from Eales and Booth, 1974, Fig.1).

The Birds River Complex, with a longer, north-westerly axis of 13.5km, is intruded into sediments of the Molteno, Red Beds and Cave Sandstone Formations of the Karroo Stormberg Group. Collapse of the roof zone sediments following "the emplacement of the gabbroic magma, led to the engulfment of dismembered fragments of Stormberg Group rocks" (Molteno, Red Beds and Cave sandstone horizons). These portions of the roof-zone country rocks that sank into the cauldron, are today exposed as often steeply dipping and highly folded xenoliths, some of large areal extent.

The upper horizons of the Molteno Formation are exposed in the area to the south of the complex, while to the north the full thickness of the Red Beds sediments, estimated at 440 metres, is exposed. Cave Sandstone has only been mapped along the steeply dipping north-eastern rim or as isolated outliers on the surrounding high ground. Eales and Booth (op.cit.) furthermore note that in the immediate vicinity of the complex in the south-western corner of Thysfontein, thick beds of massive volcanic breccia are interbedded with and overlie the Cave Sandstone horizon. Minor flows of amygdaloidal basalt are also found in some upper breccia horizons. Representative chemical analyses of the country-rock sediments, the volcanic breccias and a tholeiitic quartz basalt are presented by Eales and Booth (op.cit., Table 1). The breccias, composed essentially of coarse-grained dolerite, finer-grained basaltic fragments and fragments of Molteno, Red Beds and Cave Sandstone sediments, are also exposed in some of the larger xenoliths engulfed by gabbro within the complex. A similar occurrence though not previously mapped, has also been found in the high ground surrounding the upper reaches of Stapelbergkloof stream section (Fig. 2).

In their discussion of the shape of the complex, Eales and Booth (op.cit.) note that "to the west of a meridional line through the centre of the complex, the deduced structure conforms with that indicated by du Toit ...". Here the outer contact is in the form of a steeply-dipping dolerite dyke, having the shape of a bell-jar. However the eastern and south-eastern contacts have more the "attributes of a thick transgressive sheet" where the previously-mentioned authors contend that the magma broke out and assumed the form of a westerly dipping sheet.

The type-section for the series - gabbro-ferrogabbro-ferrotholeiite, is on the farm Denwood. A detailed geological map of this area is shown in Eales and Booth (op.cit., Fig. 3). Here the outer dolerite contact is intrusive into Molteno sandstones and dips south-west at

80°. The section exposed in this stream is shown in Eales and Robey (in press, Fig. 6) and reproduced in Fig. 11(b) of this study. The thick dyke-like mass of outer gabbro shows a sharp intrusive contact with a steeply-dipping body of intersertal, glassy, ferrotholeiites. The gabbro in the immediate contact with the ferrotholeiites is pegmatoidal in type and encloses numerous small xenoliths of the older body. This contact zone is sharp but is extremely difficult to detect in the field. Further up the stream section, the ferrotholeiites give way to dense, nearly horizontally bedded, black hornfelsic material believed to be metasomatized Red Beds sediments. At the head of the stream, just underlying the Cave Sandstone horizon, a thin band of metasomatic granophyre outcrops. (Eales and Robey, op.cit., Fig. 6; Eales and Booth, op.cit., Fig. 3).

A sketch-map of the immediate geology of the Stapelbergkloof section is shown in Fig (2). Also indicated, are the locations of the samples analysed and presented in Table 1(a). The Stapelbergkloof section is a traverse up a minor tributary of the Grootvleispruit, on the farm Stapelberg's Vlei, some 5 km to the north-west of Denwood. This tributary is cut into the south-western margin of the Birds River Complex just to the south-west of Skerprand. The area of investigation is indicated in Fig.1(a). The Stapelbergkloof traverse referred to in this study, must not be confused with the farm Stapelberg's Kloof, further to the north-west (Fig.1a).

From Fig. 2, it is seen that the Stapelbergkloof stream section is cut through gabbroic igneous rocks of both the younger gabbro and the earlier ferrotholeiites. The section is approximately 800 yards in length and in the upper reaches of the tributary, the gabbroic rocks abruptly abut against a fairly large flat-lying sedimentary xenolith of Cave Sandstone and pyroclastic breccia. The distances of the various samples from the outer dolerite - Molteno sandstone contact as shown in Fig. 2 are only approximate. These were paced out in the field. No accurate plane table surveying was undertaken.

Coarse-grained poikiliphitic gabbros outcrop for some 250 yards inwards from the outer contact. The contact between the gabbros and the glassy, ferrotholeiites has not been accurately located in this section as has been possible in the Branstone and Denwood sections (Eales and Booth, 1974). The approximate contact indicated in Fig. 2 is based purely on petrographic criteria. Whereas sample S32 is a coarse-grained, micropegmatite-rich ferrogabbro, the textures ex-

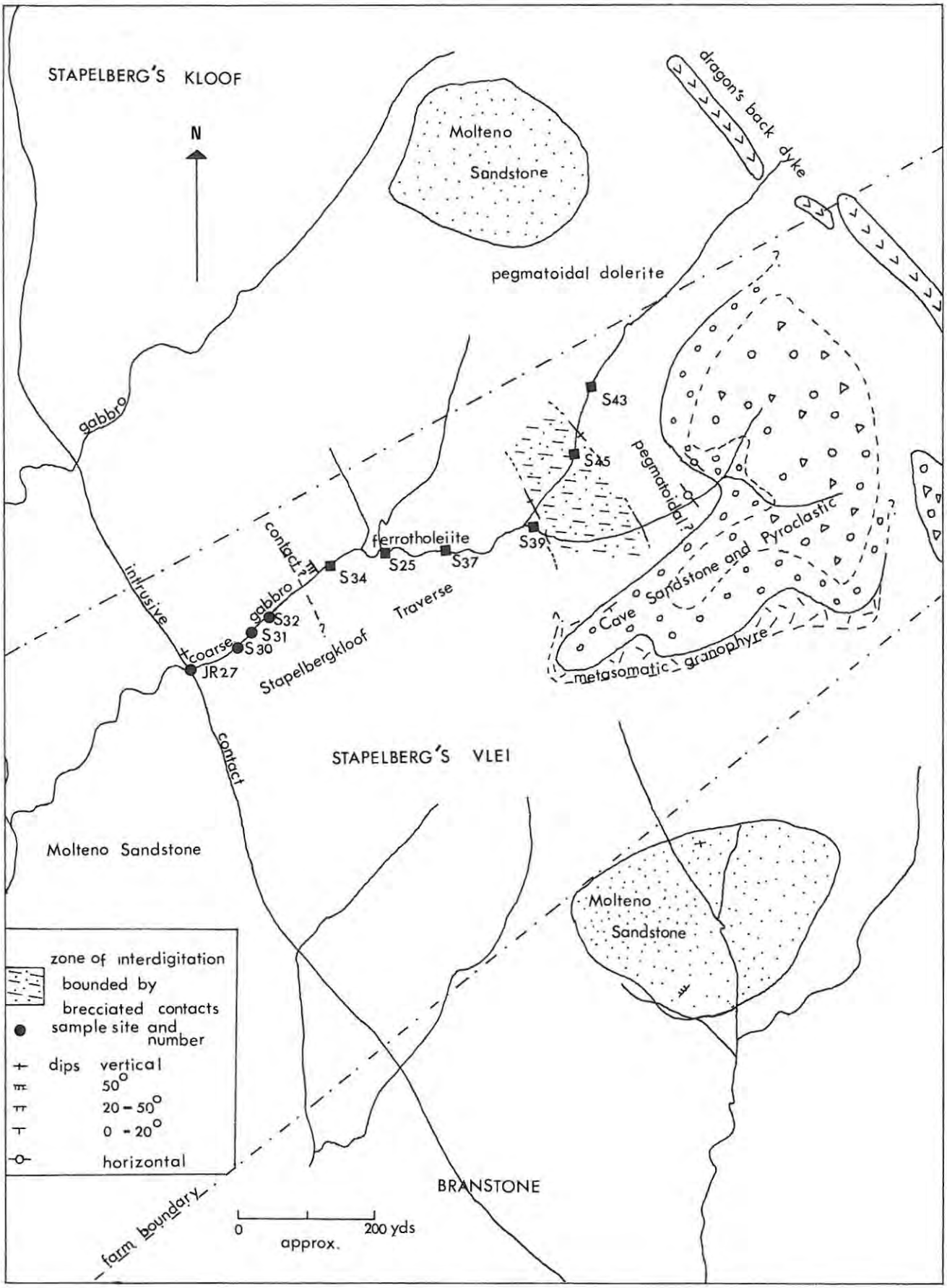

Fig.2: Map of the geology of the Stapelbergkloof stream section on the farm Stapelberg's Vlei in the Birds River area. Sample localities are indicated.

hibited by S34 are identical to textures described by Eales and Booth (op.cit.) for the porphyritic, glassy tholeiites/ferrotholeiites. These glassy ferrotholeiites, seen in hand specimen as a medium grained, dark gabbro with dense, black clots of glassy mesostasis, outcrop for some 360 yards along the main stream to sample site S39. As indicated in Fig. 2, just to the north-east of sample site S39, a narrow zone of calcite-rich breccia is encountered. A similar zone is repeated further upstream. These contact zones are nearly vertical in some sections while horizontal in others and enclose an outcrop where glassy ferrotholeiites are interdigitated with very fine hornfelsic material and coarse-grained, highly weathered granophyre (?), showing the development of large skeletal crystals and comb structures. This section is poorly exposed and highly weathered, while the scree cover on the surrounding slopes makes these contacts difficult to follow and map. The true shape of this zone of interdigitation is not known. A similar zone of interdigitation of ferrotholeiite and dense, hornfelsic metamorphozed Red Beds sediments is also found in the upper reaches of the Denwood type-section.

The gabbroic rocks directly beneath the Cave Sandstone xenolith are extremely weathered but in hand-specimen are similar to the pegmatitic facies described by Eales and Booth (op.cit.). This dolerite pegmatite, near its contact with the Cave Sandstone, contains numerous lenses of granophyric material in which excellent comb structures and large weathered skeletal crystals are found. Approximately 20 feet vertically beneath the Cave Sandstone contact, a zone of dolerite pegmatite, riddled with whitish veins is found. These veins, never more than inch in thickness, are horizontally intruded and parallel the Cave Sandstone contact. In no case were these veins observed to cut down from the overlying Cave Sandstone and it is still not clear if these represent remobilized sedimentary rheomorphic veins or true very late-stage acid differentiates of the basic rocks.

The Cave Sandstone at its contact with the dolerite pegmatite is flat-bedded and shows a thermal metamorphic zone of massive baked sandstone in which are developed small cylindrical tubes of recrystallized material, commonly seen in sedimentary rocks at the contact with intrusive dolerite. Overlying this baked zone, the Cave Sandstones revert to their normal laminated character - fine, friable sandstones showing fine bedding structures. Above the Cave Sandstone and capping the high ground at the head of the

Stapelbergkloof stream, pyroclastic breccias are found. The clasts in these breccia vary enormously in size and appear similar to the breccias previously described by Booth (1971) and Eales and Booth (1974). As shown in Fig.1(a), this xenolith of Cave Sandstone and volcanic breccia had not previously been mapped by the above-mentioned authors. The area of investigation is bounded to the north-east by the Dragon's Back dyke which forms "the jagged spine of the high ridge at an elevation well above 2000 m on (the farms) Branstone, Stapelberg's Vlei and Stapelberg's Kloof" (Eales and Booth, op.cit.). The dolerite dyke is segmented, the segments being arranged "en echelon" and is the youngest intrusive in the Birds River area, cutting through the complex and all formations in the surrounding area (Fig.1a). The Dragon's Back dyke is a sub-ophitic dolerite containing appreciable quantities of biotite and hornblende. This according to Eales and Booth (1974), suggests that the "major part of the column of Stormberg lavas was built up only after emplacement of the bell-jar (the Birds River gabbroic rocks), in which biotite and amphiboles are absent". The presence of biotite and hornblende therefore suggests that the Dragon's Back dyke "belongs to a deeper level of emplacement" relative to the gabbroic rocks from the Birds River intrusion.

2.3. Petrography.

The petrography of the representative rock types found at Birds River is described in detail by Booth (1971) and Eales and Booth (1974). It was hoped in the present study that mineralogical investigations with the aid of microprobe techniques would be possible, but unfortunately numerous factors delayed the operation of the newly-acquired microprobe at Rhodes University. Consequently little analytical work dealing with the different mineral series, was undertaken. Eales and Booth (op.cit.) present microprobe data for olivines and clinopyroxenes but no accurate data exist for the Ca-poor pyroxenes (pigeonite) series. Plagioclase compositions were determined by standard Universal Stage methods. Booth (1971) presents compositions determined from optical data for augites and pigeonites from the Birds River gabbros.

The following discussion summarizes petrographic data from Eales and Booth (op.cit.) and compares them with the petrography of the gabbroic rocks exposed in the Stapelbergkloof section.

Poikilophitic Olivine Gabbro.

The dominant basic rock type of the Birds River Complex is a coarse-grained poikilophitic olivine gabbro, characterized by early olivines and small calcic plagioclase laths set in large (up to 10 mm in diameter) host pyroxene crystals. Chemically, this gabbro closely matches the Kokstad dolerite-type of Walker and Poldervaart (1949).

The gabbros from Stapelbergkloof are identical to the olivine gabbros previously described by Eales and Booth (op.cit.). Plagioclase is the dominant mineral present while pyroxenes, both augite and pigeonite, olivine, Fe-oxides and quartz and micropegmatite form the remainder of the rock. Eales and Booth (op.cit.) note that an average modal analysis of the poikilophitic olivine gabbro shows

plagioclase - 58 %
pyroxenes - 28.5 %
olivine - 4.5 %
Fe-oxides - 2.6 %
quartz and micropegmatite - 6.4 %

Augite and pigeonite are the only pyroxenes found in these coarse gabbros from Stapelbergkloof. Pigeonite, characterized by a low 2V angle of less than 10^{o} and by a slightly higher relief, often occurs as large crystals rimmed by augite. In some instances pigeonite occurs as a small core in larger augite plates. Both pigeonite and augite exhibit mutual exsolution textures in one direction only - the 001 plane, indicating that pigeonite did not invert to orthopyroxene with decreasing subsolidus temperatures. Walker and Poldervaart (1949) believe that the presence of volatiles acts as a catalyst in the preservation of pigeonite, even in slowly cooling basic magma and note that in intrusions of Kokstad-type dolerite pigeonite often replaces orthopyroxene at higher horizons. Orthopyroxene (inverted pigeonite) has, however, been described by Eales and Booth (op.cit.) but they note that it is essentially a minor constituent in the gabbros. Primary orthopyroxene is identified in the contact dolerite at Stapelbergkloof. Here it occurs as indistinct, highly fractured phenocrysts (?) together with phenocrysts of plagioclase, augite and minor, altered olivine. Microprobe data from Eales and Booth (op.cit., Table IV, No's 1,2) show quantitatively the marginal enrichment in Fe^{2+} of the large augite crystals. The variation is from $Ca_{40}\ Mg_{47}\ Fe_{12}$ in the core

to Ca_{36} Mg_{42} Fe_{22} in the marginal zones.

Olivine varies greatly in amount in the coarse-grained gabbros from Stapelbergkloof and is often degraded to greenish bowlingite. Data from Eales and Booth (op.cit., Table II, No's 1-3) indicate that the compositions of olivines vary widely and range from Mg_{74} Fe_{26} to Mg_{44} Fe_{56}.

Plagioclase compositions were determined by measuring the extinction angle of the fast ray in sections normal to the 'a' axis.

The most calcic composition noted in the Stapelbergkloof gabbros is An_{76} but plagioclase cores range between An_{65} and An_{70}. Plagioclase crystals exhibit strong zoning textures, both normal and oscillatory, and margins are zoned to as low as An_{54}. In their discussion of the unfractionated marginal facies dolerites, which differ only from the coarse gabbros in textural criteria, Eales and Booth (op.cit.) note that calcic plagioclase (An_{78}) and olivine were the first minerals to separate. They also find that the compositions of plagioclase laths included in the poikilitic augites are abruptly terminated at An_{65} to suggest the rapid growth of pyroxene while plagioclase (An_{78-65}) was separating.

Iron ores show typical late crystallization features, being essentially confined, in the gabbros, to the interstitial areas. No iron ore is included in the poikilitic augites. This confirms observations by Eales and Booth (op.cit.) that the crystallization of the poikilitic pyroxenes was effectively complete before magnetite started crystallizing. They also show by an analysis of An content of plagioclase rims in contact with magnetite, that magnetite with exsolved ilmenite started to crystallize when plagioclase An_{61} was precipitating from the magma.

The amount of interstitial micropegmatite and free quartz increases with increasing distance, inwards from the outer contact, though no quantitative modal analyses were carried out. In the more highly differentiated gabbros and ferrogabbros, the micropegmatite becomes coarsely crystalline.

In the field the poikilitic gabbros weather to a knobbly or knotty surface texture. This texture is lost in the more differentiated gabbros where the finer grain results in a more evenly weathered surface.

Pegmatitic schlieren are quite common in the gabbros from Stapelbergkloof. These occur as relatively small patches or lenses in which crystals attain lengths of several centimetres. The pegmatitic schlieren, referred to above, are however, not late-stage

products from derivative magmas. The latter as described by Eales and Booth (op.cit.), commonly occur trapped beneath large xenoliths at Birds River, where the derivative liquids "crystallized under conditions of reduced viscosity". The schlieren found in the gabbro body are commonly highly weathered and extremely difficult to sample. One sample was obtained and analysed for the trace elements Rb, Zr, Y and Sr. The concentrations of Zr (122 ppm), Sr (250 ppm), Rb (12.4 ppm) and Y (32 ppm) indicate that these schlieren are not the derivative products of magmas undergoing fractional crystallization. Rather, theyrepresent isolated pockets of normal gabbroic material that, due to special conditions, cooled at a slower rate to enable the development of the coarse textures noted.

Ferrotholeiites.

Eales and Booth (1974) and Eales and Robey (in press) propose this name for all the more highly fractionated basic rocks that show the development of a glassy, microlite-rich mesostasis. Eales and Robey (op.cit.) define the ferrotholeiites as containing between 52 and 63% SiO_2 and as consisting essentially of a fine groundmass studded with large pyroxene, olivine, plagioclase and iron oxide crystals.

The ferrotholeiites from Stapelbergkloof texturally closely resemble their counterparts from Denwood. In the Stapelbergkloof stream section, this texture is first noted in sample, S34, though as noted before no contact between the gabbros and ferrotholeiites was found.

Large euhedral to subhedral pyroxenes, plagioclase and more-ferriferous olivines as well as highly skeletal, hopper crystals of iron oxides included in the glassy mesostasis, give this rock a porphyritic texture.

The groundmass is, with some exceptions, composed of brown glass studded with small hollow plagioclase squares and laths showing typical quench textures. Microlites of pyroxene occur either as spherulitic growths or as small trails and wisps. Later crystallizing augite and olivine show skeletal, grid, dendritic and spicular textures similar to those described by Eales and Booth (op.cit.). Skeletal olivine is often degenerated to magnetite. Apatite commonly occurs as needles or prisms some 1-2 mm in length or as squarish euhedra. Apatite in some cases is noted to occur within the larger pyroxene crystals suggesting that it may have reached a cumulus status.

The pronounced zonal structure and strong curvature of some pyroxenes described by Eales and Booth (op.cit.) are also observed in the ferrotholeiites from Stapelbergkloof. These authors note that the mosaic structure of these pyroxenes when studied under crossed nicols is "strongly suggestive of inversion from a parent polymorph, as is the case of inversion of β - wollastonite to a hedenbergitic pyroxene ...".

The extreme degree of iron enrichment in these pyroxenes is illustrated by Eales and Booth (op.cit., Fig. 4). "Ferroaugite grades continuously to ferrohedenbergite, $Ca_{42}\ Mg_{6}\ Fe_{52}$". Microprobe analyses of clinopyroxenes in the ferrotholeiites are shown in Table IV (Eales and Booth, op.cit.). These authors also note that the compositions of early formed olivines vary from Fa_{55} to Fa_{70} while the dendritic crystals found in the groundmass reach a composition of at least Fa_{89}.

In the more highly differentiated ferrotholeiites from Stapelbergkloof, the groundmass texture loses its glassy appearance and becomes a coarse "eutectoid" intergrowth of feldspar, micropegmatite, quartz and pyroxene. Texturally these may resemble the dolerite pegmatite (-oidal) facies but chemically they conform to the characteristics of the ferrotholeiites.

Eales and Booth (op.cit.) discuss at length the origin of the ferrotholeiite texture. The groundmass textures "are typically produced by rapid freezing or high viscosity of melts". These authors dismiss that rapid chilling is the sole cause for this texture since the body of ferrotholeiite is simply too large to have been suddenly quenched throughout. Rather, the influence of several factors which promote high viscosity in melts are discussed and analysed. Eales and Booth (op.cit.) conclude that the loss of H_2O to the country-rock sediments, "the increase in SiO_2 and alkalies accompanying the decrease of divalent cations and a degree of undercooling, all combine to produce the characteristic (ferrotholeiite) texture".

Pegmatitic (-oidal) derivatives, granophyres, and hybrid rocks are discussed by Eales and Booth (op.cit.) but have not been studied in the present work.

To conclude, though few new petrographic data are presented in this study, the textures noted by the above-mentioned authors confirm the presence in the Stapelbergkloof section of a substantial body of fractionated ferrotholeiite. These rocks could form the basis of an interesting mineralogical investigation aided by microprobe techniques.

2.4

Major Element Variations at Birds River.

2.4.a

Introduction:

In the first detailed analysis of major-element variations within the Birds River Complex, Eales and Booth (1974, Fig.7) discerned three trends dominated by the three variables - SiO_2, total (Fe + Mg) and total alkalies.

Briefly these trends are as follows:

(a) limited data define a basalt-quartz basalt trend showing decreasing total Fe with a subdued increase in the defined mafic index.

(b) a gabbro - gabbro pegmatite (-oid) trend showing subdued Fe-enrichment and MgO depletion but strong total alkali and silica enrichment.

(c) a dominant gabbro-ferrogabbro-ferrotholeiite trend showing strong though not extreme Fe, alkali and SiO_2 enrichment with increasing differentiation.

Eales and Booth (op. cit, Fig.7, A-B) recognise the gabbro-ferrogabbro trend as being intermediate between the extremes of the Skaergaard and calc-alkaline trends but closer to the former, suggesting crystallization under slightly decreasing PO_2 conditions. The tholeiite trend of Eales and Booth (op.cit, Fig.7, C-D) which encompasses all the rocks later defined as ferrotholeiites (Eales and Robey, in press), extends the total-Fe enrichment shown by the gabbro-ferrogabbro trend. With continued differentiation within the ferrotholeiites, total-Fe decreases sharply with a strong increase in SiO_2, suggesting increasing PO_2 conditions during crystallization. The former authors feel that the restricted size of the Bird's River intrusion, the dissociation of CO_2 in the relatively CO_2-rich country rock sediments as well as high Fe^{3+}/Fe^{2+} ratios in these sediments, played an important role in sustaining relatively high PO_2 conditions.

Furthermore they show in variation diagrams of oxide concentrations versus the defined mafic index of differentiation that the iron-enriched tholeiites of the New Amalfi and Mount Arthur intrusive complexes (Walker and Poldervaart, 1949) are chemically akin to the Birds River derivatives and that "tolerably continuous curves can be constructed by plotting these data and analyses ....on one

diagram". (Eales and Booth, 1974, Fig.5).

In the present study 10 new whole-rock and partial trace element analyses of the gabbro-ferrogabbro-ferrotholeiite trend are presented. As previously mentioned these rocks were sampled along a stream section up Stapelbergkloof (Figs. 1,2) further to the west of the Denwood type-section discussed by Eales and Robey (in press).

As noted by Eales and Booth (1974) the ferrotholeiites are not to be considered the end products of in-situ fractional crystallization within the gabbro-ferrogabbros. Rather they represent an earlier pulse of highly differentiated basic liquid derived from the fractionation of a deep-seated magma body of similar type that produced the younger gabbros and ferrogabbros. These highly fractionated, derivative ferrotholeiites were intruded along the first fractures that developed during the postulated cauldron subsidence of Stormberg Group sediments into an "underlying intrusion of gabbroic magma undergoing crystallization". (Eales and Robey, op. cit.).

This section will compare differentiation within the gabbro-ferrogabbro-ferrotholeiite suite at Stapelbergkloof to that in the Denwood type-section and will show that though a similar sequence is found in the former traverse, the ferrotholeiites from Stapelbergkloof are not as highly chemically evolved as those from Denwood. Furthermore in contrast to the Denwood section (Eales and Robey, op. cit., Fig.6) no sharp discontinuity exists between the ferrotholeiites and gabbro-ferrogabbros at Stapelbergkloof, both in the field and in major- and trace-element variations. The ferrotholeiites from Stapelberg, however, are petrographically nearly identical to the ferrotholeiites described by Eales and Booth (op.cit.) and Eales and Robey (in press) and must be classified as such. A closer sampling interval may well reveal a similar discontinuity between the ferrotholeiites and ferrogabbros from Stapelbergkloof to that shown by Eales and Robey (op. cit.). Thus, though the ferrotholeiites are derived from an earlier magma source than the later gabbro-ferrogabbros, it will be shown in both major- and trace-element variation trends that they can be equated to the differentiation and fractionation of a single body of Kokstad-type Karroo dolerite magma.

Molar ratio diagrams (Pearce, 1970) have been constructed to qualitatively define mineralogical control in the fractional crystallization sequence. These diagrams, though they are not shown, indicate that through most of the gabbro-ferrogabbro-

ferrotholeiite trend, the fractional crystallization of plagioclase, pyroxene and olivine dominated while in the more highly evolved ferrotholeiites some apatite and iron-oxide fractionation may have occurred.

A later section will deal with trace element variations in the differentiated sequence at Stapelbergkloof while the final section will be a discussion of a simple, computer-generated, fractional crystallization model which quantitatively attempts to show that both major- and some trace-element variations in the differentiated sequence at Stapelbergkloof, can be explained in terms of dominant plagioclase and pyroxene fractionation. This contradicts the view of Eales and Booth (1974) that olivine-rich gabbros underlie the Birds River Complex. Rather, a body of normal Kokstad-type gabbro, slightly feldspathic, is believed to occur at depth underneath the Birds River Complex.

2.4.b

MgO Variation Diagrams: Stapelbergkloof and Denwood - Birds River.

In accordance with Wright (1974) and Cox et al. (1967), MgO percent has been selected as a simple index of fractionation. MgO satisfies all the criteria that govern the choice of the abscissa in oxide variation diagrams of differentiated basic rock suites, having in the rocks studied, a reasonable range of values as well as decreasing steadily with increasing differentiation. The choice of MgO percent as an index of fractionation, however, is inappropriate for the very late stages of differentiation i.e. within the more highly evolved ferrotholeiites, and here an index as used by Eales and Booth (op.cit) defined as $\frac{FeO + Fe_2O_3}{FeO + Fe_2O_3 + MgO} + \frac{K_2O}{K_2O + Na_2O}$, would be better. However, since in the present study all Fe was determined as Fe_2O_3, the above index could not be used and consequently MgO percent is used throughout as the index of differentiation.

Figs. 3(a-h) show the variation of all the major oxides plotted against MgO %. All data are recalculated water-free and data from Eales and Robey (in press) for Denwood, have been recalculated to express total Fe as Fe_2O_3 for direct comparison with the new analyses from Stapelbergkloof. Symbols indicating different rock types are as defined in the caption to Figs.3(a-h) and apply throughout the discussion of the Birds River Complex. Table 1(a)

lists the major- (hydrous) and trace-element concentrations of the new samples from Stapelbergkloof, while anhydrous values are shown in Appendix 1. Data from Denwood are shown in Table 1(b).

From Figs.3(a-h) MgO is seen to decrease from 8.4% in an olivine-rich gabbro to .7% in the most highly differentiated ferrotholeiite. These are the extremes determined by Eales and Booth (1974) and the new analyses from Stapelbergkloof fall within this range.

K_2O and SiO_2 are progressively enriched to values of 3.46% and 65.8% respectively, a slight steepening of slope being evident for both elements at MgO less than 2%. (Figs.3 a,f).

Fe_2O_3 increases steadily from an average near 11% in the gabbros to a peak of 16.8% in the ferrotholeiites, but then rapidly decreases to near 10% in the most highly evolved ferrotholeiites. (Fig.3d). TiO_2 behaves similarly though peaks at a slightly earlier stage than Fe_2O_3. (Fig. 3b). CaO and Al_2O_3 decrease steadily throughout the differentiated sequence (Figs. 3c,e) and suggest plagioclase fractionation.

In the Stapelbergkloof sequence, P_2O_5 (Fig. 3h) increases from .13% in a feldspathic gabbro to a maximum of .65% in the ferrotholeiites. Data from Denwood (Eales and Booth, 1974) show P_2O_5 to increase to a well-defined peak at .8%, after which, with continued differentiation, P_2O_5 is rapidly depleted to values as low as .17%. This late sharp decrease in P_2O_5 is not noted in the Stapelbergkloof ferrotholeiites and confirms the view that these ferrotholeiites are not as highly differentiated as similar rock types from Denwood.

The relatively low Al_2O_3 content of the Denwood ferrotholeiites (generally less than 12%) as determined by Eales and Booth (op. cit.) is only matched by the more highly differentiated ferrotholeiites from Stapelbergkloof (S39, S43, S45 - Appendix 1, Fig. 3c) while the remaining ferrotholeiites from Stapelbergkloof are slightly enriched in Al_2O_3 relative to those from Denwood. The former extend the steady decrease of Al_2O_3 seen in the gabbro-ferrogabbro trend.

The variation of Na_2O (Fig. 3g) is difficult to interpret. The general trend is for a steady increase from variable but low values in the gabbros to near 3.5% in the ferrotholeiites. Three ferrotholeiites, two from Stapelbergkloof (S39, S43, Appendix 1) and one from Denwood (Eales and Booth, op.cit.Table V, No.4) have slightly depleted Na_2O% relative to ferrotholeiites with similar

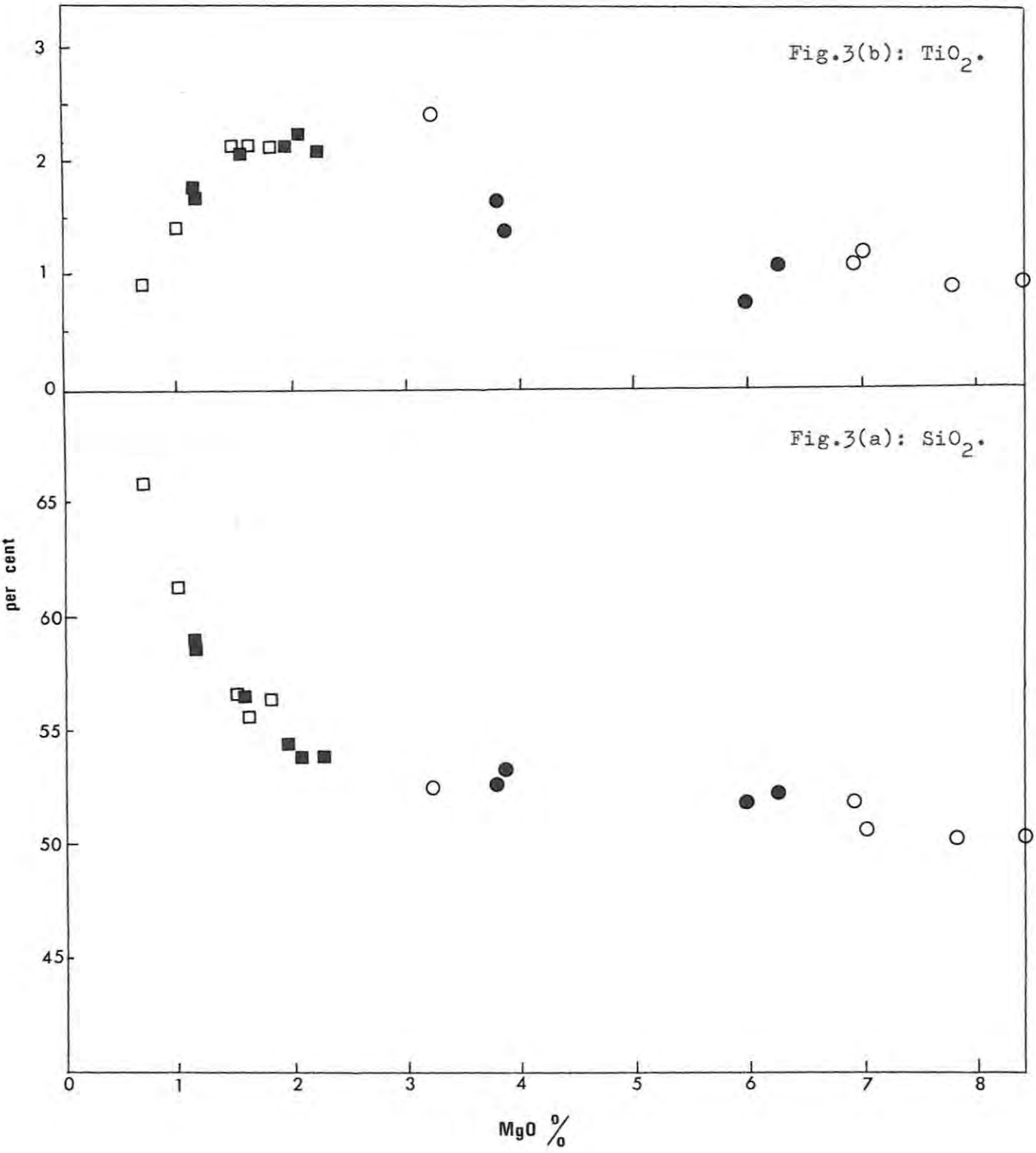

Figs. 3(a-h): Major element data (oxides) for the fractionated sequence at Birds River, plotted against MgO% the index of fractionation.

- ● Gabbro-ferrogabbro
- ■ Ferrotholeiite

– Stapelbergkloof : Table 1(a).

- ○ Gabbro-ferrogabbro
- □ Ferrotholeiites

– in part from Denwood (Eales and Booth, 1974, Tables III,V): see also Table 1(b).

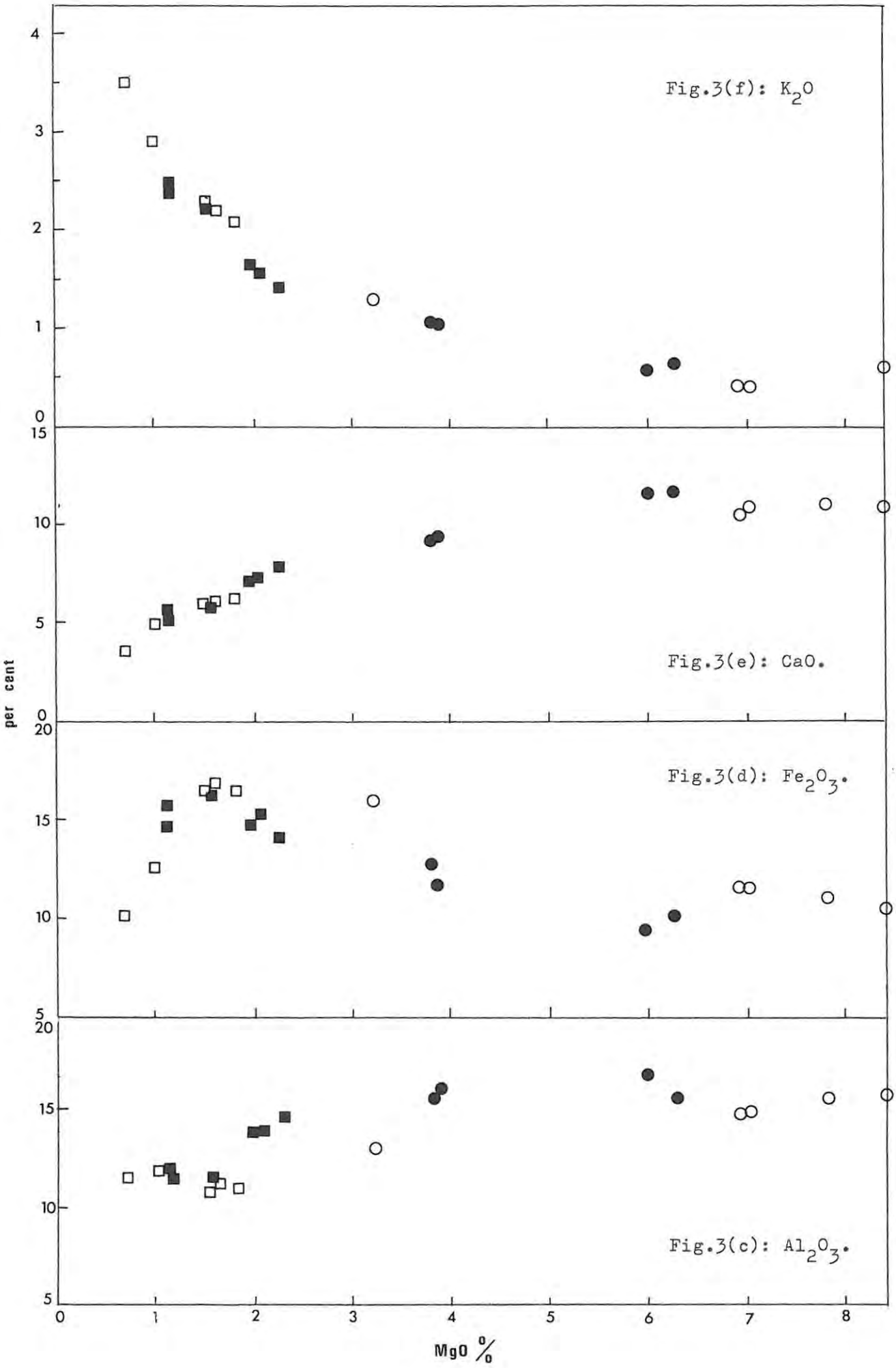
Fig.3(f): K_2O
Fig.3(e): CaO.
Fig.3(d): Fe_2O_3.
Fig.3(c): Al_2O_3.
per cent
MgO %

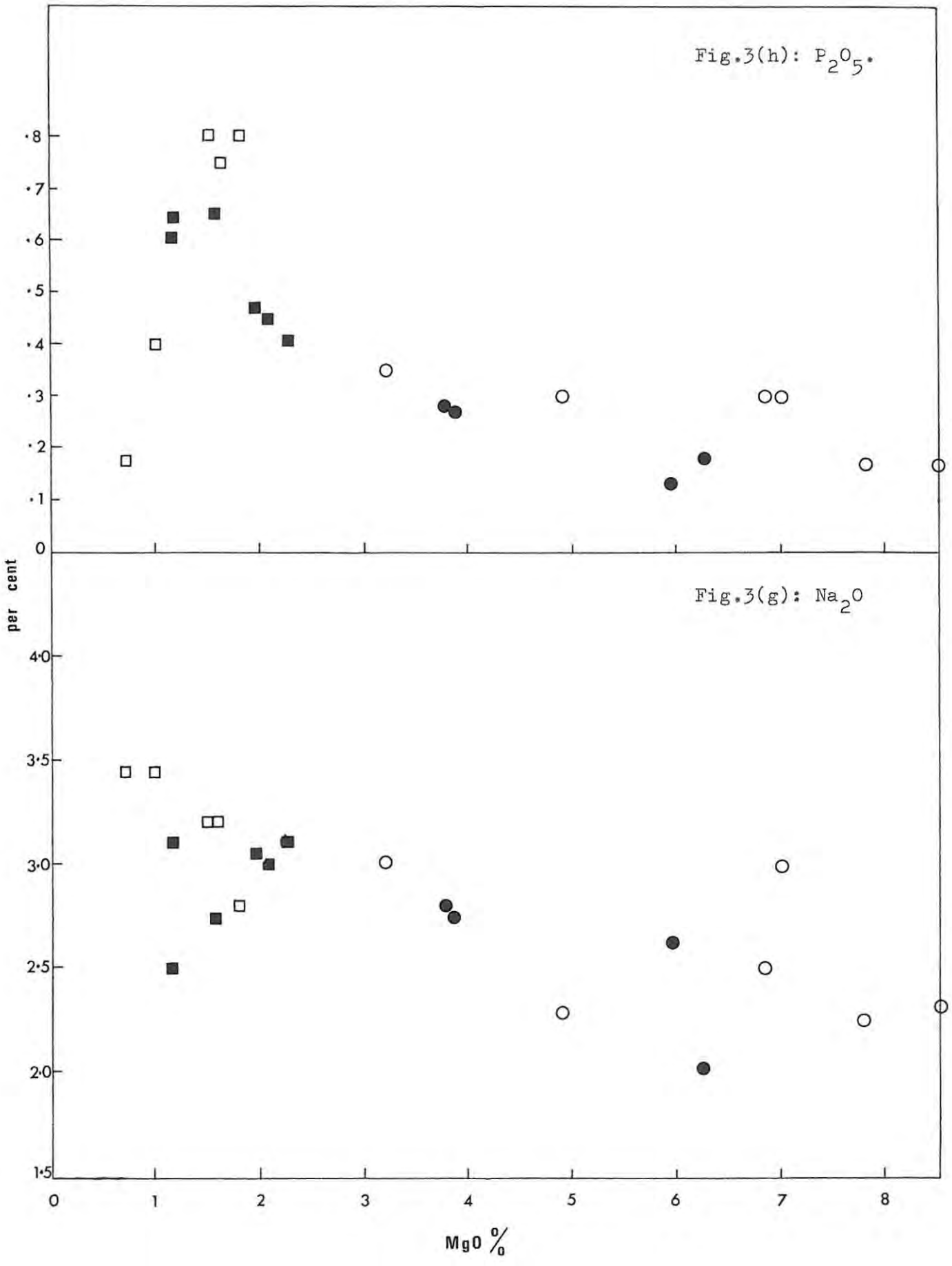
Fig.3(h): P_2O_5.
·8
·7
·6
·5
·4
·3
·2
·1
0
Fig.3(g): Na_2O
per cent
4·0
3·5
3·0
2·5
2·0
1·5
0
1
2
3
4
5
6
7
8
MgO %

MgO content and furthermore appear to plot on a trend of decreasing Na_2O% with increasing differentiation. A significant feature of these relatively Na_2O-depleted ferrotholeiites is that the groundmass in every case is coarsely crystalline and different from the glassy groundmass normally found in the ferrotholeiites. This may indicate a slower rate of cooling and the expulsion of any excess Na_2O in late-residual fractions as opposed to the trapping of any excess alkalies in the rapidly chilled, normal ferrotholeiites with glassy textures.

2.4.c

Molar Ratio Analysis:

Following the method of Pearce (1968,1970) molar ratio diagrams were constructed in an attempt to evaluate the control of fractionating phases in the gabbro-ferrogabbro-ferrotholeiite variation at Stapelbergkloof.

K_2O was chosen as the constant divisor since plagioclase and possibly late-stage TiO_2-bearing magnetite fractionation within the ferrotholeiites is suspected from the study of MgO variation diagrams. This precludes the use of either Al_2O_3 or TiO_2 as the constant divisor. K_2O increases steadily with differentiation reflecting its residual nature. Molar ratios normalized to K_2O were plotted against the ratio SiO_2/K_2O. These diagrams, with the exception of TiO_2 and P_2O_5, are however not shown but the following significant points arise from a study of these diagrams.

(a) Analyses tend to fall on smooth trends with little scatter. The use of a numerically small divisor such as K_2O invites criticism in that accuracy of determination is critical. The small degree of scatter, however, appears to confirm the accuracy of the determinations.

(b) Slopes of MgO, Al_2O_3 and CaO suggest that all three phases - plagioclase, pyroxene and olivine - were involved in fractional crystallization processes. Calculated slopes are very much lower than would be expected if any of the above phases, alone, had been involved. The positive Al_2O_3 slope indicates definite plagioclase removal from the crystallizing magma source.

(c) The TiO_2/K_2O and P_2O_5/K_2O plots are worth examining and are shown in Figs. 4 (a,b). In a basaltic system fractionating olivine, plagioclase and pyroxene, neither TiO_2 nor P_2O_5 is strongly

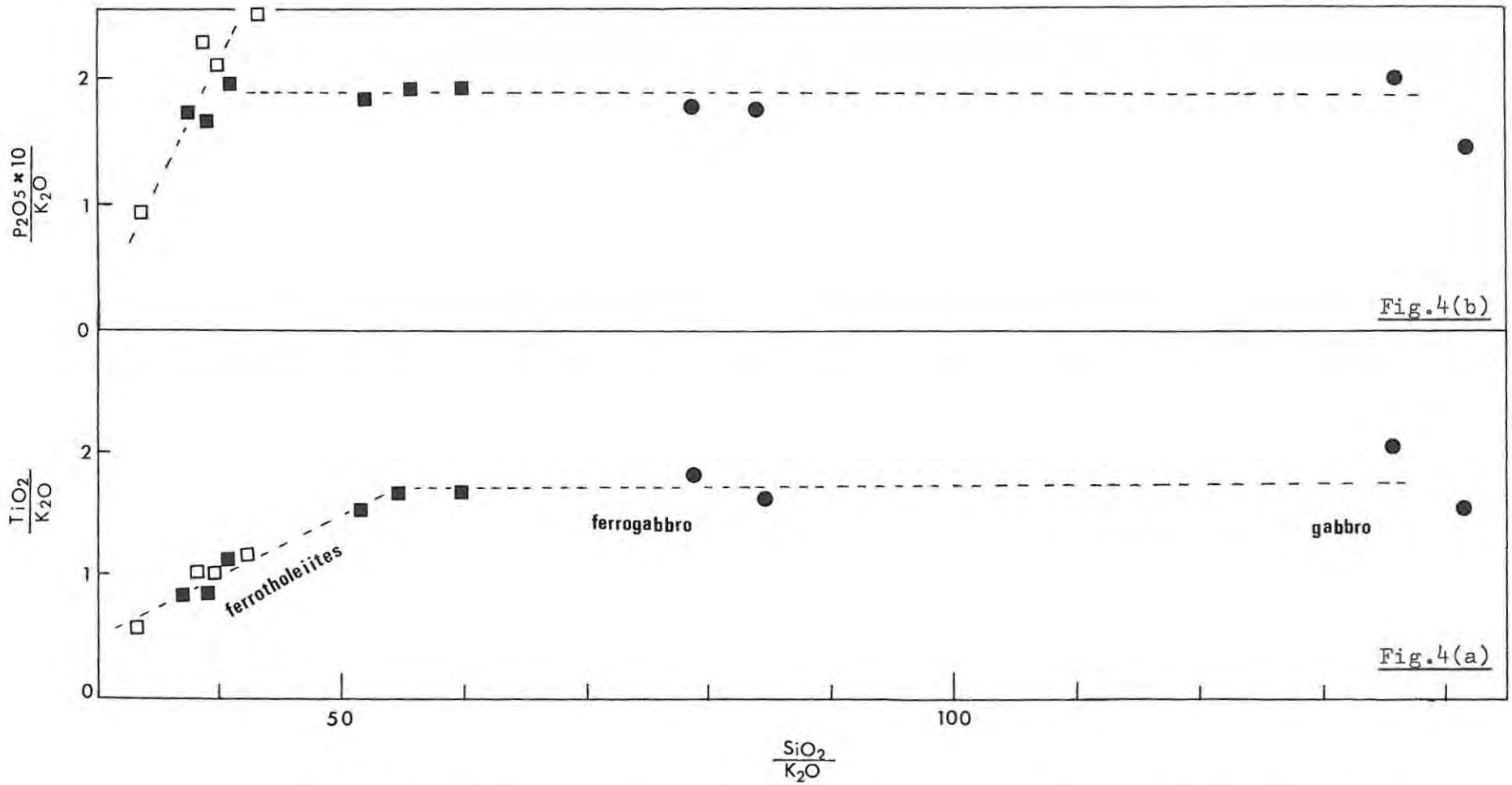

Figs. 4(a,b): Molar ratio diagrams for SiO_2, TiO_2 and P_2O_5, normalized to K_2O. These diagrams suggest that Ti-magnetite and apatite were only effectively fractionated from the Birds River magma at a very late stage of differentiation.

● Gabbro to ferrogabbro
■ Ferrotholeiites
} - Stapelbergkloof. Table 1(a).

□ Ferrotholeiites - Eales and Booth (1974, Table V).

partitioned into any of the above phases. Since K_2O is likewise concentrated in the residual liquid, the ratios TiO_2/K_2O and P_2O_5/K_2O should remain constant (i.e. have a slope of zero) until such a stage that a phase that selectively partitions TiO_2, P_2O_5 or K_2O separates from the magma. Minor amounts of TiO_2 (0.8%) are found in augites in the gabbros and ferrogabbros from Denwood (Eales and Booth, 1974, Table IV) but this is not considered too important in significantly altering the TiO_2/K_2O ratio during augite fractionation. Fig.4(a) shows the ratio TiO_2/K_2O remains constant for most of the gabbro-ferrotholeiite sequence, though decreasing significantly in the more highly differentiated ferrotholeiites from both Stapelbergkloof and Denwood. Fig.4(b) indicates that the ratio P_2O_5/K_2O also remains constant till a late stage of differentiation, after which it decreases in a manner similar to the ratio TiO_2/K_2O.

Assuming that K_2O is not depleted by the removal of a K_2O-rich phase such as alkali feldspar, these two trends suggest the late stage fractionation of a TiO_2-rich iron oxide and apatite respectively. It furthermore confirms the early crystallization features of both magnetite and apatite seen in the ferrotholeiites where both minerals form distinct euhedra. Eales and Robey (in press) note that in the ferrotholeiites apatite occurs as phenocrysts suggesting that within these quenched derivatives apatite had attained the status of a cumulus phase. The stability of the ratio TiO_2/K_2O in some less-evolved ferrotholeiites from Stapelbergkloof suggests little or no magnetite fractionation at depth while the change in this ratio in the more highly differentiated ferrotholeiites may be due to the precipitation of TiO_2-rich magnetite, as these residual liquids encountered highly oxidizing conditions during the initial emplacement episode.

Lastly, data from the Palisades sill (Pearce, 1970) were recalculated and normalized to K_2O to evaluate the method described above and to allow a direct comparison of differentiation in the Palisades sill with that at Birds River. Pearce (op.cit.), using Al_2O_3 as the constant divisor in this molar ratio method, indicates major olivine and augite, but little plagioclase fractionation within the Palisades intrusion. Using K_2O as the constant divisor, the olivine and augite fractionation trends are confirmed. Later differentiates, however, plot on a positive Al_2O_3/K_2O slope to suggest some plagioclase fractionation. This is opposite to the conclusion reached by Pearce (op.cit.).

Furthermore, certain quartz diabases (Pearce op.cit., Table 1, No's 17

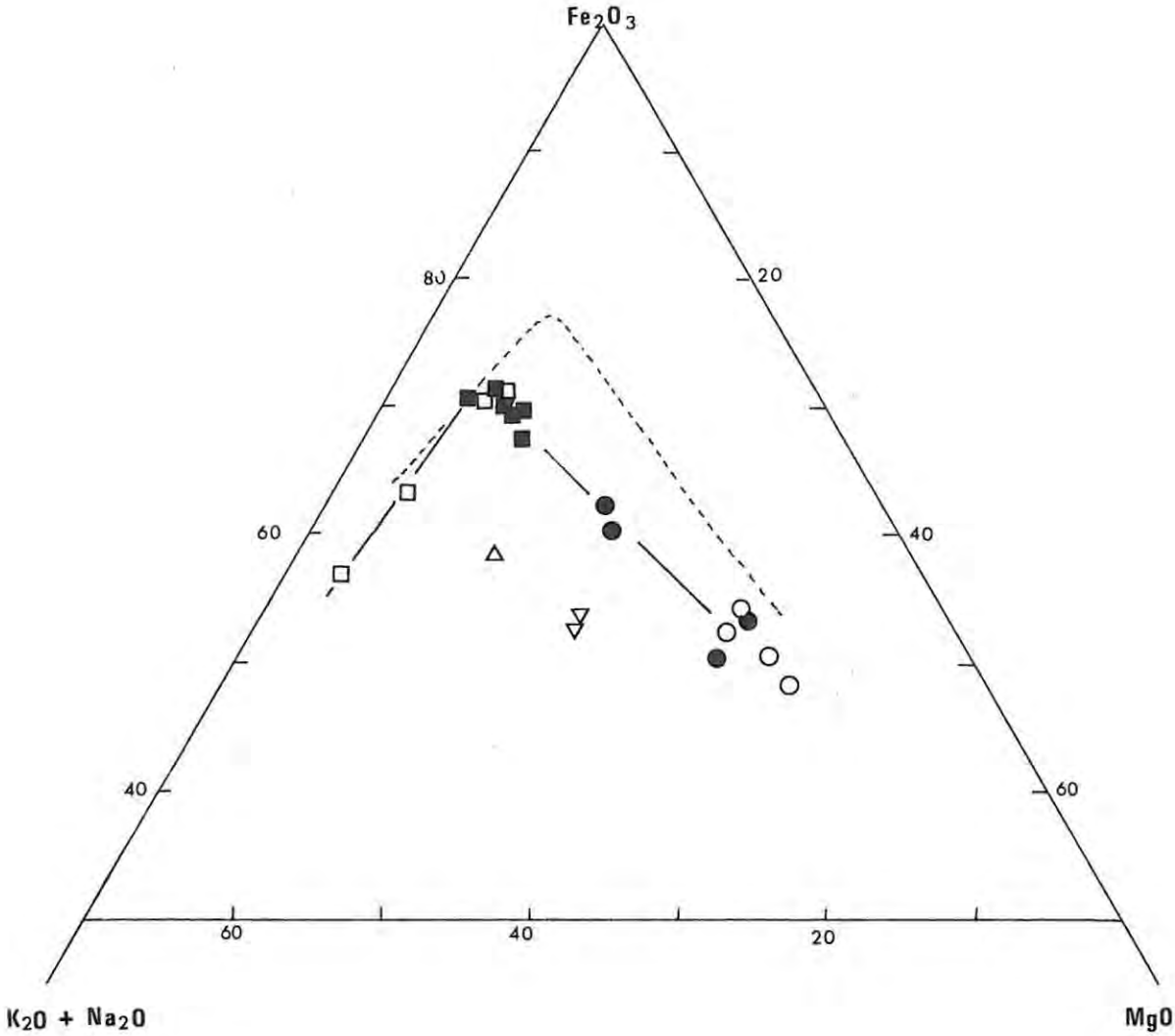

Fig.5: Strong iron enrichment seen at Birds River (_____), though moderate when compared with the iron enrichment trend for New Amalfi and Elephant's Head (-----). The dolerite pegmatites (▽) and granophyre (△) from Birds River are enriched in total alkalies relative to the dominant gabbro-ferrotholeiite trend.

● Gabbro to ferrogabbro
■ Ferrotholeiites
} — Stapelbergkloof. Table 1(a).

○ Gabbros. - Eales and Booth (1974, Table III, No's 1,2,4,5).

□ Tholeiites (ferrotholeiites) - Eales and Booth (op.cit., Table V, No's 3, 4, 6, 7).

▽ Dolerite pegmatite. - Eales and Booth (op.cit., Table III, No's 6, 7).

△ Granophyre. - Eales and Booth (op.cit., Table V, No. 9).

Data for Elephants Head and New Amalfi are from Walker and Poldervaart (1949, Table 15).

Analyses are water-free and total Fe is expressed as Fe_2O_3.

18, 27) that fall far off any of the trends defined by Pearce (1970) in his Al_2O_3-normalized plots and which are dismissed as being anomalous, plot almost exactly on the trend of the late-stage ferrogabbros and ferrotholeiites from Birds River. It can only be assumed that Pearce (1970) erred in his selection of Al_2O_3 as a constant divisor and that some plagioclase may well have fractionated from the Palisades magma.

2.4.d

Iron-enrichment at Birds River.

The strong total-Fe_2O_3 enrichment relative to MgO and total alkalies for the Stapelbergkloof sequence is shown in Fig.5 and matches the enrichment noted by Eales and Booth (1974) for the Denwood sequence, though in the latter, the more highly differentiated ferrotholeiites show the very late-stage relative enrichment of total alkalies characteristic of differentiated tholeiitic suites. This stage of enrichment in total alkalies is not reached in the Stapelbergkloof ferrotholeiites.

2.4.e

Conclusions.

Though the two sets of data presented in Tables 1 (a,b) represent analyses of the gabbro-ferrotholeiite suite sampled along two different traverses at Birds River and also analyses performed in different laboratories, the major element variation trends are nearly identical. Data from Stapelbergkloof therefore confirm the highly differentiated character of the residual rocks found at Birds River and first noted by Eales and Booth (1974).

The ferrotholeiites from Denwood are chemically more highly evolved than those from Stapelbergkloof, the latter bridging the gap between ferrogabbros and ferrotholeiites in terms of major element compositions. Though the ferrogabbros are considered in-situ differentiates of the younger gabbro and the ferrotholeiites, early-emplaced derivates from an older magma pulse (Eales and Booth, op. cit., Eales and Robey, in press), the various rock types form a continuous variation series, to suggest that the ferrotholeiites are derived from a similar parent to that of the younger gabbro.

Variation diagrams qualitatively suggest that through most of the differentiation sequence at Birds River, the crystallization

and removal of plagioclase, olivine and pyroxene and possibly the very late-stage fractionation of TiO_2-rich magnetite and apatite controlled major-element variation trends.

The similarities in the major-element variations of the Birds River Complex and other well known differentiated basic intrusions such as the Red Hill dyke (Mc Dougall, 1962), the Palisades (Walker, 1970) and Dillsburg sills (Hotz, 1953) and other differentiated Karroo-age dolerite intrusions has already been commented on in detail by Eales and Booth (1974, Table VI) and Eales and Robey (in press, Table 2, Fig.3).

Table 1a : Major and Trace Element Analyses - BIRDS RIVER COMPLEX.

STAPELBERGKLOOF TRAVERSE. (see Appendix 1).

	JR27	S30	S31	S32	S34	S25	S37	S39	S43	S45
SiO_2	51.24	52.07	52.64	52.63	53.51	53.65	54.34	57.17	55.35	57.03
TiO_2	1.04	.76	1.62	1.35	2.01	2.18	2.09	1.69	2.03	1.66
Al_2O_3	15.35	17.06	15.66	16.15	14.84	13.94	13.87	11.64	11.33	11.29
Fe_2O_3*	10.02	9.42	12.75	11.57	13.95	15.19	14.62	14.32	15.81	15.44
MnO	.19	.16	.19	.18	.19	.20	.20	.20	.22	.22
MgO	6.15	6.01	3.8	3.83	2.25	2.06	1.93	1.10	1.51	1.13
CaO	11.53	11.64	9.15	9.27	7.80	7.25	7.12	5.41	5.62	5.09
Na_2O	1.99	2.65	2.81	2.72	3.09	2.99	3.02	2.51	2.67	3.03
K_2O	.60	.58	1.06	.99	1.40	1.55	1.63	2.31	2.14	2.41
P_2O_5	.18	.13	.28	.26	.40	.44	.46	.58	.63	.63
L.O.I.	1.44	.36	.58	.63	.33	.46	.41	1.59	1.26	.76
H_2O^+	.19	.21	.28	.37	.68	.69	.87	1.42	1.46	.99
TOTAL	99.92	101.05	100.82	99.95	100.45	100.60	100.56	99.94	100.03	99.68
					p p m					
Ba	225	182	322	308	458	462	470	593	599	620
Sr	257	294	266	265	250	232	235	183	192	177
Rb	11.5	8.6	21.8	20.6	29.5	30.7	31.0	51.7	45.2	50
Y	24.2	19.0	32.4	29.6	42.0	45.5	47.1	67	62	67
Zr	96	67	137	127	196	224	228	339	316	358
Nb	9.3	5.4	15.2	12.6	22.1	24.8	26.1	30.6	29.2	34.5
Zn	91	61	89	85	98	112	110	140	140	156
Cu	71	68	131	120	168	165	147	60	98	61
Co	43.0	33.8	28.7	27.3	26.2	26.6	27.0	15.2	21.8	14.8
Ni	89	39.3	16.7	16.8	5.6	9.2	10.5	n.d.	n.d.	3.3
V	238	211	234	209	215	214	138	10.9	42.7	n.d.
Cr	235	72	25.1	19.5	15.1	9.8	12.0	12.3	16.6	6.5

* All Fe as Fe_2O_3

n.d. Concentration below L.L.D. (see Appendix 4)

JR27 Chilled, contact gabbro

S30-S32 Gabbro to ferrogabbro

S34-S45 Fractionated ferrotholeiites, mostly with glassy groundmass.

Table 1b : Major and Partial Trace Element Analyses [+]- BIRDS RIVER COMPLEX.

DENWOOD TRAVERSE.

	1	2	3	4	5	6	7
SiO_2	50.3	50.1	52.5	52.5	56.0	61.2	65.8
TiO_2	.9	.9	1.4	2.4	2.1	1.4	.9
Al_2O_3	15.8	15.7	17.1	13.3	11.6	12.0	11.7
Fe_2O_3*	10.4	11.1	10.7	15.9	16.8	12.6	10.1
MnO	.2	.2	.1	.2	.2	.2	.2
MgO	8.4	7.8	4.9	3.2	2.4	1.0	.7
CaO	10.9	11.0	10.0	7.7	5.1	4.8	3.5
Na_2O	2.32	2.25	2.28	3.01	2.85	3.44	3.46
K_2O	.62	.70	.77	1.35	2.22	2.89	3.46
P_2O_5	.17	.17	.30	.35	.84	.40	.17
Norm. Plag.	An59	An61	An58	An41	An32	An23	An16
K_2O / Na_2O	.267	.311	.338	.449	.779	.840	1.00
			p p m				
Sr	251	267	271	247	174	189	151
Rb	13	12	17	24	45	59	75
Y	21	23	29	45	77	78	86
Zr	69	75	107	184	326	401	482

\+ Data from Eales and Robey (in press.)

* Total Fe recalculated as Fe_2O_3 for direct comparison to Appendix 1 Analyses recalculated H_2O- and CO_2- free.

1-2 Poikilophitic olivine gabbro

3 Feldspathic olivine gabbro

4 Ferrogabbro with interstitial mesostasis

5-7 Fractionated ferrotholeiite suite, in part glassy.

Table 2 : C.I.P.W. Weight Percent Norms* : BIRDS RIVER COMPLEX.

STAPELBERGKLOOF TRAVERSE

	JR 27	S30	S31	S32	S34	S25	S37	S39	S43	S45
Ap.	.44	.29	.69	.64	.97	1.09	1.12	1.44	1.56	1.54
Ilm.	2.00	1.43	3.08	2.60	3.84	4.19	4.03	3.31	3.98	3.22
Or.	3.60	3.40	6.32	6.00	8.42	9.34	9.87	14.24	13.06	14.74
Ab.	17.52	22.51	24.03	23.52	26.57	25.72	26.19	22.21	23.52	26.53
An.	32.05	33.06	27.32	29.52	22.90	20.42	20.00	14.30	13.22	10.45
Mt.	2.25	2.10	2.85	2.61	3.14	3.43	3.32	3.30	3.64	3.53
En. (Di.)	5.86	5.56	2.84	2.78	1.64	1.40	1.36	.65	.92	.73
Fs. (Di.)	4.38	4.12	4.20	3.75	4.38	4.43	4.44	3.78	4.17	4.47
Wo. (Di.)	10.64	10.06	6.99	6.53	5.75	5.53	5.48	4.09	4.73	4.77
En. (Hyp.)	9.85	9.44	6.73	6.96	4.04	3.83	3.56	2.23	3.04	2.20
Fs. (Hyp.)	7.37	6.99	9.94	9.41	10.80	12.07	11.58	12.83	13.81	13.55
Qtz.	4.29	1.05	5.05	5.74	7.56	8.61	9.11	17.66	14.37	14.31
Norm.Plag.	An 64.7	An 59.5	An 53.2	An 55.7	An 46.3	An 44.3	An 43.3	An 39.2	An 36.0	An 28.3

* Oxidation ratio calculated as $\frac{Fe_2O_3}{FeO} = 0.2$

Ap. - Apatite
Ilm. - Ilmenite
Or. - Orthoclase
Ab. - Albite
An. - Anorthite
Mt. - Magnetite
En. - Enstatite
Fs. - Ferrosilite
Di. - Diopside
Wo. - Wollastonite
Hyp. - Hypersthene
Qtz. - Quartz.
Fo. - Forsterite
Fa. - Fayalite
Ol. - Olivine.

2.5
Trace Element Variations at Birds River.

2.5.a
Introduction.

Eales and Robey (in press, Table 1) report the first partial trace element analyses for representative rock types from the Birds River Complex. Rb, Sr, Zr and Y whole-rock concentrations were determined and trace element variations with differentiation and across intrusive contacts in the Denwood type-section are discussed and shown in Figs. 2,3 and 6 in the above-mentioned work.

The present study reports new determinations for eleven trace elements - Ba, Sr, Rb, Zr, Y, Nb, Zn, Cu, Co, Ni, V and Cr - for ten samples from Stapelbergkloof (Table 1(a)). This confirms trends noted by Eales and Robey (op. cit.) but also analyses the behaviour of additional trace elements not previously determined. In this study no trace element analyses of mineral separates were undertaken but some data are available from Eales and Robey (op. cit., Table 3).

Differentiation of tholeiitic magma at Birds River resulted in a progressive enrichment of Nb, Zr, Y, Rb, Ba and Zn to levels that reach a maximum in the ferrotholeiite suite. Sr and Co are gradually depleted while V remains relatively constant, only decreasing rapidly in the late-stage ferrotholeiites. Cr and Ni, relatively enriched in the chill-zone gabbro, are quickly depleted with increasing differentiation, the former stabilizing to a near constant low average of 14 ppm through most of the late stages of differentiation. Ni behaves similarly but is reduced to values below the lower limit of determination in the most highly differentiated ferrotholeiites.

K/Rb and Zr/Nb ratios are variable but average near 400 and 10 respectively, while the ratios K/Y, Zr/Y, Rb/Sr, Ba/Sr, K/Sr and K/Ba are less variable and increase steadily with increasing differentiation. Ca/Y, Ni/Co and Cr/Ni ratios generally decrease with increasing differentiation though the latter ratio varies quite considerably.

Partial trace element data for the gabbro-ferrotholeiite suite from Denwood are from Eales and Robey (op. cit.) and are shown in Table 1(b). Data for Stapelbergkloof are tabulated in Table 1(a) and shown in MgO-variation diagrams in Figs. 6(a-l). The variation of selected inter-element ratios with increasing differentiation in the Stapelbergkloof section is shown in Figs. 7(a-j), while the range of values for these ratios is compared and contrasted with data

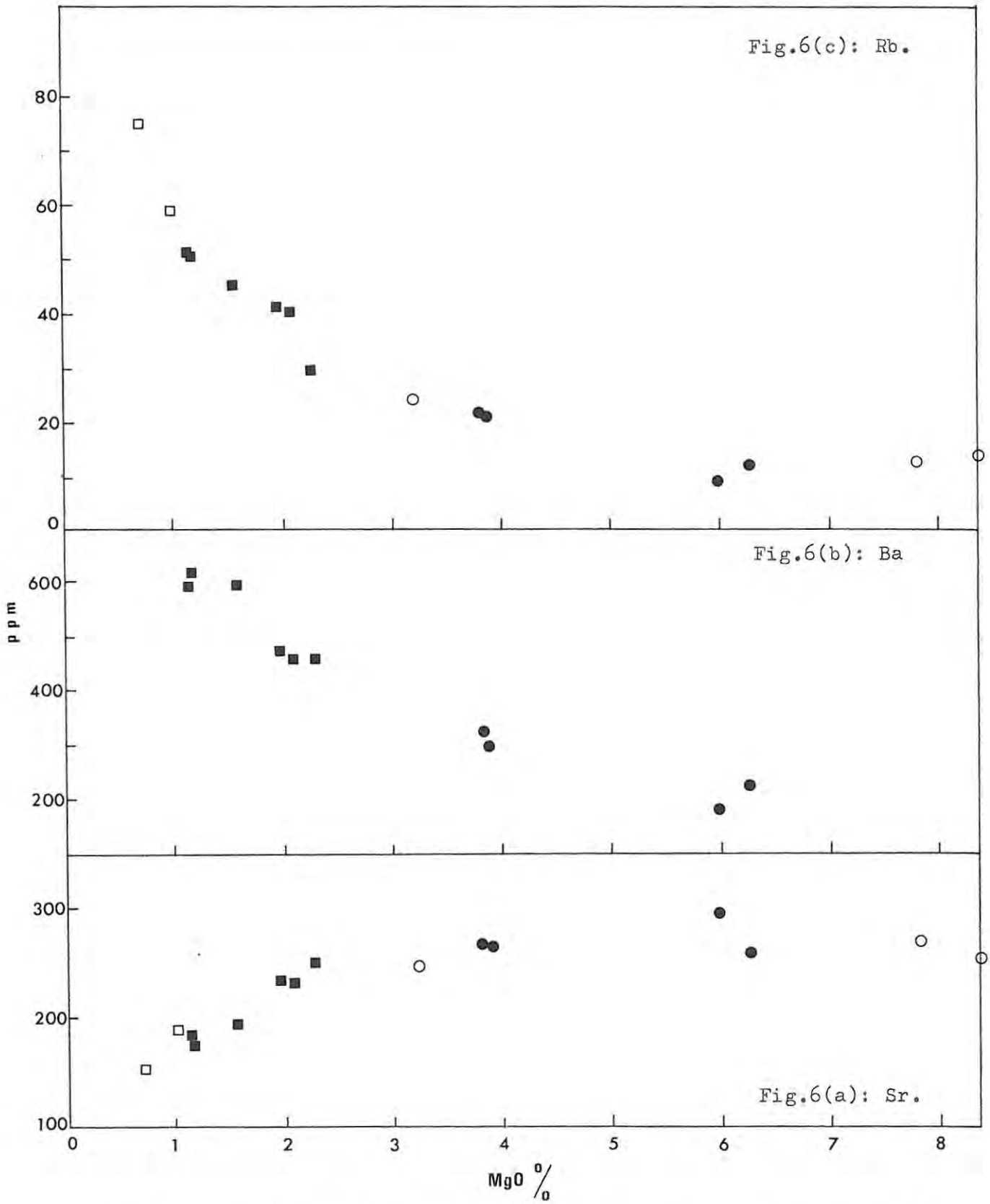

Figs.6(a-l): Trace element variations with differentiation of Birds River. Data plotted against MgO%, the index of fractionation.

- ● Gabbro-ferrogabbro
- ■ Ferrotholeiite

} – Stapelbergkloof : Table 1(a).

- ○ Gabbro-ferrogabbro
- □ Ferrotholeiite

} – Denwood : Table 1(b).

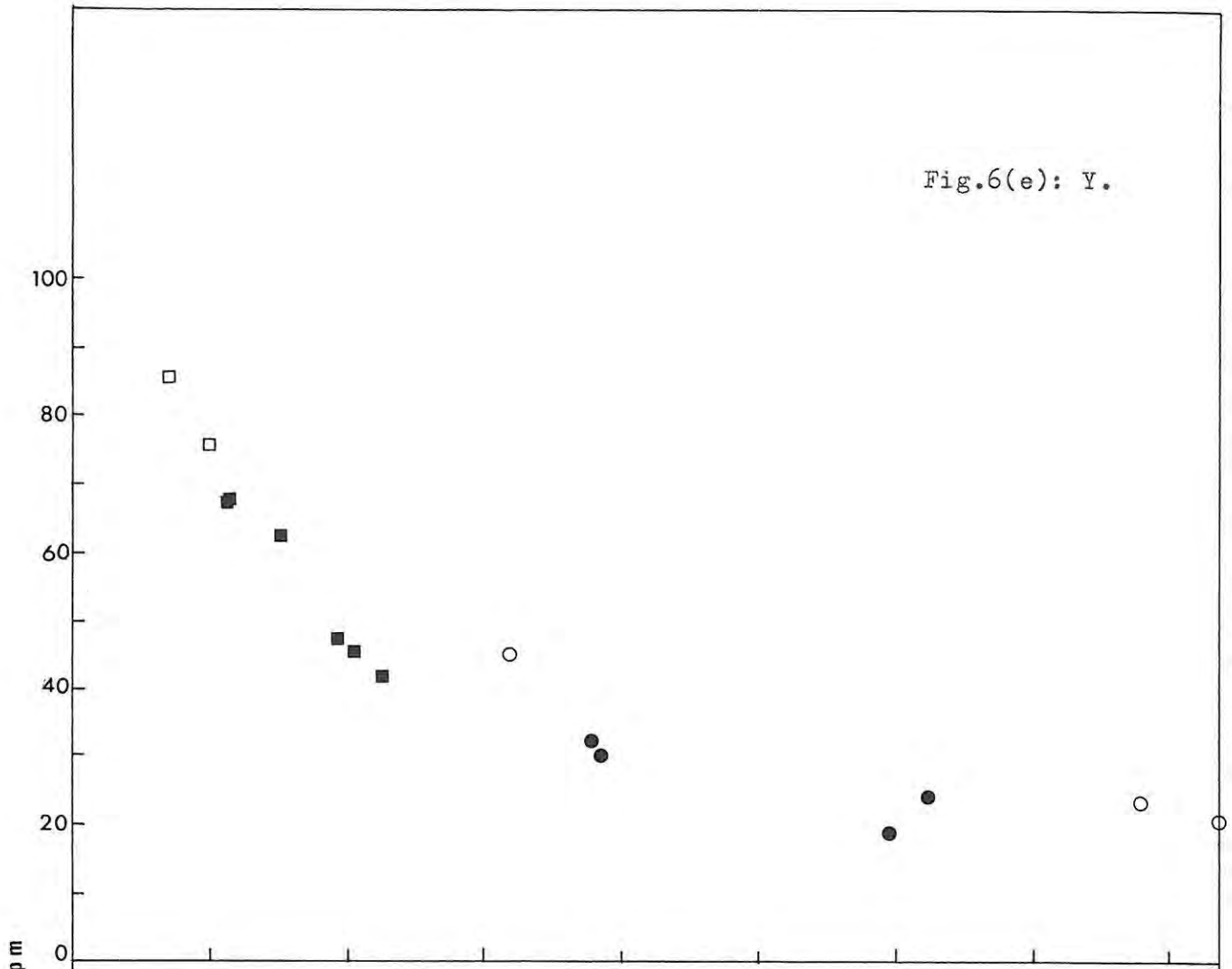

Fig.6(e): Y.

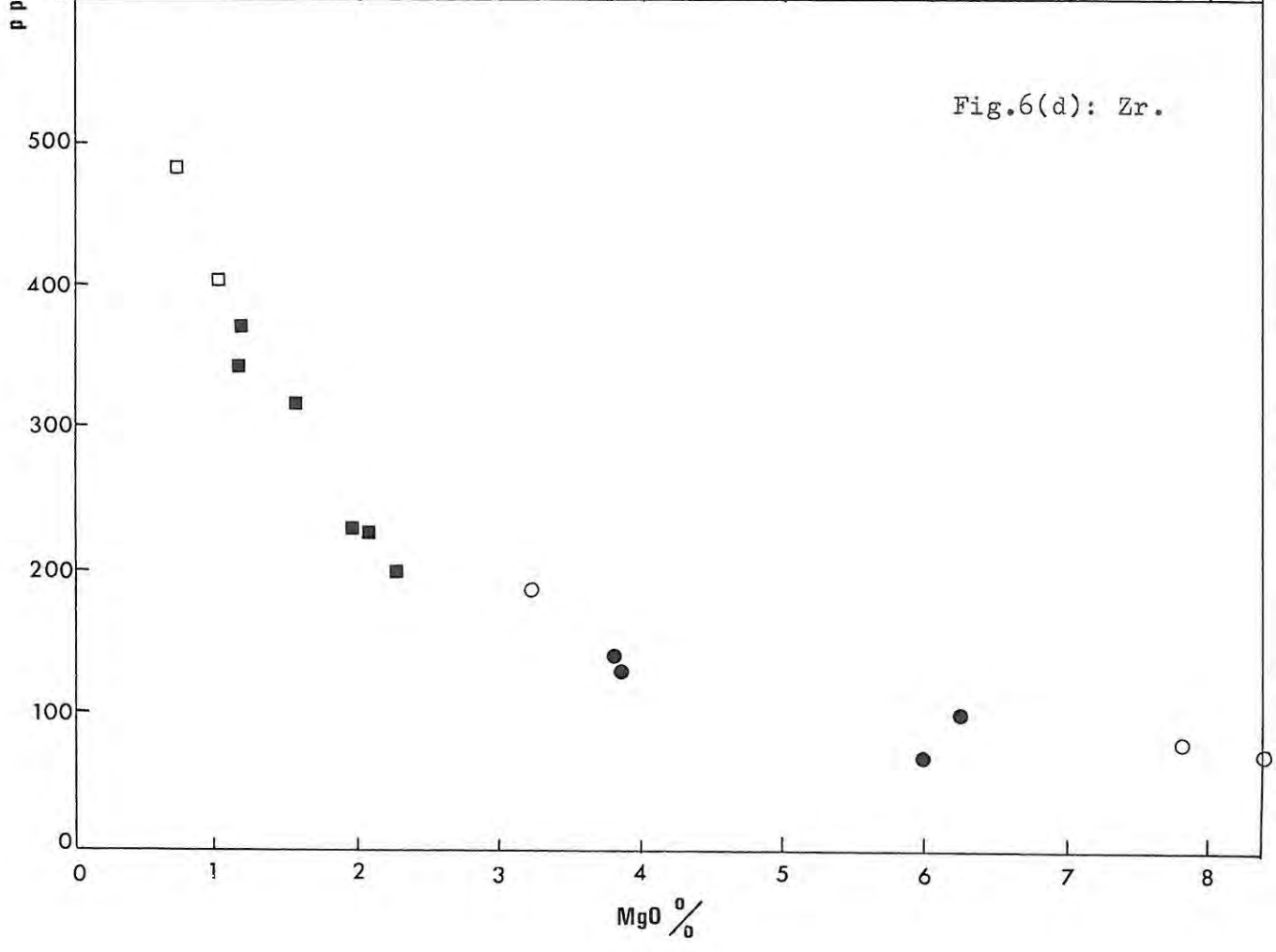

Fig.6(d): Zr.

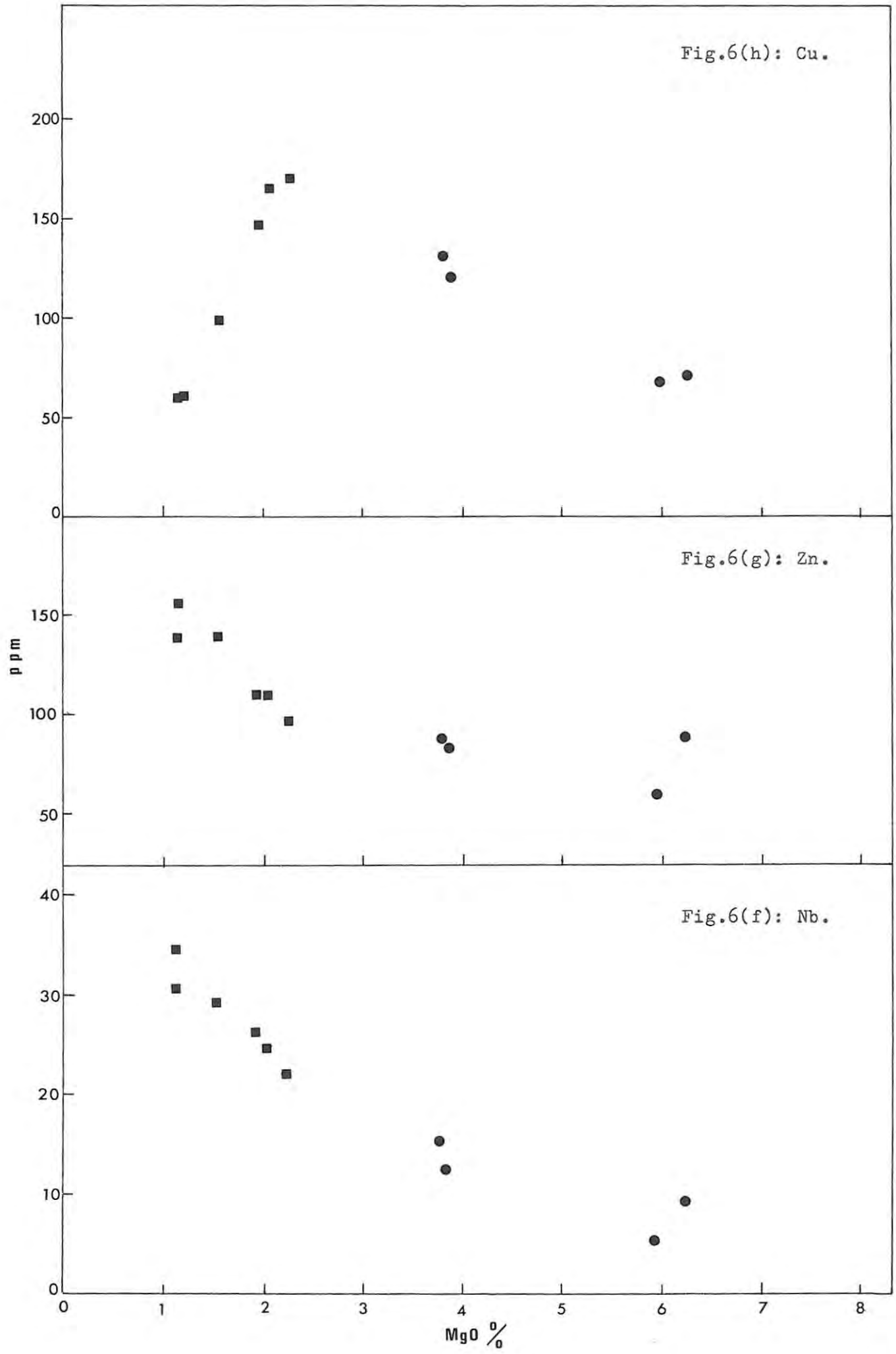
Fig.6(h): Cu.
Fig.6(g): Zn.
Fig.6(f): Nb.
ppm
MgO %
0
50
100
150
200
10
20
30
40
1
2
3
4
5
6
7
8

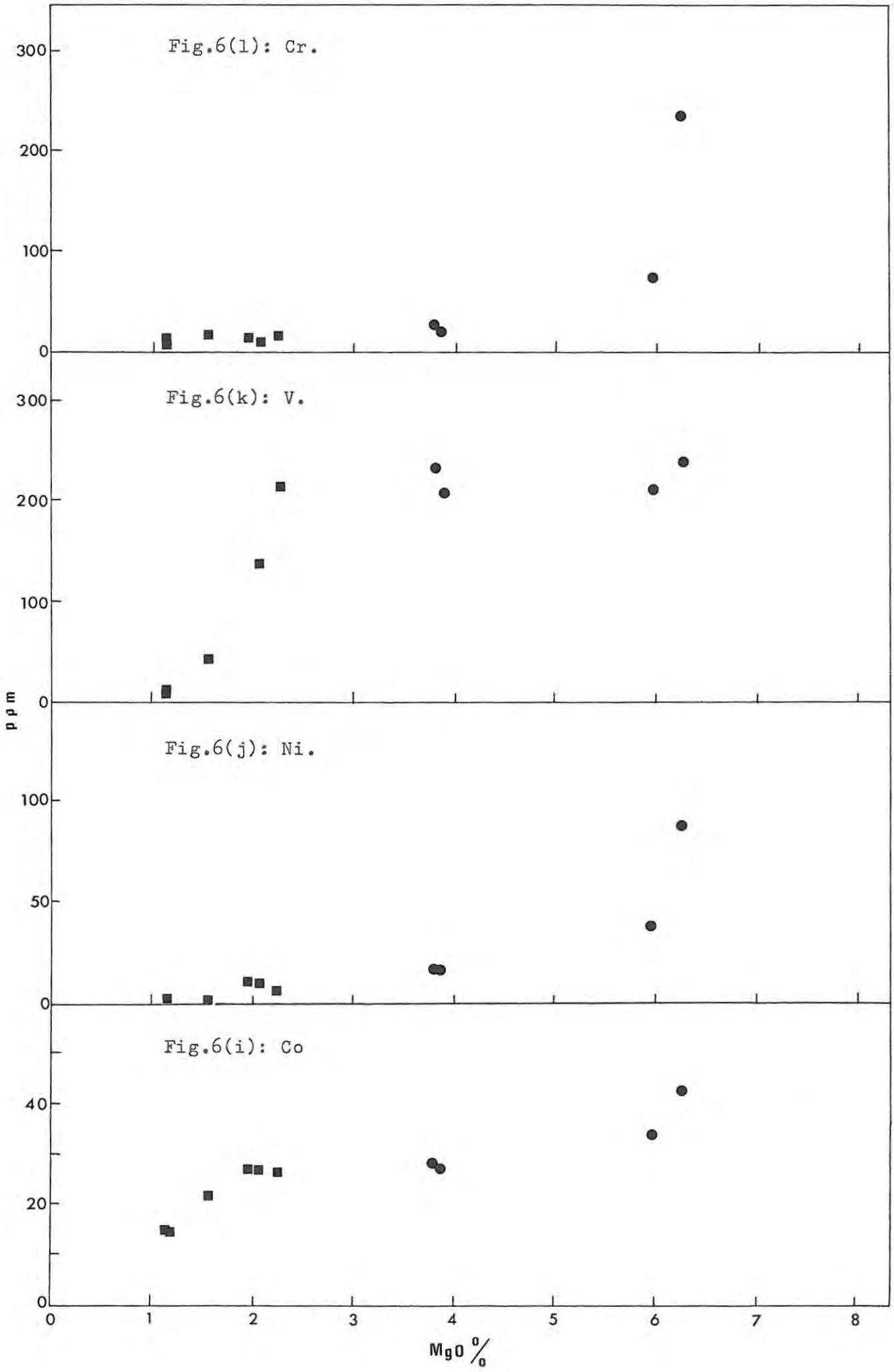
Fig.6(l): Cr.
Fig.6(k): V.
Fig.6(j): Ni.
Fig.6(i): Co
ppm
MgO %

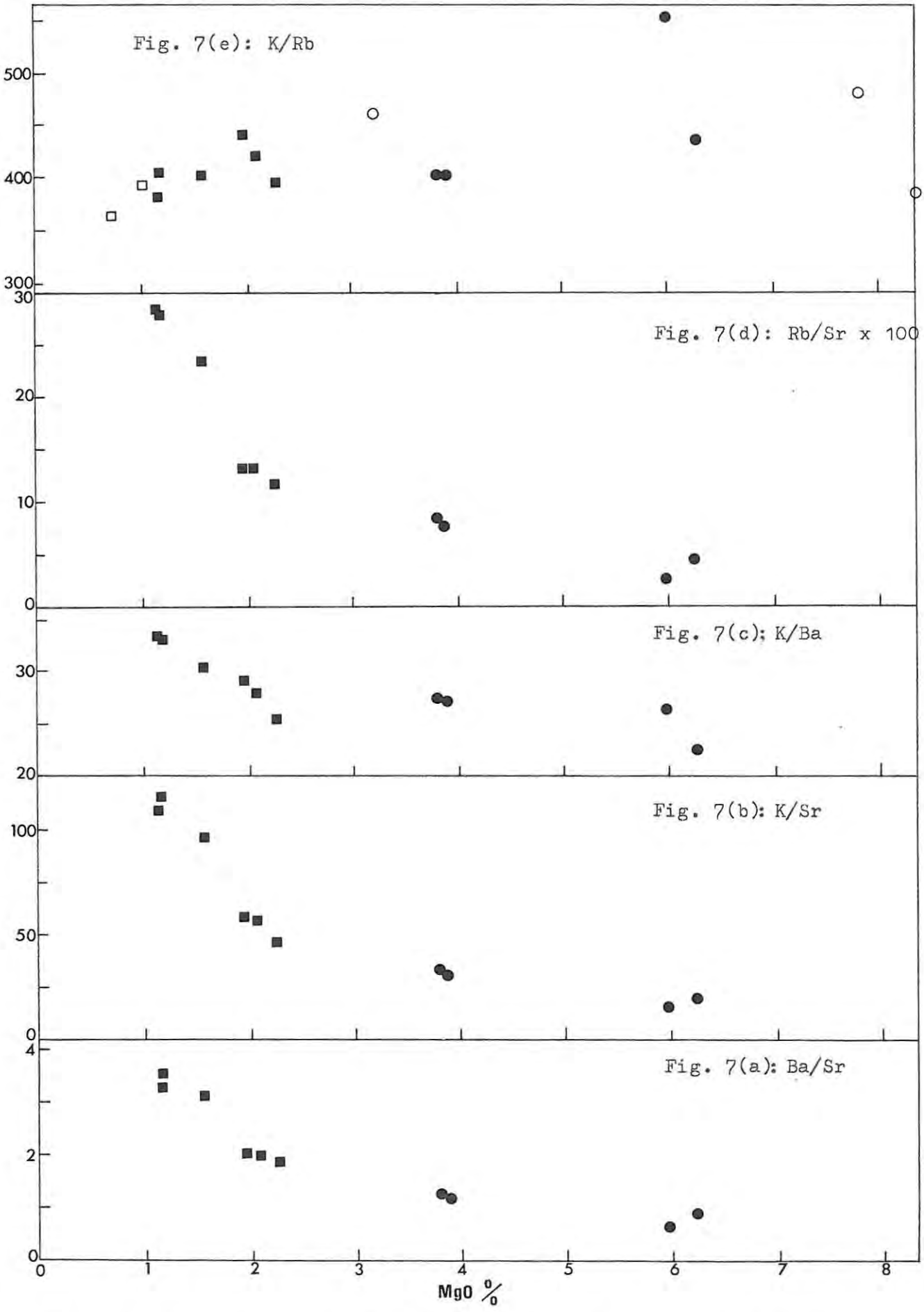

Figs.7(a-j): Variation of some inter-element ratios, with differentiation at Birds River.

Symbols as indicated in Figs. 6(a-l).

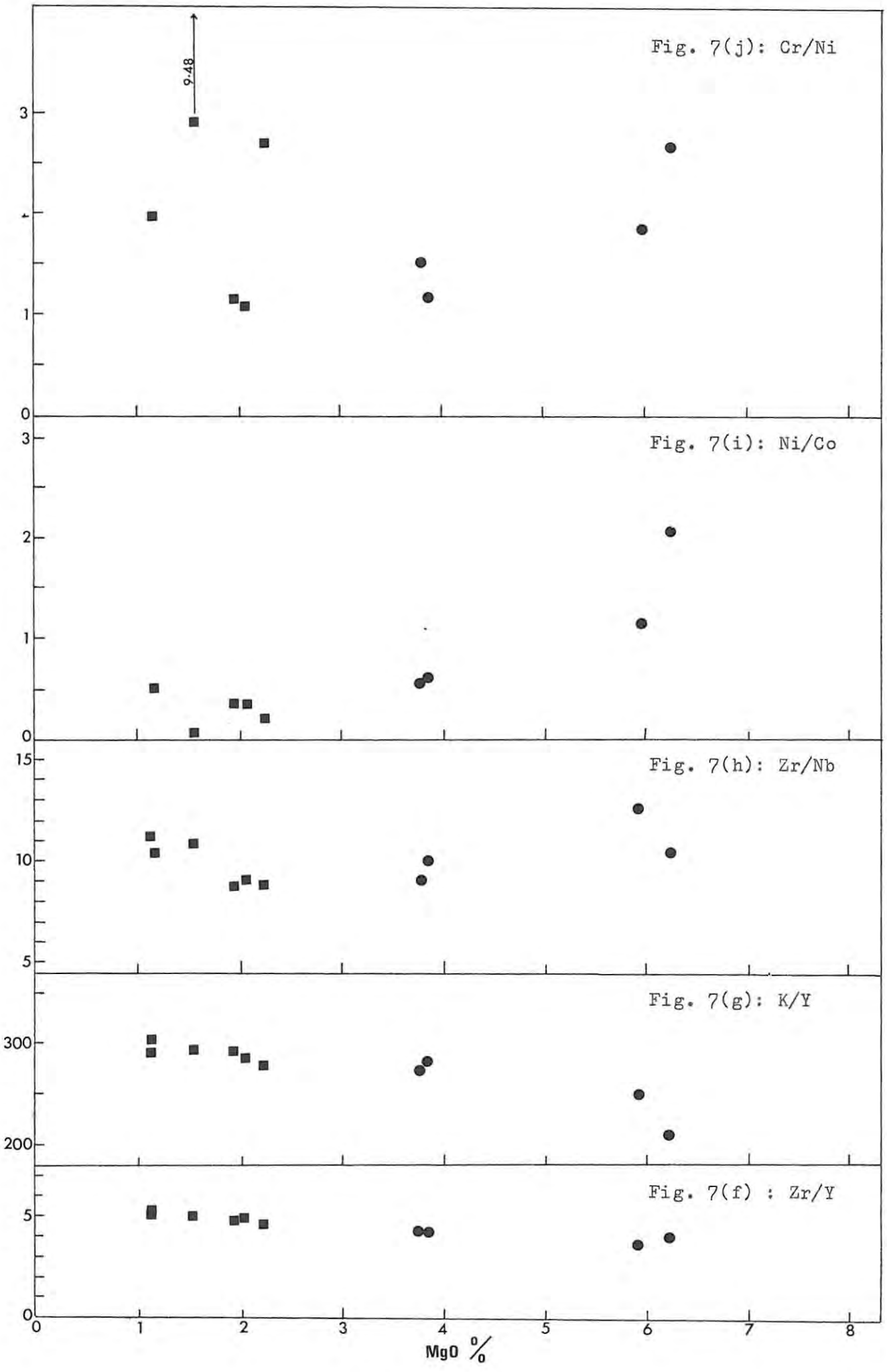
Fig. 7(j): Cr/Ni
9·48
Fig. 7(i): Ni/Co
Fig. 7(h): Zr/Nb
Fig. 7(g): K/Y
Fig. 7(f) : Zr/Y
MgO %

from the regional sample of dolerites in Table 8(c).

The following sections will discuss each trace element in turn, dealing first with the theoretical and observed geochemical behaviour and association of each trace element and then with its particular variation in the Birds River Complex.

2.5.b

Strontium.

The ionic radius of Sr (1.18 A^{o}) is intermediate in size between Ca (.99 A^{o}) and K (1.33 A^{o}) and geochemically its behaviour is dependent on the facility of Sr entry into Ca and K positions in minerals. (Taylor, 1965).

Sr, while not entering to any extent Ca positions in pyroxenes nor K positions in micas, readily enters K positions in K-feldspar and Ca positions in plagioclase and apatite. Taylor (1965) quotes data to show that in co-existing K-feldspar and plagioclase pairs, Sr preferentially enters K positions and that the Sr/Ca ratio is nearly ten times as great in K-feldspar than in co-existing plagioclase.

Strontium distribution coefficients (D_{Sr}) between plagioclase and liquid have been measured by Philpotts and Schnetzler (1970), Knorringa and Noble (1971) and others in both synthetic and natural systems. Data suggest values of $D_{Sr}^{plag.}$ vary between 1 - 3 for calcic plagioclases, the value increasing with decreasing An% of the plagioclase (Jensen, 1973).

Very little Sr enters clinopyroxenes and olivines and D_{Sr}^{cpx} and $D_{Sr}^{ol.}$ are about 0.1 and 0.001 respectively. (Hart and Brooks, 1974). Fractionation of pyroxene and olivine only would strongly enrich residual melts in Sr, the converse being true for plagioclase and K-feldspar fractionation.

The Birds River magma was, with increasing differentiation, progressively depleted in Sr (Fig.6(a)) and this is in contrast to the Sr-enrichment shown by Walker (1970) for the early stages of differentiation in the Palisades sill.

Data from Eales and Robey (in press) show an absolute decrease in Sr from 280 ppm in a feldspathic gabbro to 151 ppm in the most evolved ferrotholeiite. Data from Stapelbergkloof show a decrease from 257 ppm to 177 ppm and values fall within the range determined by Eales and Robey (op. cit.).

The decrease in Ca/Sr ratios from 326 to 210 at Stapelbergkloof

is consistent with that recorded at Denwood by the former authors and is in accord with the decrease predicted by Taylor (1965) though it is noted by Eales and Robey (op. cit.) that Ca/Sr ratios should not be interpreted entirely in terms of plagioclase fractionation since there is a strong increase in normative orthoclase (Table 2) in the ferrotholeiites relative to the gabbros.

The relatively subdued depletion of Sr in the early stages of differentiation at Birds River suggests that fractionation of pyroxene and olivine has reduced the strongly depleting effect of fractionation by plagioclase only.

The ratios Ba/Sr, K/Sr and Rb/Sr predictably increase with differentiation and are shown in Figs. 7 (a, b and d) respectively. The former increases from 0.6 in the gabbros to 3.5 in the ferrotholeiites while K/Sr and Rb/Sr (x100) ratios increase from 20 to 115 and 2.9 to 28 respectively.

2.5.c

Barium.

Ba (1.34 A^{o}) is almost identical in ionic size to K (1.33 A^{o}) and though having a more covalent bond to oxygen than K (Taylor, 1965), readily enters K positions in K-feldspars and biotites. Ba also substitutes for Ca in plagioclase and to a very much more limited extent in pyroxenes, though Ba distribution coefficients for pyroxenes are always less than unity.

$D_{Ba}^{plag.}$ values vary in a linear fashion from 0.16 (An90) to 0.42 (An30) and then increase sharply to values between 3-5 in sodic alkali feldspars. (Knorringa and Noble, 1971).

Berlin and Henderson (1969) quote similar values for $D_{Ba}^{plag.}$ and also report strong Ba fractionation by sanidine ($D_{Ba}^{sanidine}$ = 1.17 - 8.95) and biotite ($D_{Ba}^{biotite}$ = 1.16 - 15).

Barium entry into olivine and clinopyroxene is greatly restricted and though reported distribution coefficients vary greatly, data from Hart and Brooks(1974) suggest $D_{Ba}^{ol.}$ and D_{Ba}^{cpx} to be of the order of .001 and .003 respectively.

Therefore, fractionation of calcic plagioclase, clinopyroxene and olivine from a basic melt will enrich the residual liquid in Ba until such time that more sodic and K-rich feldspars dominate fractional crystallization. After this stage residual liquids would be rapidly depleted in Ba.

Similarly Ba/Sr should initially increase with differentiation reflecting the early preferential removal of Sr by calcic and intermediate plagioclase. K/Ba ratios should remain constant until K-feldspar separates from the magma afterwhich the ratio should increase since Ba preferentially enters sanidine relative to K. (Berlin and Henderson, 1969).

The concentration of Ba in the Birds River sequence has not previously been determined and variation trends are thus confined to analyses from Stapelbergkloof.

Barium increases from 225 ppm in the chill-zone gabbro to 620 ppm in the most differentiated ferrotholeiite. (Fig. 6b). The progressive enrichment of Ba is consistent with plagioclase, pyroxene and olivine crystallization, the effect of the latter two phases being to reduce the already low $D_{Ba}^{plag.}$ to give a very low bulk distribution coefficient. The high values of Ba recorded for the ferrotholeiites suggest little or no alkali feldspar removal at the late stages of differentiation. The chemically more highly evolved ferrotholeiites from Denwood may well show some late stage depletion of Ba due to sanidine fractionation but no Ba data exist for these specimens.

K/Ba ratios (Fig.7c) vary somewhat but remain relatively constant at 27 for most of the gabbro-ferrogabbro-ferrotholeiite sequence and increase slightly to 33 in the more highly differentiaed ferrotholeiites. Sanidine and sodic plagioclase are common phases in these ferrotholeiites and the slight rise in K/Ba ratios may indicate minor removal of K- or Na-feldspars.

2.5.d

Rubidium.

The close association of Rb with K is well established. Both have similar electronegativities and ionization potentials and are comparable in size, Rb (1.47 A^{o}) being slightly larger than K (1.33 A^{o}). This size difference becomes effective only under conditions of extreme differentiation and in such cases Rb is concentrated relative to K in residual liquids. (Taylor, 1965).

Rb readily enters K positions in K-feldspars and biotite and though the bulk of Rb in rocks is contained in K-feldspars, Rb shows a marked preference for entry into micas (Taylor, op.cit.).This

is reflected in reported distribution coefficients for Rb between K-feldspar and liquid and between biotite and liquid. Noble and Hedge (1970) report $D_{Rb}^{sanidine}$ = 0.25 - 0.45 while Philpotts and Schnetzler (1970) report a comparable value of 0.66. $D_{Rb}^{biotite}$ is however, generally, greater than 1. Philpotts and Schnetzler (op.cit.) report values between .94 and 3.3 while Dupuy (Marsh, 1973) reports D's for biotites in ignimbrites to range from 1.26 to 1.58. Thus "protected alkali-feldspar fractionation would enrich residual liquids in Rb whereas notable amounts of biotite removal would reverse this trend" (Marsh, op. cit) This situation however should only be expected in more alkalic suites.

Plagioclase accepts little Rb and distribution coefficients used by Arth et al. (1975) and others in modelling trace element variations, are generally less than .1. Clinopyroxenes and olivines virtually exclude Rb from their crystal lattices and data from Hart and Brooks (1974) show extremely low average distribution coefficients of .03 and .0002 respectively.

The behaviour of the K/Rb ratio during basic rock differentiation has long been the source of discussion amongst geochemists and petrologists. Fractional-crystallization effects, alone, on this ratio can best be explained only when one fully understands how this ratio is affected or changed by each mineral-liquid pair.

Philpotts and Schnetzler (1970) report $D_{K/Rb}^{plag.}$ to vary from 0.4 to 5.49 though an average near 3 is indicated. Hart and Brooks (1974) quote an even higher value of 6.9 while Goodman (1972) finds similar values. It is thus known that plagioclase-rich rocks (plagioclase cumulates) have high K/Rb ratios not due to their primitive or parental associations but simply due to the mineralogical control of plagioclase on the K/Rb ratio.

$D_{K/Rb}$'s for clinopyroxenes are variable but average near unity (Philpotts and Schnetzler, op.cit)and are in keeping with values of 0.7 - 1.18 reported by Hart and Brooks (op.cit.).Data for olivine are scarce but a $D_{K/Rb}^{ol.}$ = .99 is reported by both the above authors. Consequently olivine and clinopyroxene fractionation, either singly or together, will not radically alter the K/Rb ratio.

K-feldspars which more readily accept Rb, have $D_{K/Rb}$ values near 2 (Philpotts and Schnetzler,op.cit,while Marsh (1973) in his survey of quoted $D_{K/Rb}$'s for biotites finds values generally to be less than 1.

Thus when dealing with true residual liquids, successive residua produced by plagioclase-only fractionation should, theoretically,

show decreasing K/Rb ratios, while clinopyroxene-only and olivine-only fractionation should produce relatively constant values. Furthermore should any femic phases fractionate in appreciable quantities together with plagioclase, this would tend to lower and negate the high $D^{plag.}_{K/Rb}$ and so reduce the rate of K/Rb fall with differentiation. However, a very important point to remember is that since both Rb and K are so strongly partitioned into the liquid relative to the above phases , the absolute change in the K/Rb ratio will be very small and may be difficult to detect as being solely due to fractional crystallization unaffected by any other process. Rayleigh curves of fractional crystallization (Gast, 1968) show that to notably change an inter-element ratio such as K/Rb, where both elements strongly enter the liquid rather than the crystal phase, would require vast amounts of plagioclase, clinopyroxene and olivine fractionation from the crystallizing magma.

Conversely, an inter-element ratio is more easily changed if one of the elements is strongly partitioned into the fractionating phase, the other into the liquid. Such is the case with K-feldspar and biotite. The former, though having a $D_{K/Rb}$ less than the $D^{plag.}_{K/Rb}$ has a very much larger D_{Rb} and the relative depletion of Rb in absolute terms in the liquid would be more apparent and consequently the K/Rb ratio would be changed more radically by K-feldspar fractionation than by plagioclase-only removal.

In a basaltic system crystallizing and fractionating plagioclase, pyroxene and olivine, one would therefore expect little variation in the K/Rb ratio, although this would be dependent on the relative amounts of the various phases removed. At a later stage of differentiation when Na- and K-rich feldspars dominate the crystallization pattern and ferric phases are relatively unimportant, a stronger decrease in the K/Rb ratio should occur. Kable et al. (1972) show there to be little variation in the K/Rb ratio of a basalt-to-trachyte differentiated sequence on Tristan de Cuhna while Abbot (1967) indicates the effects of K-feldspar fractionation in markedly decreasing the K/Rb ratio.

A similar line of argument can explain the variations of the ratios K/Ba, K/Zr and K/Nb though obviously other mineral phases must be considered.

Data from Stapelbergkloof show Rb to increase from 11.5 ppm in the chill-zone gabbro to 50 ppm in the most differentiated ferrotholeiite (Fig.6c). Eales and Robey (in press) report an even

stronger enrichment to 75 ppm in the most evolved Denwood ferrotholeiite (Table 1b). Fig. 6(c) shows Rb data from both sources and it is seen that Rb increases steadily throughout the series with a similar steepening of slope to that of K_2O (Fig.3f).

The variation of K/Rb ratios at Birds River has already been discussed by Eales and Robey (op. cit.). They state that "no simple correlation exists between K/Rb ratios and fractionation index, indicating that factors other than simple crystal fractionation influence the ratio". K/Rb ratios at Stapelbergkloof range from 555 in a feldspathic gabbro to 382 in a ferrotholeiite, the variation with increasing differentiation being shown in Fig.7(e). The later-stage ferrotholeiites from both Stapelbergkloof and Denwood have slightly reduced K/Rb ratios relative to the gabbros and ferrogabbros but variations are large. Eales and Robey (op. cit.) show that K/Rb varies strongly in the Birds River gabbros (Fig.8a) and values range upwards from 260 while the ferrogabbros and ferrotholeiites (Fig.8a) show a more restricted range between 300 and 400. They furthermore find that more than half the rocks analysed had K/Rb ratios between 350 and 425 (Figs. 8a, 8b). This is consistent with data from Erlank and Hofmeyer (1966) who note Karroo dolerites to have K/Rb ratios higher than dolerites from Tasmania and Antarctica. The chill-zone gabbro from Stapelbergkloof has a K/Rb ratio of 437, close to the Karroo average of 465 reported by the former authors. The relatively high value reported for the plagioclase-rich gabbro -S30- is consistent with predictions previously discussed.

In their discussion of the variability of K/Rb ratios in the gabbros from Birds River, Eales and Robey (op. cit.) pay particular attention to the influence of mineral textures. Variation is believed to be partly dependent on the degree of crystallization processes simulating orthocumulus, mesocumulus or adcumulus growth. The former mechanism enables late residua, rich in Rb, to be trapped within crystal frameworks, so reducing the high K/Rb ratios expected when the latter mechanism predominates. With adcumulus growth, residual liquids are effectively expelled and whole-rock K/Rb ratios are then more strongly influenced by the K/Rb ratios of the mineral phases present. More simply put, the modal amounts of micropegmatite, rich in K-feldspar will strongly affect the K/Rb ratio in coarse-grained gabbros and will distort any effects caused purely by fractional crystallization.

The limited variation of K/Rb ratios within the partly glassy

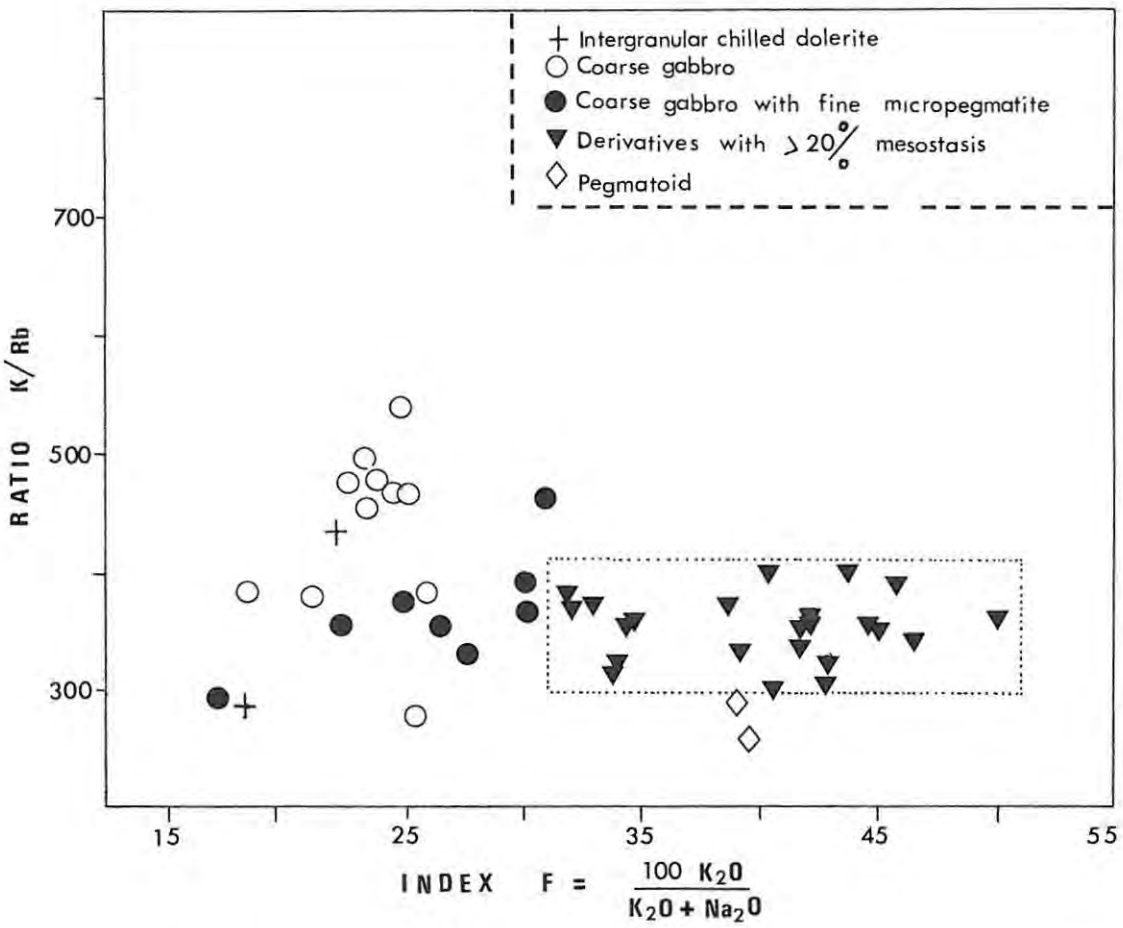

Fig.8(a): K/Rb ratios of 47 Birds River rocks plotted against a felsic index, illustrating low ratios for the pegmatitic facies of gabbro, variable values for gabbro, and restricted range for rapidly chilled rocks with more than 20 per cent mesostasis (after Eales and Robey, in press, Fig. 4).

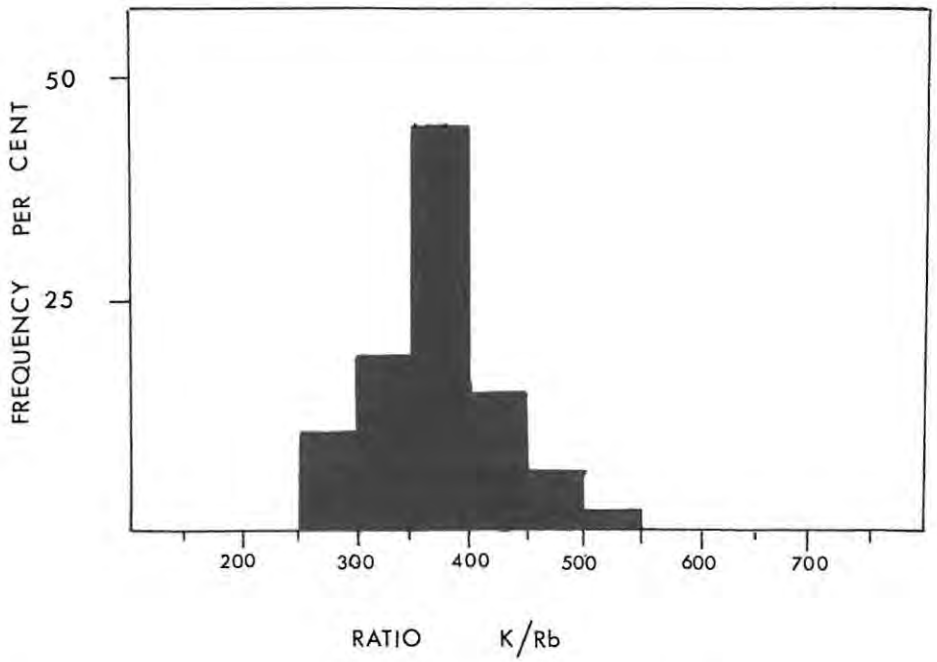

Fig.8(b): Histogram showing the frequency of occurrence of different values of K/Rb ratio in Birds River rocks (47 samples) (after Eales and Robey, op.cit., Fig. 5).

ferrotholeiites from Birds River, is probably due to their "rapid crystallization, high viscosity and inability to expel late residua during the stage when K-minerals would normally have separated" (Eales and Robey, op. cit.). Similarly the low K/Rb ratios of the gabbro pegmatoids (300) (Fig.8a), reported by the former authors, are in keeping with their truly residual nature.

In conclusion, the variation of K/Rb ratios in the coarse-grained gabbros must not only be treated in terms of fractional crystallization, for "mineralogical control" (Erlank and Hofmeyer, 1966) and "growth mechanism control" (Eales and Robey, op. cit.) are important factors to consider. Furthermore, a clear distinction should be drawn in analysing the variation of this ratio in basalts (essentially liquids) and gabbros (residual liquids and semi-cumulates or true cumulates). In the former, if variations cannot be adequately explained in terms of a fractional crystallization model, one resorts to explanations invoking the effects of varying degrees of partial melting within the mantle, mantle inhomogeneities or crustal contamination, while in coarser-grained rocks the degree of cumulus status and inclusion of micropegmatite are additional obstacles.

2.5.e

Zirconium.

Zirconium (.79 A^{o}) does not commonly enter any of the major cation sites in minerals, concentrating rather in residual liquids until it forms its own phase - zircon. Zr may substitute to a limited extent for Ti in early Ti-Fe oxides (Taylor, 1965; Walker, 1970) or enter pyroxenes and apatite. Analyses of mineral separates (Eales and Robey, in press, Table 3) show the entry of Zr into the opaque fraction but only limited entry into pyroxenes.

Virtually no published data exist for Zr distribution coefficients between mineral and liquid pairs.

The Stapelbergkloof sequence shows a strong Zr enrichment factor of greater than 5 from 67 ppm to 357 ppm (Fig.6d), while data for the Denwood ferrotholeiites (Table 1b) suggest an even stronger enrichment (by a factor of 7) to a maximum of 480 ppm in the more extreme differentiates.

The continued increase in Zr content with differentiation suggests little or no late-stage crystallization of zircon as a major phase. Walker (1970, Fig.3) reports a similar enrichment of Zr within the Palisades sill.

Eales and Robey (op.cit. Fig.3) note that the Zr variation at Birds River is similar to and extends values for Karroo-age basalts from Lesotho and Swaziland.

In the Stapelbergkloof sequence Ti/Zr ratios remain fairly constant through the gabbro and ferrotholeiites and average 63 (range 55-71) but decrease significantly to average 32 (range 28-38) in the more differentiated ferrotholeiites. This is the reverse of that predicted by Taylor (1965) but matches the TiO_2 variation (Fig.3b). Even though Zr does enter opaque oxides to some extent, distribution coefficients must be less than unity. Consequently late-stage magnetite removal from a basic magma such as crystallized at Birds River would still enrich residual liquids in Zr. The enrichment of Zr in the Founalei lavas (Ewart et al., 1973) which have crystallized magnetite early and which show decreasing V contents with increasing differentiation, clearly show this Zr enrichment.

Zr also shows a close correlation to Y, as noted by Walker (1970) and Zr/Y ratios at Birds River (Fig.7f) remain nearly constant, increasing only slightly from 4 in the chill-zone gabbro to 5 in the most differentiated ferrotholeiite. In the absence of major element data, this Zr/Y ratio may be a useful indicator or identifier of a petrographic type or province. Similarly, K/Zr ratios, with one exception, vary little and average 59 (range 66-53).

These ratios are all typical of the so-called residual trace-elements and again demonstrate the difficulty of changing an inter-element ratio when both elements strongly enter the liquid phase. (Gast, 1968).

2.5.f

Yttrium

Yttrium has an ionic radius of 0.98 A^{o} and is comparable in size to Ca and Fe^{2+} though closer to the former. The close association of Ca and Y has recently been discussed by Lambert and Holland (1974) and the following significant points emerge.

On the basis of Ca/Y ratios, these authors distinguish between "Y-accepter" and "Y-rejecter" Ca-silicates. In basaltic systems,

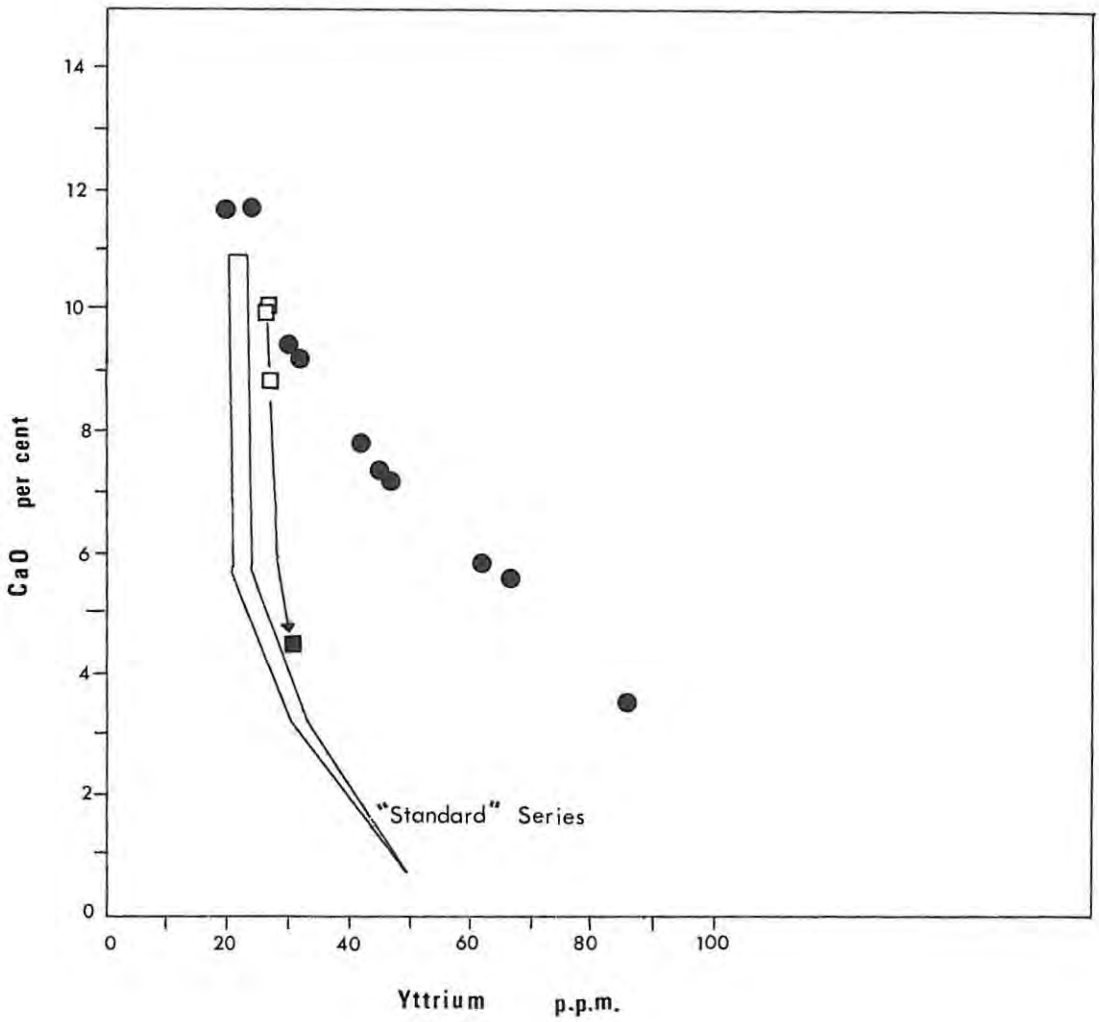

Fig. 9: Calcium - Yttrium relationships showing the strong relative enrichment of Y with decreasing CaO % for the differentiated sequence at Birds River. The more subdued Y enrichment trend for the Kraai River basalts-Belmore andesite series nearly matches the "standard" series trend of Lambert and Holland (1974).

● Gabbro to ferrotholeiite, Birds River. Data are from the present study and from Eales and Robey (in press).

□ Kraai River basalts excluding JR108A,B.

■ Belmore andesite.

augite, clinopyroxene and plagioclase take up very little Y, while hornblende, garnet, apatite, Ca-poor orthopyroxene, K-feldspar and biotite all accept enough Y to reduce the Ca/Y ratio of the mineral to less than 2000, the amount set by Lambert and Holland (op.cit.)to define a mineral as an Y-accepter or -rejecter.

Lambert and Holland (op.cit,Figs.2-4) discuss various CaO/Y fractionation trends. In all igneous series, CaO/Y ratios fall as CaO decreases but to varying degrees. Three differentiation trends are defined.

(a) A standard or calc-alkaline trend.

(b) J-type (hornblendic) trends which relative to the standard trend show Y depletion with CaO decrease. These trends appear controlled by dominant hornblende fractionation.

(c) L-type (pyroxenic) trends which, relative to the standard trend, show Y to be progressively enriched and to attain lower CaO/Y ratios than (a) or (b). This trend is dominated by strong plagioclase fractionation.

Data from both Stapelbergkloof and Denwood (Fig.6e) show Y to increase from 20 ppm in the most basic gabbro to 86 in the most differentiated ferrotholeiite, an increase by a factor of nearly 4.5. This increase is matched almost exactly by the Palisades intrusion.

Fig.9 is the Lambert and Holland (op.cit)CaO/Y plot and a clear L-type or pyroxenic trend is pronounced. The Birds River CaO/Y trend is similar to trends defined by the Aden and Little Aden volcanics (Lambert and Holland,op.cit)but is per percent CaO more Y-rich than these. This strong and persistent enrichment of Y relative to CaO at Birds River is certainly suggestive of strong plagioclase crystallization. (Lambert and Holland,op.cit,Fig.8).

At Stapelbergkloof, K/Y ratios increase steadily from 208 in the chill-zone gabbro to 303 in the most evolved ferrotholeiites and to 334 in the Denwood ferrotholeiites.

2.5.g

Niobium.

On the basis of ionic size, Nb may substitute for Ti and Zr in basic rocks, though the bulk of Nb is probably taken up in large

$(NbO_4)^{4-}$ complexes. The greater size of these complexes relative to $(SiO_4)^{4-}$ complexes causes Nb to be enriched in residual liquids with increasing differentiation (Taylor, 1965).

Data for relatively impure mineral separates (Eales and Robey, in press, Table 3) show the strong preference of Nb for the opaque oxides, where it presumably substitutes for Ti in ilmenite. Similarly, Nb substitutes for Ti in pyroxenes (Taylor, op. cit.).

The ratios Ti/Nb and Zr/Nb theoretically should decrease with increasing differentiation. However, Zr/Nb ratios for basalt and trachybasalt sequences on Marion and Prince Edward Islands (Kable et al., 1971) and in trachytic and pantelleritic volcanoes in the Kenyan and Ethiopian Rifts (Weaver et al., 1972) remain remarkably constant. Furthermore in the former case, both older and younger lavas on Marion Island have different Zr/Nb ratios to similar lavas from Prince Edward Island, while Weaver et al.(op.cit)note that this ratio also changes in different volcanoes studied. This is interpreted as being a characteristic of the lavas at their time of extrusion and suggests that Zr/Nb ratios may be used as a useful petrogenetic indicator.

Niobium data are available only for the gabbro-ferrotholeiites from Stapelbergkloof and the Nb variation trend is shown in Fig.6(f). Nb increases from 9.3 ppm in the chill-zone gabbro to 34.5 ppm in the ferrotholeiites. Since the ferrotholeiites from Stapelbergkloof are not as highly differentiated as those at Denwood, an even stronger enrichment is indicated.

Ti/Nb ratios, with one exception (JR30), decrease steadily from 670 to 288 confirming the predicted Ti/Nb decrease with increasing differentiation.

Zr/Nb ratios (Fig.7h) vary slightly, initially decreasing from 12.5 to 8.7 but then increasing to between 10 and 11.5 in the more differentiated ferrotholeiites. The Zr/Nb ratio, thus, remains fairly constant and averages about 10 for the gabbro-ferrotholeiite sequence. These ratios agree well with two unpublished values (10.9 and 12.8) for the Mt. Arthur tholeiites (A. Duncan - personal communication) but disagree with earlier data (Eales and Robey, in press, Table 3), which indicate Zr/Nb to increase from 6.9 to 9.9 in representative gabbros, ferrogabbros and ferrotholeiites from Denwood. This disagreement must be due to poor inter-laboratory correlation in the determination of Nb, for

Zr correlation (Fig.6d) is generally good. Particular care was taken in determining Nb in the samples from Stapelbergkloof and total counting times of 1200 seconds per determination - 600 seconds on peak and 300 seconds on each of the 2 background positions - reduced detection limits to near 0.8 ppm. (Appendix 4). Detection limits (unreported) for data by Eales and Robey (op. cit.) are very much higher and consequently more weight is attached to the validity of Nb determinations presented in this study.

The ratio K/Nb, similarly, should remain fairly constant with differentiation, a marked decrease only occurring with the fractionation of a K-bearing phase. K/Nb ratios at Birds River are, however, quite variable and behave in a manner similar to K/Rb. With one exception (S30 - K/Nb = 890), the K/Nb ratios range between 658 and 524 and average 581.

2.5.h

Zinc.

Zinc (0.74 A^{o}) is almost identical in ionic size to Fe^{2+} (0.75 A^{o}), though it has a more covalent bond to oxygen than Fe^{2+}. Zn is therefore enriched relative to Fe^{2+} in residual liquids (Taylor, 1965). Wager and Brown (1968) find that zinc is concentrated in magnetite in rocks from the Skaergaard intrusion while also being enriched to some extent in the late-stage granophyres.

Danchin and Ferguson (1969) note that though the geochemistry of zinc has been discussed by numerous authors such as Neuman, Wedepohl and Ahrens, there are few data for the behaviour of zinc in differentiated basic intrusions.

The variation of Zn with increasing differentiation at Stapelbergkloof is shown in Fig.6(g). The contact gabbro contains 91 ppm Zn while an overall enrichment of about 2.5 times is indicated from 61 ppm in the feldspathic gabbro, S30, to 150 ppm in the most evolved ferrotholeiite. The behaviour of Zn is thus, different to that of V, the former behaving as a true residual trace element. Bulk distribution coefficients for Zn between the fractionating phases and liquid must, however, be closer to unity than those for Rb, Zr, Y, Nb and Ba, for Zn enrichment factors are lower. This enrichment of Zn in residual liquids at Birds River supports the increase in Zn content of the granophyres from Skaergaard (Wager and

Brown, 1968) and shows a more positive correlation to differentiation than that found by Danchin and Ferguson (op.cit)for the Losberg intrusion. In the latter intrusion Zn values, throughout the differentiated sequence, remain relatively constant between 50 and 69 ppm.

2.5.i

Copper.

Cu^{2+} will substitute for Fe^{2+} in pyroxene, olivine and Fe-oxides, while Cu^{+} will substitute for Na^{+} in plagioclase. Since the Cu-O bond is more covalent than either the Fe-O and Na-O bond, Cu tends to be concentrated in residual liquids and on differentiation, the ratios Cu/Fe and Cu/Na should increase (Taylor, 1965).

In both the Skaergaard (Wager and Brown, 1968) and Red Hill (McDougall et al., 1963) intrusions, Cu increases with differentiation to reach a maximum in the mid- to late- differentiates, after-which a Cu-sulphide phase separates to deplete further residua in Cu. Wager and others (Prinz, 1967) note that in the Skaergaard intrusion, a Cu-sulphide liquid separated immiscibly when the Cu concentration in the magma reached 200 ppm. The magma became further enriched in Cu to 500 ppm at 90% solidificàtion and then was rapidly depleted in the final derivatives. Walker (1970) reports a similar behaviour of Cu in the Palisades sill.

McDougall et al.(op.cit)report an increase in Cu in pyroxenes with increasing differentiation in the Red Hill dyke, while pigeonite is reported to contain nearly three times as much Cu as co-existing augite. The concentration of Cu in plagioclases from Red Hill remains nearly constant throughout differentiation, while alkali feldspars contain less Cu than co-existing plagioclase.

The following Cu distribution coefficients are selected from data by Ewart et al. (1973) for phenocryst/groundmass pairs in some Tongan Island volcanics.

(a) $D_{Cu}^{plag.}$ - average = 0.19 (range .32 - 0.08) for plagioclase between An_{90} and An_{80}. Ewart et al.(op.cit,Fig.3) show the Cu content of plagioclase to decrease from 30 ppm at An_{90} to near 10 ppm at An_{80}. No data are available from this source for less calcic plagioclase.

(b) $D_{Cu}^{cpx.}$ - average = 0.49 but the range of values is large, (0.12 - 0.87).

(c) $D_{Cu}^{Ca\text{-poor pyroxene}}$ - average = .55 but values vary and range between 1.2 and 0.16.

(d) $D_{Cu}^{magnetite}$ - values determined for three titano-magnetites range between 1.3 and 2.3.

The broad pattern of Cu variation is, thus, for a steady increase to a maximum from the early to fairly late stages of differentiation. With continued differentiation, the Cu concentration in residual liquids is rapidly depleted either by the separation of Cu-sulphides or by the combined influence of the crystallization of minerals such as Na-rich plagioclase and magnetite that accept appreciable amounts of Cu into their structures. This rise in Cu to reach a maximum and then, its subsequent depletion, is clearly established for the Red Hill intrusion (McDougall et al., 1963) and is also strongly evident in the fractionated lava sequences from Anjouan and Grande Comores (Flower, 1973).

The variation of Cu with increasing differentiation at Stapelbergkloof, Birds River is shown in Fig 6(h). Here the chill-zone gabbro contains 71 ppm Cu and this increases to reach a maximum of 165 ppm in the ferrotholeiites. With further differentiation, the concentration of Cu rapidly decreases to near 60 ppm.

This variation is exactly as expected and virtually identical, both in terms of absolute amount and trend, to that at Red Hill. (McDougall et al.,op.cit). While chalcopyrite has been identified in the Red Hill dyke, no Cu-sulphides have been found in the Birds River rocks.

The exact cause of the strong decrease in Cu in the Birds River ferrotholeiites is difficult to determine but it may be due to the late crystallization and separation of Na-plagioclase and magnetite.

2.5.j

Cobalt.

Cobalt (0.72 A°) is intermediate in size between Fe^{2+} (0.75 A°) and Mg (0.65 A°) and is similar to Ni (0.69 A°). The larger size of the cobalt ion restricts its entry into Mg-positions in minerals to a greater degree than for Ni. Co also enters Fe-positions in

early crystallizing femic phases but again not with the same facility as Ni. The ratios Ni/Co and Fe/Co, thus, decrease and increase respectively with differentiation (Taylor, 1965).

The entry of Co into minerals is controlled by the availability of Fe-Mg sites in the following minerals. Olivine, pyroxene and Ti-magnetite readily accept Co and all have distribution coefficients greater than unity. Plagioclase, however, accepts little Co and distribution coefficients are always less than 1.

Ewart et al. (1973) calculate the following distribution coefficients for Co.

(a) clinopyroxene - average = 3.2 but values range from 1.7 to 4.9 and appear to increase with increasing Fe/Mg ratios of the pyroxenes.

(b) orthopyroxene - average = 6.2 but values range from 3.4 to 9.2, also increasing with increasing Fe/Mg of the pyroxene.

(c) titano-magnetite - values range from 6.3 to 11.1

McDougall et al. (1963) support the above observed, preferential entry of Co into orthopyroxenes relative to clinopyroxene and attribute it to the greater Fe/Mg ratio of Ca-poor pigeonite. Prinz (1968), however, points out that the Co content of pyroxenes is more a function of the total Fe-Mg sites available, rather than the Fe/Mg ratio.

Henderson and Dale (1969) studied the partitioning of Ni and Co between olivine and groundmass in some oceanic basalts. $D_{Co}^{olivine}$ varies between 1 and 4, while $D_{Ni}^{olivine}$ is very much greater at values between 10 and 16.

$D_{Co}^{plag.}$ is probably less than 0.1 (Jensen, 1973) though limited data are available.

Burns (1969) gives a concise account in terms of site preference energies, of the behaviour of the transition metals during partitioning into mineral phases. The M_1 and M_2 sites in olivine, clinopyroxene and orthopyroxene vary in their degree of approximation to octahedral symmetry. Ni has an octahedral site preference energy (O.S.P.E.) nearly three times that of Co. Henderson and Dale (op.cit.) show the direct relationship between O.S.P.E. and ln D (D being their defined distribution coefficient). Burns (op.cit) concludes that Ni and Co preferentially enter M_1 sites in olivine while in both ortho- and clinopyroxenes, Ni preferentially enters the M_1

site and Co, the M_2 site.

To conclude, Co enters clino-, orthopyroxenes, olivines and magnetite with distribution coefficients greater than 1. Plagioclase virtually excludes Co from its lattice. Fractionation of Fe-Mg silicates in basic magmas would reduce the concentration of Co in residual liquids while significant plagioclase fractionation together with these Fe-Mg silicates, would tend to reduce bulk Co distribution coefficients and so reduce the rate of Co depletion with increasing differentiation.

The concentration of Co in the Stapelbergkloof sequence (Fig.6i) is at a maximum (43 ppm) in the chill-zone gabbro and then, with increasing differentiation, decreases slightly to, but remains fairly constant at, 27 ppm. Continued differentiation to the more highly evolved ferrotholeiites reduces Co to 15 ppm.

The behaviour of Co at Birds River differs slightly to that at Red Hill (McDougall et al., 1963), where Co closely follows the Fe^{2+} trend. Co at Birds River appears more to follow a combined Fe + Mg trend. The near constancy of Co throughout most of the gabbro-ferrogabbro-ferrotholeiite sequence may be explained by dominant plagioclase crystallization, reducing the high Co distribution coefficients for olivine and pyroxene to a bulk distribution coefficient near 1. The decrease of Co in the more highly differentiated ferrotholeiites could be due to minor amounts of magnetite fractionation.

Ni/Co ratios (Fig.7i) vary slightly but predictably decrease with increasing differentiation from 2.07 in the contact gabbro to 0.5 and less in the more advanced ferrotholeiites.

2.5.k

Nickel.

Nickel, as noted before, is similar in ionic size to Co but closer to Mg than Fe^{2+}. Ni in basic magmas is rapidly depleted by early crystallizing olivine, pyroxene and Fe-oxides and is reduced to very low levels in late-stage differentiates (Taylor, 1965).

Numerous authors have measured crystal-liquid distribution coefficients for Ni. Haikli and Wright (1967) find $D_{Ni}^{olivine}$ to range from 13.5 to 16.8 in some Hawaiian tholeiites. Gunn (1971) reports a value of 10 while Henderson and Dale (1969) report

similar values for oceanic basalts from Reunion Island. Flower (1973) finds $D_{Ni}^{olivine}$ to vary from 12.0 to 3.6 in some ankaramite lavas, confirming the strong entry of Ni into the olivine structure.

Ewart et al. (1973) find orthopyroxene to accept more Ni than clinopyroxene and calculated average distribution coefficients are 9.2 and 6.5 respectively. McDougall et al. (1963), however, report less Ni in Ca-poor pigeonite than in co-existing augite from a quartz dolerite at Red Hill. The former authors also note Ni distribution coefficients near 19 for separated titano-magnetites while de Long (1974), in his fractional crystallization model, uses a $D_{Ni}^{plag.} = 0.2$.

Haikli and Wright (1967) also note that Ni concentrations in olivine and pyroxene decrease with decreasing crystallization temperatures, the rate of decrease being greater for olivine (Haikli, 1968). This differential enables the distribution of Ni between co-existing olivine and augite pairs to be used as a geothermometer (Haikli, 1968). Flower (1973), McDougall et al. (1963) and others also note this decrease in the Ni content of olivines and pyroxenes during fractional crystallization.

Miyashiro et al. (1975, Fig.7) discuss Ti, Ni, V and Cr distributions and behaviour in tholeiitic and calc-alkaline differentiated series and show that the two series can be effectively separated in SiO_2% vs. log Cr ppm and - log Ni ppm diagrams. The tholeiitic series per percent SiO_2 has lower Ni and Cr concentrations, though the degree of separation of the two trends is not as clear for Ni as it is for Cr.

Cr/Ni ratios should vary according to which mineral, olivine or pyroxene, separates in greater quantitites from a basic magma. More Ni than Cr enters the olivine structure, high Cr concentrations in olivines being generally due to tiny, disseminated inclusions of Cr-rich spinel in the olivine (Gunn, 1971). Conversely more Cr than Ni is accepted by pyroxenes. Thus, simple olivine-only fractionation would increase the Cr/Ni ratios of residual liquids, while this ratio should decrease in pyroxene-controlled fractionation paths. Data from Gunn(op.cit)confirm this conclusion. Cr/Ni ratios increase from 1.4 to 2.95 in the olivine-controlled Kilauea fractionates while ratios decrease from 2.7 to 1.6 in the Makaopuhi lava series, where some pyroxene crystallized together with olivine.

In the Stapelbergkloof sequence, Ni is rapidly depleted from

a maximum of 89 ppm in the contact gabbro to 17 ppm in the ferrogabbros. Ni then decreases rapidly to 3.3 ppm and less in the more highly differentiated ferrotholeiites. (Fig.6j).

The early depletion of Ni in differentiated basic intrusions is well-known and Birds River is thus no exception. As in the Red Hill intrusion (McDougall et al., 1963), the more silicic differentiates contain less than 5 ppm Ni. The influence of significant plagioclase fractionation combined with pyroxene and olivine removal, would again be to reduce the rate of Ni depletion with differentiation. This and other factors, such as the decrease in Ni distribution coefficients for olivine and pyroxene with decreasing crystallization temperatures, all contribute to the more gentle decrease of Ni concentrations from the mid-differentiation stage onwards at Birds River.

Cr/Ni ratios (Fig.7j) are highly variable, especially so in the ferrotholeiites. The overall decrease in this ratio in the gabbro-ferrogabbro series, however, supports a more significant pyroxene rather than olivine control in the fractional crystallization process.

Co, V and Ni inter-element variations for the Birds River sequence are shown in Fig.10. Also shown are trends for the Karroo dolerites, the Skaergaard complex and the Dillsburg sill as compiled by Ishikawa (1968). The Birds River trend of Co-V-Ni variation extends those previously reported for the Karroo dolerites and closely matches the variation found in the Dillsburg sill. The Birds River magma, on differentiation, is initially strongly enriched in V relative to Co and Ni and the trend moves to the V apex (Fig.10) at near constant Co values. On further differentiation, "in extreme cases" (Ishikawa, op.cit) as at Dillsburg and Skaergaard, the mid- and late-fractionates then swing to relative Co enrichment, the trend being parallel to the Co-V boundary. Though not as extreme as Skaergaard and very similar to the Dillsburg trend, the Co-V-Ni inter-element trend at Birds River is important in establishing the relative behaviour of these trace elements in highly differentiated Karroo magma.

2.5.1

Vanadium.

Vanadium (0.74 A^{o}) is similar in geochemical behaviour to Cr

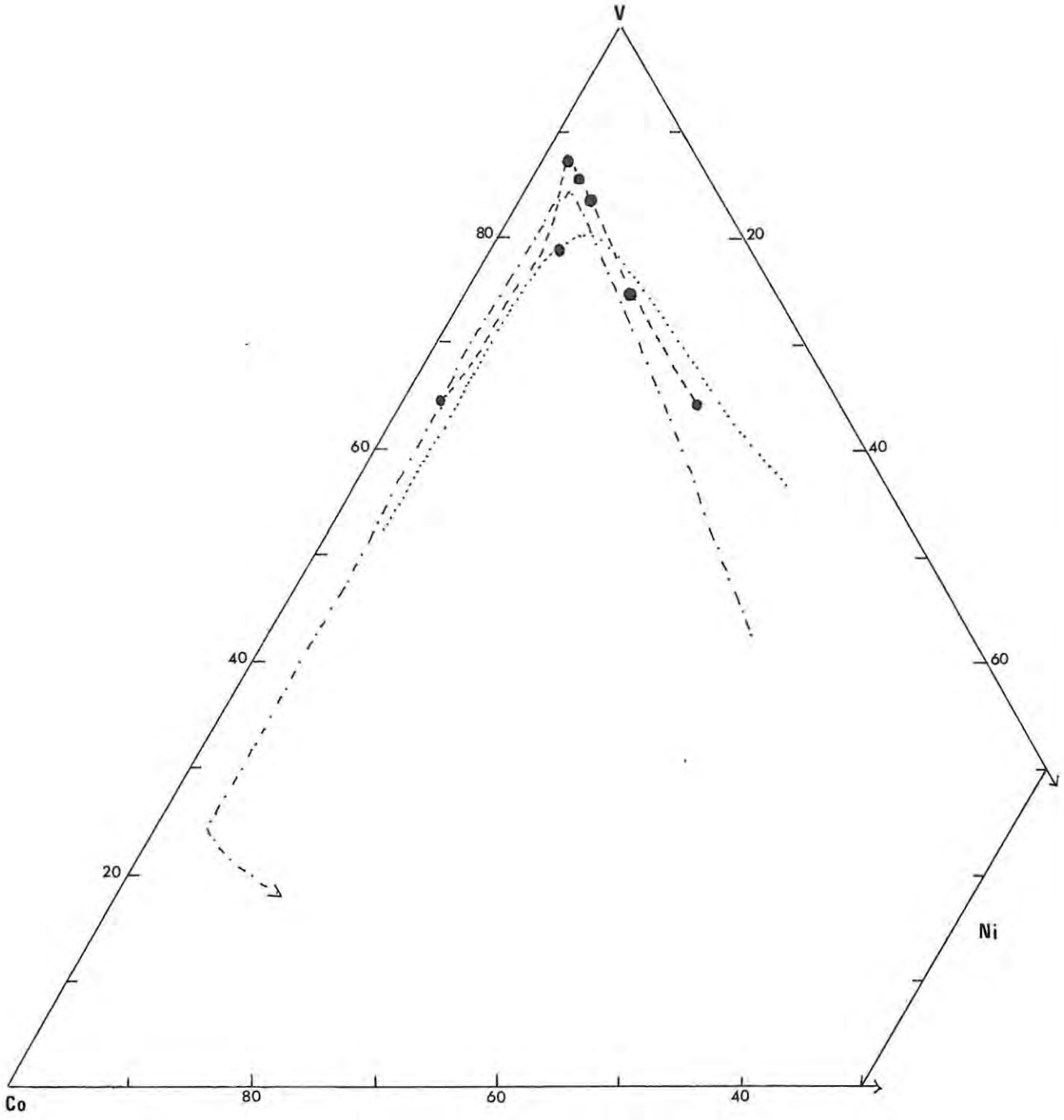

Fig. 10: Co, V and Ni inter-element ratio trends for Birds River.

● Stapelbergkloof, Birds River.

..... Dillsburg sill

-.-.-. Skaergaard intrusion } - after Ishikawa (1968).

(0.63 A^{o}) and Sc (0.81 A^{o}) and the lattice sites available for V, Cr and Sc entry into minerals are Fe^{3+}, Ti, Fe^{2+} and Mn (Walker, 1970).

V and Cr compete for available trivalent Fe lattice positions with Cr entering these sites preferentially due to its smaller ionic size. The Cr/V ratio in basic rocks therefore decreases with increasing differentiation and is a useful index of differentiation (Taylor, 1965).

V preferentially enters Fe-oxides and pyroxenes; only trace amounts are found in olivine due to the difficulty in balancing charges in Fe^{2+} positions (Taylor,op.cit) while virtually no V is accepted by plagioclase (Walker, op.cit.).

Walker(op.cit),furthermore finds that Cr enters minerals preferentially in the following order : clinopyroxene, magnetite and orthopyroxene, while for V, the order is magnetite, clinopyroxene, then orthopyroxene. Ewart et al. (1973) confirm this as shown in the following V distribution coefficients quoted by them.

$D_V^{magnetite} = 24 - 63$
$D_V^{cpx.} = 0.94 - 4.1$
$D_V^{opx.} = 0.5 - 2.3$

They also note that magnetite is virtually the only mineral that strongly removes V from a basic magma. The absolute and relative enrichment or depletion of V in successive basic differentiates would therefore, be dependent on the amounts and stages of olivine, pyroxene, plagioclase and magnetite fractionation.

This suggests that in calc-alkaline rock series, characterized by the early crystallization of magnetite, V should be depleted in successive residua and also, broadly, the calc-alkaline series should per differentiation stage be depleted in V relative to the tholeiitic series where magnetite is commonly of a late crystallization status.

The depletion of V by magnetite fractionation in basic magmas is clearly illustrated in the Founalei lavas (Ewart et al., op.cit., Fig.11), while the relative depletion of V in calc-alkaline rocks is illustrated by Miyashiro et al. (1975, Fig.8). Taylor et al. (1969) clearly illustrate the former contention and state that "the removal of one percent of magnetite will result in an average decrease of 60 ppm V in the magma; similarly the removal of 2% magnetite will cause a decrease of 120 ppm".

V, Ni and Co inter-element ratios have already been discussed in the previous section.

In the Stapelbergkloof section, the maximum V concentration is found in the contact gabbro - 238 ppm V. Fig.6(k) shows that with increasing differentiation, V remains nearly constant varying between 200 and 238 ppm in the sequence gabbro to ferrogabbro to ferrotholeiite. In the more highly differentiated ferrotholeiites, however, V rapidly decreases to concentrations as low as 10 ppm.

The constancy of V content in the initial stages of differentiation must be due to a combination of the effects of plagioclase, pyroxene and olivine crystallization, though, as will be seen in a later section, dominant plagioclase fractionation controlled the differentiation path at Birds River. Considering this and the V distribution coefficients measured in pyroxenes, the bulk distribution coefficient of the fractionating phases would be expected to be less than unity and so cause, during this stage, V to be enriched with differentiation. However, the trend indicated in Fig.6(k) suggests a bulk distribution coefficient near 1.

The strong depletion of V in the more highly evolved ferrotholeiites is, perhaps, the most convincing evidence that at least 2% magnetite (using the estimate of Taylor et al., 1969) fractionated from the magma before these rocks solidified. Eales and Booth (1974) suggest that the more calc-alkaline rather than tholeiitic trend exhibited by major element variations for the early-emplaced ferrotholeiites from Birds River, is due to these derivatives encountering highly oxidizing conditions during emplacement. This would sustain high PO_2 conditions and magnetite would freely be precipitated. The strong decrease of V in the ferrotholeiites at Stapelbergkloof would support such a conclusion.

2.5.m

Chromium.

Chromium (0.63 A°) is nearly identical in size to Fe^{3+} (0.64 A°) but has a more ionic bond with oxygen. Cr preferentially enters Fe^{3+} positions in mineral lattices and is generally, rapidly depleted at an early stage of differentiation in basic magmas (Taylor, 1965).

Pyroxenes and magnetite have a greater number of trivalent Fe positions available for Cr entry than do olivine and ilmenite. Solid-liquid distribution coefficient data reflect this preferential

entry of Cr into the former phases. Ewart et al. (1973) calculate the following Cr distribution coefficients for clino-, orthopyroxene, titano-magnetite and liquid pairs.

(a) $D_{Cr}^{cpx} = 33 - 0.75$

(b) $D_{Cr}^{opx} = 23 - 0.65$

(c) $D_{Cr}^{magnetite} = 58 - 27.$

From these data, it is apparent that Cr enters minerals in the following order : magnetite clinopyroxene orthopyroxene. A similar behaviour of Cr is indicated in data for the Red Hill dyke (McDougall et al., 1963) and the Palisades sill (Walker, 1970).

Burns (1969) reports that Cr enters the M_1 sites in both ortho- and clinopyroxenes. Furthermore, the Cr content of pyroxenes decreases with increasing differentiation (Walker, op.cit.; McDougall et al., op.cit.).

The distribution of Cr between olivine and liquid is difficult to evaluate. Theoretical considerations predict that an imbalance of charges would restrict entry of Cr^{3+} into divalent Fe positions in olivine but Flower (1973) reports $D_{Cr}^{olivine}$ to be as high as 3.1 - 10. It is more likely that most of the Cr determined in olivine phenocrysts is due to the presence of tiny inclusions of Cr-spinel in the olivine (Gunn, 1971).

As can be expected little Cr enters the plagioclase structure and as in the case of Ni, significant plagioclase fractionation together with femic phases, would reduce bulk distribution coefficients and so reduce the rate of Cr depletion in successive residua.

Taylor (1965) notes the use of the Cr content in rocks as an indicator of parent rock affinities. This is especially true in serpentinite and greenschist horizons in metamorphic terraines. Generally, high Cr contents point to a basic parent rock while low concentrations suggest a sedimentary origin.

Fig.6(1) indicates the behaviour of Cr with increasing differentiation in the Stapelbergkloof samples from Birds River. Cr is at a maximum in the chill-zone gabbro (235 ppm) and is rapidly reduced in the more differentiated ferrogabbros and ferrotholeiites, ultimately to values less than 20 ppm.

The variation of Cr in the Birds River intrusion is nearly identical to that at Red Hill (McDougall et al., op.cit), the

similar flattening-out of the curve to near constant values in the more silicic differentiates, in both cases, being very striking. Walker (1970) finds a similar pattern in the Palisades sill though here clinopyroxene - and olivine-rich layers cause large variations in Cr content when plotted against height in the sill.

As at Red Hill and the Palisades, no chrome-spinel inclusions were detected in olivines from the Birds River gabbros. Picotite inclusions have, however, been noted in olivines from some olivine-rich dolerites collected in the regional sample. These will be discussed in a later section but are shown in Table 8a (samples JR11, 105 and 124). These dolerites all contain more than 700 ppm Cr and high Cr concentrations could partly be due to the presence of Cr-rich spinel.

2.6
A model for differentiation at Birds River.

2.6.a
Introduction.

Five analyses from Stapelbergkloof have been used to model a simple fractional crystallization path for the gabbro-ferrogabbro-ferrotholeiite sequence at Birds River. No attempt is made to model through to the most highly differentiated ferrotholeiite stage, due to the uncertainty in which minerals are actually involved in fractionation. Few accurate mineral analyses for these highly differentiated rocks exist and quantitative modelling would be difficult.

Consequently, the model assumes only plagioclase, pyroxene and olivine fractional crystallization to produce the variations observed in the samples studied.

A general purpose, petrographic-mixing computer program, adapted by Dr. A. Duncan of the University of Cape Town Geochemistry Research Unit from that of Byran et al. (1969), has been used to simulate proportions of the above-mentioned phases that have controlled fractional crystallization at Birds River.

These data were then applied to trace element modelling using the Rayleigh Disequilibrium Fractionation Law (Gast, 1968) in a similar manner as that of Zielinski and Frey (1970) in their study of fractional crystallization in lavas from Gough Island.

Calculated trace element concentrations, with some exceptions, show fairly good correlations when compared with observed values and suggest that both major and trace element variations at Stapelbergkloof, for the range of differentiation studied, can be explained in terms of dominant plagioclase and pyroxene but only minor olivine fractionation. This conclusion is in accord with that deduced from the CaO/Y variation (Fig.9).

2.6.b
Major Elements.

The compositions of samples JR27, S30, S31, S32 and S34 and the phases, plagioclase, olivine, augite and pigeonite used in the model, are given in Tables 1(a) and 3 respectively. For modelling

Table 3: Compositions of Mineral Phases used in Mixing Model.

	1	2	3	4	5	6	7	8
SiO_2	48.6	52.10	39.15	36.10	52.50	51.30	54.00	53.00
TiO_2	.001	.001	.001	.001	.40	.50	.40	.40
Al_2O_3	32.36	30.60	.001	.001	2.70	3.50	.10	.10
FeO*	.40	.001	23.83	41.08	7.70	12.80	17.50	21.20
MnO	.01	.001	.001	.001	.20	.50	.01	.01
MgO	.08	.001	37.32	22.82	16.50	14.10	23.00	20.30
CaO	15.80	13.10	.001	.001	19.60	16.80	5.00	5.00
Na_2O	2.57	4.00	.001	.001	.40	.50	.01	.01
K_2O	.16	.20	.001	.001	.001	.001	.001	.001
P_2O_5	.001	.001	.001	.001	.001	.001	.001	.001

1. Plagioclase (An.78) (Ferguson and Wright, 1969, Table 1, No.28)

2. Plagioclase (An.64) (Estimate)

3,4 Olivine (Fo.73,50) (Eales and Booth, 1974, Table 2, No's 1,2)

5,6 Augite (1,2) (Eales and Booth, 1974, Table 4, No's 1,4)

7,8 Pigeonite (1,2) (Estimate)

* All Fe as FeO.

purposes, analyses were recalculated water-free and all Fe was expressed as FeO.

Diagrammatically, the model has been set up as follows.

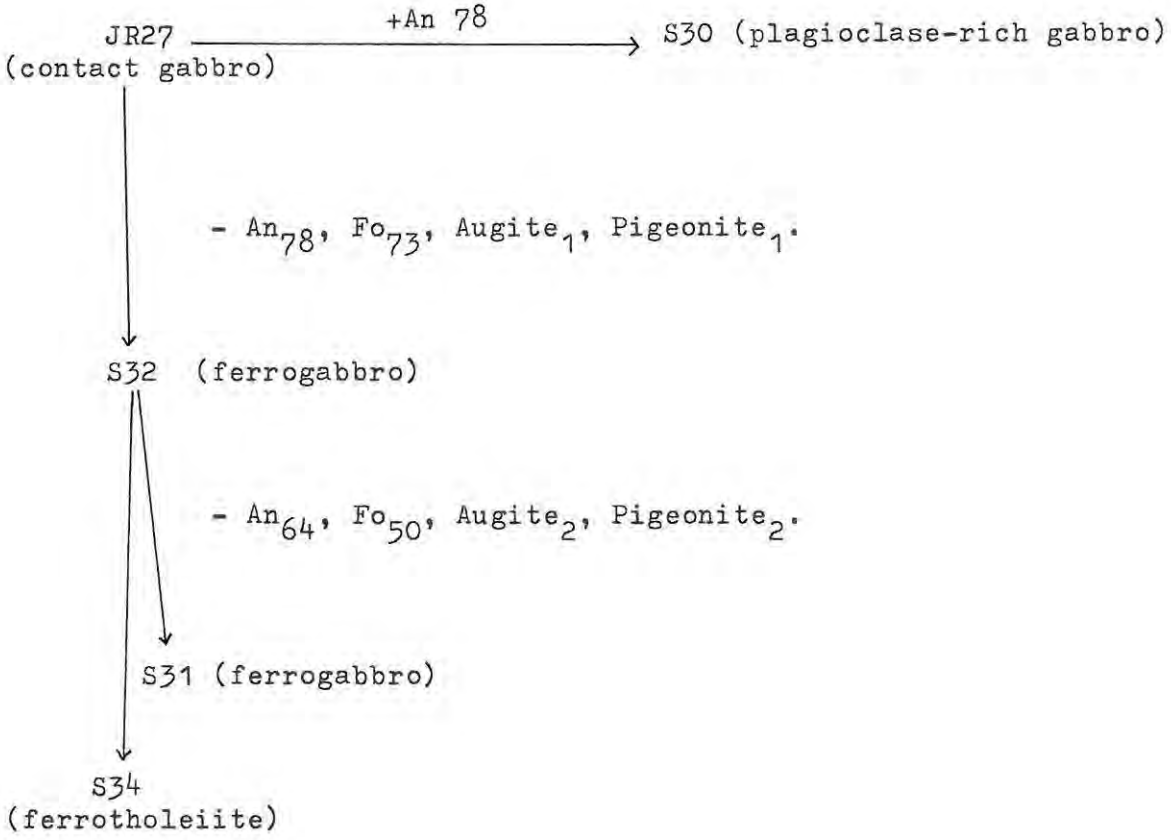

Sample JR27 has been selected as the common parent and S34, the least evolved ferrotholeiite, is derived by a two-step fractional crystallization process. The removal of calcic plagioclase, forsteritic olivine and Mg-rich pyroxenes generates a residual liquid represented by S32. The removal of more-sodic plagioclase and ferriferous pyroxene and olivine from the ferrogabbro, S32, generates residual liquids represented by the ferrogabbro, S31, and the ferrotholeiite, S34.

The criteria for establishing parent-derivative relationships have already been discussed in section 2.4. Sample S30, which has a high modal plagioclase content, high Al_2O_3 and Sr, is believed to represent a plagioclase-enriched gabbro.

A very real difficulty arises, as will always be the case when dealing with coarse-grained gabbros, in trying to decide which phases actively separated and were removed by various mechanisms, in the fractional crystallization process. It must be remembered

that, in the Birds River intrusion, all the rocks are relatively coarse-grained and that one is not dealing with a sequence of porphyritic lavas, in which the fine-grained groundmass is considered to approximate a residual liquid derived from the fractionation of the observed phenocryst phases.

The Birds River younger gabbros are clearly tholeiitic in character and, as noted by Eales and Booth (1974), calcic plagioclase and olivine were probably the first minerals to separate. This is consistent with the petrography of the rocks under discussion. Pyroxene relationships are, however, difficult to evaluate. Pigeonite is common in the gabbros and ferrogabbros and almost invariably occurs as large cores to poikilitic augites. This points to its crystallization earlier than augite. The chill-zone dolerite, JR27, is porphyritic and contains distinct phenocrysts of plagioclase, augite and altered olivine as well as large, indistinct crystals of orthopyroxene, set in a fine-grained groundmass of plagioclase and clinopyroxenes.

The gabbros and ferrogabbros (S30, S31, S32) contain both augite and uninverted pigeonite but no primary orthopyroxene, indicating that, on differentiation, Ca-poor pyroxene compositions moved beyond the orthopyroxene-pigeonite inversion point (Hess, 1949).

Eales and Booth(op.cit)show that magnetite crystallized in significant amounts only when plagioclase (An_{61}) was separating. Molar ratio diagrams (Fig.4a) suggest that the ratio TiO_2/K_2O remains constant over the range in compositions modelled. The contention that opaque oxides have had little effect on the earlier stages of fractionation is also supported by the V variation diagram (Fig.6k).

Accordingly, only 4 phases - plagioclase, olivine and two pyroxenes, were used as a first approximation to derive successive liquids from a parent gabbro composition represented by sample JR27.

That the sequence at Stapelbergkloof shows the attributes of true liquid residua, is seen in the various trace element variation trends. The residual trace elements Rb, Zr, Y, Nb, Zn and Ba increase with differentiation. Sr decreases, consistent with plagioclase fractionation, while Ni and Cr are rapidly depleted, consistent with olivine and pyroxene fractionation.

The computer mixing-program is simply a quantitative equivalent

of the graphical addition and subtraction diagrams long used by petrologists. It has the advantage, however, of treating all data in a systematic fashion to achieve a unique, though not necessarily correct, solution. Inputs are weight percent oxides in each mineral and/or rock used as a variable component, and oxides of the material to be generated. Unknowns are the weight fractions of each component, which when multiplied by the component compositions, best approximate the composition to be derived. Solutions are generated for a matrix of linear equations of the type A.X=B, with the solution matrix, X, being that which minimizes the differences between B=input and B* = calculated matrix (Byran et al., 1969; Zielinski and Frey, 1970).

In the solutions (Tables 4a-d), the matrices are set up such that the various weight fractions should be positive i.e. addition of the variable components will generate the parent composition.

Table 4a: Least squares approximation to parent JR27, calculated as a linear combination of ferrogabbro S32, + An_{78} + Fo_{73} + $Augite_1$ + $Pigeonite_1$.

	JR27 (obs.)	JR27(calc.)	Diff.	Variable	Wt. Fraction.	
SiO_2	52.56	52.60	.04	S32	.6858	
TiO_2	1.07	1.02	-.05	An78	.1221	
Al_2O_3	15.75	15.73	-.02	Fo73	.0242	
FeO	9.24	9.15	-.09	$Augite_1$	.1721	.1678
MnO	.19	.16	-.03	$Pigeonite_1$	-.004	
MgO	6.30	6.34	.04			
CaO	11.84	11.80	-.04	$\Sigma(\text{residuals})^2 = 0.09$.		
Na_2O	2.04	2.29	.25			
K_2O	.61	.71	.10			
P_2O_5	.18	.18	-			

Comments:

1) The negative TiO_2, FeO and positive MgO residuals may possibly be improved by fractionating a more ferriferous olivine or pyroxene. The TiO_2 residual suggest some magnetite may need to be fractionated, though the Birds River pigeonites may contain more TiO_2 than has been assigned in the estimated analyses (Table 3, No.7).

2) The Na_2O and K_2O residuals seem to be consistently poor in all the solutions. The Na_2O residual is always positive, showing an excess of Na in the variable components. In Table 4(a), fractionating a more calcic plagioclase may improve the CaO residual and reduce the Na_2O residual. However, this would be unrealistic for the plagioclase composition, An_{78}, is probably the most calcic to be found in the Birds River gabbros. Alternatively, excess alkalies trapped within the interstitial micropegmatite found in the gabbros, may distort the residuals for K_2O and Na_2O.

3) Table 4(a) suggests that it is feasible to derive the ferrogabbro, S32, by the removal of 12.2% An_{78}, 2.4% Fo_{73} and 16.8% pyroxene from the parent composition, JR27.

Table 4b : Parent (S32) - Derivative (S31).

	Parent S32(obs.)	S32(calc.)	Diff	Variable	Wt. Fraction.	
SiO_2	53.82	53.70	-.12	S31	.8964	
TiO_2	1.38	1.49	.11	An_{64}	.0753	
Al_2O_3	16.51	16.52	.01	Fo_{50}	-.0249	
FeO	10.64	10.59	-.05	$Augite_2$	-.0078	.0532
MnO	.18	.17	-.01	$Pigeonite_2$	.0610	
MgO	3.91	4.01	-.09			
CaO	9.47	9.47	00	$\Sigma (residuals)^2 = 0.18$		
Na_2O	2.78	2.85	.07			
K_2O	1.01	1.38	.37			
P_2O_5	.27	.26	-.01			

Comments:

1) This mix is rather poor. Residuals SiO_2, TiO_2, MgO and K_2O could possibly be improved by slightly altering the compositions of the phases being fractionated.

2) It is interesting that at this stage pigeonite is the dominant pyroxene being removed. Fractionation of plagioclase (7.53%) and pigeonite (5.32%) control differentiation, though minor olivine must be added to S32 to balance the system.

Table 4c : Parent (S32) - Ferrotholeiite (S34).

	Parent S32(obs.)	S32(calc.)	Diff.	Variable	Wt. Fraction.
SiO_2	53.82	53.98	.16	S34	=.6500
TiO_2	1.38	1.39	.01	An_{64}	=.2098
Al_2O_3	16.51	16.55	.04	Fo_{50}	=-.0025
FeO	10.64	10.67	.03	$Augite_2$	=.0698
MnO	.18	.16	-.02	$Pigeonite_2$	=.0729
MgO	3.91	3.94	.03		
CaO	9.47	9.50	.03	$\Sigma (residuals)^2 = .06$	
Na_2O	2.78	2.94	.16		
K_2O	1.01	.97	-.01		
P_2O_5	.27	.27	0.0		

Comments:

1) This is a reasonable mix and it is shown that to derive the ferrotholeiite, S34, from the ferrogabbro, S32, significant amounts of plagioclase (20.98%) and pyroxene (14.27%), though little or no olivine, must be removed from S32.

Table 4d : Parent (JR27) - plagioclase-rich gabbro (S30).

	Parent JR27(obs.)	JR27 calc	Diff.	Variable	Wt. Fraction
SiO_2	52.56	52.61	.05	S30	1.0805
TiO_2	1.07	.83	-.24	An_{78}	-.0885
Al_2O_3	15.75	15.69	-.06	Fo_{73}	-.0057
FeO	9.24	8.92	-.27	$Augite_1$	.0286
MnO	.19	.18	-.01	$Pigeonite_1$	-.0149
MgO	6.30	6.42	.12		
CaO	11.84	11.71	-.13	$\Sigma (residuals)^2 = .55$	
Na_2O	2.04	2.65	.61		
K_2O	.61	.61	0.0		
P_2O_5	.18	.14	-.04		

Comments:

1) This mix attempts to show that S30 is a plagioclase-rich equivalent of the initial parent composition. Residuals are, however, on the whole bad and quantitatively not much weight is attached to this example.

Summary.

Mixing equations have shown that reasonable solutions can be obtained by explaining the variations in major element contents between the gabbro, ferrogabbros and ferrotholeiites in terms of dominant plagioclase and pyroxene but subordinate olivine fractionation.

The following equations can be written.

$$100\ JR27 = 68.58\ S32 + 12.21\ An_{78} + 2.42\ Fo_{73} + 16.78\ Pyrox._1$$
$$100\ S32 = 89.64\ S31 + 7.53\ An_{64} - 2.49\ Fo_{50} + 5.32\ Pyrox._2$$
$$100\ S32 = 65.00\ S34 + 20.98\ An_{64} - .25\ Fo_{50} + 14.27\ Pyrox._2$$
$$100\ JR27 = 108.05\ S30 - 8.85\ An_{78} - .57\ Fo_{73} + 1.37\ Pyrox._1$$

In this simple model, the ferrotholeiite, S34, represents the residual liquid (44.58%) left after the fractional crystallization of 55.42 weight percent of the initial magma represented by the chill-zone dolerite, JR27. This is not an unrealistic amount.

2.6.c

Trace Elements.

The major element model can now be tested in terms of selected trace element variations within the range of samples studied. Should a significant correlation be obtained between the calculated and observed values, it would be a powerful argument in justifying the results of the major element model.

Trace element variations at Birds River can best be explained in terms of the Rayleigh Fractionation Law applicable to non-equilibrium systems (Gast, 1968). Zoning of both plagioclase and pyroxene is ubiquitous at Birds River (Eales and Booth, 1974) and indicates that crystal cores have not equilibrated to the residual liquids.

The formula $C_a^l / C_a^o = F^{Da-1}$ (after Gast, op.cit.) relates the enrichment of a trace element (a) in the derivative liquid (C^l) relative to the initial concentration in the parent liquid (C^o), to the weight fraction of liquid that remains (F), after the fractionation of a phase, having a distribution coefficient (D) for element (a). The distribution coefficient used here, is defined as $(\frac{\text{conc. in crystal}}{\text{conc. in liquid}})$. Where more than one phase is involved in fractionation, a bulk distribution coefficient for all the

phases, for the particular element under consideration, must be calculated. This is done by averaging the various distribution coefficients, weighted according to the proportions in which the different phases crystallize (Gast, op.cit.).

Table 5 is a list of distribution coefficients used for the various trace elements modelled.

Table 5 : Selected distribution coefficients (D).

	D_{Sr}	D_{Ba}	D_{Rb}	D_{Ni}
plagioclase	2.2[1]	.25[1]	.03[1]	.2[4]
olivine	.001[2]	.001[2]	.001[2]	16.0[3]
clinopyroxene	.10[2]	.003[3]	.003[2]	7.0[5]

References :
1. Knorringa and Noble (1971), Ewart et al. (1973).
2. Hart and Brooks (1974).
3. de Long (1974), Gunn (1971).
4. de Long (1974).
5. Ewart et al. (1973), Jensen (1973, Fig.8).

The selection of trace element distribution coefficients, if these are not actually determined, is often subjective. Furthermore, the effects of numerous variables, such as magma composition, phase composition and temperature, which influence the value of distribution coefficients, are still not quantitatively well known.

Tables 6(a), (b) and (c) compare calculated trace element concentrations with those actually observed. Fig.11(a) indicates calculated and observed values in diagrammatic form. In Tables 6(a), (b) and (c) the bulk distributions (D*), calculated according to mineral proportions predicted in Tables 4(a), (b), (c) and (d) and used in the Gast calculation, are also shown.

Table 6a : JR27 - S32

	JR27 (obs.)	S32 (obs.)	S32 (calc.)	D*
Sr	257	265	279	.780
Ba	225	307	316	.099
Rb	11.5	20	17	.013
Ni	89.10	17	18.6	5.160

Table 6b : S32 - S31

	S 32 (obs.)	S31 (obs.)	S31 (calc.)	D*
Sr	265	266	258	1.29
Ba	307	322	328	.148
Rb	20	21.8	22.1	.019
Ni	17	16.7	14.2	3.015

Table 6c : S32 - S34

	S 32 (obs.)	S34 (obs.)	S34 (calc.)	D*
Sr	265	250	230	1.340
Ba	307	458	437	.179
Rb	20	29.5	31.6	.001
Ni	17	5.61	7.3	2.953

Concentrations are in p.p.m.

2.6.d

Discussion.

Ba, Rb and Ni calculated concentrations tend to be in good agreement with observed values. Ni is of particular importance for it is the one trace element, in those modelled, that is rapidly depleted with increasing differentiation at Birds River.

The behaviour of Sr is more difficult to model. Initially, (Table 6a) S32 shows an enrichment in Sr relative to the parent composition, JR27. This is consistent with a bulk D^*_{Sr} of less than unity. The calculated concentration of Sr in S32 is, however,

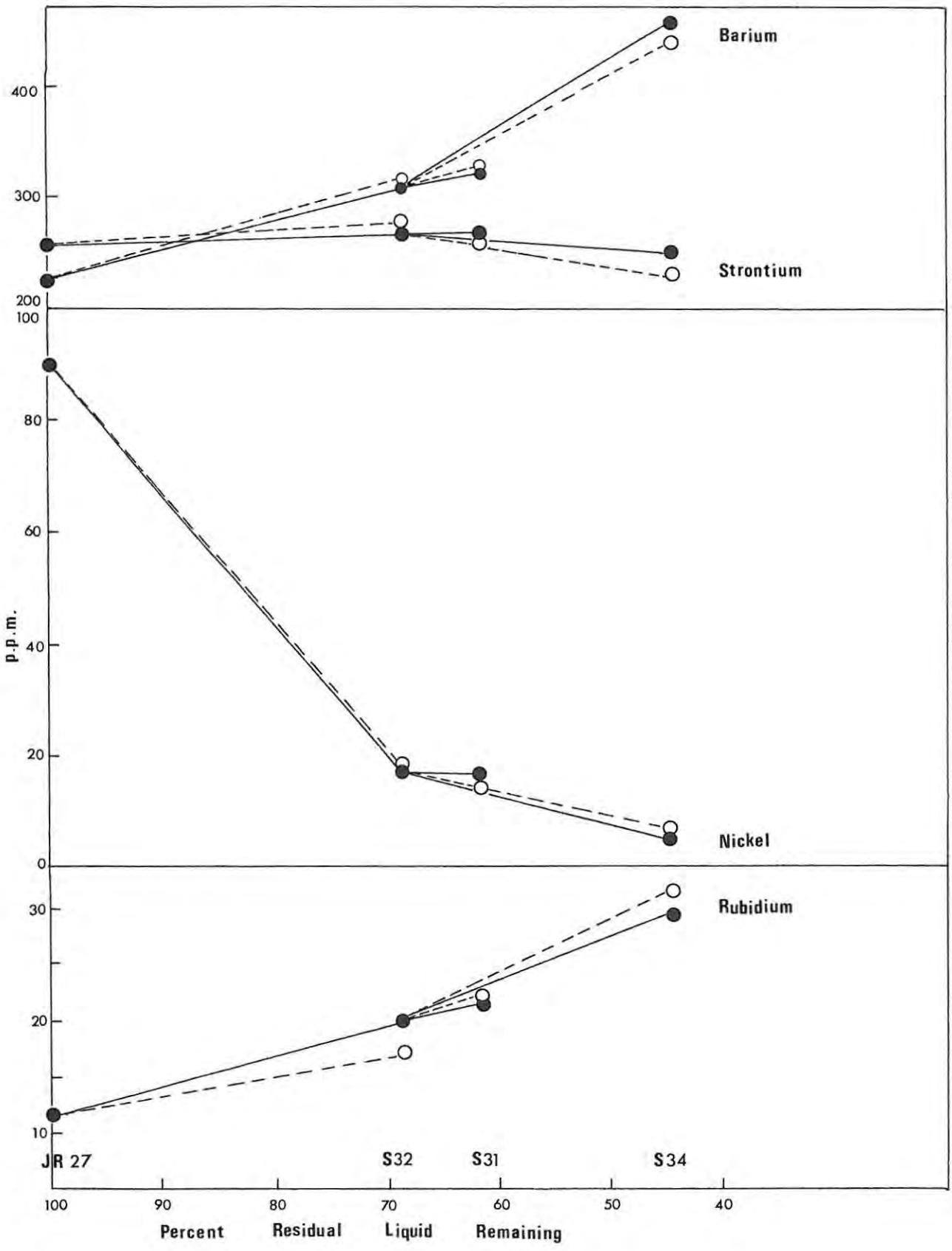

Fig.11(a): Diagrammatic representation of the Trace Element Modelling Exercise.

● Observed trace element concentration.

○ Calculated trace element concentration.

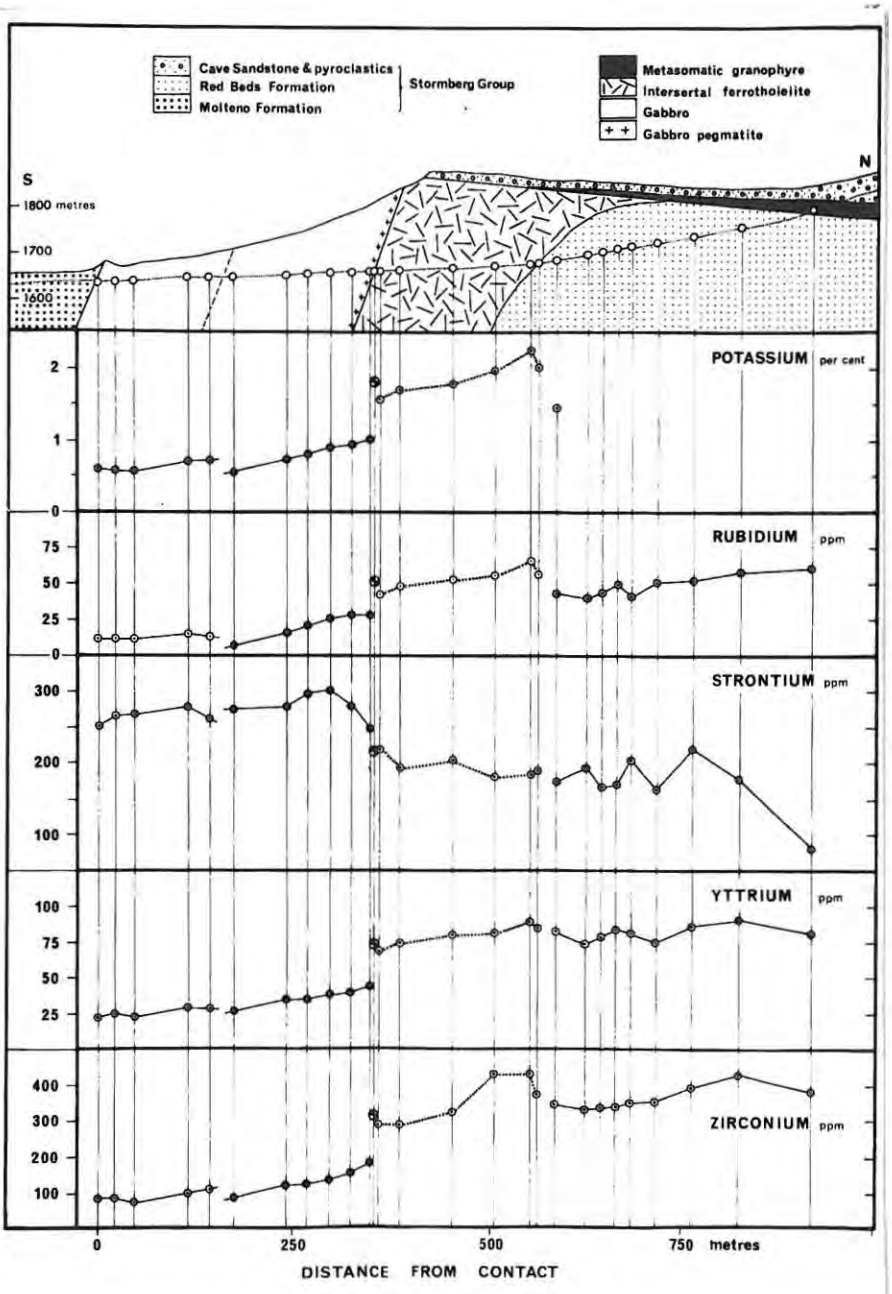

Fig.11(b): Section across south-western margin of the Birds River Complex, on the farm Denwood, showing country rock on left, xenolithic fragment on right and intrusives in centre. Variations in K and trace elements are shown for a traverse along a deeply eroded gulley (from Eales and Robey, in press, Fig.6).

too high and suggests a larger $D_{Sr}^{plag.}$ should have been used in the calculation, to increase the bulk D^*_{Sr} to near 1. However at a later stage, (Table 6c) when plagioclase, An_{64} is fractionated, the Sr calculated concentration is too low suggesting a smaller $D_{Sr}^{plag.}$ be used. This is, however, contrary to the inverse relationship of $D_{Sr}^{plag.}$ to the An% of plagioclase established by Philpotts and Schnetzler (1970). The difficulty in modelling Sr variations is similar to that of Na_2O in the major oxides. These two elements are closely associated with plagioclase and again Na- and K-rich micro-pegmatite, occurring in the gabbros and ferrogabbros, may distort the simple model employed.

Though no attempt has been made to adjust distribution coefficients to differences in mineral compositions and to changing temperatures of crystallization, the reasonably good correlation found between the calculated and observed trace element concentrations in some residual rocks at Birds River, suggests that a fractional crystallization model involving dominant plagioclase and pyroxene but minor olivine fractionation, could relate the gabbro-ferrogabbro-ferrotholeiite sequence at Stapelbergkloof. The ferrotholeiite composition (S34) is believed to represent the residual liquid left after the crystallization of 55.4% of the original Birds River magma, represented by the composition of the contact dolerite, JR27.

2.7
Conclusion.

Field evidence from the Denwood type-section at Birds River suggest the emplacement of highly fractionated magmatic residua, derived from a deeper Kokstad-type magma source, during cauldron subsidence of a mass of sediments within an annular fracture (Eales and Robey, in press). Field relationships between the older ferrotholeiites and younger gabbro-ferrogabbros are clearly seen in the Denwood section. (Fig.11b). Here it has been possible to study trace element variations across the intrusive contact between the ferrogabbros and the ferrotholeiites.

Eales and Robey (op.cit., Fig.6) note the early intrusion and rapid cooling of the residual ferrotholeiites, while the younger gabbro was emplaced in a series of closely-spaced heaves of fresh magma from the original source region. Each of these later gabbro pulses differentiated in place by inward crystallization from the

cooler outer margin, driving liquid residua inwards to the ferrotholeiite contact where they crystallized as the pegmatoidal facies.

A similar sequence of gabbro-ferrogabbro-ferrotholeiite is found at Stapelbergkloof but, in contrast to Denwood, the ferrogabbro-ferrotholeiite contact has not been accurately located in the field. Petrographic evidence i.e. the sudden appearance of glassy, porphyritic tholeiites identical to those described by Eales and Booth, (1974), however, suggest this contact must be near that indicated in Fig.2.

Furthermore, the sharp discontinuity in the levels of Rb, Zr, Y and Sr indicated in Fig.11(b) across the ferrogabbro-ferrotholeiite transition, is not seen in element variation diagrams for the sequence at Stapelbergkloof. This may partly be due to the limited number of samples analysed in this study.

The compositions of gabbros and ferrogabbros from Stapelbergkloof are similar to those at Denwood but, for the most part, the ferrotholeiites from the former section are not as highly chemically evolved as those at Denwood. Levels of the residual trace elements Ba, Zr, Rb, Nb, Y and Zn as well as the major oxides SiO_2, Fe_2O_3, K_2O, Na_2O and P_2O_5 attest to this.

A simple fractional crystallization path has been modelled for part of the gabbro-ferrotholeiite sequence at Stapelbergkloof. This assumes the ferrotholeiites to be derived from a magma source similar to that which gave rise to the younger gabbros. During the initial stages of differentiation, the fractionation of plagioclase and pyroxene and minor olivine is indicated while in the more highly differentiated ferrotholeiites, minor amounts of apatite and magnetite removal are suggested by sharply decreasing P_2O_5 and V concentrations respectively.

Though more detailed research, especially into mineralogical variations, is needed, the new major and trace element data presented in this study for the differentiated sequence at Stapelbergkloof, Birds River, clearly indicate levels to which tholeiitic magmas are differentiated in some Karroo intrusions.

3.
REGIONAL STUDY OF THE KARROO DOLERITES AND BARKLY EAST BASALTS.

3.1.a
Introduction.

New major- and trace-element data are presented for thirty Karroo dolerites from the North-Eastern Cape and Border regions. Also presented are new data for ten basalts and one andesite from the Barkly East area.

Though major element variations within the Karroo dolerites have been studied in great detail by Walker and Poldervaart (1949), the only trace element data readily available are those from Nockolds and Allen (1956). Similarly, geochemical data exist for the Basutoland (Lesotho) lavas (Cox and Hornung, 1966) while more recent major element analyses for some Barkly East basalts are reported by Lock et al. (1974, Table 1).

While not wishing to detract from the work of the above authors, the need is sorely felt for more-accurate analyses of the trace element content of both the dolerites and the basalts. The Karroo dolerites presented in this study thus represent a regional sample collected during road traverses in the North-Eastern Cape. The geochemistry of the Karroo basalts in the Barkly East area are at present being investigated in a separate project at Rhodes University and data presented in this study for some Barkly East basalts must be considered as only a preliminary pilot study to a more detailed investigation.

This second section of this dissertation thus only attempts to provide new major- and trace-element data for some Karroo dolerites and basalts. More advanced analysing techniques such as the X-ray Fluorescent method, enable the rapid analysis of a large number of samples. Trace element data previously reported by Walker and Poldervaart (op.cit.), Nockolds and Allen (op.cit.) and Cox and Hornung (op.cit.) were determined by optical spectrographic methods. Erlank and Hofmeyer (1966) in their discussion of the variation of K/Rb ratios in Karroo dolerites dismiss the wide variation of this ratio, noted by Nockolds and Allen (op.cit.) as being "almost certainly due to the semi-quantitative nature of the spectrographic method used ...", while differences in the levels of Ba, Zr and Rb determined by X-ray fluorescent techniques (X.R.F.) (analyst - G. Hornung) and by the optical spectrographic method (analyst - J.M. Rooke) in some Basutoland basalts, leave much to be desired (see

Cox and Hornung, op.cit., Table 3). This must not be interpreted as a criticism of the above-mentioned researchers, data or conclusions reached from those data. X.R.F. techniques for trace element determination have only recently come to the fore and were not available to earlier researchers.

Variations in the major- and trace-element content of the Karroo dolerites and some Barkly East basalts are discussed and compared with the aid of oxide variation diagrams. Normative chemistry is discussed following the method of Cox and Hornung (op.cit.). New trace-element data are compared with previous data (Tables 10,11), though little published data exist for certain trace elements such as Nb, Zn and Cu in Karroo dolerites and basalts.

Data are also compared with trends from the Birds River Complex, the latter intrusion being an example of strong differentiation of Karroo magma. The geochemical differences noted by Cox et al. (1967) between the northern and southern Karroo volcanic provinces are upheld, while little comment can be made on the hypothesis of Rhodes and Krohn (1972).

This study does not attempt to draw any wide-ranging conclusions as to the nature of the Karroo magmatic episode.

The area studied represents too small a portion of the whole region affected by the Karroo intrusive and extrusive cycle, to warrant such conclusions. These conclusions must rather be drawn when data for the Karroo basic rocks from the other areas of Southern Africa under investigation during the Geodynamics program, can be collated and analysed.

3.1.b

Previous Work:

Karroo dolerites:

The work of Walker and Poldervaart (1949) remains the classic study and guide-line for any investigation into the Karroo dolerites of South Africa. The general distribution, habit of intrusion and mineralogy of the dolerites are discussed while a classification based on petrographic type is presented.

Walker and Poldervaart (op.cit., Tables 15,16) present full major-element analyses for more than 80 Karroo dolerites ranging from the most basic picrites from the Elephant's Head and Insizwa

intrusions to iron-enriched marginal tholeiites from Mount Arthur and New Amalfi, to dolerites of the Perdekloof, Kokstad, Blaauwkrans and other petrographic types and through to more acid differentiates, residual pegmatites and metasomatic granophyres. The major element chemistry of the dolerites of different petrographic types are discussed, analysed and summarized in averaged compositions (Walker and Poldervaart, op.cit., Table 16) while the iron-enrichment trends with increasing differentiation in some dolerite intrusions and the trend for the province as a whole, are compared with iron-enrichment trends from the Palisade sill, Skaergaard and other areas of regional basic rock intrusive and extrusive activity (Walker and Poldervaart, op.cit., Figs. 27-35).

While the former authors only briefly discuss some trace element data (Walker and Poldervaart, op.cit., Table 14), the standard reference for such data in Karroo dolerites is Nockolds and Allen (1956, Tables 20-23).

Nockolds and Allen (op.cit.) note that Walker and Poldervaart (op.cit.) were able to recognize three trends amongst the Karroo dolerites.

(a) The main trend to which the majority of dolerites conform, is characterized by a slight absolute enrichment in Fe.

(b) An Fe-rich trend best seen in rocks from the Elephant's Head and New Amalfi intrusions and characterized by a considerable absolute Fe-enrichment factor.

(c) A third trend in which there is no absolute Fe-enrichment and which is represented by relatively few samples.

Nockolds and Allen (op.cit.) compare the behaviour of some trace elements in the normal trend with that of the Fe-rich trend. The decrease in Co content with increasing differentiation is more rapid in the Fe-rich trend, while in both trends Ni and Cr are greater than Co at the early stages of differentiation but are rapidly depleted with increasing differentiation. Moreover, Ni is higher in the earlier members of the Fe-rich trend than in corresponding members of the main trends but also falls to below detection limits earlier in the Fe-rich trend. The concentration of V does not increase to a maximum in the main trend though in the Fe-rich trend, a feeble V maximum occurs slightly earlier than the Fe^{2+} maximum. Sr is low in both trends but tends to be higher in the main trend while the increase in Y with differentiation is more pro-

nounced in later differentiates of the Fe-rich trend. K, Ba, Rb and Zr rise sharply with increasing differentiation in both trends. The increase in Rb is more marked in the main dolerite trend while Zr is relatively more-enriched in later members of the Fe-rich trend.

Trends for the Mt. Arthur tholeiites are similar to those of the main trend but these tholeiites are generally depleted in Ni and sometimes, Cr and Co. Olivine-adcumulative rocks in both trends are enriched in Cr, Ni and Co but depleted in Zr, Y, Sr and Ba.

Late-stage dolerite pegmatites from both the main and third trends are notably enriched in Zr, Sr, Ba, Rb and Y while the trace element contents of the metasomatic granophyres are "peculiar", readily distinguishing these rocks as being abnormal.

The average trace element content of 12 Karroo dolerites with MgO less than 9%, has been computed from the data of Nockolds and Allen (op.cit., Tables 20, 22, 23) and is shown in Table 10; G. With the exception of slightly lower Rb but higher Cr, the average composition is similar to that presented by Cox and Hornung (1966, Table 3; B), Table 10; F. This latter average was also compiled from data by Nockolds and Allen (op.cit.) and is the average trace element composition of 16 Karroo dolerites that cover the same range of Fe/Mg index as the Lesotho basalts studied by Cox and Hornung (op.cit.). These two averages are compared with the average trace element content of Karroo dolerites with MgO less than 9%, presented in this study.

Erlank and Hofmeyer (1966) present new K, Rb and Cs data for the Karroo dolerites and compare the average K/Rb ratio of the Karroo province with average values from the Antarctic and Tasmanian dolerites. They note that K/Rb ratios for the Karroo dolerites range between 303 and 609 and average 465, distinctly higher than the ranges 188-222 and 198-300, determined for the Tasmanian and Antarctic dolerites respectively. Further geochemical comparisons between the Mesozoic basic rocks of South Africa, Antarctica and Tasmania, are drawn by Compston et al. (1968).

Karroo basalts:

Cox and co-workers have been tireless investigators into the geochemistry of the Karroo basalts, though having tended to concentrate on the Karroo volcanics exposed in Rhodesia.

Cox and Hornung (1966) discuss the petrography of the Basutoland (Lesotho) basalts and present new major- and trace-element data for

24 basalts sampled through a sequence some 5000' thick in Northern Lesotho.

Cox et al. (1967) present new analyses for Karroo volcanics from Rhodesia and Swaziland and find that large-scale geochemical differences exist between basalts from their defined northern Karroo province (Rhodesia) and volcanics from the southern province (Lesotho, Swaziland and Karroo dolerites). Relative to the southern province, the northern province shows an absolute enrichment in K, Ti, P, Ba, Sr and Zr by factors of approximately 2-4. Nb and Y are probably enriched by a similar amount while the Ni/Mg ratios of the northern province are approximately twice those of the Karroo dolerites and Lesotho basalts, but similar to ratios for the Swaziland basalts.

A similar regional analysis of the Karroo basic rocks is discussed by Rhodes and Krohn (1972). Using a statistical approach involving trend surface analysis of available chemical data for the Karroo province, these authors propose the "basin-margins, - centre"[1] model.

From their study, Rhodes and Krohn (op.cit.) conclude that rocks from the defined central Karroo basin are significantly higher in Si, Al, Mg and Ca and lower in Fe^{3+}, Na, K, Ti and P with respect to rocks from the basin margins. Rocks from the basin margin north of 26°S are similar to those from the basin margin south of 26°S except for significant differences in Si, Ti and Fe^{3+}. Basic rocks from the central Karroo basin are significantly higher in Al, Mg and Ca but lower in Ti, Na, K and P relative to rocks from the basin margin south of 26°S. Rhodes and Krohn (op.cit.) thus note a strong tendency for trend surfaces to correspond to the configuration of the central Karroo structural basin and feel that the distinction between northern and southern provinces suggested by Cox et al. (op.cit.) does not adequately describe regional geochemical trends in the Karroo province.

Cox (1970) sets the Karroo volcanic period in the tectonic framework of Southern Africa and suggests that the "pre-existing pattern of basement cratons and orogenic belts exerted a profound influence on the development of the Karroo rocks". This was followed at a later date, by a review of the Karroo igneous cycle in Southern Africa (Cox, 1972), wherein vulcanism is related " to a single unifying thermotectonic event, postulated as initiating the disruption of Gondwanaland".

[1]-Italics are the present author's own.

More specifically, the Karroo volcanic rocks of the Barkly East area are discussed by Lock et al. (1974). These authors find that by applying normal stratigraphic mapping techniques, a number of lithostratigraphic units can be recognized.

Lock et al. (op.cit.) give a brief outline of the volcanic history of the Karroo basin and note that "evidence is accumulating that volcanic activity commenced well before the deposition of the last Stormberg sediments". The presence of the mineral laumontite; mudstones rich in devitrified glass shards (Elliot and Watts, 1974), ashbeds and greywackes rich in volcanic fragments (Martini, 1974) in Ecca and Beaufort sediments, the common occurrence of diatremes throughout the north-eastern Cape and the basalt flow lava found interbedded in Red Beds sediments near Rossouw, all suggest that "volcanism was sporadic" during most of the Karroo sedimentary cycle but that extrusive activity "became widespread only towards the close of sedimentation of the Cave Sandstone".

For details of the stratigraphy of the lower Karroo basalts in the Barkly East area, the reader is referred to Lock et al. (op.cit.). Briefly, these authors propose that the igneous Karroo extrusives be termed the "Volcanic Group", subdivided into the Lebombo and Drakensberg Subgroups.

The basalts in the Barkly East area form the lower horizons of the Drakensberg Subgroup. In this area three main Formations are mapped.

The basal formation - Moshesh's Ford Formation - is composed of the products of eruption from three localized volcanic centres - at Kelvin Grove, Broadford, Belmore and possibly from a centre slightly to the west of Barkly East that erupted the Donnybrook basalts. This formation has been subdivided into the following members (numbered from the base upwards):

Moshesh's Ford Formation.

7. Belmore Andesite Member. } developed only on the farm Moshesh's Ford.
6. Bell River Andesite Breccia Member. }
5. Dingle Tuffite Member.
4. Donnybrook Basalt Member.
3. BellKop Bedded Pyroclastic Member.
2. Jennerville Chaotic Pyroclastics Member.
1. Drumbo Basalt Member.

The Drumbo basalts are tholeiitic basalts seldom thicker than 5 metres, forming a "shield-shaped pile"; some 80 metres thick in the

type-section. These lavas are mostly of the pahoehoe type, though horizons of pillow lavas have been mapped at two localitites.

The Donnybrook basalts appear related to an eruptive centre further to the west of Barkly East. These basalts form thin individual flows, some highly amygdaloidal, and are petrographically similar to the Drumbo basalts. These basalts, 37 metres thick in the gorge of the Kraai River, opposite the 8th Reverse of the railway line between Barkly East and Aliwal North, thicken rapidly towards the west. A thickness of over 70 metres is measured in the new roadcut above the new road bridge over the Kraai River at Donnybrook.

Overlying the Dingle Tuffite of the Moshesh's Ford Formation, are the basalts and pillow lavas of the Kraai River Formation. This formation is characterized by thick, massive, generally aphanitic, tholeiitic flows with pillow-lavas developed at numerous horizons at various localities. The form, habit and petrography of these pillow-lavas are discussed in detail by Lock et al. (op.cit.), who, on this evidence, support the contention of previous workers, that "aqueous conditions persisted locally over large areas of Southern Africa at this time".

The laterally more-widespread basalts that form the thick lava succession generally referred to as the Basutoland/Lesotho lavas, overlie the Kraai River Formation. Lock et al. (op.cit.) propose these basalts be termed the Lesotho Formation in informal usage.

To summarize, the initial Karroo-age volcanic activity in the Barkly East area is represented by basalts, lahars, pyroclastics and tuffites erupted from or derived from localized centres of relatively explosive igneous activity. An example of such, is the large caldera structure preserved at Kelvin Grove (Lock et al., op.cit., Figs. 8(a), (b)). Volcaniclastic debris become less prominent during the more effusive eruptions of basalts forming the Kraai River Formation, while the lavas forming the massive pile of the Lesotho Formation were probably erupted quietly from large feeder fissure systems.

Walker and Poldervaart (1949) in their brief discussion of the Drakensberg lavas, note, apart from olivine-rich and -poor types, the presence of bronzite basalts in the Barkly East area and match these to the Hangnest type of Karroo dolerite. They present an analysis of one such bronzite basalt (Walker and Poldervaart, op.cit., Table 27; e). This composition matches very closely that of the Donny-brook basalts presented in Table 9(a).

3.2

Sample Locations and Geological Setting.

The locations of the Karroo dolerite and Barkly East basalt sampling sites are shown in Fig.12.

The sample of Karroo dolerites and some Barkly East basalts was collected during road traverses throughout the north-eastern Cape and Border regions. Five basalts (S5, S6, S9, 3/10, S17) are repeat major element analyses of samples collected by Dr. B.E. Lock and analysed by Dr. A. Paverd (Lock et al., 1974):- see Appendix 4. The distribution of trace elements in these basalts was not studied by the above-mentioned authors and trace element data presented in Table 9(a) are thus new.

Karroo dolerites:

Of the thirty dolerites presented in Table 8(a), twenty are true contact specimens. These samples were collected either directly adjacent to a contact zone with country-rock sediments or within a maximum, arbitrary distance of 20 cm from a contact. In every case, these contact dolerites are porphyritic. The terms "contact" or "chilled" dolerite used throughout this dissertation, refer only to this group of dolerites.

The remaining dolerites were sampled at distances greater than 20 cm from any contact zone. Some dolerites are very coarse-grained, while in many cases these non-contact dolerites are fine-grained, intersertal and show the development of a glassy mesostasis invariably crowded with pyroxene and plagioclase microlites and minute iron ore crystals. This intersertal texture has been described by Eales and Booth (1974) for dolerites from Birds River that belong to the near-contact facies. These authors apply the term "tholeiitic texture" to the near-contact facies dolerites "in accordance with the definition by Bailey and co-workers".

Considering the effect of different degrees of differentiation, these finer-grained dolerites are chemically, very similar to the porphyritic, contact dolerites.

An object of this study was the collection of a regional sample of Karroo dolerite contact specimens. This was with the view of studying the composition of the initial magma(s) at the time of emplacement, unaffected by any local differentiation or sediment contamination. Contrary to that expected, Karroo dolerite contact zones are often poorly exposed and/or highly weathered. Road

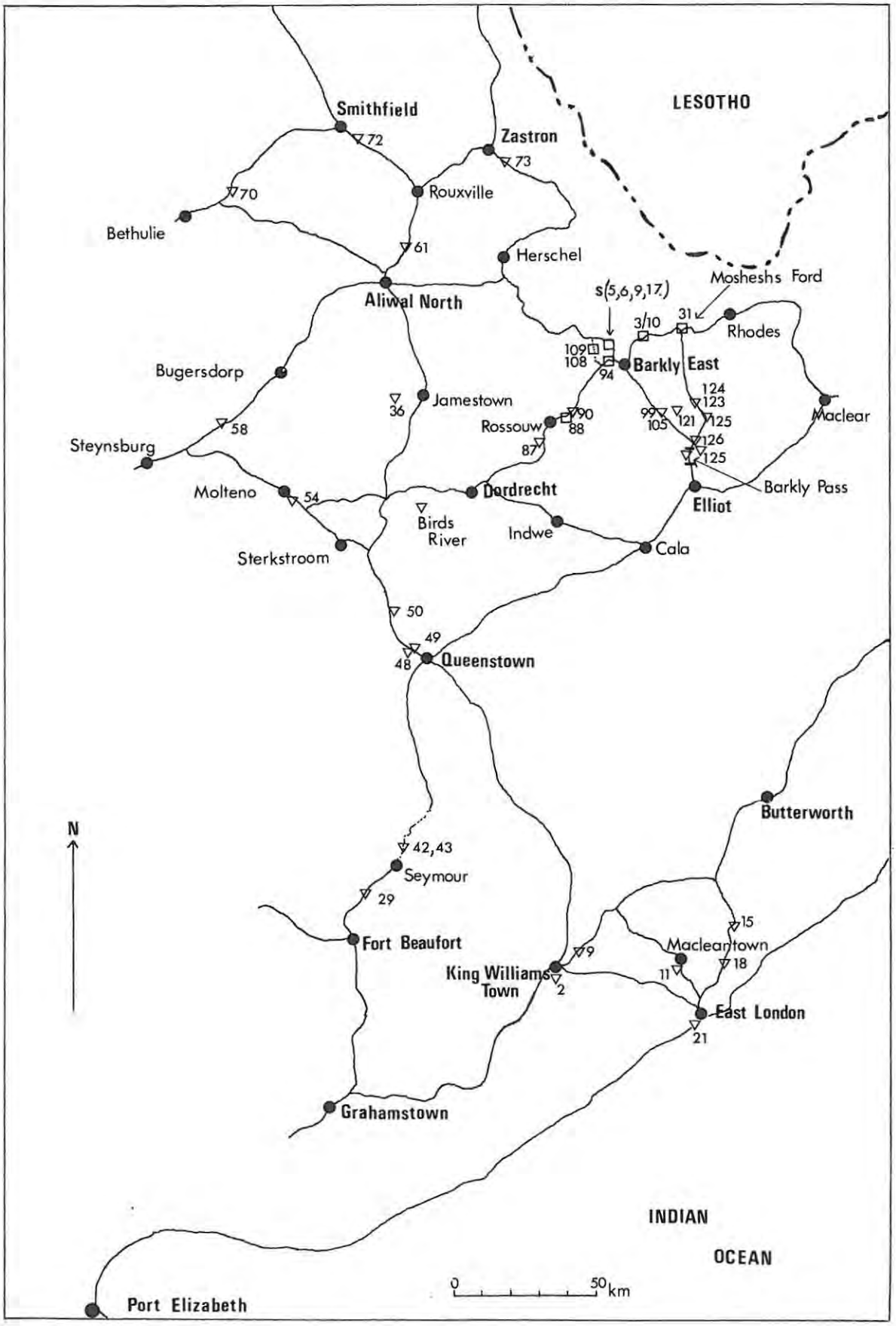

Fig.12: Location map of the sampling sites showing roads traversed in the area bounded by East London, Barkly East and Smithfield.

▽42 - Karroo dolerite
□94 - Karroo volcanics of the Barkly East area.

Sample Locations (see map, Fig.12).

Karroo dolerites

JR 2 Lower contact, Laing's Dam sill, 3 km S of King William's Town on dirt road to Peddie and Mt. Coke; sample taken near bridge over the Nqgokeweni River : 27°23'E, 32°54'S.

JR 9 Top contact, sill, 10 m thick, in road-cut 10 km from King William's Town on the road to Komga and Butterworth; 1 km past road junctions to Hanover and Frankfort : 27°27'E, 32°50'S.

JR 11 Non-contact sample, dyke, strike NE, 3 km SW of Macleantown on the Berlin road turn south to Fort Jackson; sample taken .75 km from this junction at the homestead, Driefontein : 27°42'E, 32°48'S.

JR 15 Contact, dyke, 5 m wide, vertical, strike NE, in road-cut at the Mooiplaas Hotel, just past the road junction to Haga-Haga on the national road from East London to Butterworth: 28°01'E, 32°43'S.

JR 18 Bottom contact (horizontal), thick sill, in road-cut 1 km N (Blackhill Bend) of the bridge over the Kwelera River on the East London-Butterworth road : 28°01'E, 32°49'S.

JR 21 Contact, dyke, vertical, 3 m wide, strike ENE, at Fullers Bay 4 km SW of East London : 27°53'E, 33°03'S.

JR 29 Top contact (horizontal), sill, near road junction to Amherst railway siding on the road from Fort Beaufort to Katberg and Seymour : 26°40'E, 32°48'S.

JR 36 Bottom contact (horizontal), sill, on farm Modderfontein SW of Telemachus Kop, 12 km W of Jamestown : 26°44'E, 31°03'S.

JR 42 Bottom contact, sill, half-way up new Seymour Pass over the Katberg, on the new road from Seymour to Whittlesea and Queenstown : 26°49'E, 32°31'S.

JR 43 Non-contact, sill, locality as for JR 42.

JR 48 Non-contact, Queenstown curved-sheet intrusion, large quarry, 5 km from Queenstown on national road to Jamestown: 26°49'E,31°53'S.

JR 49 Contact, dyke off-shoot from large sill (JR 48), in gulley near the Glen Farm school 5 km from Queenstown on Jamestown road; Reference as for JR 48.

JR 50 Bottom contact (horizontal), sill, in road-cut 19 km from Queenstown on Jamestown road, near the Bailey railway siding: 26°44'E, 31°46'S.

JR 54 Bottom contact (horizontal), sill, quarry off the road, 1 km SW of Molteno on road to Sterkstroom : 26°22'E, 31°24'S.

JR 58 Bottom contact (horizontal), sill, in road-cut 43 km from Molteno on new tarred road to Burgersdorp; 4 km past the homestead, Rosslands : 26°10'E, 31°09'S.

JR 61 Bottom contact (horizontal), sill, in road-cut 24 km from Aliwal North on national road to Rouxville : 26°48'E, 30°29'S.

JR 70 Dyke, 10 m wide, strike SE, sample taken within 0.5 m of assumed contact, contact not exposed; 7.3 km along road to Tampasfontein and Smithfield from the Bethulie-Aliwal North road junction : 26°07'E, 30°26'S.

JR 72 Contact, dyke, strike NE, in road-cut, 11 km S of Smithfield on the road to Rouxville : 26°36'E, 30°17'S.

JR 73 Top contact (horizontal), sill, in small quarry 7 km S of Zastron on road to Herschel and Lady Grey : 27°09'E, 30°19'S.

JR 87 Non-contact sample, 6 m below top of large sill, exposed in pass (S of Rossouw), 29 km on the road to Rossouw from the Indwe-Dordrecht road junction : 27°17'E, 31°14'S.

JR 90 Contact, dyke, vertical, 8 m wide, strike NNW, top of pass through Wasbankspruit 6 km N of Rossouw on the road to Barkly East; 2.5 km S of road junction to Lady Grey : 27°18'E, 31°07'S.

JR 99 Dyke, vertical, 10 m wide, strike ESE, sample taken within 0.5 m of contact zone; quarry on farm Ravensfell, 4 km SE of Goedvertrou on the road from Barkly East to the Barkly Pass and Elliot; dyke does not intrude through the basalts and is offset by dyke JR 105, striking ENE : 27°44'E, 31°07'S.

JR 105 Dyke, vertical, 10 m wide, strike ENE, sample taken 1 m from the contact, dyke cuts through basalts and offsets JR 99 : locality as for JR 99.

JR 101 Contact, dyke, vertical, 4 m wide, strike SE, in road-cut near the top of the Barkly Pass, north of Elliot on the road to Barkly East : 27°51'E, 31°14'S.

JR 104 Near-contact sample, dolerite plug intrusion, in valley 5 km SW of the Barkly East-Moshesh's Ford road junction at the top of the Barkly Pass, sample taken within 1 m of the contact: 27°53'E, 31°14'S.

JR 121 Non-contact sample, curved-sheet intrusion?, Rosehill homestead, up the Bottlenek Pass road, 3 km SE of Goedvertrou on the Barkly East-Barkly Pass-Elliot road : 27°47'E, 31°07'S.

JR 123 Non-contact sample, dyke, dip 80°SE, 20 m outcrop width, strike NNE, quarry near stockpens at the Nkwenkewzi road junction to the Barkly Pass-Moshesh's Ford road; dyke does not intrude through the basalts and is offset by dyke JR 124: 27°52'E, 31°07'S.

JR 124 Non-contact sample, dyke, vertical, 12 m wide, strike ESE, offsets dyke JR 123 and intrudes through the basalts exposed in the area; locality as for JR 123.

JR 125 Non-contact sample, dyke, vertical, 18 m wide, strike SE, sample taken 1 m from the contact, at junction of road to Bastervoetpad (road sign to Saamwerk, P.J. Goosen) and the Barkly Pass-Moshesh's Ford road : 27°53'E, 31°09'S.

JR 126 Non-contact sample, dyke, vertical, 16 m wide, strike NNE, quarry at road-side, 0.5 km past the Moshesh's Ford - Barkly East road junction on the road to Moshesh's Ford from the Barkly Pass : 27°51'E, 31°11'S.

Barkly East volcanics

JR 88 Red Beds basalt, Siberia, N of Rossouw in road pass through the Wasbankspruit on the road from Dordrecht to Barkly East : 27°17'E, 31°08'S.

S 17 Basalt, Donnybrook Member, Moshesh's Ford Formation (M.F.F.), type-section in gorge of Kraai River, opposite 8th Reverse of railway line between Aliwal North and Barkly East (sample Dr. B.E. Lock).

JR 94 Basalt, Donnybrook Member, M.F.F., quarry near road-side 4 km W of Barkly East on the road to Dordrecht (1 km W of junction of old road to Aliwal North from Barkly East): 27°33'E, 30°57'S.

JR 31 Andesite, Andesite Member, M.F.F., Belmore volcano at Moshesh's Ford on the road from Barkly East to Rhodes : 27°47'E, 30°51'S.

S 5 Pillow lava, Kraai River Formation (K.R.F.), Kraai River cuttings on the old road from Barkly East to Aliwal North (sample - Dr. B.E. Lock).

S 6, S9 Basalts, K.R.F., Kraai River cuttings, locality as for S 5 (samples - Dr. B.E. Lock).

3/10 Basalt, K.R.F., on farm Rebels Glen, 12 km NE of Barkly East on road to Moshesh's Ford and Rhodes (sample - Dr. B.E. Lock).

JR 109 Basalt, K.R.F., basal contact sample, pod-shaped flow above massive basalt unit (JR 108), road cuttings north of bridge on new road from Barkly East to Aliwal North, 17 km W of Barkly East on the farm Donnybrook Outspan : 27°29'E, 30°55'S.

JR 108A,B Coarse-grained basalt, flow 2 m thick, A = basal sample, B = upper feldspathic zone. Flow JR 108 is the basal flow in a sequence of coarsely crystalline flows that directly underlie basalts of the Kraai River Formation; locality as for JR 109.

traverses were undertaken with the view of sampling dolerites exposed in recent road-cuts.

Considering the volume and nature of dolerites intruded into Karroo-age sediments in the area studied and the method of sampling, it is obviously difficult to determine the relative ages of the samples collected. Likewise, the detailed mapping of dolerites in the area studied was beyond the scope of this work. Consequently, during sampling, the habit, thickness, dip and strike (where necessary or possible) of the dolerite intrusion was noted. Only for some dolerites sampled in the Barkly East area, could any relative ages be assigned. In this area,Karroo basalts overlie the upper Karroo (Stormberg Group) sediments. In the sediments directly underlying the Karroo basalts, the most common habit of dolerite intrusion appears to be dyke-like. Very few large sills were noted, these being more frequently intruded into lower-Stormberg and Beaufort Group sediments in the area south and west of Barkly East.

Of interest in the Barkly East area is that some dolerite intrusions appear to be truncated by the overlying basalts while others intrude through the basalt pile. Two dykes that on aerial photographs are clearly seen to intrude through the sequence of basalts exposed, were sampled. These are samples JR105 and JR124. Both intrusions are near-vertical dykes, approximately 10 metres in width, and both cut and offset pre-existing dykes (JR99 and JR123 respectively).

These latter, older dykes appear to be truncated by the lowermost lavas and pyroclastic horizons in the area. The two dolerite dykes (JR105, 124) that clearly cut the lower lavas are both olivine-rich types and differ from the other dolerites by having slightly enriched Co, Cr and Ni concentrations. Also of interest is the tentative identification (Dr. B.E. Lock - personal communication) of a fairly large, curved-sheet (Walker and Poldervaart, 1949) dolerite intrusion in the Bottlenek Pass area to the east of Barkly East. This intrusion, which also appears to be truncated by the lower lavas, has a circular outcrop some 8 kilometres in diameter. Dips are radially inwards to the centre and the intrusion appears very similar to the curved, undulated sheets described by Walker and Poldervaart (op.cit.) in the Queenstown area. A single sample (JR121) of this sheet was collected. Petrographically it matches the Perdekloof dolerite type (Walker and Poldervaart, op.cit.) of the Queenstown basin-shaped intrusions. Mapping in the area by Dr. B.E. Lock, has not been fully completed and this structure and the apparent truncation of certain

dolerites by the lower lavas are to be more fully investigated. Extensive scree deposits derived from the basalts and generally friable, pyroclastic/volcaniclastic horizons, in nearly every case obscure the immediate contact between some dolerite intrusive bodies and the overlying horizontally-bedded basalts. It is thus difficult to decide if these dolerites are actually truncated by or intruded into the lower-most basalt horizons.

Highly vesicular, rounded basalt inclusions of varying sizes, were found in one dolerite dyke. This dyke (JR125), 18 metres wide and striking S.E., is exposed in a road quarry just north of the Barkly Pass-Barkly East-Moshesh's Ford road junction on the Moshesh's Ford road. Though this dyke today is intruded into Cave Sandstone and dies out before any basalt outcrop, the presence of basalt inclusions suggests that it may have cut basalts of a higher level. Alternatively, this dyke might have sampled minor basalts interbedded with Cave Sandstone and upper Red Beds sediments at a lower stratigraphic level. Basalts interbedded with Cave Sandstone and Red Beds Sediments have been noted by numerous authors and a site of vulcanicity during Red Beds times is today found exposed at Siberia, just north of Rossouw on the Dordrecht-Barkly East road (see sample JR88, Table 9a).

Barkly East basalts:

As discussed in Section 3.1.b, Lock et al. (1974) divide the basalts and volcaniclastic horizons of the lower part of the Drakensberg Subgroup into 3 formations : the basal Moshesh's Ford Formation, the intermediate Kraai River Formation and the overlying Lesotho Formation.

The basalts and andesite collected and analysed in this study and collectively termed the "Barkly East basalts", are exclusively confined to lavas from the Moshesh's Ford and Kraai River Formations.

No basalts from the more voluminous Lesotho Formation are included, these being studied in a separate investigation underway at present. The Basutoland basalts studied by Cox and Hornung (1966) fall into the Lesotho Formation of Lock et al. (op.cit.).

Five samples (S5, S6, S9, 3/10, S17) were kindly given to the author by Dr. B.E. Lock. The major element analyses of three of these basalts (S5, 3/10, S17) are reported by Lock et al. (op.cit., Table 1). The remaining samples presented in Table 9(a) were collected during a field trip to the Barkly East area. The following summary assigns the samples to the stratigraphic formations of

Lock et al. (op.cit.):

a) Red Beds lava, Siberia : JR88 (see also Lock et al., op.cit., Table 1, S1).

b) Moshesh's Ford Formation : Donnybrook Member - S17, JR94.
Belmore Andesite Member - JR31.

c) Kraai River Formation : S5, S6, S9, 3/10, JR109.

The exact stratigraphic position of basalt flow JR108A,B is difficult to define. This flow is exposed in a newly opened road cut north of the new bridge over the Kraai River on the Barkly East - Lady Grey road. Preliminary investigations (B.E.Lock, H. Minne - personal communications) show that a thick, massive, coarsely crystalline basalt unit some 57 metres thick and overlain by a sequence of 11 to 12 similar, individual flows varying in thickness between 1 and 2 metres, overlies the Donnybrook basalts, Bell Kop pyroclastics and Dingle tuffites of the upper Moshesh's Ford Formation but underlies lavas of the Kraai River Formation. More detailed investigations into this sequence of lavas are being undertaken and it is possible that they will be mapped as a new member of the Moshesh's Ford Formation. Samples JR108A,B are the basal and near upper contacts respectively of the lowermost basalt flow in the sequence of 11 to 12 individual flows that cap the massive unit.

The geochemistry of these basalts is at present being investigated and the preliminary results presented for JR108A,B in this study (Table 9a) indicate that these basalts are quite different from basalts of the Moshesh's Ford and Kraai River Formations. They also differ markedly in their petrography, being characteristically very coarse-grained while geochemically, in nearly every aspect, they match the compositions of the Karroo dolerites.

The single andesite, JR31, was collected from the andesites that cap the ancient Belmore volcano at Moshesh's Ford.

Basalt JR88, is from the Red Beds lava site at Siberia, near Rossouw, as previously mentioned by Lock et al. (op.cit.).

3.3
Petrography.

Karroo dolerites:

Walker and Poldervaart (1949) find that most of the Karroo dolerites can be classified into four common petrographic types. Briefly summarized these are :

a) Perdekloof type: medium- to fine-grained ophitic, olivine dolerites characterized by large ophitic augites and the absence of orthopyroxene and columnar pigeonite.

b) Blaauwkrans type: medium-grained subophitic olivine dolerites characterized by the subophitic texture and the common occurrence of columnar pigeonite cores in the augitic pyroxenes. Orthopyroxene is absent and plagioclase rarely exceeds 50 per cent by volume.

c) Kokstad type: coarse-grained subophitic olivine dolerites in which augite is accompanied by orthopyroxene or pigeonite. Plagioclase generally forms more than 50 per cent by volume and micropegmatite may occur interstitially.

d) Hangnest type: medium- to coarse-grained, subophitic bronzite dolerites, in which augite occurs with orthopyroxene. Pigeonite may be present but olivine is absent.

Dolerites of the other types - Downes Mountain, Hanover, marginal tholeiites, Kranskop, picrites, dolerite-pegmatite, Kentani and metasomatic granophyre - are rarer and not as widespread in their distribution as the four common types.

Walker and Poldervaart (op.cit.) in analyzing the relative frequency of the main dolerite types, find that throughout the whole Karroo province, dolerites of the Perdekloof type are most common, forming 28% of the sample.The Blaauwkrans- , Kokstad-and Hangnest-types constituent 24%, 15% and 9% respectively of the distribution, while the other types make up the remaining 24 per cent. There are however regional variations.i.e. dolerites of Hangnest-type are more common in the western Karroo and Natal while the Kokstad-type dolerites are more frequently found in the Transkei (Walker and Poldervaart, op.cit., Table 1).

These authors also briefly discuss the petrography of chilled selvages of the Karroo dolerites.

Plagioclase, augite and olivine phenocrysts commonly occur in chilled phases of dolerites of the Blaauwkrans-, Kokstad- and Perdekloof-types. Plagioclase is the most common and most abundant phenocryst phase and, in the Blaauwkrans- and Kokstad-type dolerites, often forms glomeroporphyritic aggregates. Dolerites of the Hangnest type contain plagioclase and bronzite phenocrysts. Walker and Poldervaart (op.cit., Table 4) present micrometric analyses of the phenocrysts in contact dolerites of the four main petrographic types. They find that on average, phenocrysts make up 6.7% of the chilled dolerite. This total is made up of 63% plagioclase (average composition, An70-80), 19% olivine (Fo80-85), 12% augite (Wo39 En50 Fs11) and 6% bronzite (Of15-20).

As mentioned in Section 3.2, the dolerites presented in this study are from three environments of crystallization: the porphyritic samples collected from true contact zones, the intersertal dolerites of the "near-contact facies" and the coarse-grained dolerites, sampled some distance from a contact.

The phenocryst assemblages identified in the contact samples are indicated in Table 8(a). No micrometric analyses were undertaken, neither were the compositions of the phenocryst phases accurately determined. It was hoped to study the compositions of some phenocryst assemblages with the aid of the microprobe but this has not been possible.

The mineralogy and petrography of the Karroo dolerites is discussed in detail by Walker and Poldervaart (op.cit.). The present study has concentrated on presenting new geochemical data for the dolerites. Consequently detailed petrographic studies were not undertaken.

The following discussion notes the salient petrographic features of the dolerites studied.

Porphyritic dolerites:

The most common phenocrysts observed in the contact dolerites are plagioclase, augite and olivine. Pigeonite is present in some samples (e.g. JR9) but no orthopyroxene phenocrysts have been identified. This suggests that all the contact dolerites sampled can be classified as belonging to either the Blaauwkrans, Kokstad or Perdekloof types of Walker and Poldervaart (op.cit.). The absence of any Hangnest-type dolerites confirms the relative paucity in the distribution of this dolerite type in the north-eastern Cape as

noted by the former authors.

Data from Walker and Poldervaart (op.cit., Table 4) suggest similar phenocryst assemblages for the Perdekloof, Kokstad and Blaauwkransdolerite types. The very common occurrence of glomeroporphyritic aggregates of plagioclase in many contact dolerites included in this study suggests they be classified as Blaauwkrans- or Kokstad-type dolerites. Some chilled dolerites e.g. JR50, 29 contain phenocrysts of augite as well as large, slightly resorbed, ophitic augite xenocrysts of a possibly intratelluric origin. The strongly ophitic character of the augite xenocrysts suggests these dolerites be of the Perdekloof type.

Plagioclase phenocrysts invariably occur as glomeroporphyritic aggregates while in some ultra-fine-grained dolerites, plagioclase microphenocrysts are lath -shaped and show typical quench textures.

Olivine varies greatly in abundance though being commonly degraded to greenish bowlingite. The sizes of the olivine phenocrysts also vary greatly. In some specimens (JR36, 18) large euhedral olivines showing slight resorption textures are observed while in others the olivines are microphenocrystic and more anhedral in shape.

A single picritic sample (JR18) was collected. In this specimen large olivine euhedra with minute inclusions of brownish picotite (spinel), are set in a variolitic groundmass. This rock is nearly identical to variolitic picritics shown by Walker and Poldervaart (op.cit., Figs. 11A,B). Another interesting texture observed is the apparent fining of the groundmass in a zone around large olivine (JR36) and augite (JR29) phenocrysts. This texture is not a reaction rim or halo. Rather, the groundmass appears "chilled" in the immediate vicinity of these phenocrysts.

The dominant pyroxene phenocryst observed is augite. Augite occurs either as discrete euhedra, or slightly ragged, ophitic plates containing tiny plagioclase laths or in one specimen (JR9), as abundant glomeroporphyritic aggregates. Pigeonite occurs as discrete crystals but is often very difficult to distinguish from augite, especially in the finer-grained specimens.

Groundmass textures vary considerably. In some specimens (e.g. JR18) the groundmass is strongly variolitic, while in others the groundmass is very fine-grained and more felsitic in appearance. More commonly the groundmass is a fine-grained intergranular intergrowth of plagioclase, pyroxene, iron ores and sometimes biotite. Slightly coarser-grained contact dolerites have intersertal to subophitic groundmass textures. Brownish glass, often altered, is also observed.

Intersertal dolerites:

These dolerites characteristically do not contain any distinct phenocrysts though tiny microphenocrysts of often highly-altered olivines are observed. The texture is dominantly fine-grained intersertal. In some specimens intergrowths of elongate plagioclase and pyroxene approximate coarse spherulitic textures while the brown, glassy mesostasis is crowded with quenched plagioclase, pyroxene and Fe-oxide microlites.

Medium- to Coarse-grained dolerites:

Samples JR11, 43 are coarse-grained, subophitic, olivine dolerites containing abundant plagioclase. Augite, inverted pigeonite (orthopyroxene) and pigeonite occurring as digested cores to the augites, are present while iron ores, biotite and micropegmatite make up the minor constituents of the rocks. These dolerites are of the Kokstad-type.

Dolerites (e.g. JR121, 87) containing abundant, large augite plates ophitically enclosing tiny plagioclase laths are representative of the Perdekloof dolerite type.

Two olivine-rich dolerite dykes that intrude and cut through the lower basalts of the Lesotho Formation (Lock et al., 1974) in the Barkly East area were sampled (e.g. JR105, 124). These dolerites both form negative outcrops and contact zones are highly weathered and difficult to sample. These dolerites are coarse-grained, olivine-rich, varieties showing prominent subophitic to complex intergrowth textures of pyroxene (augite) and plagioclase. In both cases a glassy mesostasis rich in quench plagioclase and iron ores occurs interstitially. Minute inclusions of picotite(?) are observed in some of the larger, euhedral olivine crystals. These dolerites may be olivine-enriched accumulative rocks, the olivine settling under gravitation in static, slowly crystallizing feeder dykes. These dykes have however not been investigated in great detail and an alternative argument could be that the samples were collected from a zone enriched in olivine through a mechanism such as flow differentiation. The presence of a glassy residuum, however, suggests some degree of chilling.

Brief petrographic descriptions of the dolerites included in this study are given in Appendix 5.

Barkly East basalts:

Cox and Hornung (1966) discuss the petrography of the Basutoland (Lesotho Formation) basalts and note that while these basalts rarely appear porphyritic in the field, microphenocrysts of plagioclase and altered olivine are almost always present in chilled specimens from flow bases. The central portions of the more-massive flows are generally rather coarse-grained, with ophitic to subophitic intergrowths between plagioclase and augite giving the basalt a doleritic appearance in thin section.

Donnybrook basalts, Moshesh's Ford Formation.

Lock et al. (1974) note that the Donnybrook basalts are petrographically indistinguishable from the lower Drumbo basalts. "In thin section, the (Drumbo) basalts are seen to consist of plagioclase (zoned An40-An65), pigeonite and augite, with phenocrystic olivine and various accessories". Two Donnybrook basalts (S17, JR94) have been examined. In thin section, they consist of fractured and altered glomeroporphyritic plagioclase set in a partly glassy, fine-grained granular groundmass of pyroxene, plagioclase and iron ore. Pseudomorphs of reddish iddingsite after olivine represent very minor, microphenocrytic olivine while a single, highly eroded phenocryst of clinopyroxene was also observed. Orthopyroxene (bronzite), common in the aphanitic Kraai River basalts, has not been positively identified in the Donnybrook basalts. The two basalts sampled are slightly weathered and are somewhat amygdaloidal.

Belmore andesite, Moshesh's Ford Formation.

Du Toit (1904), Lock et al. (op.cit.) note the presence of enstatite - and plagioclase-phyric, glassy andesites capping the ancient Belmore volcano. The single sample studied (JR31) confirms the above observations. Small lath -shaped plagioclase and stumpy enstatite phenocrysts as well as smaller plagioclase and more granular, anhedral orthopyroxenes crowd and are set in a clear, brown glassy groundmass.

Kraai River basalts, Kraai River Formation.

Lock et al. (op.cit.) offer little petrographic information for the Kraai River basalts. The samples provided by Dr. B.E. Lock and analysed in the present study are interesting in that some contain

orthopyroxene (bronzite) as a common phenocryst phase together with plagioclase. These basalts thus, petrographically, approximate the Hangnest-type dolerite and as mentioned before, have been noted in the Barkly East area by Walker and Poldervaart (1949). Plagioclase phenocrysts occur either as largish individual laths (An50-60) or as glomeroporphyritic clusters. Orthopyroxene occurs as partly altered, stumpy crystals, up to 1mm in length. Orthopyroxene is frequently mantled by a thin rim of clinopyroxene. Groundmass textures show generally very fine-grained intergrowths of plagioclase and clinopyroxene, set in a glassy mesostasis crowded with iron ores. Elongate groundmass clinopyroxene and plagioclase intergrowth in coarser varieties often resemble spherulitic textures. These basalts are all amygdaloidal to some degree. In sample crushing, the larger amygdales were removed but in thin sections, small veins and bubbles of amygdales persist.

The coarse-grained basalt flow JR108 discussed in an earlier section, is clearly different from the normal, finer-grained Kraai River basalts. Sample JR108A, from near the base of a single flow about 2 m thick, is a very coarse-grained basalt, rich in plagioclase, augite and pigeonite. Augite subophitically encloses plagioclase laths while pigeonite occurs as cores in the larger augite plates. No fresh olivine is observed but abundant brownish to greenish chlorophaeite present in this rock might represent products of the late-stage, hydrothermal alteration of olivine. Olivine is a common constituent in samples collected from different flows in this coarse-grained basalt unit (H. Minne - personal communication). Micropegmatite occurs as a minor constituent in the interstices. Sample JR108B collected near the upper contact of this flow is similar to JR108A but shows the development of abundant, coarsely crystalline micropegmatite. Pyroxenes are generally also more strongly zoned. Chemically, this sample is strongly differentiated with respect to the basal sample, JR108A.

Red Beds basalt, near Rossouw

Thin section examination shows this basalt (JR88) to contain discrete and glomeroporphyritic plagioclase, minor pigeonite and augite(?) phenocrysts set in a very fine-grained, glassy groundmass. The groundmass also contains abundant plagioclase microphenocrysts arranged along flow lines to give a trachytic-like texture. The glassy groundmass is highly altered and oxidized and contains abundant, minute granules of iron ore.

To conclude, plagioclase is the most common phenocryst in the porphyritic basalts studied. In some Kraai River basalts, orthopyroxene is observed together with plagioclase in the phenocryst assemblage. Augite and pigeonite may occur as phenocrysts in the Donnybrook and Red Beds lava while very little phenocrystic olivine has been observed. The groundmass is generally glassy but coarser varieties show complex intergrowths between plagioclase and clinopyroxene with iron ore generally being confined to interstitial, glassy areas.

The coarse-grained basalt flow JR108, is petrographically similar to the Kokstad-type coarse-grained dolerites. In this flow, differentiation has strongly enriched the upper portion in micropegmatite.

3.4

Major Element Variations.

Major element variations within the Karroo dolerites and Barkly East basalts included in this study, are discussed with the aid of MgO variation diagrams, the total alkalies vs. silica plot (Kuno, 1968), AF*M diagrams and also in terms of normative chemistry following the method of Cox and Hornung (1966).

New major (hydrous) and trace element data for 30 Karroo dolerites are presented in Table 8(a). Anhydrous analyses used in the construction of the variation diagrams are shown in Appendix 2. New data for 10 Barkly East basalts and 1 andesite are similarly shown in Fig.9(a) and Appendix 3.

All major element data quoted in the following discussion, are anhydrous values. Total Fe was determined as Fe_2O_3 throughout.

3.4.a

Karroo dolerites : Major element variation diagrams.

Figs.13 (a-h) show major element variations for both the Karroo dolerites and the Barkly East basalts, plotted versus MgO%. Also indicated are the trends defined by differentiation at Birds River, as discussed in Section 2.4. This allows direct comparisons of all rock suites presented in this study.

The true contact dolerites, the compositions of which, accurately reflect compositions of the magma at the time of emplacement, show a limited variation in MgO content from 8.04% to 4.95%.

The fields defined in Figs.13 (a-h) thus tend to be clustered. This is also seen in trace element variation diagrams shown in Figs.14 (a-l).

The dolerites have, tentatively, been subdivided into two groups on the basis of K_2O content (Table 8a). The low-K_2O group is defined as those contact dolerites with K_2O less than 0.4%. The normal-K_2O group has K_2O greater than 0.4%. These two groups are indicated with different symbols in Figs.13 (a-h) and 14 (a-l).

In Fig.13(g), K_2O increases with increasing differentiation, as expected in differentiated basic magmas. Some dolerites (and basalts), however, have an abnormally low K_2O content and low K_2O/Na_2O ratios (< 0.2, Appendix 2) for their differentiation stage. These few specimens are all porphyritic dolerites with MgO values ranging

from 7.29 to 6.53%. Unfortunately, low K_2O appears to be about the only characteristic of this group and naturally this may lead to speculation as to the validity of the determinations. Analyses on duplicate fusion discs, however, are within the limits of variation imposed by the method of determination. Sample JR50, with a very low K_2O content of 0.11%, was independently reanalysed in duplicate. An average value of 0.10% K_2O was determined (H.V. Eales and J. Pemberton - personal communication.). This suggests that the low K_2O values reported in Fig.8(a) are valid. Trace element concentrations, particularly the K-related elements Rb and Ba, do not as a whole characterize this group with sympathetically low values (Table 8a, Figs. 14b,c). Individually, some dolerites (JR29, 21) do show correspondingly low Ba and Rb. This leads to an immediate indication that factors other than crystal fractionation control major and trace element variations in the Karroo dolerites.

In Figs. 13 (a-h), the Karroo dolerites sampled show relatively strong increases in SiO_2 (49.3-54.7%), Al_2O_3 (13.6-16.2%) and K_2O (0.35-1.03%) from the olivine-rich dolerites to the more differentiated samples. Na_2O% and P_2O_5% increase in a more subdued manner, while CaO% initially increases but then varies considerably at lower MgO values. Some dolerites (JR58, 70) are relatively depleted in CaO ($<$10%) and in CaO content are similar to the low CaO values of the northern Karroo province (Cox et al., 1967). The behaviour of TiO_2 and Fe_2O_3 is erratic, especially in the more MgO-rich and coarser-grained dolerites, where variations in the modal amounts of TiO_2-rich Fe-oxides are probably important. Within the contact dolerites, TiO_2 and to a lesser degree Fe_2O_3, do appear to increase with increasing differentiation but trends are by no means clear (Figs.13 b,d).

Fig.15(a) shows the dolerites plotted in the AF*M diagram. The relatively undifferentiated nature of most of the dolerites sampled is clear, though some degree of total-Fe enrichment is seen from the more basic dolerites to dolerites with moderate MgO contents. Nockolds and Allen (1956) using the data of Walker and Poldervaart (1949), note that the Karroo dolerites are characterised by three Fe-enrichment trends. The dominant trend is one of moderate Fe-enrichment, while certain differentiated dolerite intrusions such as New Amalfi and Elephant's Head show strong Fe-enrichment trends, though not as extreme as that for the Skaergaard intrusion (Walker and Poldervaart, op.cit., Fig.28). A third trend is characterised by little or no Fe-enrichment but is only seen in a few samples.

Table 8a : Major and Trace Element Analyses - KARROO DOLERITES.

	JR 70	JR 90	JR 36	JR 54	JR 61	JR 2	JR 15	JR 21	JR 29	JR 42
SiO_2	54.27	52.25	52.81	50.69	52.42	52.51	51.51	51.12	51.08	51.60
TiO_2	.87	1.02	.87	1.06	1.04	1.01	.96	.82	.98	.99
Al_2O_3	14.98	15.13	15.20	15.11	15.52	14.93	15.59	15.03	14.98	14.89
$Fe_2O_3^+$	10.09	11.58	10.25	11.20	10.62	11.53	11.78	13.22	11.27	11.19
MnO	.17	.18	.16	.17	.17	.19	.18	.20	.18	.17
MgO	5.96	6.12	7.27	6.83	5.99	6.36	6.66	6.59	6.64	8.08
CaO	9.63	10.16	10.37	10.56	10.85	10.76	10.72	11.23	10.55	10.67
Na_2O	2.03	2.32	2.56	2.30	2.32	2.53	2.41	2.16	2.27	2.30
K_2O	.95	.77	.29	.72	.68	.74	.61	.34	.29	.47
P_2O_5	.13	.19	.14	.20	.19	.16	.16	.07	.17	.15
L.O.I.	.67	.64	.61	.55	.99	-.41	-.02	-.04	.82	.24
H_2O^+	.27	.36	.29	.19	.25	.08	.10	.07	.13	.03
TOTAL	100.02	100.72	100.81	99.58	101.04	100.40	100.68	100.85	99.34	100.78
				p p m						
Ba	252	235	192	343	239	231	201	99	136	167
Sr	168	200	224	242	251	192	190	84	244	215
Rb	22.9	16.1	9.6	14.6	12.3	16.6	11.9	10.6	2.4	9.3
Y	27.7	25.5	23.2	23.2	25.6	26.7	25.5	25.7	26.7	24.2
Zr	121	110	103	97	104	104	98	52	97	77
Nb	5.7	9.2	4.8	10.8	8.0	7.0	6.4	n.d.	5.6	6.9
Zn	82	89	75	80	81	86	85	87	105	81
Cu	86	82	87	90	86	98	111	155	118	92
Co	37.1	34.4	43.1	42.8	39.5	41.9	43.8	49.4	44.2	46.3
Ni	54	44.3	127	82	74	56	84	75	90	137
V	235	192	228	232	238	261	252	304	242	242
Cr	208	147	336	212	253	201	191	125	242	404
			1.			2	2	1,2	1,2	2
Ph.	plag. only.		plag. +olivine			plag.+olivine +augite+pigeonite			plag.+olivine +augite	

Table 8a (contd.)

Table 8a (contd.) Karroo Dolerites

	JR 49	JR 50	JR 99	JR 48	JR 72	JR 73	JR 101	JR 18	JR 9	JR 58
SiO_2	50.91	50.70	50.36	51.87	51.38	52.59	49.36	50.58	51.66	53.43
TiO_2	.90	1.08	.94	.93	.99	1.09	.96	.83	1.01	1.22
Al_2O_3	15.23	15.25	15.11	15.38	15.28	15.90	15.74	14.12	15.29	14.42
Fe_2O_3	11.12	11.41	11.14	11.19	11.15	9.97	11.21	11.10	11.62	10.67
MnO	.17	.19	.18	.17	.17	.14	.24	.17	.17	.17
MgO	7.27	6.69	6.67	7.18	7.10	4.85	6.06	11.03	6.00	5.50
CaO	10.64	10.61	10.95	10.93	10.93	10.09	11.15	10.05	10.05	8.98
Na_2O	2.09	1.94	2.07	2.33	2.14	2.24	1.98	2.07	2.22	2.26
K_2O	.29	.10	.35	.65	.57	.96	.60	.41	1.02	.83
P_2O_5	.16	.21	.16	.15	.17	.21	.17	.14	.17	.21
L.O.I.	.77	1.59	1.05	-.13	.28	1.30	1.47	.15	.59	1.86
H_2O^+	.15	.21	.82	.11	.18	.78	.89	.06	.40	.12
TOTAL	99.70	99.98	99.79	100.75	100.34	100.12	99.83	100.71	100.20	99.66
Ba	-	123	214	201	185	256	-	129	364	287
Sr	202	205	206	197	208	264	204	176	224	202
Rb	6.3	11.8	5.8	13.9	9.5	20.1	9.9	9.6	37.2	19.0
Y	24.9	25.6	24.5	24.2	23.6	27.6	24.7	20.8	27.5	30.9
Zr	97	98	104	92	75	158	105	64	109	135
Nb	5.9	11.3	5.5	5.4	5.4	18.7	5.9	3.9	6.1	4.4
Zn	86	82	76	77	82	87	82	83	90	91
Cu	89	89	89	87	91	96	92	94	101	19.2
Co	45.9	45.5	44.2	42.1	43.7	34.3	44	58	35.7	36.7
Ni	103	77	84	84	100	71	89	271	55	3.5
V	233	248	230	232	231	235	242	224	242	229
Cr	272	248	279	261	311	193	299	651	246	188
	1	1	1					2	2	
Ph.	plag. + olivine + augite							olivine only	plag.+augite + pigeonite	

Table 8a (contd.)

Table 8a (contd.) Karroo Dolerites

	JR 43	JR 87	JR 104	JR 121	JR 126	JR 123	JR 125	JR 11	JR 105	JR 124
SiO_2	50.97	51.24	51.25	51.07	51.48	51.68	51.65	49.47	48.26	48.09
TiO_2	.86	.74	.91	.95	.90	.96	.97	73.	1.00	.95
Al_2O_3	15.63	15.56	15.06	14.93	15.13	15.16	15.44	13.64	14.04	13.38
Fe_2O_3	10.83	10.26	11.04	11.20	11.24	11.29	10.59	11.72	12.21	12.32
MnO	.16	.16	.17	.17	.17	.21	.21	.17	.16	.18
MgO	9.01	7.72	7.06	7.09	7.19	6.40	6.54	12.65	9.02	12.34
CaO	10.72	11.28	10.85	10.66	10.91	11.01	11.00	9.53	10.33	9.89
Na_2O	2.35	2.17	2.45	2.48	2.25	2.19	2.15	2.02	1.80	1.97
K_2O	.46	.56	.34	.62	.65	.53	.54	.36	.40	.38
P_2O_5	.13	.13	.16	.16	.16	.16	.16	.12	.13	.12
L.O.I.	-.18	.16	.81	.35	.37	.58	.81	.06	1.74	.41
H_2O^+	.10	.15	.54	.25	.18	.45	.54	.07	.77	.48
TOTAL	101.03	100.13	100.64	99.93	100.63	100.62	100.60	100.53	99.86	100.51
Ba	148	-	201	201	360	193	249	117	152	183
Sr	221	191	203	195	215	198	208	171	196	193
Rb	8.2	11.5	27.7	11.8	12.1	8.8	9.1	5.8	9.6	10.2
Y	21.2	19.7	24.4	24.3	25.1	22.1	24.4	17.8	21.4	21.0
Zr	62	78	98	88	103	87	86	50	83	83
Nb	5.6	2.1	5.3	5.1	5.1	5.2	4.7	3.0	1.6	4.2
Zn	72	67	76	79	79	82	78	71	77	76
Cu	77	64	86	88	88	90	89	70	106	103
Co	51	43.6	42.1	44.4	43.8	44.8	48.7	67	73	71
Ni	165	190	82	94	79	98	101	300	539	513
V	210	212	222	229	232	239	246	193	240	228
Cr	407	345	284	286	293	283	291	786	799	767
	2							2		
	medium- to coarse-grained dolerites							coarse-grained olivine-rich dolerites		

n.d. Concentration below L.L.D. (see Appendix 4)

* All Fe determined as Fe_2O_3

1 Chilled dolerites with K_2O less than .4 %

2 Dolerites sampled within southern basin margin (Rhodes & Krohn, 1972)

Ph. Phenocrysts present in chilled dolerites.

In Fig.15(a) the Fe-enrichment trend for the Birds River intrusion is indicated and compared with the field covered by the Karroo dolerites of this study. Most of the dolerites plot exactly in the field defined by the relatively undifferentiated gabbros from Birds River and none reach the degree of Fe-enrichment noted for the Birds River ferrogabbros and ferrotholeiites. A comparison of the dolerite trend, the Birds River trend and the New Amalfi - Elephant's Head trend suggests that the degree of iron enrichment at Birds River is a true example of the moderate Fe-enrichment trend of Nockolds and Allen (1956), extending the degree of iron enrichment for the dolerites of this study.

The alkali-silica plot (Kuno, 1968) - Fig 16 - indicates the tholeiitic nature of these Karroo intrusives. The plotted points fall exclusively within the tholeiitic field and do not transgress into the high-Al basalt field as shown by Kuno (1968). Only the true contact samples are plotted in Fig.16. These more accurately reflect the initial composition of the Karroo magma at the time of emplacement, unaffected by internal differentiation within dykes or sills or by reaction with country-rock sediments. The strongly tholeiitic character of the Karroo magma, previously noted by Walker and Poldervaart (1949), is thus confirmed.

The tholeiitic character of the Karroo dolerites can further be demonstrated by classification according to the scheme of Irvine and Baragar (1971). Norms presented in Table 8(b) are conventional C.I.P.W. weight percent norms and not the Niggli-Barth katanorms used by the abovementioned authors in constructing their diagrams. Consequently, direct comparisons cannot be made without recalculating the norms. However, considering both the similarity between these two normative calculations and the relatively high Fe_2O_3/FeO ratio (0.2) used in the calculation of the norms in Table 8(b), the Karroo dolerites of this study fall well within tholeiitic fields defined by Irvine and Baragar (op.cit.).

Major element concentrations presented in Table 8(a) confirm the differences noted by Cox et al. (1967) between the southern and northern Karroo provinces. The Karroo dolerites from the Eastern Cape are relatively enriched in Al_2O_3, CaO and depleted in TiO_2 and K_2O and are characteristic of the defined southern Karroo province. Trace element concentrations, generally, also confirm this conclusion.

Considering the rather small sample of dolerites presented in this study, the basin centre-basin margin hypothesis of Rhodes and

Krohn (1972) cannot be fully tested. Rhodes and Krohn (op.cit., Fig.2, Table 1) find that basaltic rocks from their defined central Karroo basin contain significantly more Al_2O_3, MgO and CaO and lower TiO_2, Na_2O, K_2O and P_2O_5 than basaltic rocks from the basin margins south of 26°S latitude. Dolerites sampled within the southern basin area, as delineated by Rhodes and Krohn (op.cit.), are indicated in Table 8(a). An examination of these analyses (especially K_2O concentrations) suggests that the pattern evolved by these authors does not hold true in individual cases, e.g. JR29, 21. No detailed comment is possible on this hypothesis until it can be tested, by similar statistical methods, when more data are available for the various areas under study during the Geodynamics program.

3.4.

The Barkly East basalts.

To enable direct comparison with the Karroo dolerites, the Barkly East basalts are included in Figs.13 (a-h). Basalts belonging to the different formations as named by Lock et al. (1974) are indicated with different symbols, as defined in the caption to Figs.13 (a-h). Analyses S5, S17 and 3/10 are repeat major element analyses of those presented in Fig.1 (Lock et al., op.cit.), though trace element data are new.

As previously mentioned, most of the basalts (S5, S6, S9, 3/10, JR109) belong to the Kraai River Formation. There is some doubt as to the exact stratigraphic position of basalt flow JR108 (A,B). Samples JR94 and S17 belong to the older Donnybrook Member while JR31 is the andesite lava capping Belmore volcano. Sample JR88 is from the very early Karroo lava exposure, interbedded with Red Beds sediments at Siberia, near Barkly East.

In Figs.13 (a-h) clear trends of strong SiO_2, more subdued Al_2O_3 and P_2O_5 enrichment and CaO and Fe_2O_3 depletion with increasing differentiation are seen in the aphanitic basalts of the Kraai River Formation. TiO_2 remains fairly constant while Na_2O and K_2O trends are erratic. Internal differentiation from the base (A) to the top (B) of flow JR108, which petrographically is quite different from the other Kraai River basalts in that it is coarsely crystalline and does not contain orthopyroxene, differs quite markedly from the overall Kraai River differentiation trends. Differentiation of flow JR108 results in a strong increase in Fe_2O_3 and TiO_2 but decrease in

Table 9a:

MAJOR AND TRACE ELEMENT ANALYSES - BARKLY EAST BASALTS.

(see Appendix 3)

	JR 88	JR 94	S 17	S 5	S 6	S 9	3/10	JR 109	JR 108A	JR 108B	JR 31
SiO_2	50.03	53.84	52.98	52.52	50.68	53.04	55.77	53.30	50.50	53.19	62.88
TiO_2	1.15	.86	.85	.85	.85	.82	.85	.87	.84	1.13	.76
Al_2O_3	14.61	15.09	14.95	14.65	15.01	14.62	14.81	14.86	15.37	13.72	15.46
Fe_2O_3*	12.87	9.87	9.65	9.71	9.99	10.04	8.79	9.85	10.26	11.45	6.74
MnO	.18	.15	.14	.15	.15	.16	.13	.18	.16	.18	.10
MgO	6.63	6.18	6.03	6.74	6.87	6.44	4.67	6.61	7.82	5.92	2.83
CaO	9.50	9.55	9.15	9.75	9.80	10.35	8.51	9.74	11.07	10.89	4.29
Na_2O	2.02	2.03	2.15	1.89	1.89	2.01	1.82	2.07	2.01	2.42	2.58
K_2O	.25	1.08	1.09	.44	.42	.25	.42	.83	.38	.51	2.04
P_2O_5	.17	.15	.15	.13	.14	.13	.16	.14	.12	.17	.16
L.O.I.	2.01	1.17	1.35	1.77	2.66	1.86	2.89	1.39	1.18	.74	2.17
H_2O^+	.90	.41	.26	1.39	1.05	.64	.53	.85	.69	.26	.20
TOTAL	100.03	100.38	98.70	99.99	99.52	100.36	99.39	100.69	100,40	100.58	100.21
					p p m						
Ba	283	214	238	129	149	148	183	177	130	186	610
Sr	239	184	181	183	205	190	236	220	183	189	279
Rb	n.d.	33.7	34.3	11.7	11.8	17.6	21.0	22.9	4.6	9.0	111
Y	27.7	27.0	25.1	26.2	25.7	24.3	29.0	26.0	21.2	31.2	30.2
Zr	122	112	113	108	112	103	158	113	65	99	205
Nb	2.3	5.1	5.6	4.2	5.3	5.3	8.0	5.7	2.4	5.2	12.2
Zn	95	78	90	80	80	76	83	79	68	82	79
Cu	92	57	71	63	67	60	47.0	64	89	127	29.7
Co	36	35.2	35.9	37.2	38.7	33.3	28.8	35.7	44.2	35.2	16.1
Ni	51	47.7	51	53	54	51	32.5	42.2	115	47.0	21.5
V	255	221	223	230	237	216	189	242	228	284	120
Cr	163	223	218	249	255	236	121	246	370	153	75

* All Fe determined as Fe_2O_3

n.d. Concentration below L.L.D. (see Appendix 4)

JR88 - Red Beds basalt

JR94, S17 - Donnybrook basalts.

S5, S6, S9, 3/10, JR109 - Kraai River basalts.

JR108A, B - Kraai River basalt? - differentiated flow (A- near base of flow)
(B- near top of flow)

JR31 - Belmore Andesite.

Al_2O_3 percent.

The two analyses of the Donnybrook basalts are virtually identical (Table 9a) in both major and trace element concentrations and no variation can therefore be discussed. Their plotted points fall on the Kraai River trends (Figs.13 a-h), with the important distinction that the Donnybrook basalts are significantly richer in K_2O content (1.0%) and the K-related trace elements, Ba and Rb. K_2O/Na_2O ratios (Appendix 3) are also higher (0.50) than for the other basalts (average = 0.26).

JR88, the early Red Beds lava, is distinctive by its relatively high TiO_2 (1.18%), Fe_2O_3 (15.04%) and low K_2O (0.26%) contents, while the K_2O/Na_2O ratio is also abnormally low (0.125).

The andesite, JR31, with the exception of Na_2O and K_2O, plots virtually on the extension of the Kraai River major element trends, though it belongs to an earlier episode of vulcanism. It is characterized by high SiO_2, Al_2O_3, K_2O and Na_2O but low CaO, Fe_2O_3, MgO and TiO_2. Similarities in the phenocryst petrography of the andesite to the Kraai River basalts (i.e. the common occurrence of orthopyroxene as a phenocryst) also suggest that the andesite may be an extreme differentiate from a magma source similar to that that gave rise to the Kraai River basalts.

Fig.15(b) shows the basalts plotted in the AF*M diagram. Though trends are not clear, the Kraai River basalts do show some degree of relative Fe-enrichment, with increasing differentiation to 3/10. The Donnybrook basalts and the andesite appear to be on a more calc-alkaline trend showing no relative Fe-enrichment. The Kraai River basalt trend of Fe-enrichment is matched by that of flow JR108(A,B), though the former basalts all show decreasing absolute Fe_2O_3 with decreasing MgO.

Fig.16 is a plot of the Barkly East basalts on the alkali-silica diagram (Kuno, 1968). The strongly tholeiitic nature of the Barkly East basalts is clearly evident and confirms such a conclusion by Lock et al. (1974). Should this diagram be a measure of the degree of tholeiitic character of a magma, then the basalts are clearly more tholeiitic than the Karroo dolerites. This strong tholeiitic character is also seen in their normative chemistry, where hyperthene forms up to 26 weight percent of the norm.

The scheme of Irvine and Baragar (1971) has been adopted in an attempt to classify the Belmore andesite. Du Toit (1904) discusses the petrography and silica content of an andesite from

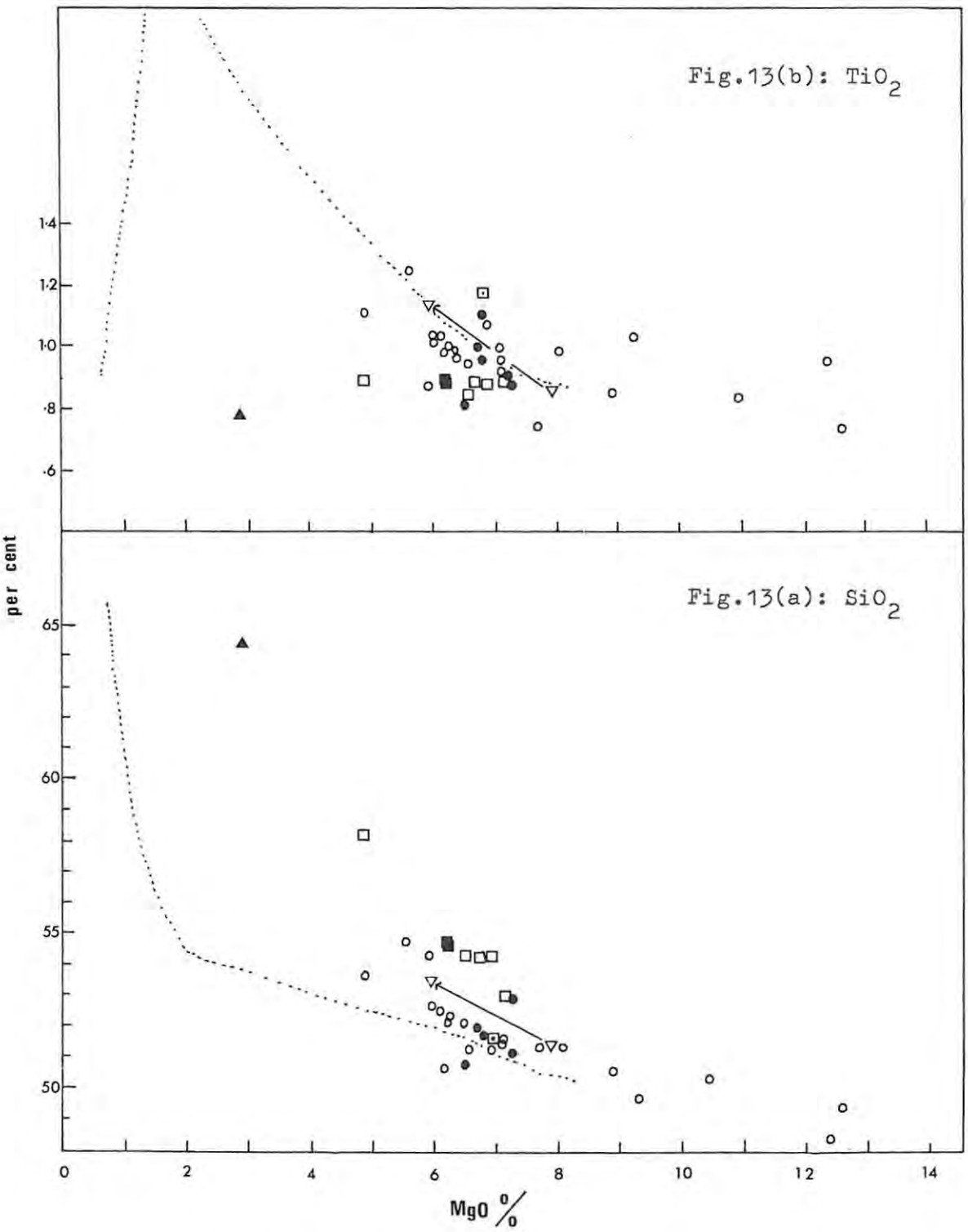

Figs.13(a-h): Major element data (oxides) for the Karroo dolerites and Barkly East volcanics, plotted against MgO%, the index of fractionation.

- ● Chilled Karroo dolerites with $K_2O < .4\%$.
- ○ Karroo dolerites. (contact and non-contact samples).
- ⊡ Red Beds basalt.
- ■ Donnybrook basalts.
- ▲ Belmore andesite.
- □ Kraai River basalts.
- ▽→▽ Basalt flow JR108(A→B).

(...) - Variation at Birds River; (---) - Geochemical "boundaries" between northern and southern Karroo provinces (Cox et al., 1967).

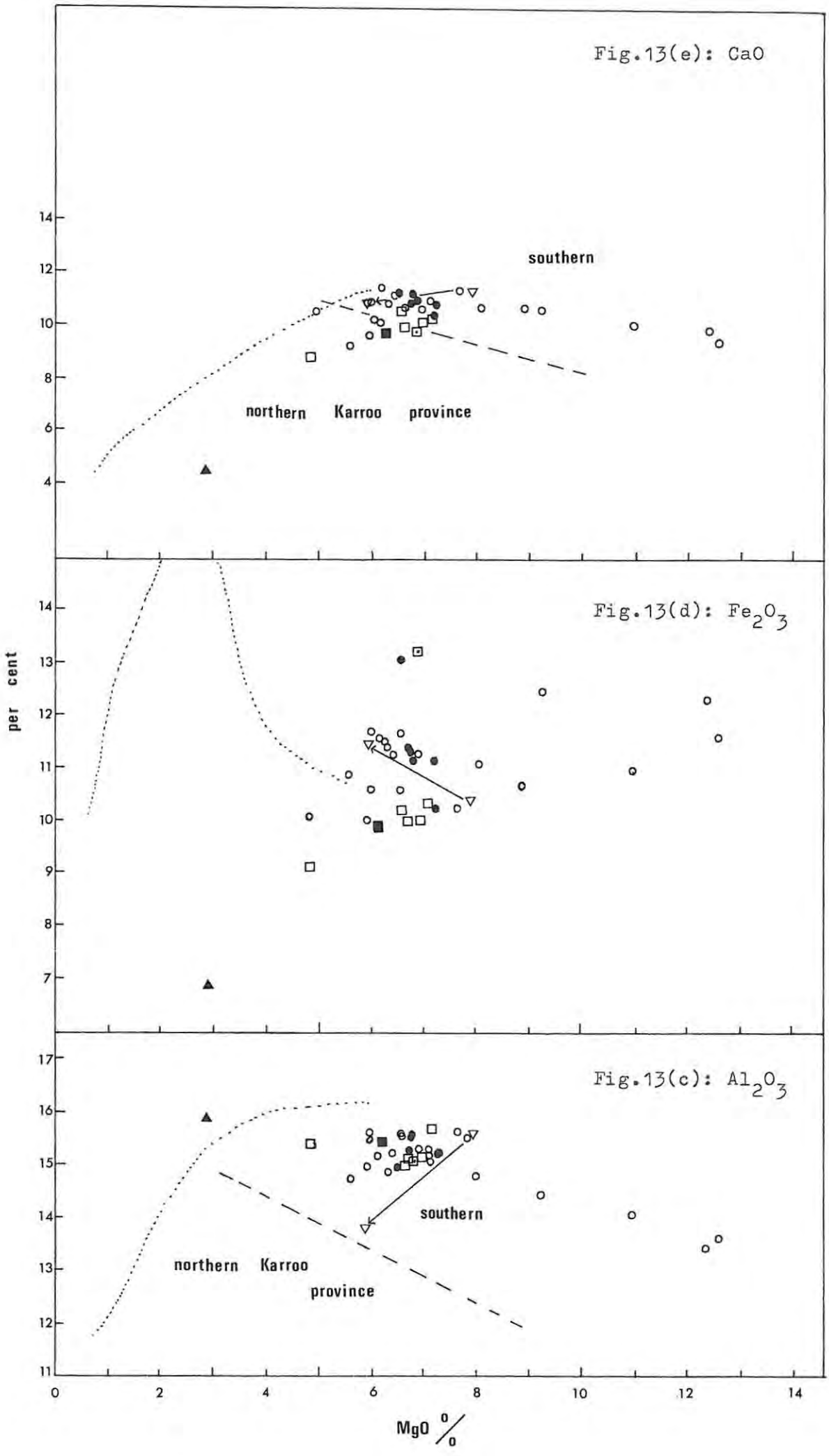
Fig.13(e): CaO
southern
northern Karroo province
Fig.13(d): Fe_2O_3
per cent
Fig.13(c): Al_2O_3
southern
northern Karroo province
MgO %

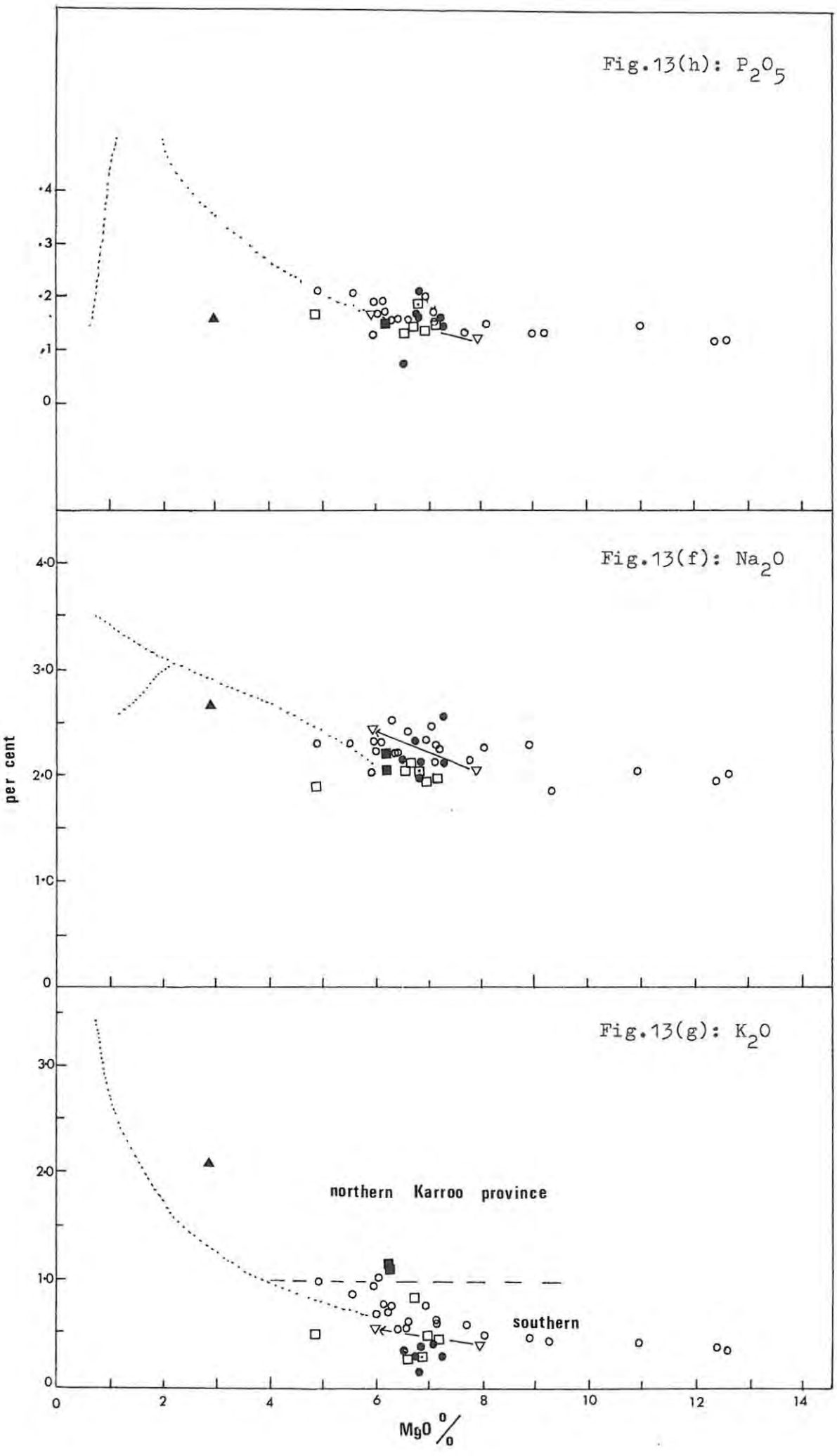
Fig.13(h): P_2O_5
Fig.13(f): Na_2O
Fig.13(g): K_2O
per cent
northern Karroo province
southern
MgO %

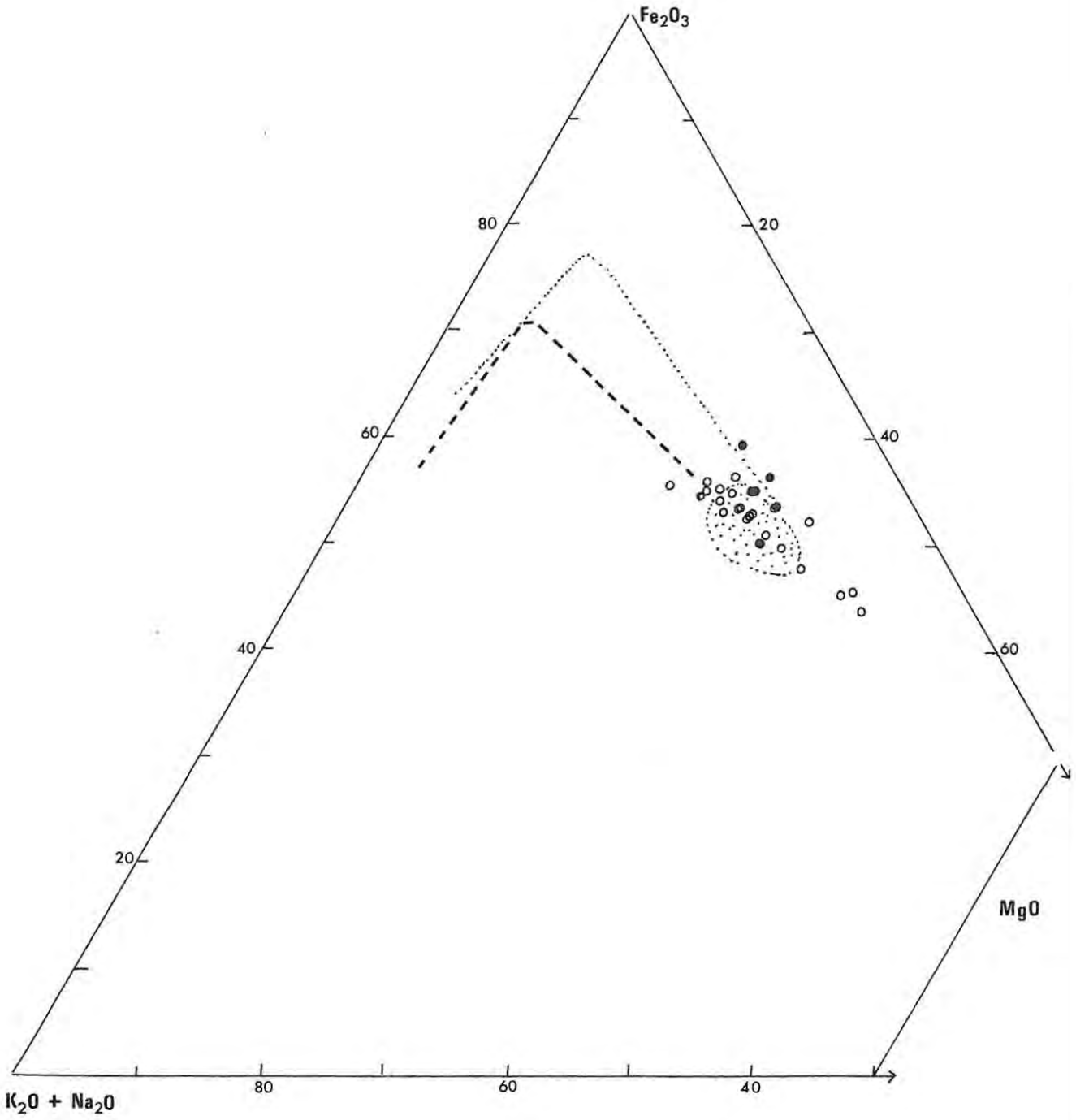

Fig. 15(a): AF*M diagram for the Karroo dolerites. Also shown are iron-enrichment trends for Birds River and Elephant's Head/New Amalfi, and the field covered by the Birds River gabbros (see Fig. 5).

- ● Chilled Karroo dolerites with $K_2O < 0.4\%$.
- ○ Karroo dolerites (contact and non-contact samples).
- ⁘ Birds River gabbros.

All Fe as Fe_2O_3.

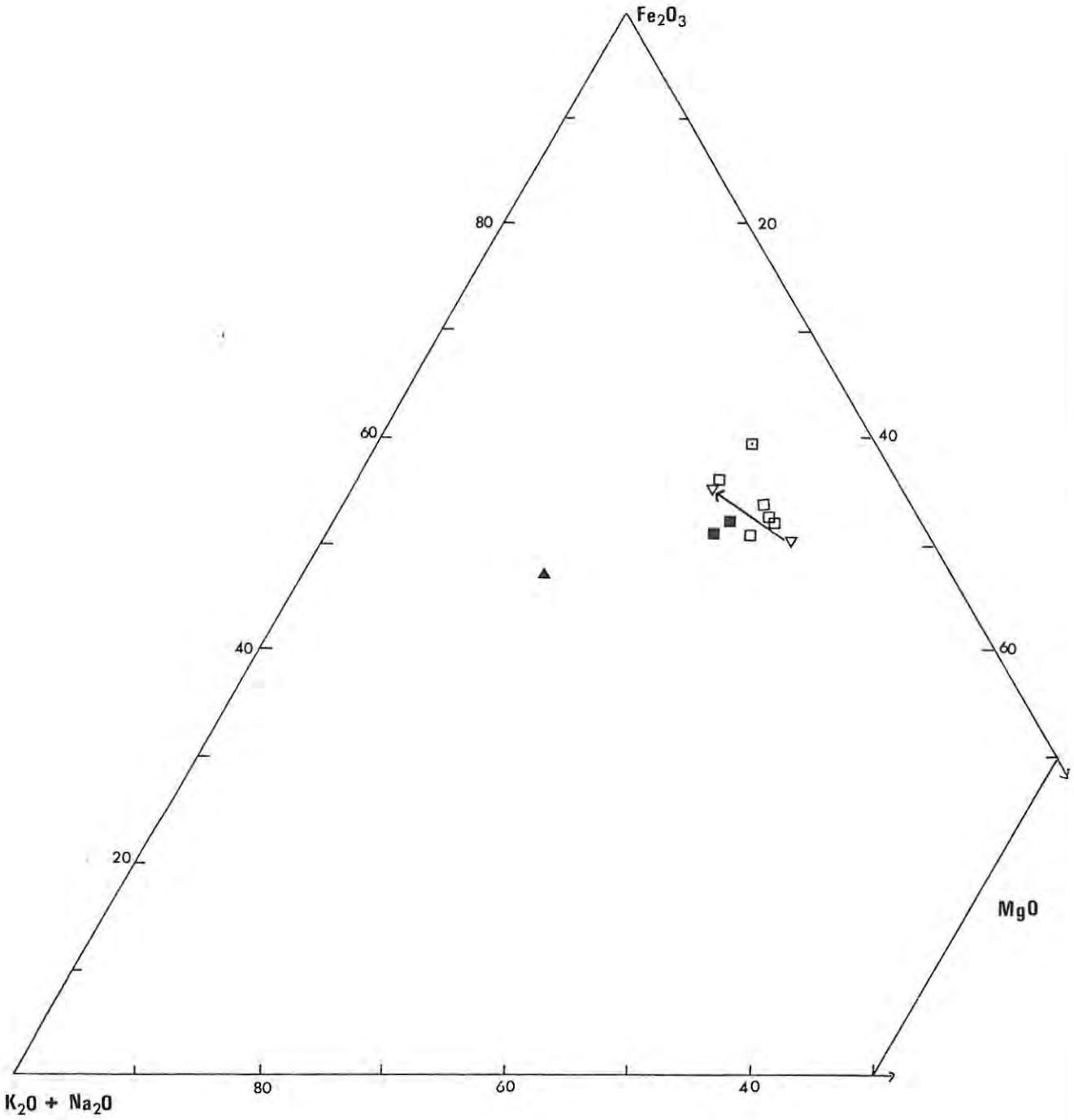

Fig. 15(b): AF*M diagram for the Barkly East volcanics. The Kraai River basalts, the Red Beds lava and flow JR108(A-B) show some degree of relative iron-enrichment. The Donnybrook basalts and the andesite plot on a more calc-alkaline trend.

- ⊡ Red Beds basalt.
- ■ Donnybrook basalts.
- ▲ Belmore andesite.
- □ Kraai River basalts.
- ▽→▽ Basalt flow JR108(A-B).

All Fe as Fe_2O_3.

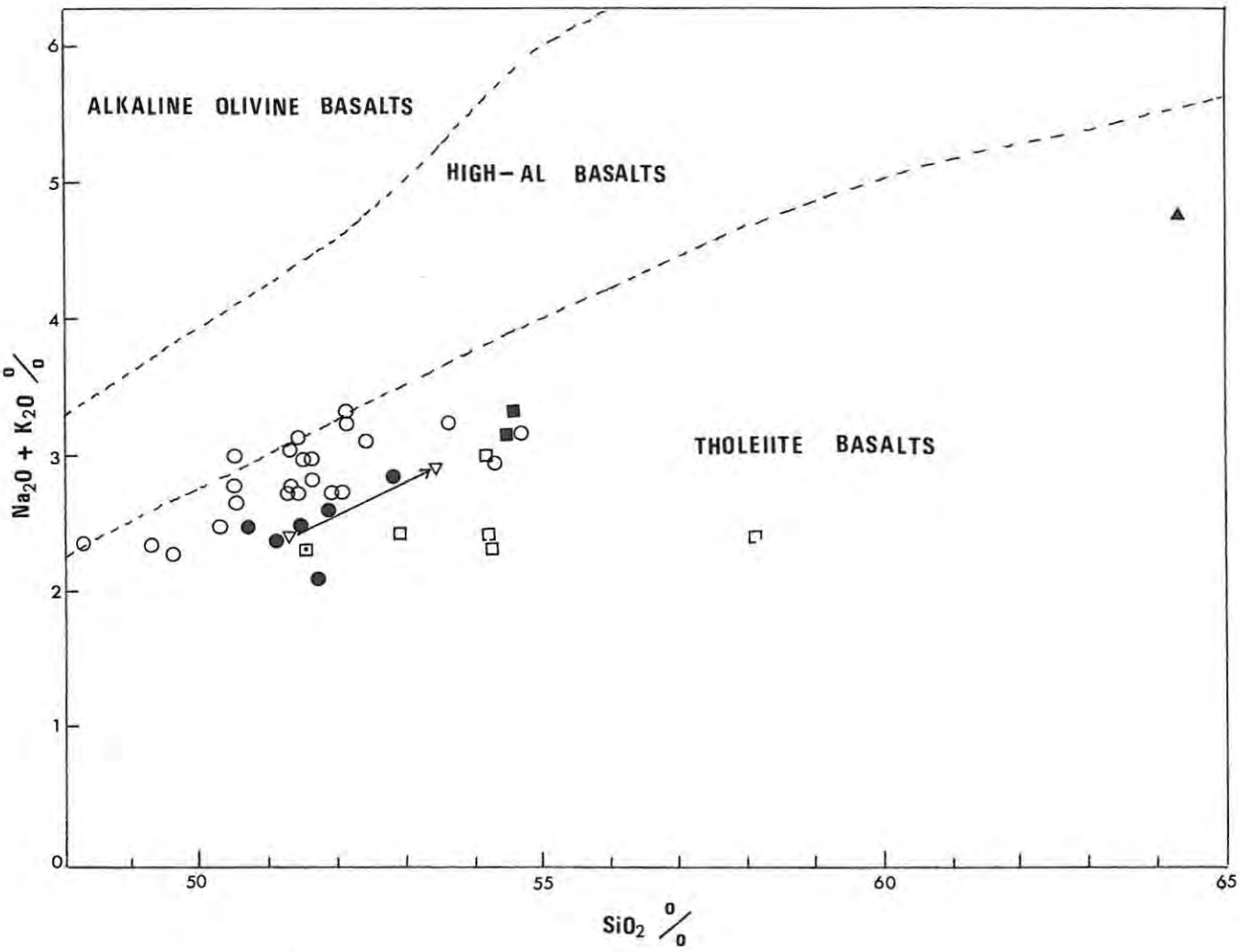

Fig. 16: Alkali-silica diagram (after Kuno, 1968) for the Karroo dolerites and Barkly East volcanics.

- ● Chilled Karroo dolerites with $K_2O < 0.4\%$.
- ○ Karroo dolerites (contact and non-contact samples).
- ⊡ Red Beds basalt.
- ■ Donnybrook basalts.
- ▲ Belmore andesite.
- □ Kraai River basalts.
- ▽→▽ Basalt flow JR108(A-B).

the Belmore locality and notes that it is a "typical siliceous enstatite andesite" with SiO_2 greater than 60%. The Niggli Katanorm (Hutchison, 1974) was calculated for JR31 (Table 9b) to enable direct comparisons with Figs.6, 7 and 8 of Irvine and Baragar (op.cit.). In the norm calculation, the oxidation ratio, Fe_2O_3/FeO, was reduced to 0.1.

In the Al_2O_3 vs. normative An% diagram (Irvine and Baragar, op.cit., Fig.6), rocks from the calc-alkaline series have higher Al_2O_3 per An% than the tholeiitic series. JR31 plots near the boundary separating the two fields. The calc-alkaline affinity of JR31 is, however, shown in the normative An% vs. colour index diagram (Irvine and Baragar, op.cit., Fig.7), where calc-alkaline andesites have a lower colour index per normative percent An%, than do tholeiitic andesites.

The analysis of the Belmore andesite (Table 9a), therefore, confirms the highly siliceous character noted by du Toit (1904) while the low absolute Fe_2O_3 content, the low degree of Fe-enrichment and parameters defined by Irvine and Baragar (op.cit.) suggest a calc-alkaline affinity. The high Al_2O_3 but low CaO content of this andesite, forms corundum in the normative calculation and in this respect, it also differs from normal calc-alkaline andesites. The andesite flow at Belmore overlies a fragmented-quartz-rich andesite breccia, showing ignimbritic textures (Lock et al. 1974) and the possibility that its chemistry may in part be due to sediment contamination cannot be discounted.

3.4.c

Comparison of the Barkly East basalts with the Karroo dolerites (this study) and basalts from the northern Karroo province.

In Figs.13 (a-h), the main differences in major element chemistry between the Barkly East basalts and the Karroo dolerites are clearly seen. The basalts, overall, are enriched in SiO_2 but depleted in Fe_2O_3, CaO and TiO_2 relative to the dolerites. Na_2O may be slightly depleted in the basalts but like K_2O, is highly variable. Some basalts (S9, JR88) have low K_2O ($< 0.3\%$) and low K_2O/Na_2O ratios (< 0.20), corresponding to similar low values in some Karroo dolerites - JR29, 21 and 36. There is little difference in the levels of Al_2O_3 and P_2O_5. Table 11 lists the average major and trace element content of the Barkly East basalts and the Karroo

dolerites and compares these with the average Lesotho, Swaziland and Nuanetsi basalt from data by Cox and Hornung (1966) and Cox et al. (1967).

Table 10 compares new data for the Karroo dolerites with average data from Walker and Poldervaart (1949) and with average data for chilled dolerites from Tasmanian and Antarctica.

Comparisons of the Barkly East basalts with basalts from the northern Karroo province can be made. Shown in Figs.13 (c, e, g) are the boundaries (Cox et al., op.cit., Figs.2,3,4) indicating the low-Al_2O_3-CaO and high-K_2O nature of basalts from Rhodesia relative to basalts from Lesotho and Swaziland. In Al_2O_3 and K_2O content, the Barkly East basalts fall within the limits of the southern province. Some Barkly East basalts have a low CaO content, more like those from Rhodesia. These boundaries must, however, not be interpreted too literally for they are gradational and attempt only to show very broad geochemical differences. As will be seen in a later section, low Ba, Sr, Zr, Nb and Y trace element concentrations within the Barkly East basalts, confirm the broad conclusions of Cox et al. (op.cit.).

3.4.d

Variations in MgO content and the ratio K_2O/Na_2O.

Cox (1972, Figs.3a-f) discusses MgO and K_2O/Na_2O variation trends in relation to height in the stratigraphic sequence at three localities of Karroo vulcanism - Nuanetsi, Tuli and Lesotho.

In relating the MgO content of the lavas to eruption temperatures, Cox (op.cit., Fig.4) draws an idealized volcanic cycle where,

(a) an initial period of eruption is characterised by low MgO concentrations indicating low eruption temperatures. These early extrusives would, presumably, have been most subjected to the cooling effects of country-rock through which they intruded prior to eruption.

(b) a culmination stage, closely following the initial stage, is characterised by high but variable MgO% and highly variable K_2O/Na_2O ratios. The olivine-rich basalts of Nuanetsi and Tuli belong to this stage. Highly variable K_2O/Na_2O ratios suggest a considerable range of parental magma compositions, since variation of this ratio cannot be due to plagioclase fractionation in these rocks.

(c) a steady state phase, best represented by the lavas from Lesotho, the Interbedded and Upper Basalts from Nuanetsi and the olivine-free basalts from Tuli, follows the culmination stage. In this stage, uniformly low MgO% and low but relatively constant K_2O/Na_2O ratios suggest a period of quiescent upwelling of magma from near-related parental melts.

(d) the final or termination stage is possibly in part represented by the Cretaceous kimberlites of Southern Africa.

The olivine-rich Lesotho basalts (Cox and Hornung, 1966, Table 1, No's 66,67 and 71), found near the base of the sequence are indicated in Fig.3c (Cox, 1972) as belonging to basalts from the culmination stage. A clear distinction between these basalts and olivine-rich types from Nuanetsi is not drawn by Cox (op.cit.). The latter are not parental to or related to the Interbedded and Upper Basalts by fractional crystallization (Cox and Jamieson, 1974). The olivine-rich basalts from Lesotho are not similar to those at Nuanetsi but are probably related to the average Lesotho basalt by low-pressure olivine accumulation.

The Barkly East basalts sampled in this study possibly represent the earliest Lesotho lavas and are obviously not widespread, for similar rock types are not reported from other basal horizons in the Lesotho sequence. The possibility that these basalts may represent basalts from the initial or culminatory stages as defined, can now be discussed. The following points emerge.

(a) The Barkly East basalts do not have significantly higher or lower MgO concentrations than the average overlying Lesotho basalt Table 11) and, in terms of MgO content, don't fall within the initial or culmination stage

(b) The average K_2O/Na_2O ratio of the Lesotho basalts (Cox and Hornung, 1966, Table 2,A) is 0.32 and this value remains steady throughout a vertical succession of nearly 1.5km (Cox, 1972, Fig.3f), suggesting a near similar parent basalt composition for these lavas. K_2O/Na_2O ratios for the Barkly East basalts vary between 0.13 and 0.53 and are not as stable as those for the Lesotho lavas. The early Red Beds basalt, JR88, has a low K_2O/Na_2O ratio of 0.13 while the older Donnybrook lavas have higher ratios, averaging 0.53. The overlying Kraai River basalts have ratios varying between 0.13 and 0.4 but average 0.26, slightly lower than that for the average Lesotho basalt, though similar to the average

chill-zone dolerite of this study (Table 10,A).

The variation of K_2O/Na_2O ratios within the Barkly East basalts and the porphyritic Karroo dolerites is even more difficult to analyse for, unlike the olivine-rich basalts from Nuanetsi, they commonly contain plagioclase as a phenocryst phase. Any variation in the degree of plagioclase fractionation or flotation, as these magmas migrate to upper crustal levels, would affect the final K_2O/Na_2O ratio of the rock. Plagioclase fractionation could account for minor variations in the K_2O/Na_2O ratio but, certainly, in the low-K_2O dolerites and basalts, low K_2O/Na_2O ratios must reflect unitial abundance variations for plagioclase fractionation must increase this ratio. This is clearly seen in the variation of K_2O/Na_2O at Birds River - (Appendix 1).

3.4.e

Normative chemistry : A comparison of the Karroo chilled dolerites, Lesotho lavas and Barkly East basalts in the basalt system, Diopside-Anorthite-Forsterite-Silica.

1) Method of Projection:

C.I.P.W. weight percent norms for the dolerites (Table 8b) and Barkly East basalts (Table 9b) were calculated assuming an oxidation ratio, $Fe_2O_3/FeO = 0.2$. To enable direct comparison with the Lesotho lavas studied by Cox and Hornung (1966), their data was recalculated assuming the same oxidation ratio. This results in a slight shift of the field defined by the Lesotho lavas (Cox and Hornung, op.cit., Fig.4) towards the quartz apex of the basalt tetrahedron. (Fig.17b).

Normative data were recalculated in the following way, to give the 4 components of the generalized basalt tetrahedron shown in Fig. 17(a).

1) An. - albite + anorthite
2) Di. - diopsidic (entatite + ferrosilite + wollastonite)
3) Ol. - olivine + normative olivine component of hyperthene.
4) Si. - quartz + normative quartz component of olivine.

As Cox and Hornung (op.cit.) note, this method ignores normative orthoclase, ilmenite, magnetite and apatite but "constitutes an average 91% of the original anhydrous analysis".

Table 8b : C.I.P.W. Weight Percent Norms* - KARROO DOLERITES.

(chilled samples only)

	JR 70	JR 90	JR 36	JR 54	JR 61	JR 2	JR 15	JR 21	JR 29	JR 42
Ap.	.30	.45	.33	.47	.45	.39	.37	.17	.40	.36
Ilm.	1.65	1.93	1.62	2.04	1.97	1.90	1.81	1.54	1.88	1.86
Or.	5.73	4.61	1.71	4.31	4.02	4.37	3.63	2.01	1.71	2.84
Ab.	17.51	19.88	21.87	19.84	19.88	21.49	20.48	18.28	19.71	19.54
An.	29.46	28.98	29.43	29.44	30.26	27.29	30.06	30.45	30.63	29.01
Mt.	2.28	2.60	2.29	2.52	2.38	2.67	2.61	2.93	2.55	2.48
En. (Di.)	4.14	4.50	5.19	5.22	5.10	5.43	4.93	5.24	4.95	5.61
Fs. (Di.)	3.28	3.97	3.43	3.95	4.17	4.81	4.10	5.07	3.92	3.63
Wo. (Di.)	7.68	8.70	9.02	9.51	9.57	10.51	9.32	10.52	9.18	9.68
En. (Hyp.)	10.98	10.94	13.09	12.16	9.97	10.47	11.71	11.23	12.03	14.59
Fs. (Hyp.)	8.70	9.63	8.66	9.21	8.16	9.27	9.76	10.88	9.54	9.44
Qtz.	8.32	3.82	3.37	1.33	4.09	1.43	1.23	1.70	3.48	.98
Fo. (Ol.)										
Fa. (Ol.)										
Norm. Plag.	An 62.7	An 59.3	An 57.3	An 59.7	An 60.4	An 60.1	An 59.5	An 62.5	An 60.8	An 59.8

Table 8b (contd.)

Table 8b (contd.)

	JR 49	JR 50	JR 99	JR 48	JR 72	JR 73	JR 101	JR 18	JR 9	JR 58
Ap.	.37	.52	.40	.36	.40	.49	.41	.33	.40	.52
Ilm.	1.73	2.08	1.79	1.75	1.86	2.11	1.86	1.57	1.91	2.37
Or.	1.71	.65	2.10	3.84	3.37	5.86	3.66	2.42	6.15	5.08
Ab.	18.11	16.92	18.06	19.71	18.32	19.63	17.39	17.60	19.08	19.71
An.	32.01	33.52	31.88	29.67	30.75	31.54	33.42	28.16	29.29	27.66
Mt.	2.51	2.60	2.55	2.48	2.49	2.28	2.57	2.46	2.61	2.44
En. (Di.)	4.89	4.31	5.21	5.49	5.33	4.01	4.94	5.56	4.35	3.67
Fs. (Di.)	3.52	3.41	4.07	4.02	3.90	3.71	4.30	2.66	3.89	3.21
Wo. (Di.)	8.75	7.99	9.61	9.88	9.08	7.90	9.51	8.77	8.51	7.07
En. (Hyp.)	13.63	12.82	11.89	12.42	12.56	8.48	10.71	16.95	10.85	10.47
Fs. (Hyp.)	9.80	10.11	9.32	9.09	9.19	7.87	9.35	8.10	9.81	9.14
Qtz.	2.99	5.08	3.09	1.31	2.27	6.15	1.87	-	3.09	8.67
Fo. (Ol.)								3.56		
Fa. (Ol.)								1.87		
Norm. Plag.	An 63.9	An 66.5	An 63.8	An 60.1	An 62.7	An 61.6	An 65.4	An 61.5	An 59.5	An 58.4

* Norms calculated to an oxidation of $\frac{Fe_2O_3}{FeO} = 0.2$

Abbreviations for normative minerals as in Table 2.

Table 9b : C.I.P.W. Weight Percent Norms - BARKLY EAST BASALTS.

	JR 88	JR 94	S 17	S 5	S 6	S 9	3/10	JR 109	JR 108A	JR 108B	JR 31*
Ap.	.40	.37	.36	.32	.36	.32	.39	.34	.29	.42	.34
Ilm.	2.24	1.66	1.65	1.64	1.69	1.60	1.68	1.66	1.61	2.14	1.12
Or.	1.51	6.50	6.68	2.69	2.66	1.54	2.87	5.05	2.27	3.04	12.55
Ab.	17.72	17.54	18.87	16.67	16.84	17.51	16.16	17.80	17.39	20.79	24.23
An.	31.25	29.46	29.03	31.46	32.88	31.05	32.41	29.51	32.60	25.46	21.13
Mt.	2.95	2.22	2.22	2.24	2.32	2.28	2.04	2.23	2.32	2.56	1.74
C.[1]											1.81
En. (Di.)	3.55	4.12	3.94	4.32	4.13	4.86	2.36	4.49	5.60	5.06	-
Fs. (Di.)	3.20	3.06	2.94	2.90	2.80	3.55	2.05	3.13	3.46	5.40	-
Wo. (Di.)	6.93	7.47	7.15	7.54	7.24	8.76	4.54	7.96	9.53	11.78	-
En. (Hyp.)	13.59	11.60	11.65	13.18	13.90	11.67	9.87	12.33	14.32	8.88	8.16
Fs. (Hyp.)	12.25	8.64	8.69	8.86	9.43	8.55	8.52	8.65	8.85	7.90	7.39
Qtz.	4.41	7.36	6.85	8.19	5.76	8.29	17.11	6.71	1.75	5.60	22.54
Norm. Plag.	An 64	An 63	An 61	An 65	An 66	An 64	An 67	An 62	An 65	An 55	An 47

* Barth-Niggli Katanorm calculated for JR31 assuming $\frac{Fe_2O_3}{FeO} = .1$

All other norms as C.I.P.W. Weight Percent calculations.

1 C. - Corundum. Abbreviations for normative minerals as in Table 2.

Fig.17(b) is the projection from the An. apex of the basalt tetrahedron and is identical to that discussed by Cox and Hornung (op.cit., Fig.4), with the exception that the divariant line An + Py + Si + liquid is also shown.

2) The System : Forsterite - Anorthite - Diopside - Silica.

Fig.17(a) is a reproduction of the 4-component system, Fo-An-Di-Si, as shown by Coombs (1963, Fig.2); also shown is the subdivision of the pyroxene primary phase volume into the diopside and proto-enstatite phase volumes (Schairer and Yoder, 1962; Hyoten and Schairer, 1960). The subdivisions and phases boundaries are shown diagrammatically.

This system is discussed in detail by Coombs (1963) and only the salient features need be pointed out. Seen from the An. apex, the plagioclase primary phase volume forms a roof to the spinel, forsterite, pyroxene and silica volumes and meets these volumes in the trivariant surfaces A,B,C and D (Fig.17a), where An + Sp, An + Fo, An + Pyr. and An + Si are in equilibrium with liquid respectively. Other trivariant surfaces are Fo + Sp + liquid, Fo + Pyr. + liquid and Pyr + Sr + liquid.

Of importance in the present study, are the trivariant surfaces B,C and D. Surface B meets C in the divariant line (ab) along which 3 phases, An + Fo + Py coexist with liquid. Similarly, C meets D along the line (cd) where An + Pyr + Si + liquid are in equilibrium. Thermal minima occur along (ab) and (cd) at X and Y, respectively. The line XY is the divariant line along which 2 Pyr + An + liquid coexist. X and Y therefore mark univariant points, where a 4 phase + liquid assemblage is stable. e.g. X = An + Fo + 2 Pyr + liquid. X is the univariant point indicated at $1250^{\circ} \pm 10^{\circ}$ in Fig.4 (Cox and Hœrnung, 1966).

In the general case, a basaltic liquid originating in the olivine primary phase volume will first precipitate olivine. The liquid composition may then move towards either the Fo + An + liquid or the Fo + Pyr + liquid trivariant surface where a second phase would begin to precipitate. In the latter case, pyroxene precipitates directly and also forms from the reaction, olivine + liquid = pyroxene. Residual liquid compositions then move to the divariant (ab), where a third phase, An or Pyr, crystallizes. Further crystallization drives the compositions of residual liquids to X where the stable assemblage is An + Fo + 2 Pyr + liquid. Liquids originating in the undersaturated portion of the olivine primary phase volume cease crystalli-

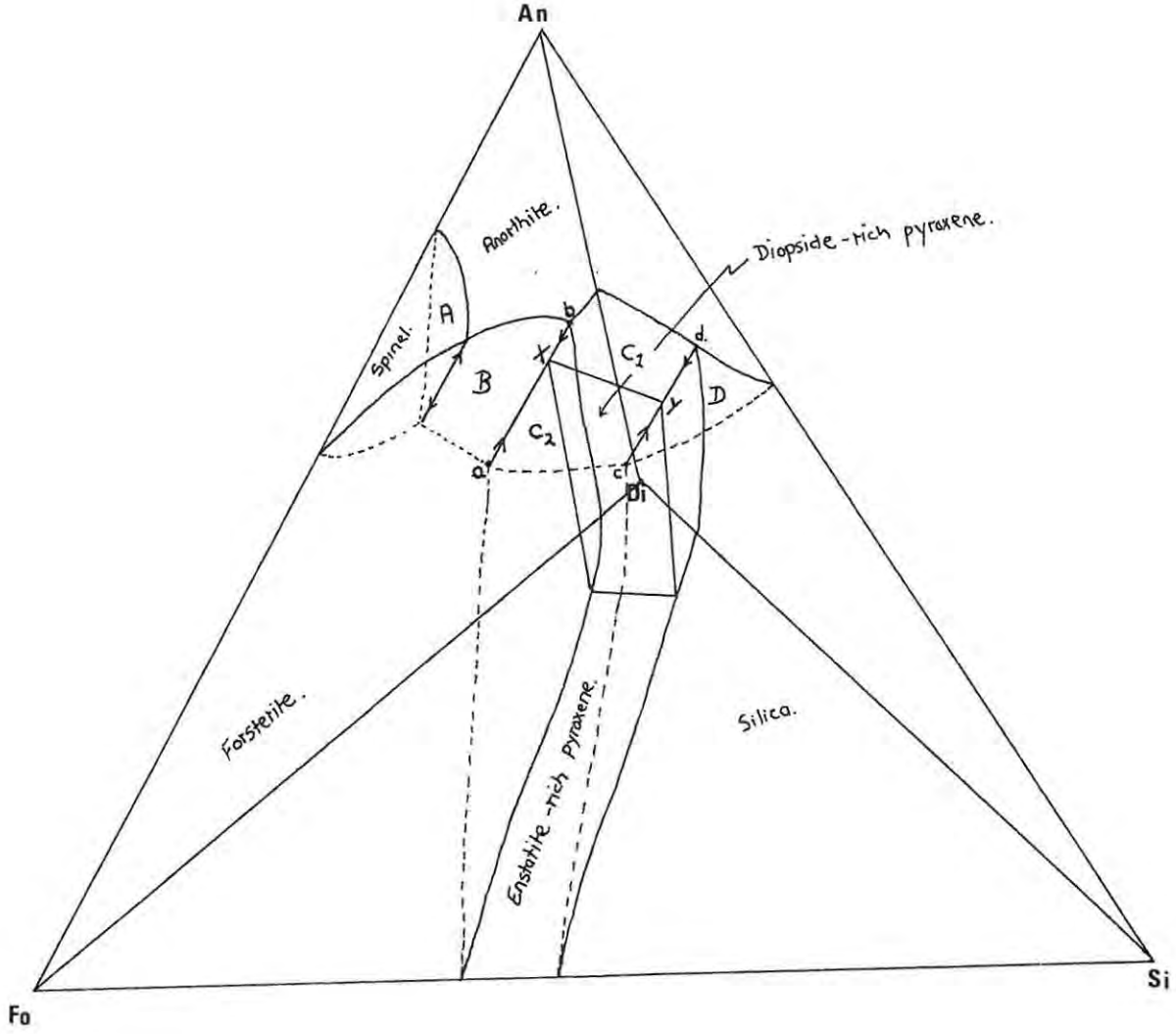

Fig.17(a): Schematic representation of relations in the 4 component basalt system - Anorthite, Diopside, Silica and Forsterite. The pyroxene volume has been subdivided into the Enstatite-rich and Diopside-rich volumes. The "floor" of the Anorthite volume is shown shaded. It is crossed by four four-phase divariant lines : anorthite-spinel-forsterite-liquid, anorthite-forsterite-pyroxene-liquid, (ab), anorthite-2 pyroxenes-liquid (XY), anorthite-pyroxene-silica-liquid, (cd), where it intersects other boundary surfaces (after Coombs, 1963, Fig. 2).

zation at point X, while saturated liquids continue crystallization along XY.

From Fig.17(a), the numerous paths a basaltic liquid could take on equilibrium crystallization, are evident.

3) Application of Results.

These diagrams (Fig.17a,b) have been included to compare the new dolerite and basalt analyses with basaltic lavas from Lesotho.

Cox and Hornung (1966, Fig.4) show that the majority of the Lesotho basalts lie on or very close to the trivariant surface, Fo + An + liquid. This corresponds with the dominant phenocryst assemblage - olivine + plagioclase - found in these lavas. Olivine-rich basalts (Cox and Hornung, op.cit., Table 1, No's 66, 67 and 71) lie displaced towards the olivine apex and may be considered low pressure, cumulus-enriched varieties of the overlying basalts. Cox and Hornung (op.cit.) note that variations within the Lesotho lavas cannot be explained simply in terms of olivine and plagioclase fractionation. The field defined does not lie along a single olivine-plagioclase control line but rather, projects across such a line, to show some component of pyroxene control. Furthermore, they maintain that since the Lesotho lavas project to points that straddle the join, enstatite-diopside, this thermal barrier did not exist when these basalts achieved their present compositions. Boyd and England (1961) find this thermal barrier to be effective at pressures greater than 10 kb.

The projected fields defined by the Karroo chill-zone dolerites and the Barkly East basalts, are shown in Fig.17(b). Three points are immediately clear.

(a) The displacement of projected points towards the Si apex, caused by using a higher Fe_2O_3/FeO ratio than that used by Cox and Hurnung (op.cit.) in the normative calculations, must not be confused with the "thermal barrier" effect mentioned earlier.

(b) The majority of Karroo dolerite analyses presented in this study project exactly into the field delineated by Cox and Hornung (op. cit.) for the Lesotho basalts. This suggests that the Karroo dolerites may also have achieved their compositions, at the time of intrusion, at pressures less than 10 kb. The common occurrence of clinopyroxene as a phenocryst phase in the dolerites is, however, problematic.

(c) Most of the Barkly East basalts project in the field En + An +

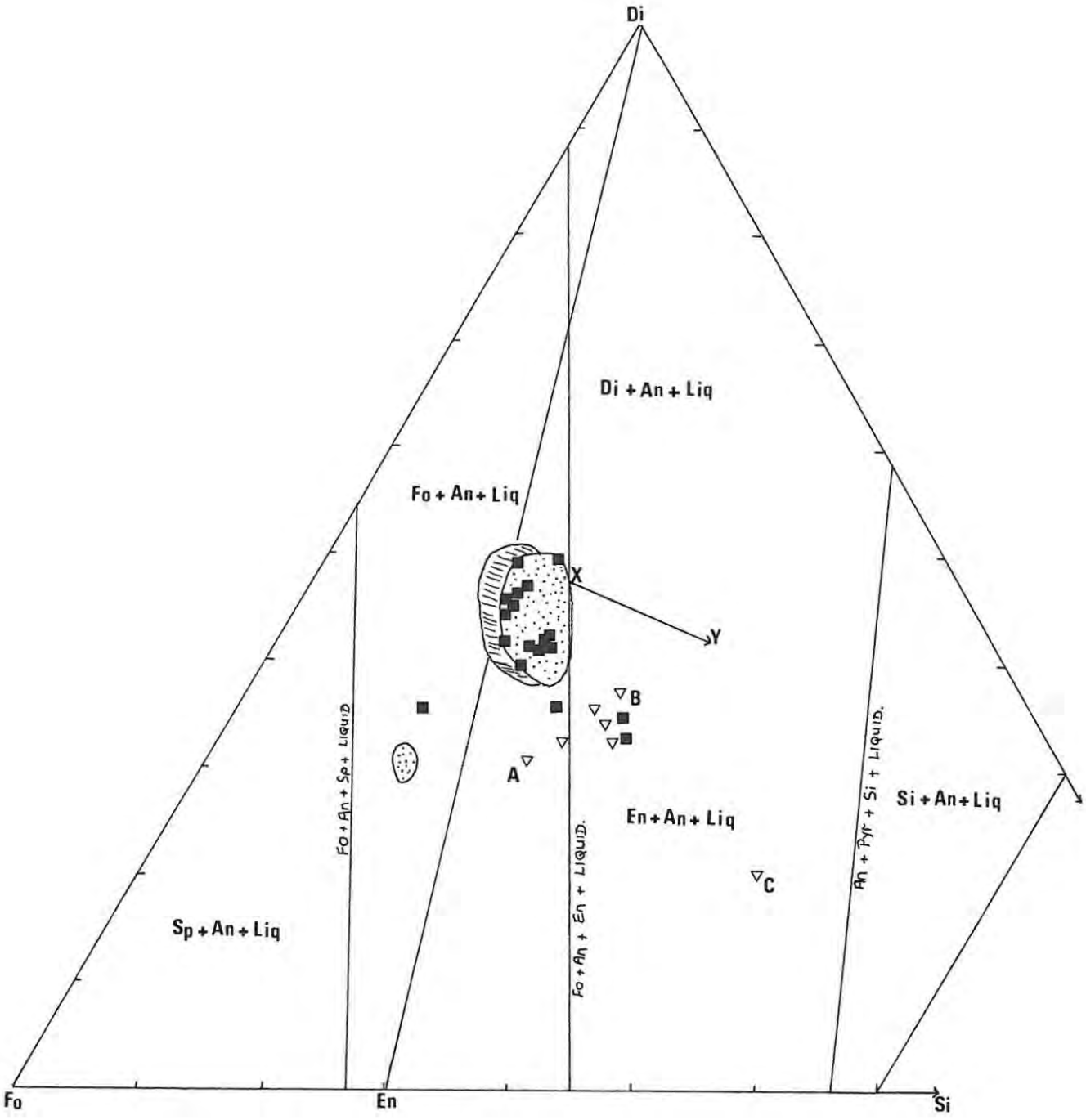

Fig.17(b): The Anorthite Projection of the Basalt System, An-Di-Fo-Si, similar to that discussed by Cox and Hornung (1966). Shown are the projections of the spinel, forsterite, pyroxene and silica primary phase volumes as well as the projection of the divariant lines Fo+An+Sp+liq., Fo+An+ Pyr+liq. and An+Si+Pyr+liq. Di= diopside, Fo= Forsterite, An= Anorthite, Si= Silica, En= Enstatite, liq.= liquid.

Field delineated by the Lesotho basalts (Cox & Hornung, op. cit.), assuming an oxidation ratio of $Fe_2O_3/FeO = 0.2$

Field delineated by the Lesotho basalts from normative data by Cox & Hornung (op.cit.). Oxidation ratio $Fe_2O_3/FeO = 0.123$.

■ Contact Karroo dolerites.

▽ Barkly East basalts, with the exception of JR108A,B.

All normative data calculated assuming $Fe_2O_3/FeO = 0.2$.

liquid. This field is the projection of the En + An + liquid trivariant surface (Fig.17a, C2) onto the base of the tetrahedron.

Orthopyroxene and plagioclase form the most common phenocryst assemblage found in these basalts. This suggests that, with the exception of JR88, their compositions lie on or very close to, the En + An + liquid surface. The Red Beds lava, JR88, projects into the Fo + An + liquid field but shows the phenocryst assemblage, plagioclase + pigeonite.

4) Discussion.

Though the Karroo dolerites project into the same field occupied by the Lesotho lavas, they contain more variable phenocryst assemblages than the latter. Most of the porphyritic dolerites contain a three-phenocryst assemblage, (olivine + plagioclase + clinopyroxene) and in Fig.17(a) appear less primitive than the two-phenocryst Lesotho lavas. One- (plagioclase or olivine) and two- (plagioclase + olivine or plagioclase + clinopyroxene) phenocryst assemblages are also common in the dolerites sampled. Some dolerites show a four-phenocryst assemblage (olivine + plagioclase + augite + pigeonite), suggesting that the univariant point X (Fig.17a) had been reached. No orthopyroxene phenocrysts have been identified in the dolerites from this study, though orthopyroxene phenocrysts are characteristic of chilled margins of Hangnest-type dolerite intrusions. (Walker and Poldervaart, 1949).

The prevalence of clinopyroxene as a common phenocryst phase in the Karroo dolerites but not in the Lesotho lavas, may be due to the expansion of the clinopyroxene primary phase volume at higher pressures (O'Hara, 1968). The exact positions of the various phase boundaries in the basalt tetrahedron are strongly sensitive to pressure-temperature conditions. Variable phenocryst assemblages, assuming equilibrium, may thus reflect subtle changes in pressure-temperature conditions in the environment of crystallization.

As mentioned before orthopyroxene and plagioclase phenocryst assemblages in the Barkly East basalts agree well with their projected position in Fig.17(b). Considering only these basalts (Fig.17b), two trends are apparent. Trend A-B suggests olivine + plagioclase fractionation to derive the main group of Barkly East basalts from an initial composition more basic than that of JR88. A second trend, B-C, suggest some pyroxene fractionation to produce the more differentiated basalt 3/10. Similar "kinked" trends are discussed by Coombs

(1963, Figs.8,9).

Ni and Cr concentrations in JR88 (Table 9a), however, do not satisfy the contention that the Barkly East basalts are related to JR88 by olivine fractionation.

Fig.17(b) indicates that had the norms of the Barkly East basalts been calculated assuming an oxidation ratio $Fe_2O_3/FeO = .123$ (Cox and Hornung, 1966), the majority would project very close to the divariant line Fo + An + En + liquid. The absence of olivine as a phenocryst in these basalts may, in part, be due to its reaction relationship with residual liquids and to its removal by a mechanism such as gravitational settling.

The trend of the projected Barkly East basalt compositions towards the silica apex (Fig.17b) suggests that residual liquids were moving across the trivariant surface En + An + liquid, at the time of eruption and solidification. The general absence of clinopyroxene as a phenocryst phase in these basalts, is confusing. Residual liquids would be expected to move across the An + Pyr + liquid surface at higher temperatures during equilibrium crystallization. A rapid decrease in the confining pressure immediately prior to eruption may have reduced the clinopyroxene primary phase volume. Any clinopyroxene phenocrysts were therefore likely to be resorbed, though relicts should be observed. Sparse, highly-eroded clinopyroxene phenocrysts are seen in only one basalt - JR94.

O'Hara (1968) discusses the trend of the Lesotho lavas in the type of normative diagram shown in Fig.17b. He cautions that, though there appears to be evidence for a more extensive clinopyroxene field at higher pressures, continuous olivine fractionation from high-pressure partial melting products will project residual liquids at the loci of liquids in low pressure equilibrium with anorthite, forsterite and pyroxene. Such a projection will give the spurious appearance of basalts having suffered low-pressure fractionation of olivine, plagioclase and clinopyroxene.

The Barkly East basalts in normative chemistry, thus extend the trend noted by Cox and Hornung (1966) for the Lesotho lavas, into the An + En + liquid field. Petrographically and in terms of silica enrichment, they match the Hangnest dolerite-type of Walker and Poldervaart (1949). The Barkly East basalts are clearly different in both major and trace element content, to the orthopyroxene-bearing Nuanetsi olivine dolerites (Cox and Jamieson, 1974). In a later section dealing with trace elements, it will be seen that the Barkly East basalts are only significantly depleted in Ni relative to the

average Lesotho basalt (Cox and Hornung, op.cit.).

The overall trend indicated in Fig.17(b) needs further analysis. Whether the Barkly East basalts are related to the overlying Lesotho basalts by low-pressure olivine, plagioclase and clinopyroxene fractionation from a similar parent magma, is difficult to analyse. At this stage, the author can only repeat the view of O'Hara (1968) that "the occurrence of a series of lavas with compositions connected in an obvious low-pressure geochemical fractionation series, is no guarantee whatever that these magmas are related to one another by such a process".

3.5.
Trace Element Variations.

3.5.a
Introduction.

New trace element data for some Karroo dolerites and Barkly East lavas are presented in Tables 8(a) and 9(a) respectively. All analyses were determined by standard X.R.F. techniques (Appendix 4).

Previous published trace element data for the Karroo dolerites are confined to Walker and Poldervaart (1949) and Nockolds and Allen (1956). Prinz (1967), in a broad survey of data for basic igneous suites, reviews trace element data for the Karroo dolerite province. Trace element data for the Lesotho basalts are from Cox and Hornung (1966) while data for Karroo volcanics in Rhodesia and Swaziland are from Cox et al. (1967). These data are summarized in Tables 10 and 11.

Cox et al. (op.cit.) find that large geochemical differences exist between the northern (Rhodesia) and southern (Lesotho and Swaziland) Karroo basalt provinces. The Karroo dolerites and the Lesotho and Swaziland basalts are depleted by factors of approximately 2 to 4 in the trace elements Ba, Sr, Zr and probably Y and Nb relative to Karroo lavas from Rhodesia.

This section will discuss trace element and inter-element variations within the Karroo dolerites and the Barkly East basalts. Trace element variations with differentiation are discussed with the aid of MgO variation diagrams (Figs.14 a-l). Selected inter-element variations are shown in histogram form. (Fig.18 a-j), and summarized in Tables 8(c) and 9(c).

To avoid unnecessary repetition, a comparison of the new data to previous data by the abovementioned authors, will be discussed in Section 3.6.

3.5.b
Strontium.

Dolerites:

The slight increase in Sr (Fig.14a) with differentiation, from 175 ppm in the olivine-rich dolerites to an average of 203 ppm in the contact dolerites, is typical of the early to middle stages of

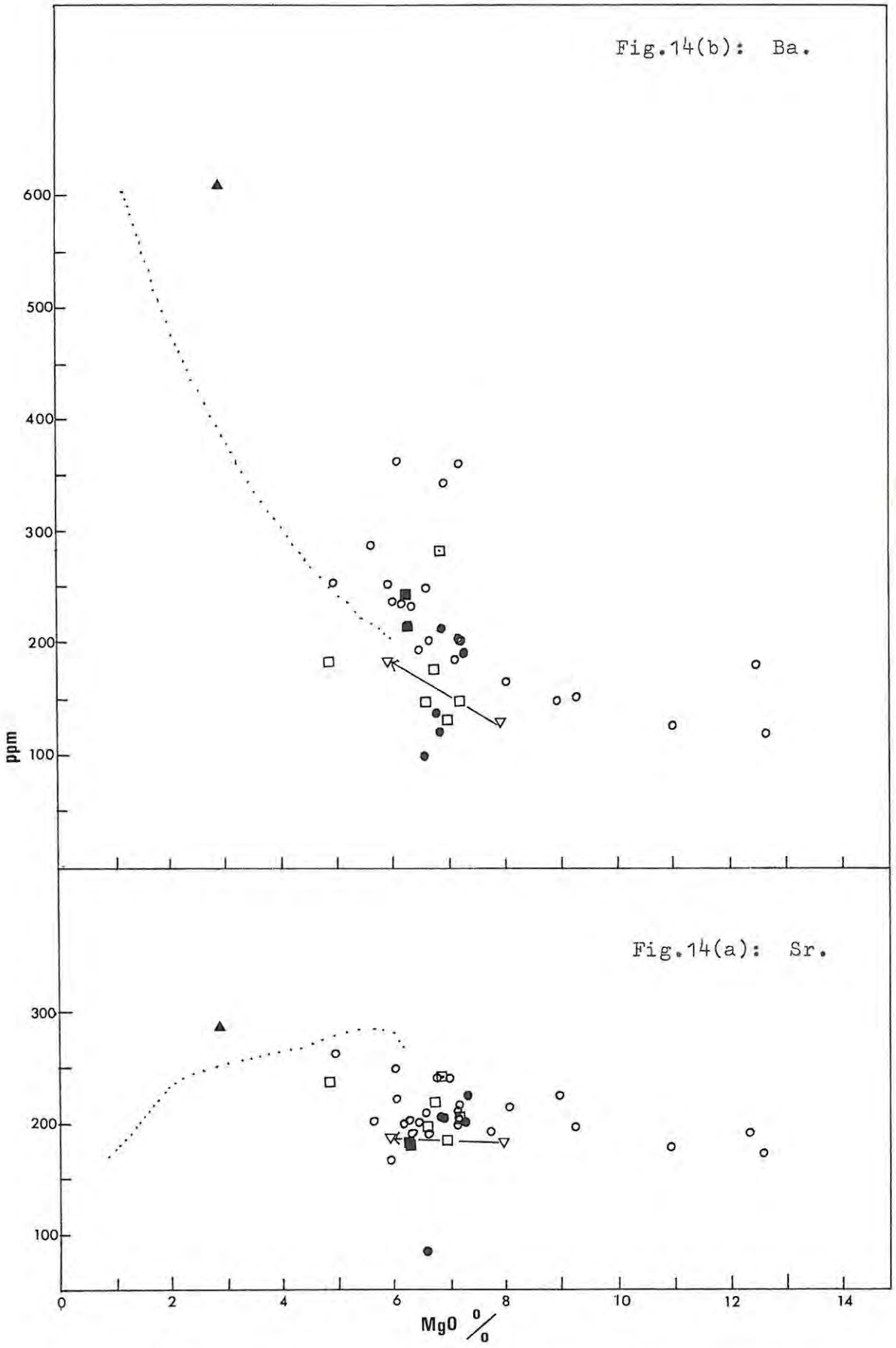

Figs.14(a-l): Trace element variations within the Karroo dolerites and Barkly East volcanics, plotted against MgO%. Symbols as for Figs.13(a-h).

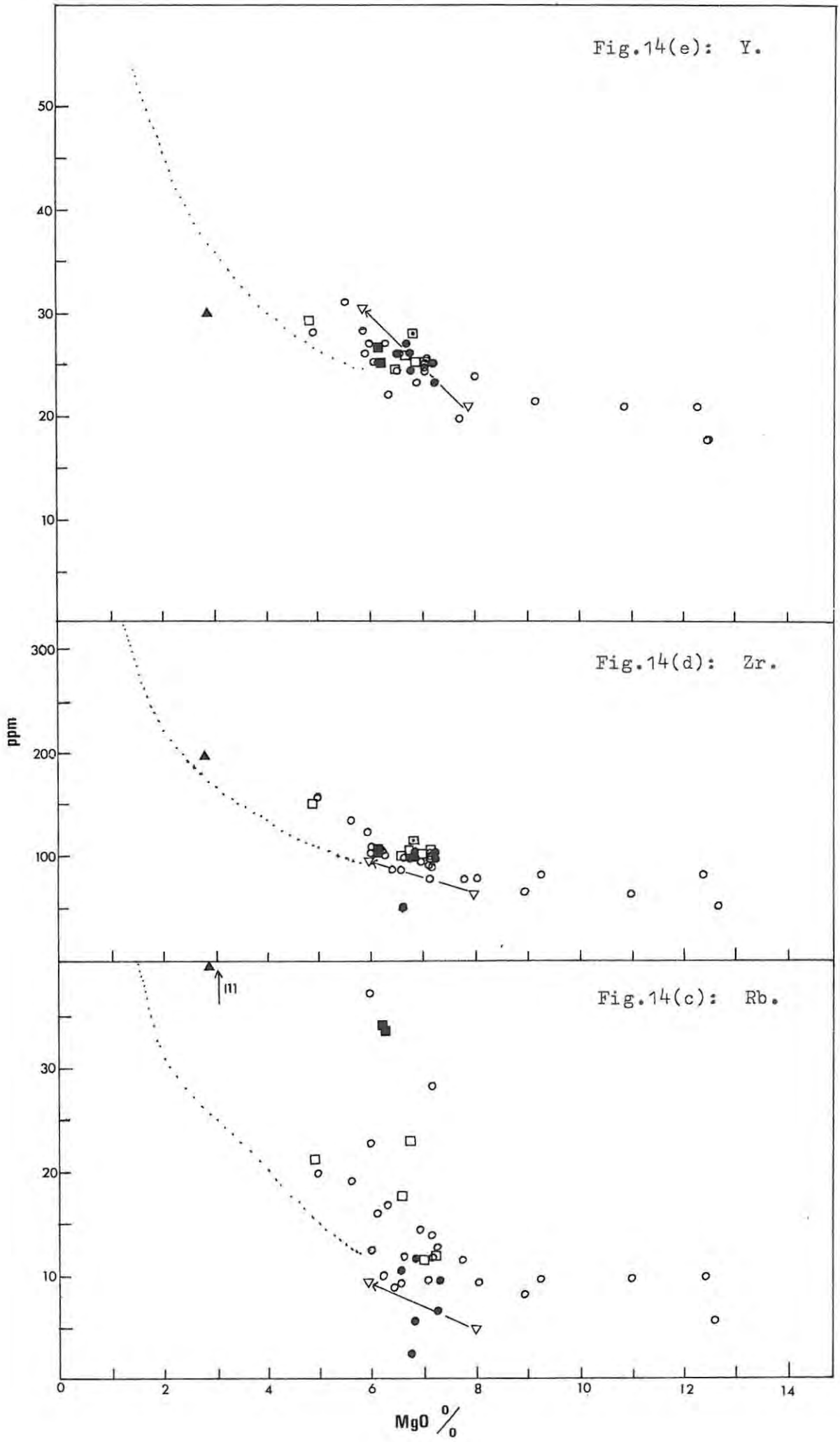
Fig.14(e): Y.
Fig.14(d): Zr.
Fig.14(c): Rb.
ppm
MgO %
50
40
30
20
10
300
200
100
30
20
10
0
2
4
6
8
10
12
14

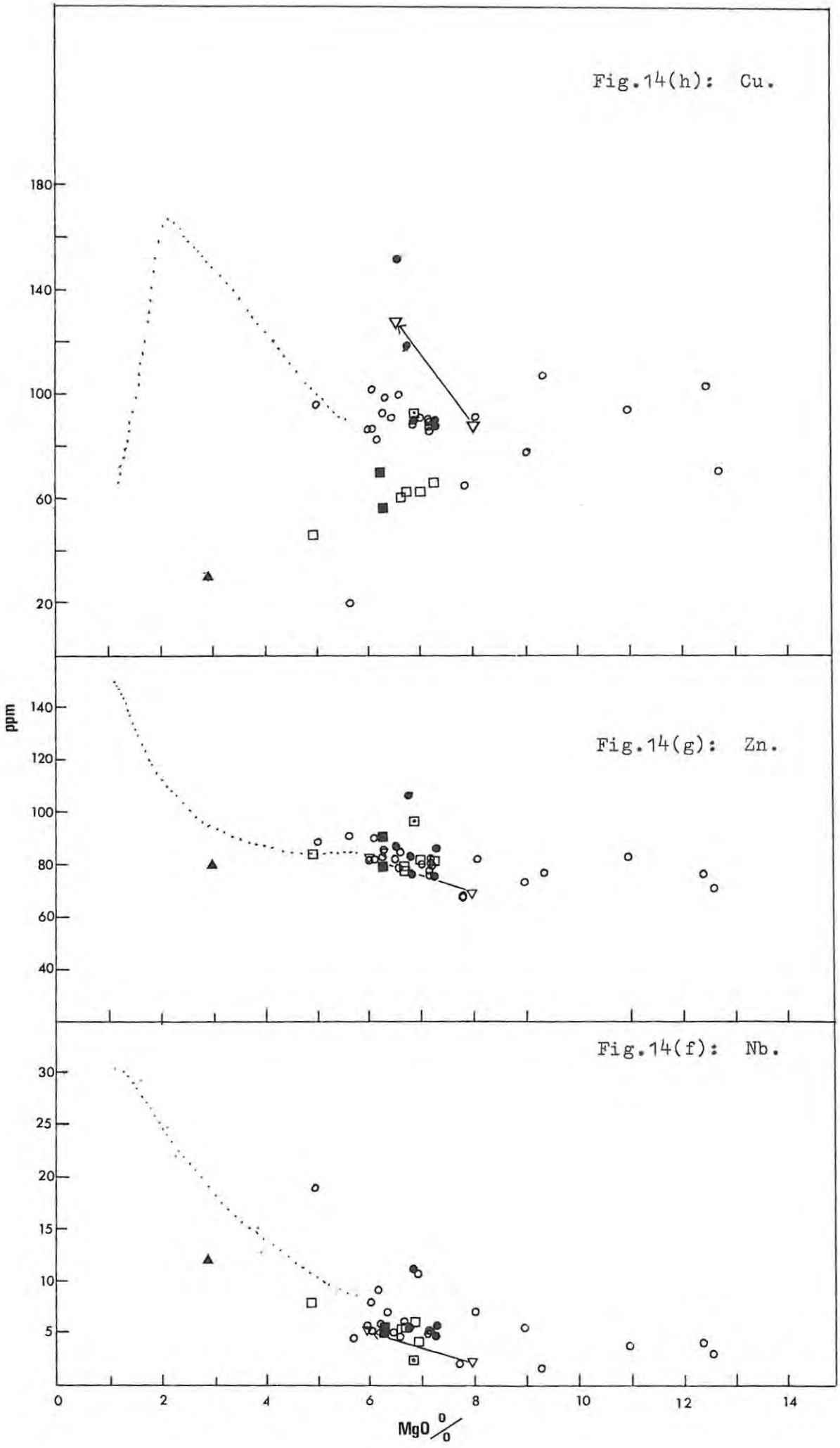
Fig.14(h): Cu.
180
140
100
60
20
ppm
Fig.14(g): Zn.
140
120
100
80
60
40
Fig.14(f): Nb.
30
25
20
15
10
5
0
2
4
6
8
10
12
14
MgO %

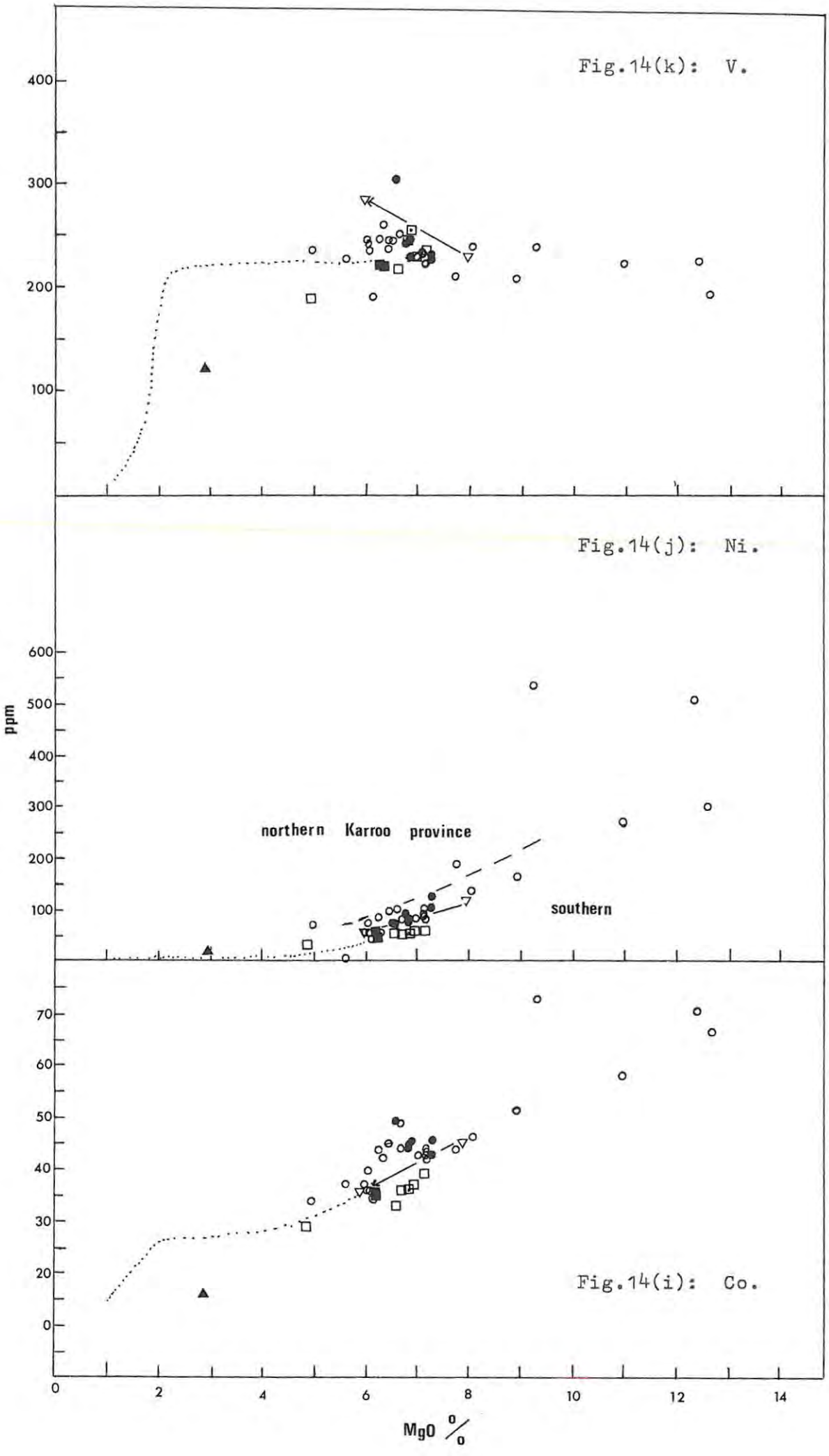
Fig.14(k): V.
Fig.14(j): Ni.
Fig.14(i): Co.
ppm
northern Karroo province
southern
MgO %

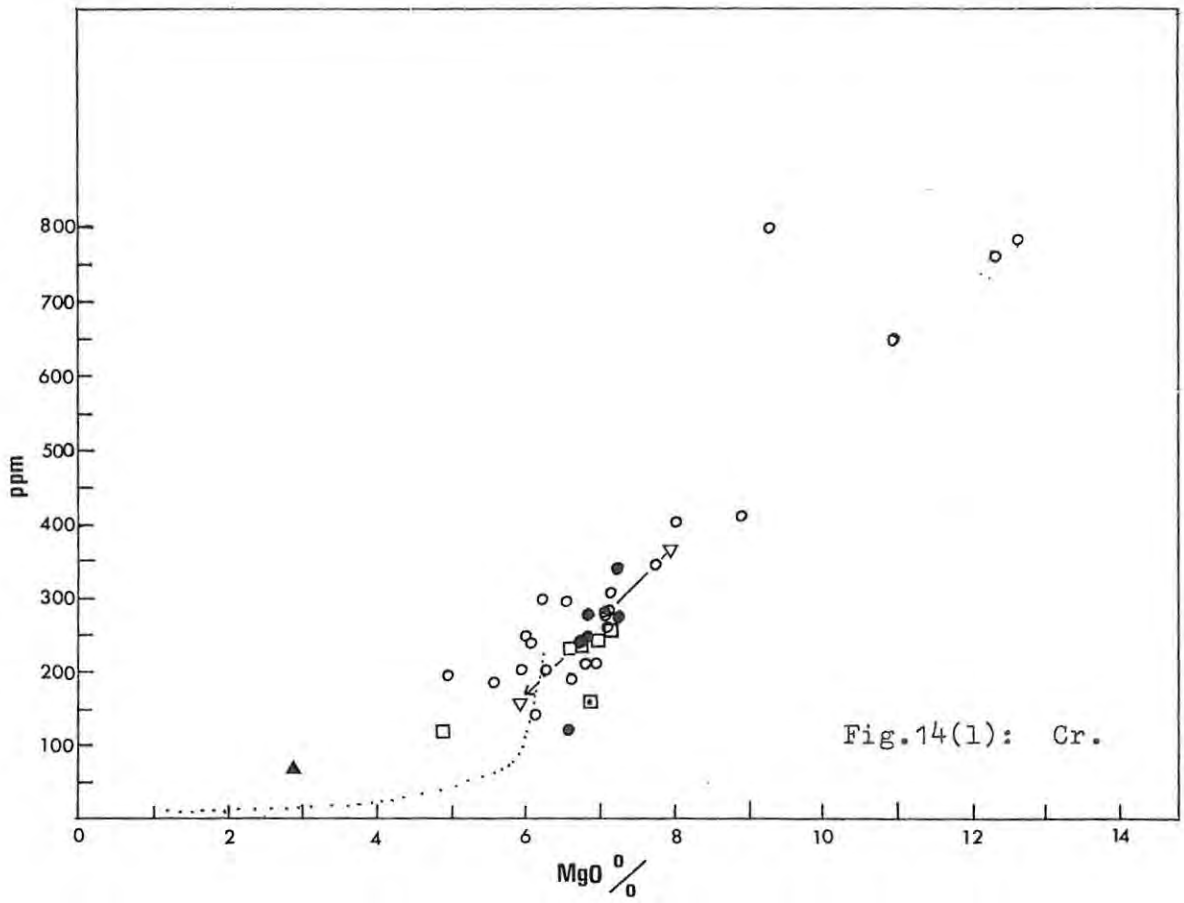

Fig.14(1): Cr.

differentiation in basic magmas. This trend of increasing Sr suggests dominant femic mineral control in fractionation processes, while the steady decrease in Sr, noted for the Birds River intrusion, has already been discussed in terms of strong plagioclase fractionation.

The contact dolerites show no single Sr variation trend, and values range between 165 ppm and 250 ppm. The average value is 206 ppm (Table 10,A).

There is little correlation between petrographic type (based on phenocryst assemblages) and Sr content. Only the plagioclase + olivine-phyric dolerites (JR36, 54, 61, Table 8a) contain consistently higher Sr concentrations than the average concentration. Furthermore, with the exception of JR21, the low-K_2O dolerites have normal Sr levels.

The low Sr (84 ppm) and Ba (99 ppm) levels in sample JR21, are difficult to explain. Included glomeroporphyritic plagioclase in JR21 is relatively calcic (normative plagioclase is An_{63}) and protracted Na-plagioclase fractionation must be ruled out. These concentrations must reflect initial abundance variations or differing degrees of partial melting of the parent mantle rock.

Ca/Sr ratios average 397 (range 423-279), with the exception of JR21 (Ca/Sr = 948). Ba/Sr ratios average 0.94 but range from 1.63 to 0.67.

Barkly East basalts:

The range of Sr concentrations in the Barkly East basalts (239 ppm to 184 ppm) is well within the range found in Karroo dolerites with similar MgO percent (Fig.14a).

Sr increases with differentiation to 236 ppm in the more highly differentiated basalt, 3/10, and to 279 ppm in the andesite. There is little change in Sr content from the base to the top of flow JR108 (183 to 189 ppm Sr). This is surprising, for the strong decrease in Al_2O_3 percent with differentiation of flow JR108, suggests strong plagioclase crystallization.

The average Ba/Sr ratio for these basalts (excluding the andesite) is 0.92 (range = 0.71-0.72), close to the value determined for the Karroo dolerites. The andesite shows a strong enrichment of Ba relative to Sr (Ba/Sr = 2.18) and matches values found in the late-stage derivatives from Stapelbergkloof, Birds River.

3.5.c

Barium.

Dolerites:

For the most part, a well defined trend of increasing Ba with differentiation is seen in Fig.14(b). Ba increases from 117 ppm in an olivine-rich dolerite to between 250 and 290 ppm in the more differentiated samples. Within this trend, the degree of scatter is relatively small and variations might be explained by varying amounts of olivine, plagioclase and pyroxene fractionation.

Some dolerites (JR49, 126, 9 and 124), however, show relatively enriched Ba concentrations (average = 350 ppm Ba) while dolerites JR21, 29 and 50, are depleted to Ba levels of less than 150 ppm. In the high Ba group of dolerites, only JR9 shows a sympathetic enrichment of Rb and K_2O%. These residual element concentrations could be due to protracted femic phase fractionation. However, the concentrations of other residual trace elements such as Nb, Zr and Y are not similarly enriched (Table 8a), as would be expected with such a process.

Low Ba concentrations are confined exclusively to the low-K_2O dolerites but the corollary is not true. i.e. not all the low-K_2O dolerites have low Ba levels (Fig.14b). Low Ba concentrations cannot be due to frational crystallization processes involving the removal of alkali- or sodic-feldspars or biotite for these phases are not observed in these samples. This suggests that factors other than low pressure crystal fractionation influence the levels of Ba determined in the Karroo dolerites.

Lower K/Ba and Ba/Zr ratios characterize the low-K_2O dolerites (Table 8c, Figs.18d,f). Considering only the contact dolerites, K/Ba ratios for the dolerites with K_2O 0.4%, average 26, while for the low-K_2O dolerites, average 16. Similarly Ba/Zr ratios average 2.3 and 1.7 respectively.

Figs.18 (d,f) indicate the large variation in K/Ba and Ba/Zr for the Karroo dolerites when compared with the range in these ratios for the differentiated sequence at Birds River.

Barkly East basalts:

Fig.14(b) indicates that, though concentrations vary, Ba increases with differentiation from 130 to 183 ppm in the Kraai River basalts. Differentiation of flow JR108 has enriched Ba from 130 ppm (A) to 189 ppm in the upper contact (B).

Table 8c : Selected Inter-element Ratios* - KARROO DOLERITES.

Ratio	A	B	C	D	E	Fig 18
K/Rb	262[1] (74-509)	398 (229-514)	401 (74-975)	401 (74-975)	(382-555)	a
K/Y	92 (34-120)	230 (161-311)	189 (34-311)	177 (34-311)	(208-303)	b
K/Zr	27 (9-53)	57 (48-78)	48 (9-78)	49 (9-78)	(52-71)	c
K/Ba	16 (9-28)	26 (32-23)	23 (7-32)	22 (7-32)	(22-33)	d
Ba/Rb	(9-56)	16 (10-20)	18 (9-56)	19 (9-56)	(12-21)	e
Ba/Zr	1.7 (1.3-2.1)	2.3 (1.6-3.5)	2.2 (1.3-3.5)	2.3 (1.3-3.5)	(1.7-2.7)	f
Zr/Nb	16 (9-22)	16 (8-31)	16 (8-31)	16 (8-31)	(9-13)	g
Zr/Y	3.7 (2.0-4.4)	4.0 (3.2-5.7)	3.9 (2.0-5.7)	3.8 (2.0-5.7)	(3.6-5.3)	h
Ni/Co	2.1 (3.0-1.7)	2.0 (.1-4.7)	2.0 (.1-4.7)	-	(.1-2.1)	i
Cr/Ni	2.7 (1.7-3.3)	3.2[2] (2.3-4.5)	3.0[2] (1.7-4.5)			j

* Ratios are averaged. Range indicated in brackets.

1 excluding JR29 (K/Rb = 975)

2 excluding JR58 (Cr/Ni = 54)

A. Chilled dolerites with $K_2O < .4$ %

B. Chilled dolerites with $K_2O > .4$ %

C. All chilled dolerites

D. All dolerites sampled.

E. Range determined for fractionated sequence at Stapelbergkloof, Birds River.

Table 9c: Selected Inter-element Ratios* - BARKLY EAST BASALTS.

Ratio	A	B	C	D	Fig 18
K/Rb	250[1] (322-122)	270 (268-272)	-	155	a
K/Y	153 (270- 89)	353 (268-272)	76	574	b
K/Zr	38 (21-62)	81 (80-82)	17	84	c
K/Ba	25 (15-39)	41 (39-42)	7.4	28	d
Ba/Rb	10[1] (8-13)	6.7 (6.4-6.9)	-	5.5	e
Ba/Zr	1.5 (1.2-2.0)	2.0 (1.9-2.1)	2.3	3.0	f
Zr/Nb	22 (19-27)	21 (20-22)	54	17	g
Zr/Y	4.5[1] (4.1-5.5)	4.3	4.4	6.8	h
Ni/Co	1.3[1] (1.1-1.5)	1.4	1.4	1.3	i
Cr/Ni	4.7[1] (3.7-5.8)	4.5	3.2	3.5	j

* Ratios are averaged. Range indicated in brackets.

1 excluding JR108A, B.

A. Kraai River basalts.

B. Donnybrook basalts.

C. Red Beds lava from Siberia.

D. Belmore andesite.

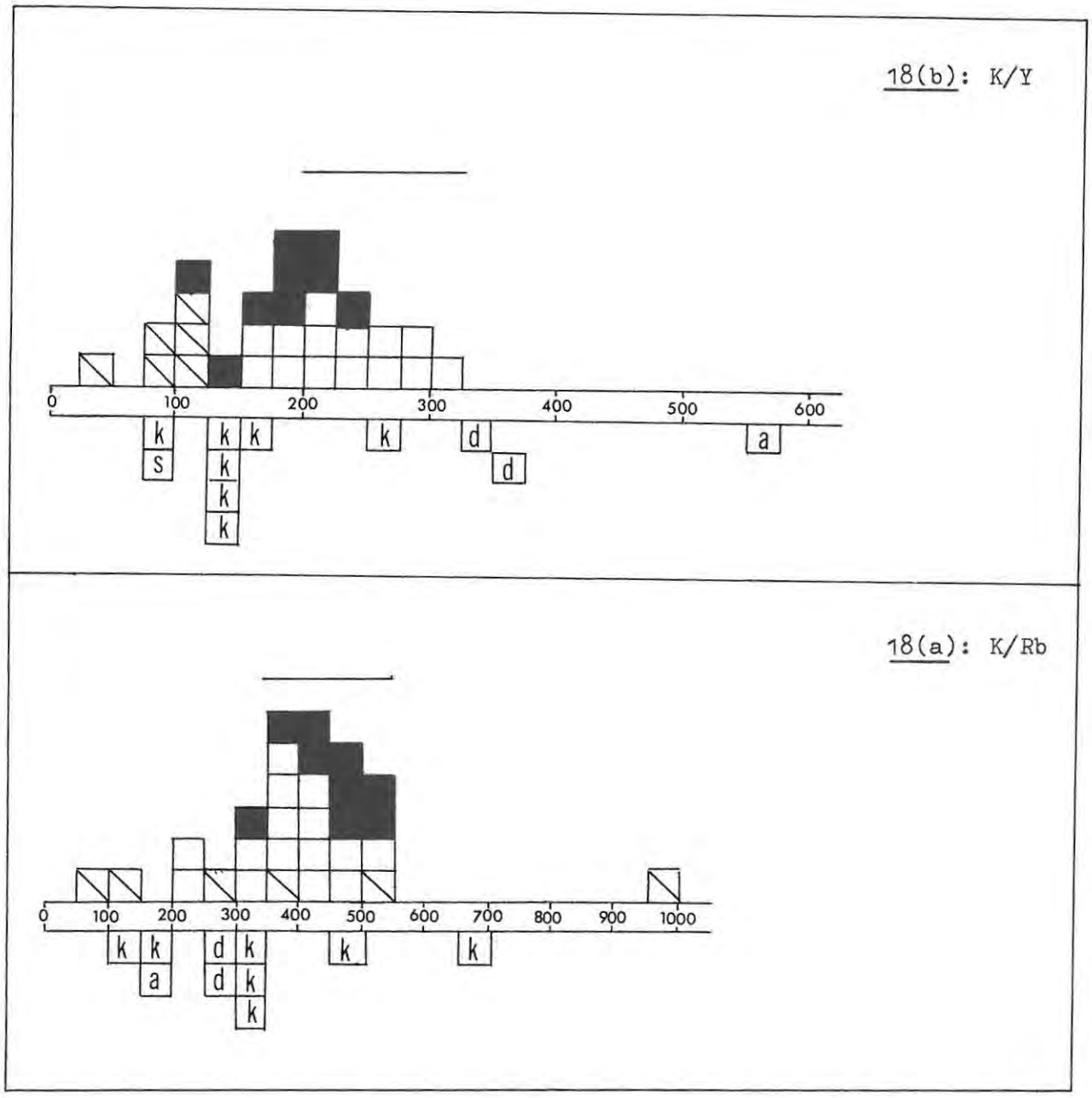

Figs. 18(a-j) : Selected inter-element ratios - Karroo dolerites and Barkly East basalts.

Contact dolerites with $K_2O < 0.4\%$ (the low-K_2O group).

Contact dolerites with $K_2O > 0.4\%$ (the normal-K_2O group).

Non-contact dolerites.

k Kraai River basalts including JR108A,B.

d Donnybrook basalts.

a Belmore andesite.

s Red Beds basalt, Siberia.

The range of ratios determined for the sequence at Stapelbergkloof, Birds River is also indicated.

18(e): Ba/Rb

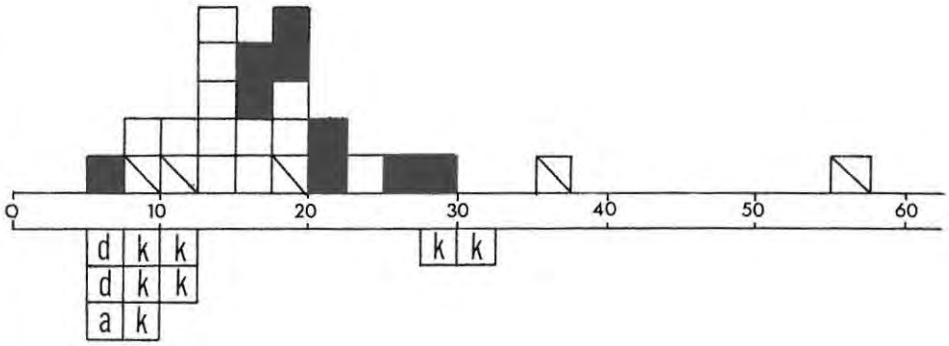

18(d): K/Ba

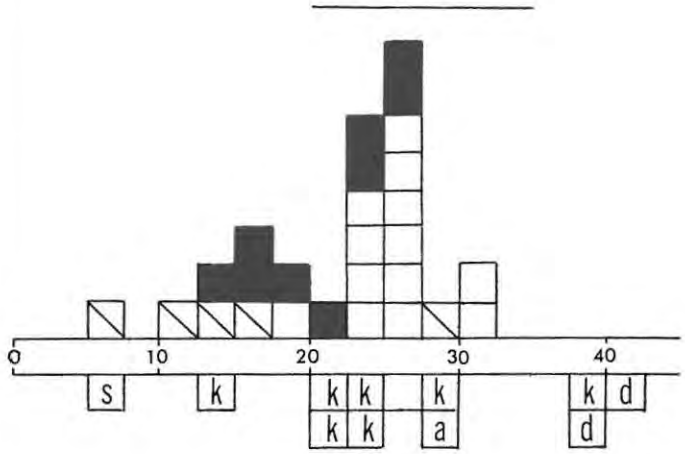

18(c): K/Zr

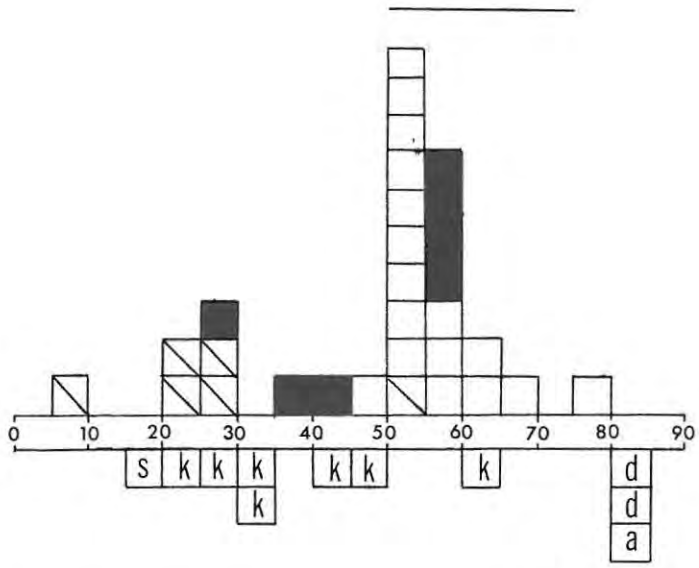

18(h): Zr/Y

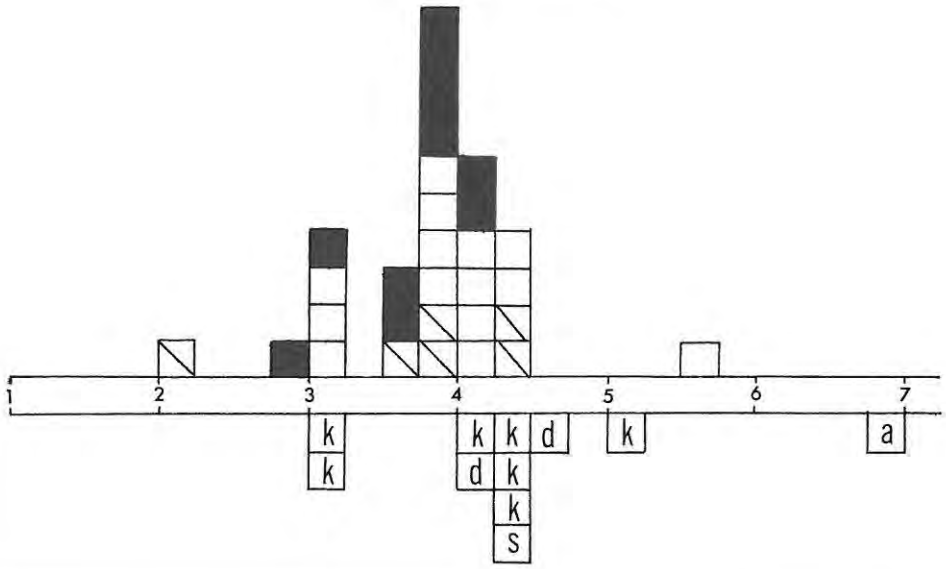

18(g): Zr/Nb

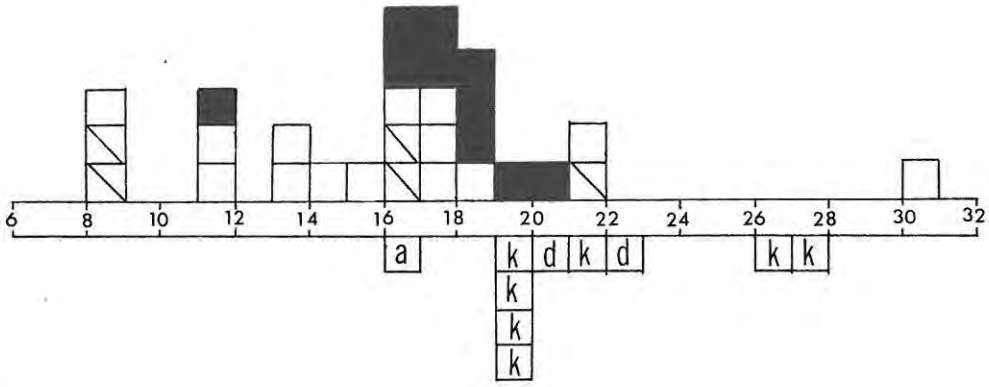

18(f): Ba/Zr

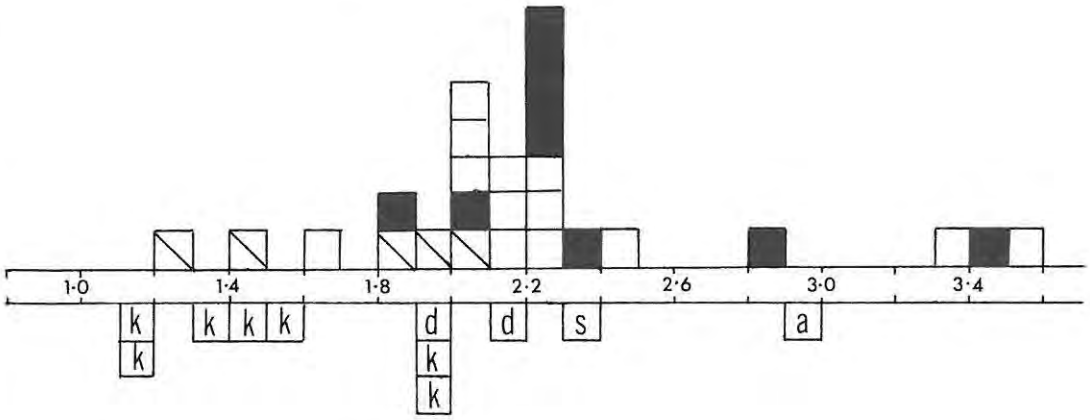

18(j): Cr/Ni

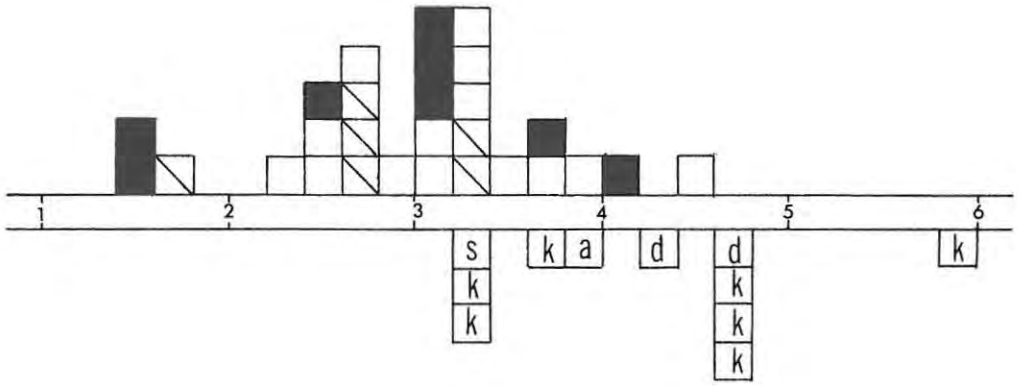

18(i): Ni/Co

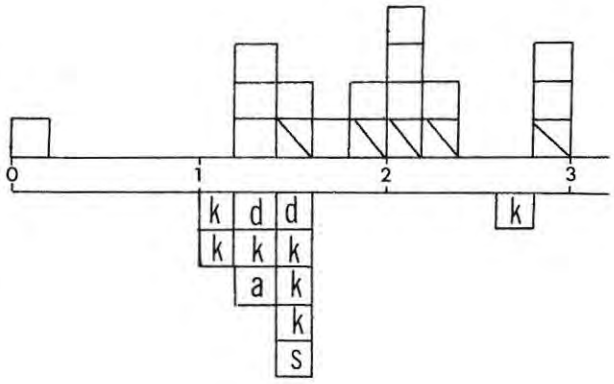

The Donnybrook basalts (JR94, S17) are sympathetically enriched in Ba, Rb and K_2O% relative to the Kraai River basalts, and average 226 ppm Ba.

K/Ba and Ba/Zr ratios are, similarly, higher in the Donnybrook basalts (Table 9c) and average 41 and 2.0 respectively, but average 25 and 1.5 in the Kraai River basalts. These ratios are, however, quite variable (Figs.18d, f).

Ba is strongly enriched (610 ppm) in the andesite, while the K/Ba ratio (28) is similar to the average value for the Kraai River basalts.

The range of K/Ba and Ba/Zr ratios for the Kraai River basalts, the Red Beds lava and the andesite is similar to the range determined for the Karroo dolerites (Fig.18d,f). The Donnybrook basalts, alone, have very high K/Ba ratios nearly double that of the average Karroo dolerite (Tables 8c, 9c).

3.5.d
Rubidium

Dolerites:

The variation of Rb within the dolerites (Fig.14c) is similar to that seen for Ba. Again a main trend of increasing Rb with differentiation contrasts isolated high and low Rb concentrations.

In the main trend, Rb increases from 5.8 ppm in an olivine-rich dolerite to between 20 and 23 ppm in the more highly differentiated samples. The relatively high Rb content of JR9 (37 ppm) correlates to high Ba and K_2O levels. As a group the low-K_2O dolerites show a wide range in Rb content (2.4-28 ppm) and only in some samples (JR29, 49 and 99) does low Rb match low K_2O%.

The average Rb concentration for all the chilled dolerites sampled, is 13.6 ppm (Table 10,A).

The wide range in Rb content within the dolerites, is reflected in the variation of the ratios, K/Rb and Ba/Rb.

Table 8(c) and Fig.18(a) indicate that in the chilled dolerites with $K_2O < 0.4$%, K/Rb ratios range from 229 to 514 and, with one exception (JR9 - K/Rb = 229), fall within the range determined by Erlank and Hofmeyer (1966). However, K/Rb ratios for the low-K_2O dolerites are highly variable and range from 74 to 501, averaging 262.

This exludes the high K/Rb (975) determined for JR29.

Treated individually, it seems almost impossible to explain this range in terms of fractional crystallization effects only. JR50 and JR104 (K/Rb = 74, 103 respectively) are not unduly altered samples though both have glassy groundmass textures. This texture is, however, also common in dolerites with normal Karroo K/Rb ratios. K/Rb ratios for JR36, 21 and 9 (246, 261 and 229, respectively) are more in keeping with ratios reported for the Tasmanian and Antarctic dolerites (Erlank and Hofmeyer, op.cit.). Only JR9, however, has a major element chemistry similar to that of the average chilled Tasmanian dolerite (Table 10). The very high K/Rb determined for JR29 (975) is more in keeping with K/Rb ratios reported for oceanic tholeiites (Engel et al., 1965). The concentration of Ba in JR29 is, however, too high for any oceanic tholeiite affinity.

Considering all these variations, the average K/Rb for all the chilled dolerites is 401 (Table 8c), slightly lower than the average (465) quoted by Erlank and Hofmeyer (op.cit.) for Karroo dolerites. The generally lower K/Rb ratios of the low-K_2O dolerites are problematic. Low K_2O concentrations in these dolerites argue against any crustal contamination theory. Crustal contamination has been argued to account for the generally lower K/Rb ratios of the Tasmanian and Antarctic dolerites but as pointed out by Erlank and Hofmeyer (op.cit.), Rb would have to be selectively added to a magma, relative to K_2O, in such a process.

The variation of K/Rb ratios reported in this study, in part confirms the large variations in the K/Rb ratios reported for Karroo dolerites by Nockolds and Allen (1956). Erlank and Hofmeyer (op.cit.) dismiss the large variations reported by the former authors, considering them to be due to the semi-quantitative method of determination of Rb.

Ba/Rb ratios for the dolerites are summarized in Table 8(c) and Fig.18(e). The average Ba/Rb for all the chilled dolerites is 18 but the range is large, 9 to 56. The high Ba/Rb (56) and high K/Rb (975) ratios of JR29 must be considered anomalous values.

Barkly East basalts:

Fig.14(c) illustrates the wide variation in Rb determined for the Barkly East basalts.

Within the Kraai River basalts, Rb increases sharply from 11.7 ppm to 21 ppm in sample 3/10, while in flow JR108 differentiation enriches Rb from 4.6 ppm in the basal sample (A) to 9.0 ppm in the upper contact (B).

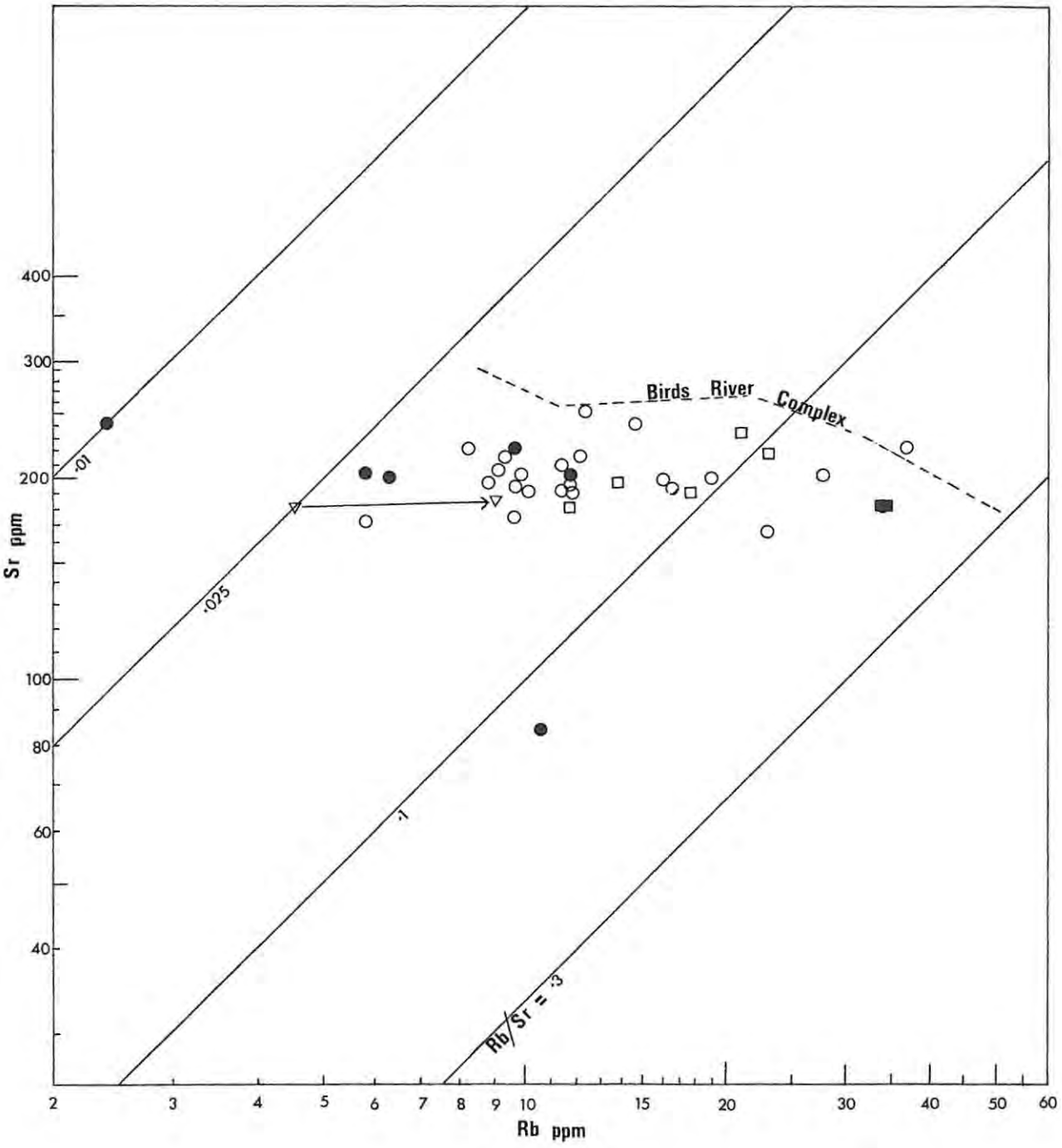

Fig. 19(a): Variation of the ratio Rb/Sr in the Karroo dolerites and Barkly East volcanics compared with Rb/Sr variation at Birds River (Stapelbergkloof section). Logarithmic scale.

- ● Chilled Karroo dolerites with $K_2O < .4\%$.
- ○ Karroo dolerites (contact and non-contact samples).
- ▣ Red Beds basalt.
- ■ Donnybrook basalts.
- ▲ Belmore andesite.
- □ Kraai River basalts.
- ▽→▽ Basalt flow JR108(A→B).

The Donnybrook basalts are enriched in Rb (34 ppm) relative to the Kraai River basalts. The andesite is similarly enriched to 111 ppm Rb but the Red Beds lava, JR88, has a Rb content below detection limits.

K/Rb ratios are summarized in Table 9(c) and Fig.18(a). With the exception of JR108A,B, the Kraai River and Donnybrook basalts have average K/Rb ratios of 250 and 270 respectively. These are lower than the average K/Rb (401) determined for the chilled Karroo dolerites. The K/Rb ratios for flow JR108 are very much higher and change from 693 in the basal sample (A) to 474 in the upper contact (B). This emphasizes the variation that can be expected within individual flows and points to the need for systematic sampling, if the K/Rb ratios of numerous flows are to be compared.

With the exception of high Ba/Rb ratios (28,30) for flow JR108, the average Ba/Rb ratios of the Kraai River and Donnybrook basalts - 10 and 6.7 respectively, are lower than that of the average chilled Karroo dolerite (18) - Tables 8(c), 9(c), Fig.18e. This is due to generally lower Ba levels in the basalts (Fig.14b).

The wide variation of Rb/Sr ratios within the Karroo dolerites and the Barkly East basalts is shown in Fig.19(a). With the exception of dolerite JR29 (Rb/Sr = 0.01) and the andesite, JR31 (Rb/Sr = 0.4), Rb/Sr ratios for both the dolerites and the basalts range between 0.025 to 0.19.

3.5.e
Yttrium.

Dolerites:

The steady increase from 17.8 ppm to 31 ppm Y with increasing differentiation in the dolerites is indicated in Fig.14(e). The degree of scatter in this trend is relatively small and there is little difference in the Y content of the low- and normal-K_2O dolerites. The average Y concentration for all the chilled dolerites analysed, is 25.7 ppm.

As expected K/Y ratios are lower for the low-K_2O dolerites (Table 8c, Fig.18b). The average K/Y ratio of the normal-K_2O dolerites is 230, while the former average 92. The average K/Y for all the chilled dolerites is 189.

The relatively low and stable Y concentrations of the chilled

dolerites are as expected in relatively undifferentiated basic magma and the trend shown in Fig.14(e) merely extends the Y variation seen in the Birds River intrusion to lower levels of differentiation.

Barkly East basalts:

The Barkly East basalts have an almost identical Y content as the chilled Karroo dolerites (Fig.14e).

In the Kraai River basalts, Y increases with differentiation from 24 to 29 ppm. Differentiation of flow JR108 results in a more marked increase in Y from 21 ppm in the basal sample (A) to 31 ppm in the upper contact (B). The Donnybrook basalts average 26 ppm and lie on the Kraai River Y trend, while the andesite, JR31, shows a relatively subdued increase in Y to 30 ppm.

The more highly differentiated Kraai River basalt, 3/10, and the andesite, JR31, plot on a CaO/Y variation trend (Fig.9) that closely matches that of the "Standard" series (Lambert and Holland, 1974).

The subdued increase in Y with decreasing CaO% is characteristic of dominant pyroxene fractionation. While it is debatable that the andesite, JR31, can be derived by fractional crystallization from a parent magma similar to that which gave rise to the Kraai River basalts, the controls on fractional crystallization in terms of CaO/Y variation, are clearly different to that operative during differentiation at Birds River.

K/Y ratios within the basalts are more variable than in the dolerites (Table 9c, Fig.18b). The Kraai River basalts have an average K/Y ratio of 153, lower than that of the Donnybrook basalts (353). The subdued Y but high K_2O content of the andesite is reflected in its high K/Y value (574). On average, the Kraai River basalts have slightly lower K/Y ratios than the chilled Karroo dolerites while the Donnybrook basalts and the andesite have much higher values.

3.5.f
Zirconium.

Dolerites:

Fig.14(d) indicates the more than 3-fold increase in Zr with differentiation from 50 ppm in an olivine-rich dolerite to 158 ppm

in the most differentiated contact dolerite.

As with Y, there is little difference in the Zr content of the low- and normal-K_2O dolerites. The low Zr concentration of JR21 (52 ppm) is matched by low Ba, Sr, Nb and Cr levels, and is anomalous for its differentiation stage. The more highly differentiated contact dolerites are slightly enriched in Zr relative to gabbros, with similar MgO levels, from the Birds River intrusion. This influences Zr/Nb ratios, discussed in the section dealing with Niobium. The average Zr concentration of the chilled dolerites is 102 ppm.

K/Zr and Zr/Y ratios are summarized in Table 8c and are shown diagrammatically in Figs.18 (c,h) respectively. K/Zr ratios emphasize the difference in K_2O% in the low- and normal-K_2O dolerites. The former have an average K/Zr ratio of 27; the latter average 57, while the average for all the chilled dolerites is 48. The range in K/Zr ratios (9-78) within all the dolerites sampled, is far greater than the range determined for K/Zr in the Birds River sequence.

As shown in Fig.18(h), there is little difference in Zr/Y between the low- and normal-K_2O dolerites. The low-K_2O dolerites have an average Zr/Y ratio of 3.7, close to the average of 4.0 for chilled dolerites with K_2O 0.4%. The average Zr/Y for all the chilled samples is 3.9 but values range from 2.0-5.7 (Table 8c).

Barkly East basalts:

In the Kraai River basalts, Zr rises to a maximum of 158 ppm in the more highly differentiated basalt, 3/10. The relatively undifferentiated Kraai River and Donnybrook basalts have Zr concentrations matching those of Karroo dolerites of similar MgO percent (Fig. 14d). Zr increases from 65 to 99 ppm with the differentiation in flow JR108, an enrichment of nearly 50%. This enrichment factor matches that noted for Y.

As with Ba, the Red Beds lava (JR88) is slightly enriched in Zr (122 ppm). The enrichment of Ba, Zr and possibly Y in this basalt is however, not matched by similar increased values for the other two common residual trace elements, Nb and Rb. The highly differentiated andesite contains 205 ppm Zr and extends the Zr enrichment in these Barkly East lavas, to levels found in the more differentiated ferrogabbro and ferrotholeiites from Birds River.

K/Zr ratios average 38 for the Kraai River basalts but are higher - 81 - in the Donnybrook lavas. Zr/Y ratios are, however,

more stable than the former ratio and average 4.5, 4.3 and 4.3 for the Kraai River lavas, the Donnybrook lavas and the Red Beds basalt. The high Zr/Y ratio (6.8) for the andesite, JR31, again emphasizes the subdued Y enrichment previously noted. These ratios are summarized in Table 9(c) and are compared with the dolerites in Figs. 18 (c,h).

3.5.g
Niobium:

Dolerites:

Two trends of increasing Nb with increasing differentiation are seen in Fig.14(f).

A trend showing relatively high Nb enrichment is indicated by the dolerites JR73, 50, 54, 42 and 43. All except JR43, are contact dolerites. In this trend Nb increases from approximately 3.0 ppm in the olivine-rich dolerites to 18.7 ppm in JR73.

The bulk of the dolerites, however, plot on a trend showing a more subdued increase in Nb with differentiation. In this trend, Nb increases from 3.0 ppm to values less than 10 ppm. This latter trend appears to be extended at higher levels of differentiation by the Birds River Nb trend.

As previously mentioned, Zr/Nb ratios are considered by some authors to be of petrogenetic interest. Table 8(c), Fig.18(g) and Fig.19(b) summarize Zr/Nb ratios in the Karroo dolerites.

In Fig.7(h), it is seen that this ratio does not change drastically with strong differentiation at Birds River. Fig.18(g), combining data from Birds River, suggests there is a bimodal distribution of Zr/Nb ratios for the Karroo dolerites. Though varying, the Zr/Nb ratios of the derites, reflect the high- and low-Nb trends noted in Fig.14(f). The high-Nb dolerites have Zr/Nb ratios that range from 8.5 to 11.9, covering the same range noted for the Birds River intrusion. The dolerites with slightly depleted Nb concentrations, have a Zr/Nb distribution that shows a strong mode between 17 and 18.

However, the low Zr/Nb ratios of the Birds River intrusion are due more to low Zr rather than high Nb values. This is seen in Figs.14(d,f). Thus two trends, one enriched in Nb, the other depleted in Zr, have the same range and nearly identical average Zr/Nb ratios.

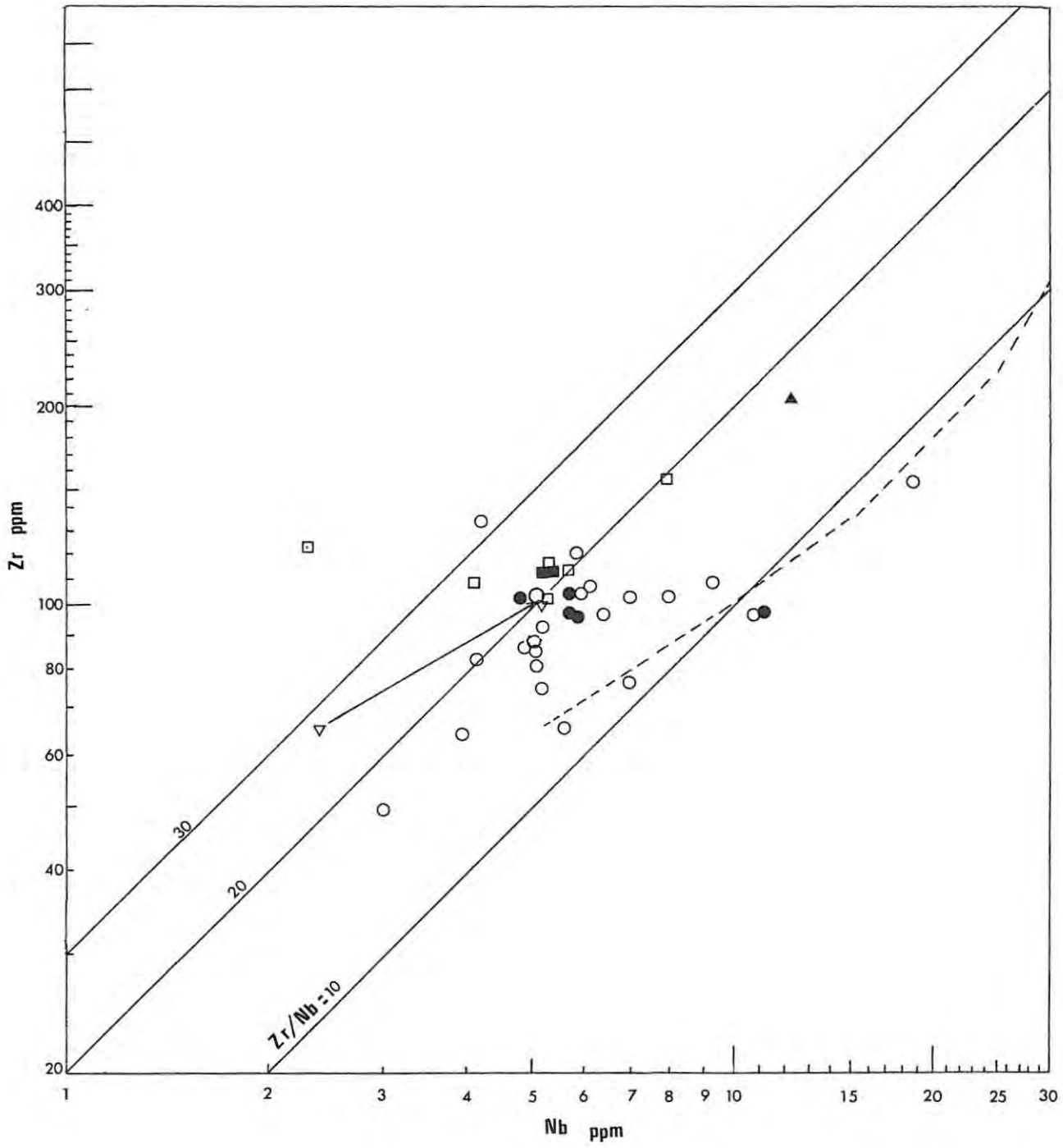

Fig. 19(b): Variation of Zr/Nb ratios in the Karroo dolerites and Barkly East volcanics compared with Zr/Nb variation at Birds River (Stapelbergkloof section). Logarithmic scale.

Symbols as in Fig. 19(a).

The limited variation of the Zr/Nb ratio at Birds River but its wide variation in the Karroo contact dolerites, is a further indicator that low-pressure fractionation of the common phenocrysts-olivine, plagioclase and pyroxene - cannot solely explain fluctuations of this ratio in the Karroo dolerites.

An important point to consider in the analysis of Zr/Nb ratios in the Karroo dolerites, is that Nb is a relatively difficult element to determine by X.R.F. techniques. Zr tail-overlap and line interferences that depend on the accuracy of Y and Rb determinations, all influence the final Nb determination.

Since the Nb content of the dolerites is generally low, any error in Nb determination is compounded by dividing into a denominator (Zr) with a concentration very much larger than that of Nb. Zr/Nb ratios determined by Weaver (1972) remain remarkably constant in differentiated basalt to trachyte lava series in some Kenyan Rift volcanoes. However, here, especially in the more salic derivatives, Zr and Nb concentrations are generally greater than 1000 ppm.

Since little quantitative, published data exist for the Nb content of the Karroo dolerites, the validity of the apparent bimodal distribution of Zr/Nb ratios noted in the present study, cannot be fully appraised.

Barkly East basalts:

The Barkly East basalts (Fig.14f) as a group, are slightly depleted in Nb relative to the Karroo dolerites of similar MgO content. There is little difference in the Nb content of the Kraai River and Donnybrook lavas. In these lavas, Nb increases from 4.2 to 8.0 ppm with differentiation to basalt, 3/10. The Red Beds lava is strongly depleted in Nb (2.3 ppm), while the andesite extends the Kraai River Nb enrichment trend to 30 ppm.

The slightly lower Nb content of the Barkly East basalts relative to the Karroo dolerites, is reflected in their slightly higher Zr/Nb ratios (Table 9c, Figs.18g, 19b), though there is some degree of overlap. The average Zr/Nb ratio for the Kraai River and Donnybrook lavas is 22. The low Nb but normal Zr content of the Red Beds basalt, gives this rock a rather high Zr/Nb ratio of 54.

3.5.h
Zinc.

Dolerites:

The concentration of Zn in the Karroo dolerites is rather variable but does appear to increase slightly with differentiation, from 71 ppm in the most MgO-rich dolerite to nearly 90 ppm in the more differentiated samples (Fig.14g).

The variation of Zn at Birds River indicates that only in the final stages of differentiation is Zn strongly concentrated in residual basic liquids. As such, considering both trends, the overall enrichment of Zn over a range of nearly 12 percent MgO, is relatively small (71-150 ppm). This indicates that though Zn behaves as a residual trace element, similar to Zr, Y, Rb, Nb and Ba, in the differentiation of Karroo magma, its greater affinity for entry into Fe^{2+} positions in early crystallizing femic phases, reduces its overall enrichment factor relative to those of the other residual trace elements.

The average Zn concentration in the chilled Karroo dolerites, is 84 ppm (range 71-105).

Barkly East basalts:

Little can be deduced from the variation of Zn in the Barkly East basalts (Fig.14g). The range in values (68-95 ppm) is similar to that determined for the Karroo dolerites.

From the base (A) to the top (B) of flow JR108, Zn increases from 68 to 82 ppm. The more highly differentiated Kraai River basalt, 3/10, and the andesite, JR31, show relatively subdued Zn concentrations of 90 and 79 ppm, respectively. The subdued concentration of Zn in the andesite is matched by low Cu and V concentrations.

The average Zn concentration of the Barkly East basalts is 83 ppm, nearly identical to that of the average chilled Karroo dolerite 82 ppm (Table 11).

3.5.i
Copper.

Dolerites:

Fig.14(h) shows the large variation in the Cu content of the Karroo dolerites. With two exceptions, JR21 and JR58, the chilled dolerites (MgO 8.04%) generally show a lower degree of variation in Cu concentrations than the more coarse-grained and olivine-rich types.

The high Cu content (155 ppm) of JR21 is anomalous considering that the maximum enrichment found in the Birds River intrusion is only 169 ppm. The high Cu content of JR21 is, moreover, matched by a high V concentration (304 ppm). The low Cu content (19 ppm) of dolerite JR58 is also anomalous but in this case correlates to a very low Ni content of 3.5 ppm.

The average Cu concentration in the chilled dolerites is 93 ppm but values range between 19 and 155 ppm. From this variation, it is unlikely that Cu can be considered an important trace element in geochemical studies of the Karroo dolerites.

Barkly East basalts:

In contrast to the behaviour of Cu in the Karroo dolerites, the variation of Cu in the Barkly East basalts is more interesting. A clear trend of steadily decreasing Cu with increasing differentiation characterizes most of these basalts. Differentiation of flow JR108, however, results in an opposing Cu-enrichment trend (Fig.14h).

Cu decreases in a smooth trend from 67 ppm in the Kraai River basalts to 30 ppm in the andesite, JR31. One Donnybrook basalt, S17, plots off this trend, having a slightly higher Cu concentration of 71 ppm. The Red Beds lava is also slightly enriched in Cu (92 ppm), while differentiation from the base (A) to the top (B) of flow JR108, enriches the residual liquid from 89 to 127 ppm Cu.

As will be seen, the variation of V is nearly identical to the above trends.

The distribution coefficient of Cu between Ti-magnetite and liquid is greater than 1, but generally less than 1 for both Ca-rich and Ca-poor pyroxenes. Likewise, V is more strongly partitioned into Ti-magnetite than into pyroxene.

The trend of decreasing Cu seen with increasing differentiation in the basalt-andesite series at Barkly East, suggests some magnetite

removal from the crystallizing parent magma(s). This will be discussed in more detail in the section dealing with Vanadium.

3.5.j
Cobalt.

Dolerites:

The steady decrease in Co with increasing differentiation, from approximately 70 ppm in the olivine-rich dolerites to 34 ppm in the most differentiated contact dolerite, is very striking (Fig.14i).

With the exception of JR105, the plotted points fall on a relatively smooth trend. Co readily enters olivines and pyroxenes and the steady decrease noted must in part, be attributed to the removal of these phases under conditions of low-pressure crystal fractionation. The flattening-out of the trend during the ferrogabbro-ferrotholeiite stage at Birds River has already been discussed as due to major plagioclase fractionation. The sharp drop in Co in the very late stages of differentiation at Birds River may be due to the crystallization and removal of Ti-magnetite.

Thus the overall trend of Co variation seen for both the regional dolerites and the Birds River intrusion, indicates the effects of early olivine and pyroxene, later plagioclase and very late stage Fe-oxide crystallization in basic Karroo magmas.

The high Co concentration noted for dolerite JR105 (73 ppm), matches that of JR124 (71 ppm). These two dolerites - both dykes - are similarly enriched in Ni (539, 513 ppm) and Cr (799, 767 ppm), though differing in MgO% and therefore in degree of differentiation in MgO-type variation diagrams. In Section 3-2 it is noted that both these dykes are relatively young in age and intrude through the lower lavas of the Lesotho formation (Lock et al., 1974) in the Barkly East area.

The average Co concentration for the chilled dolerites is 41.7 ppm (Table 10).

Barkly East basalts:

Fig.14(i) indicates that a similar trend of decreasing Co with increasing differentiation characterizes the Barkly East basalts. Also seen, is that the Barkly East basalts are, with

the exception of JR108 A,B, generally depleted in Co relative to the Karroo dolerites. A similar relative depletion in Ni concentrations is also observed (Fig.14j).

Co decreases from 39 ppm to 29 ppm in the Kraai River basalts and to 16 ppm in the andesite. Differentiation of flow JR108 reduces Co from 44 ppm in the basal sample (A) to 35 ppm in the upper contact (B).

The average Co concentration of the Barkly East basalts is 35.1 ppm (Table 11), slightly lower than the average value determined for the chilled Karroo dolerites.

The lower Co content of these basalts may suggest that the basalts are related to the Karroo dolerites by olivine fractionation. This is also supported by the generally lower Ni concentrations in these basalts. However, trace element variations within the Barkly East basalts themselves cannot be due solely to olivine fractionation from the parent Barkly East basalt magma(s). The variation of Ni is not consistent with such a conclusion.

The variation of Co, Ni and Cr in these basalts may be due to the removal of orthopyroxene during fractional crystallization but this has not been quantitatively tested. Orthopyroxene is a common phenocryst phase in many of these basalts.

3.5.k
Vanadium.

Dolerites:

The very slight increase in V from the olivine-rich dolerites to the more highly differentiated types is illustrated in Fig.14(k). As seen in the Cu variation trend, the degree of variation in the V content of the dolerites is more pronounced in the less differentiated dolerites.

With two exceptions JR21 and 90 (V = 304, 192 ppm respectively, Table 8a), the range in V concentrations in the chilled dolerites is quite restricted (261-228 ppm). The average for all the chilled dolerites sampled, is 239 ppm V (Table 10).

The sequence of Co, Ni and V interelement ratios determined by Ishikawa (1968) during various stages of differentiation of tholeiitic magma is confirmed when data for the regional dolerites and the

differentiated sequence at Birds River are compared. Initially in the olivine-rich dolerites, the sequence is Ni > V > Co. Then in the majority of the relatively undifferentiated dolerite contact samples, V > Ni > Co while in the Birds River series, the trend is V > Co > Ni.

Barkly East basalts:

Fig.14(k) shows that while the less differentiated Kraai River basalts have a V content similar to the chilled Karroo dolerites, on increasing differentiation to basalt, 3/10, and to the andesite, JR31, the trend is for a steady decrease in V levels to 189 and 120 ppm respectively.

This decrease in V in these basalts matches the variations of Fe_2O_3, TiO_2, Cu, Zn, Co, Ni and Cr and must be attributed to the removal of minor amounts of Ti-magnetite from the crystallizing magma(s). The removal of orthopyroxene will reduce Co, Cr and Ni concentrations but will not reduce the V content by the amounts observed, while any significant plagioclase fractionation would tend to enrich residual liquids in V.

Opposing this trend of V depletion seen in the more highly differentiated Kraai River basalt and in the andesite, is the V enrichment trend of flow JR108. Differentiation of flow JR108 results in an enrichment of V in the residual liquid (B), from 228 to 284 ppm.

The inter-element relationships of Ni, Co and V in the Barkly East basalts are interesting. Even in the most highly differentiated basalt and andesite, the sequence remains V > Ni > Co. The strong depletion of Co relative to Ni supports the view that orthopyroxene and not olivine fractionation, is, in part, responsible for trace element variations in these basalts and andesite.

3.5.1
Nickel.

Dolerites:

With two exceptions (JR105, 124), the observed Ni concentrations in the dolerites plot on a smooth trend of decreasing Ni. Ni decreases from 300 ppm in an olivine-rich dolerite to approximately 45 ppm in the more highly differentiated samples (Fig.14j). Sample JR58 (Table 8a) has an abnormally low Ni concentration of 3.5 ppm

when compared with other contact dolerites of a similar MgO%. The low Ni content of this dolerite is matched by a very low Cu concentration (19.2 ppm).

The two coarse-grained, olivine-rich dolerites JR105 and 124, contain 539 and 513 ppm Ni respectively and plot well off the normal Ni trend for the Karroo dolerites. Their enriched Ni, Co and Cr concentrations are more similar to the picrites from the Elephant's Head intrusion (Nockolds and Allen, 1956), than to the average Karroo dolerite from this study.

The average Ni concentration for all the chilled Karroo dolerites is 78 ppm.

Ni/Co ratios in the Karroo dolerites are summarized in Table 8(c) and Fig.18(i). The average Ni/Co ratio for all the chilled dolerites is 2.0 but values range from 0.1 to 4.7. The high Ni/Co ratios for JR105 and 124 (7.4, 7.2) are distinctive to these high-Ni dolerites. Though the Ni/Co ratio is strongly affected by differentiation, the average value for the chilled Karroo dolerites is in accordance with the conclusions of Taylor et al. (1969). These authors find that Ni/Co ratios in tholeiitic basalts are generally greater than 2, while those of high-Al and calc-alkaline andesites are generally less than 1.

Barkly East basalts:

The depletion of Ni with increasing differentiation in most of the Barkly East basalts, is not as marked as that seen for the Karroo dolerites (Fig.14j). Furthermore the average Ni content of these basalts (48 ppm, Table 11) is lower than that of the average chilled Karroo dolerite - 78 ppm.

All the basalts, with the exception of JR108 A,B which plot on the dolerite trend, show a relatively smooth trend of decreasing Ni. Ni is reduced from 55 ppm in the less differentiated Kraai River basalts to 33 ppm in basalt 3/10, and to 22 ppm in the andesite, JR31. Differentiation of flow JR108, however, reduces Ni at a more considerable rate, from 115 ppm in the basal sample (A) to 47 ppm in the upper portion (B) of the flow.

The relatively subdued decrease of Ni in the former trend, must rule out any major olivine fractionation in this series.

The lower Ni and Co characteristics of the average Barkly East basalt relative to the average Karroo dolerite of similar MgO content

(Table 11), suggests a parent basalt already depleted in Ni and Co.

Ni/Co ratios in the Barkly East basalts and andesite are shown in Table 9(c) and Fig.18(i). The average Ni/Co ratio of the basalts and andesite is 1.4. The strong depletion of Ni with differentiation in flow JR108 is indicated by Ni/Co ratios that decrease from 2.6 to 1.3. As previously mentioned, Ni/Co ratios in the basalt-andesite series from Barkly East, always remain greater than 1, while the Ni/Co ratio in the derivative rocks from Birds River decrease to values less than 1. The Ni/Co ratio (1.3) of the andesite is not in keeping with its calc-alkaline affinity, determined in the section dealing with major element variations. Calc-alkaline andesites generally have Ni/Co ratios of less than 1 (Taylor et al., 1969).

3.5.m

Chromium.

Dolerites:

Chromium, like Ni and Co, is commonly rapidly depleted during the early stages of differentiation in basic magmas. The strong correlation between decreasing Cr and decreasing MgO% in the Karroo dolerites, is shown in Fig.14(l). Cr decreases from 786 ppm in the most MgO-rich dolerite to approximately 200 ppm in the more differentiated dolerites.

As seen in the variation of Ni (Fig.14j), the olivine-rich dolerite JR105, is, for its stage of differentiation, enriched in Cr (799 ppm), and plots off the trend observed for the remaining dolerites. In contrast to Ni, Cr is more highly variable in the chilled Karroo dolerites. Varying amounts of pyroxene fractionation together with olivine and plagioclase, may account for the greater spread of Cr values in the chilled dolerites.

The high Cr concentrations observed in the more olivine-rich dolerites must, in part, be due to Cr-rich spinel inclusions, observed in olivines from these dolerites. These inclusions occur as tiny, brownish euhedra, and are identified as picotite.

Thus the initial strong depletion of Cr in the more basic dolerites is probably due to the fractionation of minor amounts of Cr-rich spinel.

The average Cr content of the chilled dolerites is 243 ppm. Ci/Ni ratios are summarized in Table 8(c) and Fig.18(j). Excluding

JR58 (Cr/Ni = 54), the average Cr/Ni ratio of all the chilled dolerites is 3.0 (range 1.7-4.5). The high-Ni, high-Co dolerites JR105 and 124, are characterized by a low Cr/Ni ratio of 1.5.

Barkly East basalts:

Fig.14(1) shows that the Kraai River and Donnybrook basalts plot on a single trend of decreasing Cr with increasing differentiation. The concentration of Cr decreases from 255 ppm in the less differentiated basalts to 121 ppm in basalt, 3/10. The andesite, JR31, is slightly enriched in Cr (75 ppm) relative to this trend.

A similar though more marked decrease in Cr is seen in the differentiation trend for flow JR108. Here, Cr is depleted from 370 ppm in the basal sample (A) to 153 ppm in the upper contact (B).

The Red Beds lava, JR88, has an anomalously low Cr content of 163 ppm. This could possibly be due to protracted pyroxene fractionation which would give the observed enrichments noted for the residual trace element Zr, Ba, Y and Sr. However, the relatively low concentrations of K_2O%, Rb and Nb in this basalt is difficult to explain by this process.

The average Cr concentration for the Barkly East basalts is 213 ppm (Table 11), lower than the value for the average chilled Karroo dolerite.

Cr/Ni ratios (Table 9c, Fig.18j) for the Barkly East basalts are generally higher than those for the Karroo dolerites. The Kraai River and Donnybrook basalts have an average Cr/Ni ratio of 4.6 while JR108 A,B, the Red Beds lava and the andesite have slightly lower ratios of 3.3, 3.2 and 3.5 respectively.

3.5.n

Karroo dolerites - Variation in trace element content with height in the stratigraphic column.

This section briefly explores the possibility that the Karroo magma column is differentiated with respect to height in the stratigraphic sequence through which it intruded. The concentrations of Ba, Rb, Zr and Ni were plotted against the height above sea level of the sample site. The heights of the sampling sites are uncorrected for any regional dip in the stratigraphic sequence of the area studied. Ba, Rb, Zr and Ni were selected for these trace elements should be the most strongly affected by increasing differentiation.

In Figs. 20 (a-d), there is little indication of any marked trend with increasing height of intrusions. There is some tendency for Ba to increase with increasing height but the Zr and Rb distributions are highly scattered. In a similar manner Cr and Ni distributions are highly variable and show little tendency to decrease with increasing height. High Ni- and-Cr dolerites were sampled at both a low and high level in the sedimentary sequence.

Cox and Hornung (1966) find that Fe/Mg ratios in the Lesotho basalts increase with increasing height in the volcanic sequence. They note that two possible interpretations could apply:

a) the fractionation stage depends upon the height the magma column reached before extrusion.

b) the fractionation stage depends upon the time elapsed since the beginning of the volcanic episode.

Cox and Hornung (op.cit.) note that very few Karroo dolerites have a more fractionated aspect than the analysed Lesotho basalts. Should the basalts and dolerites be broadly contemporaneous in age, then the degree of fractionation of the basalts could depend on the height of the magma column. Conversely should the dolerites be older than the basalts, both "could be derived by successive tapping of a continuously fractionating, possibly static, magma chamber, without significant subsequent fractionation in the conduits."

Figs. 20(a-d) indicate that it will be difficult to detect any fractionation trends that can be directly related to the height of the Karroo magma column in the north-eastern Cape regions.

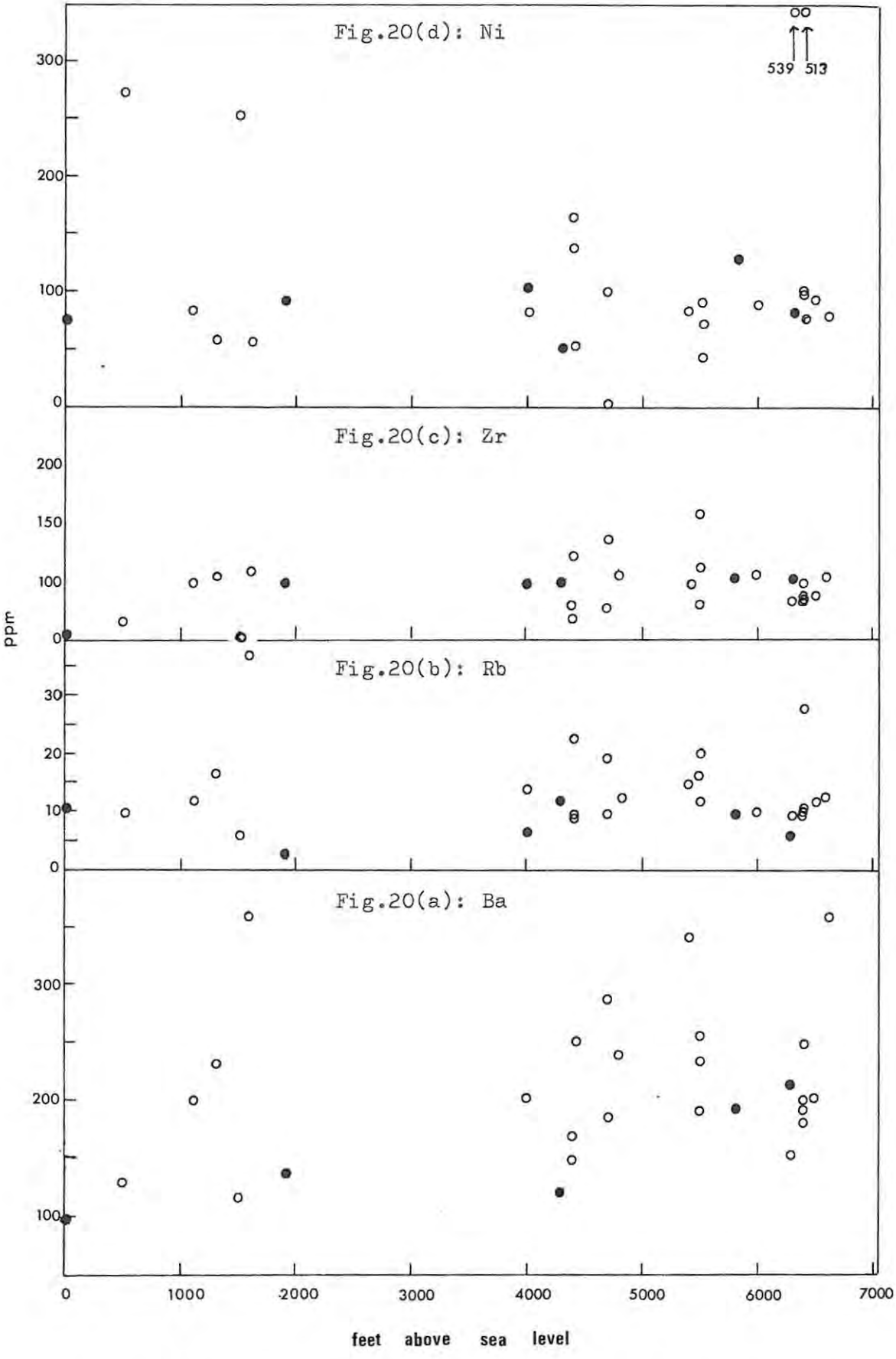

Figs.20(a-d): Variations in the Ba, Rb, Zr and Ni contents of Karroo dolerites plotted against the approximate heights above sea level of the intrusions. Symbols as for Fig 19.

3.6

Comparisons with previous data.

3.6.a

Karroo dolerites:

Table 10 compares data for the average chilled Karroo dolerite presented in this study with averaged data from Walker and Poldervaart (1949) and Nockolds and Allen (1956).

The average contact dolerite (this study) is slightly enriched in Si, Ca and Na but depleted in Mg relative to the average chilled dolerite of Walker and Poldervaart (op.cit.) but is similar to the average Karroo dolerite computed by Cox and Hornung (1966). In trace element content, new data for dolerites with MgO less than 9.0% are compared with data from Nockolds and Allen (op.cit.) for dolerites with similar MgO values, and with the average trace element content computed by Cox and Hornung (op.cit.). The agreement with the exception of Rb, Sr and Cr, is generally good. New data suggest that the average Rb and Cr content is slightly lower than previously determined while the new Sr average is slightly higher than previous values. The size of 1 standard deviation in each trace element distribution is also indicated in Table 10. This serves as a measure of variance. Rb, Nb, Ba and Cu distributions show a relatively large degree of scatter while Sr, Zn, Y and Co show a lesser degree of variance.

The relatively low-Si, low-K character of the Karroo dolerites when compared with similarly-aged intrusions from Antarctica and Tasmania, is confirmed.

The variation of selected inter-element ratios in the Karroo dolerites are compared with data from Birds River and the Barkly East basalts in Figs. 18(a-j) and are summarized in Table 8(c). The variation of K/Rb ratios has already been discussed and compared with data from Erlank and Hofmeyer (1966). New data suggest that the range of K/Rb ratios in Karroo dolerites is greater than that previously determined by the above-mentioned authors.

The geochemical differences noted by Cox et al. (1967) between the northern and southern Karroo igneous provinces are upheld but in individual cases (especially K_2O content) the hypothesis of Rhodes and Krohn (1972) is not supported. Dolerites sampled within the defined southern marginal area of Rhodes and Krohn (op.cit.) are indicated in Table 8(a). A more detailed statistical analysis of

Table 10 :

	A	B	C	D	E	F	G
SiO_2	52.58	51.9	53.8	53.9	52.7	52.41	-
TiO_2	1.00	1.1	.6	.7	1.16	.98	-
Al_2O_3	15.47	15.6	15.5	16.1	15.4	15.46	-
Fe_2O_3	1.71*	1.0	.8	.8	1.38	1.69*	-
FeO	8.69*	9.7	8.5	7.4	9.35	8.63	-
MnO	.18	.3	.1	.1	.22	.18	-
MgO	6.63	8.2	6.7	7.0	6.6	6.83	-
CaO	10.69	9.7	11.2	11.1	9.96	10.79	-
Na_2O	2.27	1.8	1.7	1.8	2.22	2.28	-
K_2O	.61	.7	1.0	1.0	.87	.59	-
P_2O_5	.17	.1	.1	-	.16	.16	-
Ba	220(69)[a]				200	219(67)	204
Sr	206(37)				168	206(32)	164
Rb	13.6(7.4)				17	13.4(7.2)	11
Y	27.7(1.9)				22	24.9(2.3)	22
Zr	102(21)				88	98(20)	91
Nb	7.4 (3.3)				-	6.8 (3.0)	-
Zn	84 (6.6)				-	82 (7.4)	-
Cu	93 (24)				-	90 (21)	-
Co	41.7 (4.2)				38	42.7 (4.2)	39
Ni	78 (29)				70	84 (30)	80
V	239 (20)				225	236 (19)	220
Cr	243 (65)				293	262 (67)	335

* Feo recalculated assuming $\frac{Fe^{3+}}{Fe^{2+}+Fe^{3+}} = 0.15$

a. Values shown in brackets are for 1 Standard Deviation.

A. Average chilled Karroo dolerite (this study) - excluding JR18. (19 samples)

B. Average chilled Karroo dolerite (Walker & Poldervaart, 1949, Table 17;3)

C. Average chilled Tasmanian dolerite (McDougall, 1962, Table 8; 2)

D. Average chilled Antarctic dolerite (McDougall, 1962, Table 8; 3)

E. Average Karroo dolerite (Cox & Hornung, 1966, Table 2; B, Table 3; B)

F. Average Karroo dolerite - MgO < 9.0% including chilled samples (this study) - (26 samples).

G. Average Karroo dolerite - MgO < 9.0% (Nockolds and Allen, 1956, Tables 20, 22, 23) - 12 samples. (trace element data only)

the new data must, however, be undertaken before this hypothesis is rejected/accepted.

3.6.b

Barkly East basalts:

Table 11 compares the average Barkly East basalt with the new average for Karroo dolerites with MgO less than 9.0% (i.e. covering more or less the same range of differentiation). Averaged data for the Lesotho, Swaziland and Nuanetsi basalts are from Cox et al. (op.cit.). The average major-element composition of the Hangnest-type dolerite of Walker and Poldervaart (op.cit.) is also included because some Barkly East basalts show a similar petrography to these dolerites.

When compared with the new average Karroo dolerite composition, the average Barkly East basalt is enriched in Si, Rb and possibly Zr but markedly depleted in Co and Ni. When compared with the average Lesotho basalt of Cox et al. (op.cit.), the Barkly East basalts are enriched in Si but depleted in Nb, Ni and possibly V.

The size of 1 standard deviation in each trace element distribution has been calculated for the data of Cox et al. (op.cit.). Values indicate the wide scatter in Ba, Sr, Rb and V distributions. This makes differences in averaged compositions from different data difficult to analyse.

The Hangnest-type dolerites of Walker and Poldervaart (op.cit.) contain a phenocryst assemblage similar to that noted in some Kraai River basalts. The average Hangnest dolerite and Barkly East basalt are both enriched in Si but depleted in Ca relative to the average Karroo dolerite. No trace element data are available for dolerites of the Hangnest-type. Walker and Poldervaart (op.cit.) in their discussion of the origin of this dolerite type, note that Hangnest-type compositions are difficult to derive by normal fractional crystallization processes and consider a model whereby igneous fractionation is combined with sediment assimilation (Walker and Poldervaart, op.cit., Table 20). That the compositions of the Barkly East basalts could be derived by a similar process can be qualitatively assessed in terms of their trace element contents. The addition of a normal argillaceous sediment to a basic magma would enrich the magma in K_2O, Ba, Rb and possibly Zr and by dilution, deplete the magma in Ni, Co and Cr. Only the Donnybrook basalts

Table 11.

	A	B	C	D	E	F
SiO_2	52.41	55.02	51.8	51.6	51.4	54.4
TiO_2	.98	.91	1.13	1.65	3.18	1.1
Al_2O_3	15.46	15.32	14.8	15.3	13.05	14.8
Fe_2O_3	1.69*	1.57*	3.92	2.45	3.00	1.3
FeO	8.63	7.98	7.26	9.47	8.95	8.9
MnO	.18	.16	.17	.16	.16	.2
MgO	6.83	6.48	7.1	5.56	6.78	7.2
CaO	10.79	9.74	10.57	10.29	9.03	9.0
Na_2O	2.28	2.05	2.40	2.96	2.51	2.1
K_2O	.59	.62	.74	.36	1.52	.9
P_2O_5	.16	.15	.13	.14	.43	.1
Ba	219 (67)[a]	190 (48)	233[1] (46)	184 (113)	630	
Sr	207 (32)	205 (22)	213 (55)	264 (76)	706	
Rb	13.4 (7.2)	21.8 (8.6)	29[1] (10)	50	-	
Y	24.9 (2.3)	26.4 (1.5)	23 (9.6)	22 (8.8)	39	
Zr	98 (20)	118 (16.2)	109[1] (24)	70 (22)	196	
Nb	6.8 (3.0)	5.2 (1.5)	11.6	19 (8)	47	
Zn	82 (7.4)	83 (6.1)	-	-	-	
Cu	90 (21)	65 (12)	-	-	-	
Co	42.7 (4.2)	35.1 (2.8)	34 (4.7)	33 (2.5)	29	
Ni	84 (30)	48.0 (6.7)	73 (32)	86 (20)	170	
V	236 (19)	226 (19)	300 (46)	279 (52)	292	
Cr	262 (67)	213 (44)	317	156 (60)	280	

* FeO recalculated assuming $\frac{Fe^{3+}}{Fe^{2+} + Fe^{3+}} = 0.15$

a. Values shown in brackets are for 1 Standard Deviation

1. X.R.F. determinations by Hornung. (Cox & Hornung, 1966, Table 3)

A. Average Karroo dolerite with MgO<9.0% - Table 10; F

B. Average Barkly East basalt - excluding JR108A,B - this study (8 samples

C. Average Lesotho basalt (Cox & Hornung, 1966, Table 2; A, Table 3; A)

D. Average Swaziland basalt (Cox et al., 1967, Table 3; F)

E. Average Nuanetsi basalt - MgO 5-8% - (Cox et al., 1967, Table 3; D_2)

F. Average Hangnest dolerite-type. (Walker & Poldervaart, 1949, Table 16;I

show any enrichment of K_2O, Ba and Rb. Normal crystal fractionation could possibly produce these enrichments but then Zr, Y and Nb should be similarly enriched. The latter elements as well as Co, Cr and V however show normal concentrations.

The Kraai River basalts generally contain low K_2O concentrations but K/Rb ratios are also low (Table 9c), suggesting some enrichment of Rb relative to K. Sediment assimilation is only viable if Rb can be selectively added to the magma. Ba levels in all the basalts studied are generally low to normal and are not considered high enough to warrant sediment assimilation. A more detailed, quantitative analysis of this problem is, however, called for.

Reduced levels of Ni in the Barkly East basalts when compared with the Karroo dolerites and Lesotho basalts suggest the former may be related to the latter by fractional crystallization processes involving the removal of olivine. Variations within the Barkly East basalts themselves cannot however be due to major olivine fractionation. Only very minor amounts of olivine microphenocrysts are seen in some of these basalts. The dominant femic phenocryst phase is orthopyroxene. Any fractionation model must consider the effects of orthopyroxene and plagioclase removal to explain geochemical variations within these basalts.

The variation of selected inter-element ratios in the Barkly East basalts is summarized in Table 9(c) and compared with the Karroo dolerites in Figs. 18(a-j). The ratios K/Rb and Ni/Co are generally lower in the Barkly East basalts than in the Karroo dolerites, while the reverse is true for the ratios, Cr/Ni and Zr/Nb. K/Rb ratios calculated for the Lesotho basalts (Cox and Hornung, Table 3 - Rb analyses by X.R.F. - G. Hornung) range between 707-112 but average 238. K/Rb ratios within the aphanitic Barkly East basalts show a more restricted range (322-122), if the high values (693, 474) recorded for flow JR108(A,B) are ignored.

Finally, the regional geochemical differences noted by Cox et al. (op.cit.) are further enhanced by new data for strongly tholeiitic basalts from the Barkly East area.

3.7 Conclusions.

3.7.a Karroo dolerites:

The following conclusions can be drawn from a geochemical study of some Karroo dolerites sampled in the north-eastern Cape. These conclusions are presented in point form.

a) The new average major and trace element composition of twenty contact dolerites is very similar to average compositions calculated by Cox et al. (1967) from data by Walker and Poldervaart (1949) and Nockolds and Allen (1956). New data suggest slightly lower average Rb and Cr concentrations but slightly higher Sr. Nb levels are generally low in the Karroo dolerites.

b) MgO-variation diagrams confirm that during the early- to middle-stages of differentiation, the Karroo magma is enriched in Si, Al, Ca, Na, K and P. The trace elements Ba, Zr, Rb, Y, Sr and Zn, all increase with differentiation. Mg, Co, Cr and Ni are rapidly depleted, consistent with early olivine, pyroxene and possibly Cr-spinel fractionation. The overall behaviour of Fe , Ti and Cu is more difficult to interpret for these distributions show quite a large degree of variation.

c) It is especially noted that the concentrations of the K-related elements i.e. K, Ba and Rb, are highly variable in some Karroo dolerites while trends for the Mg, Fe-related trace elements i.e. Co, Cr, V and Ni, are slightly less scattered or variable.

d) Major- and trace-element variations, particularly K_2O, Ba and Rb suggest that crystal fractionation processes alone cannot account for all the individual variations observed. The low-K_2O dolerites are problematic. Levels of Ba and Rb in some of these dolerites are sympathetically low, while in other low-K_2O dolerites, Rb levels are high. Crustal contamination can only account for the dolerites with low K/Rb ratios, if Rb is selectively added with respect to K. The low-K_2O dolerites may possibly be explained in terms of a partial melting model. Jamieson and Clarke (1970, Table 1) indicate that "90% of the total K and associated elements is in the liquid phase when 10% partial melting (of the host mantle rock) has occurred". Low

K, Ba and Rb concentrations in some dolerites could thus be related to extensive partial melting. i.e. melting more than 10% of the host rock will effectively, by dilution, reduce the levels of Ba, Rb and K in the partial melt. Alternatively the source mantle may be depleted in these elements. Partial melting and source area variations have not been considered in detail in this study.

e) The main group of dolerite contacts (i.e. excluding the picritic contact, JR18) is essentially undifferentiated. There is with some exceptions, little correlation between the phenocryst assemblage of the contact dolerites and their trace element contents. Most of the dolerites sampled can be classified as belonging to either the Perdekloof-,Blaauwkrans- or Kokstad-types of Walker and Poldervaart (1949). It was hoped to be able to classify the Karroo dolerite contact samples in terms of their different phenocryst assemblages and to correlate these with compositional variations. This has not been successful. The phenocryst assemblages of the above-mentioned three main petrographic dolerite types are very similar. Furthermore, Yoder and Tilley (1962) note that under normal P-T conditions, the three main phases olivine, pyroxene and plagioclase begin to separate from basic magmas within a very restricted temperature range.

f) In terms of normative chemistry, the tholeiitic nature of the initial Karroo magma is confirmed. All analyses contain hypersthene in the norm. and most can be classified as quartz (oversaturated) tholeiites, following the scheme of Yoder and Tilley (op.cit.). The high normative quartz seen in Table 8(b) is, however, in part due to the oxidation ratio ($Fe_2O_3/FeO = .2$) used in the calculation.

g) A brief examination of the trace element variation with increasing height of intrusion in the area studied, has revealed little information. Ba, Rb and Zr concentrations, show little or no tendency to increase with increasing height in the magma column. Similarly, Ni and Cr are not depleted. The range in stratigraphic heights of the intrusions studied, however, covers but the small upper part of the whole Karroo magma column and no conclusion can be drawn at this stage, as to whether the magma column is differentiated with respect to height.

h) The main object of this study was to provide new major- and -trace element data for a representative sample of Karroo dolerite chilled margins in the north-eastern Cape. It is hoped that this data will form a fruitful contribution to the geochemical studies being undertaken in the Karroo province during the Geodynamics Program.

3.7.b

Barkly East basalts:

Geochemical data presented in this study for some basalts and one andesite from the lower formations of the Drakensberg Subgroup (Lock et al., 1974) must be considered only as a preliminary investigation into the volcanic rocks of the Barkly East area. The volcanic history of the area is at present being interpreted by Dr. Lock and co-workers. A preliminary report of the volcanic stratigraphy of the area appears in Lock et al. (op.cit.). A more thorough geochemical investigation of basalts in the area is at present being undertaken in the Department of Geology, Rhodes University.

The following can be concluded from the study of the Barkly East basalts.

a) Chemically, many of the basalts studied differ from the overlying Lesotho basalts in that the former are enriched in Si but depleted in Mg, Ca and Ni. The former also commonly contain orthopyroxene + plagioclase $\pm$ pigeonite phenocrysts but little or no olivine. The Lesotho basalts commonly contain the phenocryst assemblage - plagioclase + olivine (Cox and Hornung, 1966).

b) In terms of normative chemistry, the Barkly East basalts are strongly tholeiitic and in the An-projection of the basalt system Fo-An-Di-Si, these basalts project into the En-rich pyroxene + An + liquid field. The projected positions of these basalts in this normative diagram extends the trend noted by Cox and Hornung (op.cit.) for the Lesotho basalts.

c) From MgO-variation diagrams, it is difficult to judge if the Donnybrook and Kraai River basalts form a fractionation sequence that, at higher levels of differentiation, could lead to the formation of andesitic compositions, similar to JR31. What is clear however, is that flow JR108 is internally differentiated in a manner different to the Kraai River basalt-Donnybrook basalt-Belmore andesite differentiation trend.

d) The most obvious differences in trace element variations between the Barkly East basalts and the Karroo dolerites, are that Cu and V decrease steadily with increasing differentiation in the basalts. Ni is also reduced at a lower rate. Considering the range basalt to andesite, a more calc-alkaline nature of differentiation is indicated. This is partly supported by the relative iron-enrichment trends. A trend of decreasing V with increasing differentiation strongly suggests magnetite fractionation. This does not imply that the initial magma was calc-alkaline. Rather the tholeiitic character of the initial magma was probably changed to a more calc-alkaline affinity in the near surface environment, in a similar manner as that that applied to the ferrotholeiites from Birds River (Eales and Booth, 1974). Residual basalt liquids encountered highly oxidizing conditions as they penetrated upper Stormberg sediments prior to eruption. Magnetite was freely precipitated and lavas extruded at the surface showed certain characteristics of calc-alkaline volcanics.

e) While the average Barkly East aphanitic basalt has a composition similar to that of the average Hangnest-type dolerite, trace element data does not seem to support a model involving sediment assimilation into the parent magma(s).

f) The Donnybrook basalts are characteristically enriched in K, Ba and Rb relative to the Kraai River basalts. Any fractional crystallization model expounded for this basalt series must consider the fractional crystallization of orthopyroxene rather than olivine. The low rate of Ni depletion in these basalts is consistent with such a view.

APPENDIX 1 : MAJOR ELEMENTS - BIRD'S RIVER COMPLEX. (recalculated L.O.I.-and H_2O^+-free)

STAPELBERGKLOOF TRAVERSE. (see Table 1a)

	JR 27	S30	S32	S31	S34	S25	S37	S39	S43	S45
SiO_2	52.14	51.83	53.16	52.66	53.82	53.94	54.51	58.97	56.88	58.24
TiO_2	1.06	0.75	1.37	1.62	2.02	2.20	2.12	1.74	2.08	1.69
Al_2O_3	15.62	16.98	16.32	15.67	14.90	14.01	14.05	12.01	11.65	11.53
Fe_2O_3	10.19	9.37	11.69	12.75	14.03	15.27	14.80	14.77	16.24	15.76
MnO	0.19	0.16	0.18	0.19	0.20	0.20	0.20	0.21	0.23	0.22
MgO	6.25	5.98	3.87	3.80	2.26	2.07	1.95	1.14	1.56	1.16
CaO	11.74	11.59	9.36	9.16	7.84	7.29	7.21	5.59	5.77	5.20
Na_2O	2.02	2.64	2.75	2.81	3.11	3.00	3.05	2.59	2.74	3.10
K_2O	0.61	0.57	1.00	1.06	1.41	1.55	1.65	2.38	2.20	2.47
P_2O_5	0.18	0.13	0.27	0.28	0.41	0.45	0.47	0.60	0.65	0.64
K_2O/Na_2O	0.302	0.216	0.364	0.377	0.453	0.517	0.541	0.919	0.803	0.797

APPENDIX 2 : MAJOR ELEMENTS - KARROO DOLERITES (recalculated L.O.I.-and H_2O-free)

(see Table 8a)

	JR 70	JR 90	JR 36	JR 54	JR 61	JR2	JR 15	JR 21	JR 29	JR 42	JR 49	JR 50	JR 72	JR 99	JR 48
SiO_2	54.27	52.40	52.81	51.28	52.53	52.13	51.21	50.69	51.92	51.34	51.06	51.74	51.44	51.42	51.48
TiO_2	.87	1.02	.87	1.07	1.04	1.00	.95	.81	1.00	.98	.90	1.10	.99	.96	.92
Al_2O_3	14.98	15.17	15.20	15.29	15.55	14.82	15.50	14.90	15.23	14.81	15.28	15.56	15.30	15.43	15.27
Fe_2O_3	10.09	11.61	10.25	11.33	10.65	11.45	11.71	13.11	11.45	11.13	11.15	11.64	11.16	11.34	11.11
MnO	.17	.18	.16	.17	.17	.19	.18	.20	.18	.17	.17	.19	.17	.18	.17
MgO	5.96	6.14	7.27	6.91	6.00	6.31	6.62	6.53	6.75	8.04	7.29	6.83	7.11	6.81	7.13
CaO	9.63	10.19	10.37	10.68	10.87	10.68	10.66	11.14	10.72	10.62	10.67	10.83	10.94	11.18	10.85
Na_2O	2.03	2.33	2.56	2.33	2.32	2.51	2.40	2.14	2.31	2.29	2.10	1.98	2.14	2.11	2.31
K_2O	.95	.77	.29	.73	.68	.73	.61	.34	.29	.47	.29	.11	.57	.36	.65
P_2O_5	.13	.19	.14	.20	.19	.16	.16	.07	.17	.15	.16	.21	.17	.16	.15
K_2O/Na_2O	.468	.332	.113	.313	.293	.292	.253	.157	.128	.204	.139	.05	.266	.169	.279

Appendix 2 (contd.)

Appendix 2 (contd.)

	JR101	JR 73	JR9	JR 58	JR 43	JR 87	JR104	JR121	JR126	JR123	JR125	JR 11	JR105	JR124	JR 18
SiO_2	50.64	53.64	52.07	54.70	50.50	51.33	51.62	51.41	51.48	51.89	52.04	49.27	49.57	48.27	50.33
TiO_2	.98	1.11	1.02	1.25	.85	.74	.92	.96	.90	.96	.98	.73	1.03	.95	.83
Al_2O_3	16.15	16.22	15.41	14.76	15.49	15.59	15.17	15.03	15.13	15.22	15.56	13.59	14.42	13.43	14.06
Fe_2O_3	11.50	10.17	11.71	10.92	10.73	10.28	11.12	11.28	11.21	11.34	10.67	11.67	12.54	12.37	11.04
MnO	.24	.14	.17	.17	.16	.16	.17	.17	.17	.21	.21	.17	.16	.18	.17
MgO	6.22	4.95	6.05	5.63	8.93	7.73	7.11	7.14	7.19	6.43	6.59	12.60	9.27	12.39	10.98
CaO	11.44	10.29	10.13	9.13	10.62	11.30	10.93	10.73	10.91	11.06	11.08	9.49	10.61	9.93	10.00
Na_2O	2.03	2.28	2.24	2.31	2.33	2.17	2.47	2.50	2.25	2.20	2.17	2.01	1.85	1.98	2.06
K_2O	.62	.98	1.03	.85	.46	.56	.34	.62	.65	.53	.54	.35	.41	.38	.41
P_2O_5	.17	.21	.17	.21	.13	.13	.13	.16	.16	.16	.16	.12	.13	.12	.14
K_2O/Na_2O	.303	.428	.459	.367	.196	.258	.138	.250	.289	.242	.251	.175	.222	.193	.198

APPENDIX 3 : MAJOR ELEMENTS - BARKLY EAST BASALTS (calculated L.O.I.-and H_2O^+-free)

(see Table 9a)

	JR 88	JR 94	S 17	S 5	S 6	S 9	3/10	JR 109	JR 108A	JR 108B	JR 31
SiO_2	51.51	54.49	54.55	54.24	52.90	54.2	58.11	54.14	51.25	53.41	64.27
TiO_2	1.18	.87	.88	.88	.89	.84	.89	.88	.85	1.13	.78
Al_2O_3	15.04	15.27	15.39	15.13	15.67	14.94	15.43	15.09	15.60	13.78	15.80
Fe_2O_3	13.25	9.99	9.94	10.03	10.43	10.26	9.16	10.01	10.41	11.50	6.89
MnO	.19	.15	.14	.15	.16	.16	.14	.18	.16	.18	.10
MgO	6.83	6.26	6.21	6.96	7.17	6.58	4.87	6.71	7.94	5.94	2.89
CaO	9.78	9.67	9.42	10.07	10.23	10.58	8.87	9.89	11.24	10.94	4.38
Na_2O	2.08	2.05	2.21	1.95	1.97	2.05	1.90	2.10	2.04	2.43	2.64
K_2O	.26	1.09	1.12	.45	.44	.26	.48	.84	.39	.51	2.09
P_2O_5	.18	.15	.15	.13	.15	.13	.17	.14	.12	.17	.16
K_2O/Na_2O	.125	.532	.508	.231	.223	.127	.253	.400	.191	.210	.790

APPENDIX 4.

A) Chemical Analyses:

All the whole rock chemical analyses were performed by the author during a period as a visiting student in the Department of Geochemistry, University of Cape Town (U.C.T.). All analyses were conducted by x-ray fluorescence procedures adopted and devised by the Department of Geochemistry, U.C.T.

Rocks from the Birds River Complex were crushed in the Department of Geology, Rhodes University. Samples were split in a jaw crusher, crushed to $\pm$ 120 mesh size in a roller mill and then crushed to $\pm$ 300 mesh size by hand in an agate mortar.Powder briquettes, using approximately 3 grams of fine powder, were prepared for X.R.F. analysis for Zr, Y, Rb and Sr. These samples were subsequently re-analysed at U.C.T.

The Karroo dolerites and Barkly East basalts were crushed at U.C.T. Samples were initially split in a jaw crusher;then about 200 grams of powder was crushed to less than 120 mesh size in an agate "Sieb" mill. Ten grams of this powder was then crushed to approximately 300 mesh size in automatic agate mortars. Aliquots of sample 3/10 (basalt) were crushed both at Rhodes and at U.C.T. to determine if there was any contamination introduced by the steel roller mill used for crushing at Rhodes University. These aliquots were separately analysed in full. The results are shown in Table B. Also shown in Table B is the chemical analysis reported for this rock (3/10) by Lock et al. (1974).

Na, Ba, Sr, Rb, Zr, Y, Nb, Zn, Cu, Ni, Co, Cr and V were determined on pressed powder briquettes. Si, Al, Ti, Ca, K, Mg and P were analysed on duplicate fusion discs prepared after the method of Norrish and Hutton (1969). Mass absorption coefficients at the Rb wavelength were determined on the powder briquettes using measurement on the Compton Scatter peak.

Mass absorption coefficients and Ba were determined on a manually operated PW 1540 spectrometer. The remaining elements were analysed using a semi-automatic PW 1220 spectrometer.

Raw data were processed using standard computer programs written in the Department of Geochemistry, U.C.T. In all the programs, working curves are calculated from determinations on international and departmental (U.C.T.) rock standards. Values used for the standards are those adopted in the Geochemistry Dept., U.C.T.

Spectral line interferences were reduced and applied to the raw data from determinations on blank and synthetic standards. Matrix effects and dead-time corrections were applied to the raw data in the computer programs. Mass absorption coefficients necessary for the reduction of Co, Cr, V and Ba data were calculated using a computer program, from major element data. For these calculations, the old Birks' values were used.

All the fusion discs including the international and N.I.M. rock standards, were cast using flux purchased by the Department of Geology, Rhodes University. These standards were returned to Rhodes and are now in use in geochemical analytical determinations carried out by this department.

H_2O^- was determined by heating the sample at 110°C for at lease 6 hours and measuring the weight differential. Similarly, H_2O^+ was determined by ignition at 950°C for at least 12 hours in a large furnace. All Fe was determined as Fe_2O_3. FeO was not separately determined. Normative calculations assume an oxidation ratio of $Fe_2O_3/FeO = 0.2$.

Analytical conditions for the major and trace element determinations are shown summarized in Table A. Averaged lower limits of determination are indicated in Table C.

Table A : Analytical Conditions

Major Elements

	Fe	Mn	Ti	Ca	K	P	Si	Al	Mg	Na	Rb mass. abs. coeff.
Tube	W		Cr								Mo (Y_2O_3-filter)
Kv	55										50
mA	36										20
Counter	Flow										Scintillation
Collimator	Fine		Coarse	Fine		Coarse			Fine	Coarse	Fine
Crystal	LiF(220)		LiF(200)			PET			TLAP		LiF(220)
Counting time on peak (sec).	10	40	10	10	20	100	100	100	200	200	preset count to 300,000

Trace Elements

	Ba	Sr	Rb	Zr	Y	Nb	Zn	Cu	Ni	Co	Cr	V
Tube	Cr	W					Au			W		
kV	50	70					60					
mA	20	28					32					
Counter	Flow	Scintillation					Flow and Scint.			Flow		
Collimator	Fine											
Crystal	LiF(220)											
Counting time on peak (sec.)	3x100	120				600	200					

Table B

Sample 3/10 (basalt)

	1	2A	2B	3A	3B
SiO_2	56.9	55.75	55.78	56.05	55.95
TiO_2	0.93	0.85	0.86	0.87	0.87
Al_2O_3	15.0	14.82	14.79	14.89	14.89
FeO	5.96	8.82*	8.77*	8.83*	8.92*
Fe_2O_3	1.96				
MnO	0.15	0.13	0.13	0.13	0.13
MgO	4.10	4.64	4.72	4.65	4.68
CaO	8.20	8.51	8.51	8.53	8.49
Na_2O	1.96	1.82[a]	1.82	1.85	1.85
K_2O	0.53	0.46	0.46	0.46	0.46
P_2O_5	0.22	0.16	0.16	0.15	0.14
$H_2O(T)$	3.27	3.42	3.42	3.37	3.37
TOTAL	99.18	99.38	99.38	99.80	99.76

Trace Elements ppm

	2	3
Ba	182	183
Sr	235	236
Rb	21.0	20.9
Y	29.3	28.7
Zr	157	159
Nb	7.8	7.4
Zn	82	85
Cu	45	51
Co	28.5	29.3
Ni	31.8	32.9
V	191	188
Cr	121	122

No's

1. Lock et al. (1974, Table 1, Sample 3/10).

2A,B. Aliquot of sample 3/10, crushed at U.C.T.

3A,B. Aliquot of sample 3/10, crushed at R.U.

* All Fe determined as Fe_2O_3.

(A,B) Duplicate fusion discs for major element analyses.

a. Na and trace elements determined on single powder briquettes.

$H_2O(T)$ Total water (L.O.I. + H_2O^-).

Table C

Average Lower Limits of determination (L.L.D.) and errors of determination.

	Average L.L.D.	Average absolute error	Average % error
Fe	.020%	.077%	1.04
Mn	.008	.006	4.28
Ti	.006	.017	2.53
Ca	.010	.044	1.12
K	.003	.041	2.49
P	.018	.006	2.79
S	.031	.286	.51
Al	.025	.073	.60
Mg	.108	.101	4.83
Na	.080	.062	2.17
Ba	4.0 ppm	2.20 ppm	
Sr	2.6	1.18	
Rb	2.6	.86	
Y	2.4	.85	
Zr	2.6	1.00	
Nb	1.4	.40	
Zn	1.0	.45	
Cu	1.5	.60	
Co	5.3	1.35	
Ni	1.9	.80	
V	4.0	1.50	
Cr	2.8	1.40	

Note: Lower limits of determination are calculated by data reduction computer programs written in the Dept. of Geochemistry, U.C.T.

$$\text{L.L.D.} = \frac{6.0}{Ip/m} \times \sqrt{\frac{Ib}{T}}$$

where Ip = Peak intensity
Ib = Background(s) intensity
T = Total counting time
M = Counts per sec. per % of element

As a general rule, the lower limit of determination is about three times the lower limit of detection (Jenkins, 1974). Data quoted in Table C are lower limits of determination. Detection limits are consequently about three times smaller than the L.L.D.

APPENDIX 5

Brief petrographic descriptions of the Karroo dolerites, basalts and andesite presented in Tables 8(a), 9(a).

Karroo dolerites:

JR2. Porphyritic : olivine, plagioclase, augite and pigeonite(?) phenocrysts. Groundmass fine-grained intersertal, containing plagioclase, pyroxene, biotite and minor Fe-oxide. (Augite and pigeonite are not distinct phenocrysts but are larger than the normal groundmass minerals. Augite is strongly zoned).

JR9. Porphyritic : plagioclase, augite and pigeonite phenocrysts. Both pyroxenes and plagioclase phenocrysts also occur as glomeroporphyritic aggregates. Groundmass - very fine-grained plagioclase, pyroxene. and Fe-oxide. No olivine.

JR11. Coarse-grained olivine dolerite with subophitic augite. Orthopyroxene is inverted pigeonite; pigeonite also occurs as cores in augite. Minor Fe-oxide and micropegmatite - Kokstad-type.

JR15. Porphyritic : plagioclase, resorbed augite, pigeonite(?) and minor, fresh olivine phenocrysts. Augite phenocrysts are large plates with included plagioclase lathes (Perdekloof-type). Groundmass - fine-grained, intersertal plagioclase, pyroxene and Fe-oxide.

JR18. Porphyritic, variolitic picrite dolerite. Olivine-only phenocrysts with inclusions of spinel (picotite?) set in variolitic groundmass of fibrous plagioclase and pyroxene.

JR21. Porphyritic : plagioclase (glomeroporphyritic), augite, pigeonite(?) and very minor, altered olivine phenocrysts. Groundmass - intersertal to subophitic plagioclase, pyroxene and Fe-oxide.

JR29. Porphyritic : large euhedral augite (slightly resorbed) phenocrysts and plagioclase and altered olivine microphenocrysts. Apparent fining of groundmass around cpx.

Appendix 5 (contd.)

phenocrysts (see JR36). Groundmass - very fine-grained granular plagioclase and pyroxene.

JR36. Porphyritic : large, euhedral, partly altered olivine and glomeroporphyritic plagioclase phenocrysts. Groundmass - fine-grained, granular, plagioclase, pyroxene and Fe-oxide.

JR42. Porphyritic : plagioclase and large olivine phenocrysts. Augite may be phenocrystic. Groundmass - relatively coarse-grained intersertal plagioclase, augite, minor biotite and Fe-oxide. Altered glass occurs interstitially.

JR43. Coarse-grained, subophitic olivine dolerite. Plagioclase, augite and inverted pigeonite (opx.). Minor biotite, Fe-oxide and micropegmatite. Kokstad-type.

JR48. Coarse-grained ophitic to subophitic olivine dolerite. Augite up to 1mm in length (clearly visible in hand specimen), minor Fe-oxide. Perdekloof-type.

JR49. Porphyritic : altered olivine and quench plagioclase microphenocrysts. Groundmass - very fine-grained, partly glassy.

JR50. Porphyritic : plagioclase, augite and small, altered olivine microphenocrysts. Augite are ophitic and resorbed (Perdekloof-type). Groundmass - fine-grained intersertal plagioclase and pyroxene; interstitial glassy mesostasis crowded with Fe-oxide.

JR54. Porphyritic : glomeroporphyritic plagioclase, olivine phenocrysts. Groundmass - relatively coarse-grained, subophitic to coarse spherulitic intergrowths of elongate plagioclase and pyroxene; minor Fe-oxides.

JR58. Porphyritic, altered : highly altered, glomeroporphyritic plagioclase, altered olivine and augite(?) phenocrysts. Groundmass - micro-crystalline.

Appendix 5 (contd.)

JR61. Porphyritic : plagioclase and highly altered olivine phenocrysts. Groundmass - quenched plagioclase and pyroxene microlites set in a dense variolitic groundmass.

JR70. Porphyritic : gromeroporphyritic plagioclase phenocrysts only. Groundmass - intersertal; plagioclase and especially pyroxene are elongate and often intergrown in coarse bowtie (or spherulitic) textures. Typical hollow, quench plagioclases also found in groundmass.

JR72. Porphyritic : glomeroporphyritic plagioclase, olivine and augite (micro)phenocrysts. Groundmass - intersertal; plagioclase, pyroxene and Fe-oxide. Plagioclase and augite are often elongate and completely intergrown.

JR73. Porphyritic : plagioclase, augite and altered olivine microphenocrysts. Groundmass - intersertal; elongate plagioclase and pyroxene with spherulitic intergrowths. Quench plagioclase and Fe-oxide microlites in glassy residuum.

JR87. Medium-grained dolerite; ophitic augite plates, similar to JR121 but rock is more plagioclase-rich. Minor micropegmatite. Perdekloof-type.

JR90. Porphyritic : glomeroporphyritic and large, eroded laths of plagioclase. Microphenocrystic olivine(?). Groundmass - fine-grained intersertal plagioclase and pyroxene with iron oxide crowded in glassy residuum.

JR99. Generally fine-grained dolerite. Microphenocrysts of olivine; plagioclase and augite in subophitic to intersertal intergrowth. Groundmass - iron oxide-rich, glassy mesostasis.

JR101. Sparsely porphyritic : microphenocrysts of olivine (altered), plagioclase and augite(?). Groundmass - dense intersertal to spherulitic intergrowths of elongate plagioclase and clinopyroxene. Glassy residuum rich in Fe-oxide.

Appendix 5 (contd.)

JR104. Medium-grained, subophitic; augite and plagioclase. Minor microphenocrystic olivine. Glassy mesostasis rich in Fe-oxide.

JR105. Coarse-grained, olivine-rich dolerite. Plagioclase and augite show subophitic to coarse spherulitic-eutectoid intergrowths. Interstitial glassy residuum. Olivines large, fresh and show minor inclusions of brownish spinel (picotite?).

JR121. Medium-grained, Perdekloof-type dolerite. Large ophitic augite plates constitute bulk of rock. Minor olivine microphenocrysts. Glassy residuum rich in Fe-oxide and plagioclase microlites occurs interstitially.

JR123, 125, 126. Fine- to medium-grained dolerite. Plagioclase and highly-zoned augite occur in subophitic to intersertal intergrowths. Glassy residuum is rich in Fe-oxides.

JR124. Coarse-grained, olivine-rich dolerite (similar to JR105) with augite and plagioclase showing subophitic textures. Glassy mesostasis is crowded with Fe-oxide and quench plagioclase microlites.

Barkly East basalts:

JR88. Red Beds basalt : glomeroporphyritic plagioclase, pigeonite and highly altered clinopyroxene(?) phenocrysts. Microphenocrystic plagioclase laths show flow textures (trachytic). Groundmass - dense, altered pyroxene and plagioclase with altered, oxidized glass and granular Fe-oxide.

S17. Donnybrook basalt : highly altered plagioclase glomeroporphyritic aggregates and discrete laths . Minor, very small, highly altered olivine pseudomorphs. Groundmass - very fine-grained, partly glassy; plagioclase, pyroxene and Fe-oxide. Altered specimen.

JR94. Donnybrook basalt : very similar to S17 but shows a single, highly eroded clinopyroxene phenocryst.

Appendix 5 (contd.)

JR31.	Belmore andesite : abundant (micro)phenocrysts of plagioclase and orthopyroxene (enstatite). Groundmass - clear, brown glass.
S5.	Pillow lava, Kraai River Formation. Sparse plagioclase phenocrysts set in a very fine-grained groundmass, partly glassy and versicular.
S6.	Kraai River basalt : Sparsely plagioclase phyric. Groundmass - microcrystalline, plagioclase, pyroxene, Fe-oxides and altered glass. Vesicular.
S9.	Kraai River basalt : Glomeroporphyritic plagioclase and resorbed orthopyroxene phenocrysts. Orthopyroxene is often finely rimmed by groundmass clinopyroxene. Groundmass - fine-grained, intersertal; plagioclase and augite often elongate , curved and intergrown. Glassy mesostasis is rich in Fe-oxides.
3/10.	Kraai River basalt : massive lava; plagioclase and orthopyroxene phenocrysts. Groundmass - fine-grained plagioclase and pyroxene, in part glassy.
JR109.	Kraai River basalt : Glomeroporphyritic plagioclase phenocrysts only. Groundmass - ultra-fine-grained; slightly versicular.
JR108A.	Coarse-grained basalt. Subophitic augite and plagioclase. Pigeonite occurs as cores to augite. Abundant greenish to brownish chlorophaeite. Minor micropegmatite occurs interstitially. No fresh olivine.
JR108B.	Similar to JR108A. Augites are more strongly zoned and the rock contains abundant micropegmatite. No fresh olivine.

REFERENCES

ABBOT, M.J., 1967, K and Rb in a continental alkaline igneous rock suite: Geochim. et Cosmochim., v.31, p.1035-1041.

ARTH, J.G., and HANSON, G.N., 1975, Geochemistry and origin of the early Pre-Cambrian crust of northeastern Minnesota: Geochim. et Cosmochim., v.39, p.325-362.

BERLIN, R., and HENDERSON, C.M.B., 1969, The distribution of Sr and Ba between the alkali feldspar, plagioclase and groundmass phases of porphyritic trachytes and phonolites: Geochim. et Cosmochim., v.33, p.247-255.

BOOTH, P.W.K., 1971, The Birds River gabbro complex: unpubl. M.Sc. thesis, Rhodes University.

BOYD, F.R., and ENGLAND, J.L., 1961, Melting of silicates at high pressure: Carnegie Inst. Wash. Yb., 60, p.113-125.

BURNS, R.G., 1969/70, Site preferences of transition metal ions in silicate crystal structures: Chem. Geol., v.5, p.275-283.

BYRAN, W.B., FINGER, L.W., and CHAYES, F., 1969, Estimating proportions in petrographic mixing equations by least-squares approximation: Science, v.163, p.926-927.

COMPSTON, W., McDOUGALL, I., and HEIER, H.S., 1968, Geochemical comparison of the Mesozoic basaltic rocks of Antarctica, South Africa, South America and Tasmania: Geochim. et Cosmochim., v.32, p.129-149.

COOMBS, D.S., 1963, Trends and affinities of basaltic magmas and pyroxenes as illustrated on the diopside-olivine-silica diagram: Min. Soc. America, Spec. Paper, 1, p.227-250.

COX, K.G., 1970, Tectonics and vulcanism of the Karroo period and their bearing on the postulated fragmentation of Gondwanaland: In CLIFFORD, T.N., and GASS, I.G. (eds.), African Magmatism and Tectonics. Oliver and Boyd, Edinburgh.

_____, 1972, The Karroo volcanic cycle: J. Geol. Soc. London, v.128, p.311-331.

_____, and HORNUNG, G., 1966, The petrology of the Karroo basalts of Basutoland: Amer. Min., v.51, p.1415-1432.

_____, and JAMIESON, B.G., 1974, The olivine-rich lavas of Nuanetsi: a study of polybaric magmatic evolution: J. Petrology, v.15, p.269-301.

_____, MACDONALD, R., and HORNUNG, G., 1967, Geochemical and petrographic provinces of the Karroo basalts of Southern Africa: Amer. Min., v.52, p.1451-1474.

DANCHIN, R.V., and FERGUSON, J., 1969, The geochemistry of the Losberg intrusion, Fochville, Transvaal: Geol. Soc. South Africa, Spec. Publ., 1, p.689-714.

de LONG, S.E., 1974, Distribution of Rb, Sr and Ni in igneous rocks, central and western Aleution Islands, Alaska: Geochim. et Cosmochim., v.38, p.325-362.

du TOIT, A.L., 1904, Geological survey of Aliwal North, Herschel, Barkly East and part of Wodehouse: 9th Ann. Rpt. Geol. Commission, Colony of Cape of Good Hope, p.69-110.

_____, A.L., 1911, Geological survey of parts of the Stormbergen: 16th Ann. Rpt. Geol. Commission, Colony of Cape of Good Hope, p.113-136.

_____, A.L., 1920, The Karroo dolerites of South Africa: Trans. Geol. Soc. South Africa, v.23, p.1-42.

EALES, H.V., and BOOTH, P.W.K., 1974, The Birds River gabbro complex, Dordrecht district: Trans. Geol. Soc. South Africa, v.77, p.1-15.

———., and ROBEY, J. van A., in press, Differentiation of tholeiitic Karroo magma at Birds River, South Africa.

ELLIOT, D.H., and WATTS, D.R., 1974, The nature and origin of volcaniclastic material in some Karroo and Beacon rocks: Trans. Geol. Soc. South Africa, v.77, p.109-111.

ENGEL, A.E.J., ENGEL, C.G., and HAVENS, R.G., 1965, Chemical characteristics of oceanic basalts and the upper mantle: Geol. Soc. America, Bull., v.76, p.719-734.

ERLANK, A.J., and HOFMEYER, P.K., 1966, K/Rb and K/Cs ratios in Karroo dolerites from South Africa: J. Geophys. Res., v.71, p.5439-5445.

EWART, A., BYRAN, W.B., and GILL, J.B., 1973, Mineralogy and geochemistry of the younger volcanic islands of Tonga, S.W. Pacific: J. Petrology, v.14, p.429-465.

FERGUSON, J., and WRIGHT, I.H., 1970, Compositional variation of plagioclases in the Critical Series, Bushveld Complex: Geol. Soc. South Africa, Spec. Publ., 1, p.59-66.

FLOWER, M.J., 1973, Trace element distribution in lavas from Anjouan and Grande Comore, Western Indian Ocean: Chem. Geol., v.12, p.81-98.

GAST, P.W., 1968, Trace element fractionation and origin of tholeiitic and alkaline magma types: Geochim. et Cosmochim., v.32, p.1057-1086.

GOODMAN, R.J., 1972, Distribution of Ga and Rb in coexisting groundmass and phenocryst phases of some basic volcanic rocks: Geochim. et Cosmochim., v.36, p.303-317.

GUNN, B.M., 1971, Trace element partition during olivine fractionation of Hawaiian basalts: Chem. Geol., v.8, p.1-13.

HAIKLI, T.A., 1968, An attempt to apply Makaopuhi nickel fractionation data to the temperature determination of a basic intrusive: Geochim. et Cosmochim., v.32,

_____, and WRIGHT, T.L., 1967, The fractionation of nickel between olivine and augite as a geothermometer: Geochim. et Cosmochim., v.31, p.877-884.

HART, S.R., and BROOKS, C., 1974, Clinopyroxene - matrix partitioning of K, Rb, Cs, Sr and Ba: Geochim. et Cosmochim., v.38, p.1799-1806.

HENDERSON, P., and DALE, I.M., 1969/70, The partitioning of selected transition ions between olivine and groundmass of oceanic basalts: Chem. Geol., v.5, p.267-274.

HESS, H.H., 1949, Chemical compositions and optical properties of common clinopyroxenes: Amer. Min., v.34, p.621-666.

HOTZ, P.E., 1953, Petrology of granophyre in diabase near Dillsburg, Pennsylvania: Geol. Soc. America, Bull., v.64, p.675-704.

HUTCHISON, C.S., 1974, Laboratory Handbook of Petrographic Techniques. Wiley, New York.

HYOTEN, K., and SCHAIRER, J.F., 1960/61, The plane enstatite-anorthite-diopside and its relation to basalts: Carnegie Inst. Wash. Yb., 60, p.125-141.

IRVINE, T.N., and BARAGAR, W.R.A., 1971/70 A guide to the chemical classification of the common volcanic rocks: Canadian J. Earth. Sc., v.8, p.543-548.

ISHIKWAWA, H., 1968, Some aspects of geochemical trends and fields of ratios of V, Ni and Co: Geochim. et Cosmochim., v.32, p.1913-1917.

JAMIESON, B.G., and CLARKE, D.B., 1970, Potassium and associated elements in tholeiitic basalts: J. Petrology, v.11, p.183-204.

JENKINS, R., 1974, An Introduction to X-ray Spectrometry. Heyden, London.

JENSEN, B.B., 1973, Patterns of trace element partitioning: Geochim. et Cosmochim., v.37, p.2227-2242.

KABLE, E.J.D., ERLANK, A.J., and CHERRY, R.D., 1971, Geochemical features of lavas: In van Zinderen BAKKER Sr, E.M., WINTERBOTTOM, J.M., and DYER, R.A. (eds.), Marion and Prince Edward Islands, Balkema, Cape Town, p.78-88.

KORRINGA, M.K., and NOBLE, D.C., 1971, Distribution of Sr and Ba between natural feldspar and igneous melt: Earth and Planet. Sc. Letters, v.11, p.147-151.

KUNO, H., 1967, Differentiation of basalt magmas: In HESS, H.H., and POLDERVAART, A. (eds.), Basalts, v.2, Wiley, New York, p.623-689.

LAMBERT, R. St. J., and HOLLAND, J.G., 1973, Yttrium geochemistry applied to petrogenesis utilizing calcium-yttrium relationships in minerals and rocks: Geochim. et Cosmochim., v.38, p.1393-1414.

LOCK, B.E., PAVERD, A.L., and BRODERICK, T.J., 1974, Stratigraphy of the Karroo volcanic rocks of the Barkly East district: Trans. Geol. Soc. South Africa, v.77, p.117-129.

MARSH, J.S., 1973, Alkaline igneous rocks of the coastal belt, south of Luderitz, South West Africa: a petrological study: Unpubl. Ph.D. thesis, University of Cape Town.

MARTINI, J.E.J., 1974, On the presence of ash beds and volcanic fragments in the graywackes of the Karroo System in the southern Cape Province (South Africa): Trans. Geol. Soc. South Africa, v.77, p.113-116.

McDOUGALL, I., 1962, Differentiation of the Tasmanian dolerites: Red Hill dolerite-granophyre association: Geol. Soc. America, Bull., v.73, p.279-315.

_____, and LOVERING, J.F., 1963, Fractionation of chromium, nickel, cobalt and copper in a differentiated dolerite-granophyre sequence at Red Hill, Tasmania: J. Geol. Soc. Australia, v.10, p.325-338.

MIYASHIRO, A., and SHIDO, F., 1975, Tholeiitic and calc-alkaline series in relation to the behaviours of titanium, vanadium, chromium and nickel: American J. Sc., v.275, p.215-277.

NOCKOLDS, S.R., and ALLEN, R., 1956, The geochemistry of some igneous rock series, 3: Geochim. et Cosmochim., v.9, p.34-77.

O'HARA, M.J., 1968, The bearing of phase equilibria studies in synthetic and natural systems on the origin and evolution of basic and ultrabasic rocks: Earth. Sc. Reviews, v.4, p.69-133.

PEARCE, T.H., 1968, A contribution to the theory of variation diagrams: Contr. Min. Pet., v.19, p.142-157.

_____, 1970, Chemical variations in the Palisade sill: J. Petrology, v.11, p.15-32.

PHILPOTTS, J.A., and SCHNETZLER, C.C., 1970, Phenocryst - matrix partition coefficients for K, Rb, Sr and Ba, with applications to anorthosite and basalt genesis: Geochim. et Cosmochim., v.34, p.307-322.

PRINZ, M., 1967, Geochemistry of the basaltic rocks: trace elements: In HESS, H.H., and POLDERVAART, A. (eds.), Basalts, v.1, Wiley, New York, p.271-323.

RHODES, R.C., and KROHN, D.H., 1972, Tectonic control over regional geochemical variation in the Karroo basaltic province of South Africa: Trans. Geol. Soc. South Africa, v.75, p.11-21.

SHAIRER, J.F., and YODER Jr., H.S., 1961/62, The system diopside-enstatite-silica: Carnegie Inst. Wash. Yb., 60, p.125-141.

TAYLOR, S.R., 1965, The application of trace element data to problems in petrology: Phys. Chem. Earth, v.6, p.133-214.

_____, KAYE, M., WHITE, A.J.R., DUNCAN, A.R., and EWART, A., 1969, Genetic significance of Co, Cr, Ni, Sc and V content of andesites: Geochim. et Cosmochim., v.33, p.275-286.

WAGER, L.R., and BROWN, G.M., 1968, Layered Igneous Rocks. Oliver and Boyd, London.

WALKER, F., and POLDERVAART, A., 1949, Karroo dolerites of the Union of South Africa: Geol. Soc. America, Bull., v.60, p.591-706.

WALKER, K.R., 1970, The Palisade sill, New Jersey: a reinvestigation: Geol. Soc. America, Spec. Paper, 111.

WEAVER, S.D., SCEAL, J.S.C., and GIBSON, I.L., 1972, Trace element data relevant to the origin of trachytic and pantelleritic lavas in the East Africa Rift System: Contr. Min. Pet., v.36, p.181-194.

WRIGHT, T.L., 1974, Presentation and interpretation of chemical data for igneous rocks: Contr. Min. Pet., v.48, p.233-248.

YODER, Jr., H.S., and TILLEY, C.E., 1962, Origin of basalt magmas: an experimental study of natural and synthetic rock systems: J. Petrology, v.3, p.342-532.

ZIELINSKI, R.A., and FREY, F.A., 1970, Gough Island - evaluation of a fractional crystallization model: Contr. Min. Pet., v.29, p.242-254.